

**The establishment of non-viral reprogramming methods and
pancreatic differentiation in organotypic models
for the production of patient-specific pancreatic cells**

Dissertation

zur Erlangung des
Doktorgrades der Naturwissenschaften (Dr. rer. nat.)

der

Naturwissenschaftlichen Fakultät I – Biowissenschaften –

der Martin-Luther-Universität
Halle-Wittenberg,

vorgelegt

von Herrn Matthias Jung

geb. am 13.01.1984 in Jena

Gutachter:

1. Prof. Dr. Gerald Moritz
2. Prof. Dr. Dr. Bernd Fischer
3. Prof. Dr. Heike Walles

Öffentliche Verteidigung am 08.12.2014 in Halle an der Saale

*I lovingly dedicate this thesis to
my family
for their love and care*

ACKNOWLEDGEMENTS

I would like to express my very great appreciation to Dr. Insa S. Schroeder for the opportunity to work in her junior research group and for her patient guidance, enthusiastic encouragement, and useful critiques of this work. I would like to offer my special thanks to Prof. Bernd Fischer and Prof. Gerald Moritz for their continuous support and their valuable and constructive suggestions. I would like to extend my thanks to Prof. Anna M. Wobus for her generous support.

I would also like to express my very great appreciation to all present and former members of the junior research group of Dr. Insa S. Schroeder. All of them created a friendly, enjoyable, inspiring, and motivating working atmosphere. I am particularly grateful for the help provided by Dr. Sabine Sulzbacher, Dr. Sabine Foja, Dr. Sandrina Schweyen, and Dr. Judith Czarnota. Assistance provided by Bernadette Harwardt was greatly appreciated. Further, I wish to acknowledge the help provided by Christina Baumbach, Liubov Stavitskaya, Stephanie Kuhn, Diana Rarisch and Ulrike Gresch. I would also like to thank the staff of the TRM Leipzig for their support.

My special thanks are extended to the group of Prof. Bernd Fischer and the people at the Department of Anatomy and Cell Biology. PD Dr. Anne Navarrete-Santos, Dr. Juliane-Susanne Schmidt, Dr. Martin Schicht, Dr. Ronald Biemann, Dr. Heiko Baisch, Dr. Rene Thieme, and Dr. Julia Knelangen gave insightful feedback, comments, and suggestions. I would like to thank the following people for excellent technical support: Christine Fröhlich, Sabine Schrötter, Michaele Kirstein, Susann Möschter, Stephanie Beilecke, Franziska Knöfel, Hans-Joachim Heine, Elisabeth George, Evelyn Axmann, and Patrizia Zwarg. To all of them I would like to thank for making it a nice, friendly, and enjoyable time.

I would like to express my special thanks to PD Dr. Dagmar Riemann, Prof. Heike Walles & Johanna Schanz, Prof. Helge Taubert, Dr. Wolfgang Knolle, and Angelika Steller for contributing to this work with technical support, instruments, methods, and materials.

I would like to express my gratitude to the MLU Halle and the TRM Leipzig for their financial support.

My deepest heartfelt thanks and appreciation belongs to my wife, my son, and my parents. I would like to thank particularly my wonderful Juliane for always supporting me and for giving me strength and motivation to finish this work. I love you! Further, my gratitude belongs to my whole family, who supported me always. I am also very grateful for all my friends for their support in many ways.

Everything counts.

LIST OF FIGURES

- FIGURE 1: Potency of stem cells and progenitors during embryogenesis and reprogramming.
- FIGURE 2: Cells for the analysis of induction and maintenance of pluripotency.
- FIGURE 3: Signaling pathways for induction and maintenance of pluripotency.
- FIGURE 4: Induction, maintenance, and loss of pluripotency and involved miRs.
- FIGURE 5: Procedure of patient- and disease-specific iPS cell generation.
- FIGURE 6: Pancreas development *in vivo* and pancreatic differentiation *in vitro*.
- FIGURE 7: Mouse and human pancreatic differentiation models applied in the present study.
- FIGURE 8: Primary keratinocytes obtained from human plucked hair.
- FIGURE 9: Analysis of pluripotency markers in BJ-5ta fibroblasts, L87 MSCs, and primary keratinocytes.
- FIGURE 10: Delivery of STEMcircles™ into L87 and BJ-5ta cells.
- FIGURE 11: Induction of ONSL, Klf4, and c-Myc by STEMcircles™.
- FIGURE 12: Induction of endogenous ONSL expression.
- FIGURE 13: Analysis of the transfection procedure using novel miR-1.
- FIGURE 14: Flow cytometry and IF analysis of miR-delivery.
- FIGURE 15: Prediction of target mRNA possibly involved in reprogramming.
- FIGURE 16: Expression analysis of predicted miR-302a-d & 372 target mRNAs Ccna1, Klf13, Dnmt1, and Wdr61.
- FIGURE 17: Induction of mature and precursor miR-302a-d & 372 expression.
- FIGURE 18: Regulation of Oct4 and Nanog by miR-302a-d & 372.
- FIGURE 19: Regulation of Dnmt1 by miR-302a-d & 372.
- FIGURE 20: Direct interaction of mature miR-302a-d & 372 with the 3'UTR of Dnmt1 transcripts.
- FIGURE 21: Regulation of the Oct4 promoter methylation by miR-302a-d & 372.
- FIGURE 22: Regulation of Dnmt3a and Dnmt3b by miR-302a-d & 372.
- FIGURE 23: Induction of Oct4A and Nanog by miR-302a-d & 372 is regulated by ES cell-specific conditions and hypoxia.
- FIGURE 24: Induction of endogenous miR-302a expression by synthetic miR-302a-d & 372 is regulated by hypoxia.
- FIGURE 25: STEMcircles™-mediated induction of Oct4, Nanog, Sox2, and Lin28 is regulated by hypoxia.
- FIGURE 26: Proliferation is regulated by hypoxia and FGF2.
- FIGURE 27: Epigenetic modulators promote maintenance of undergoing reprogramming by miR-302a-d & 372 delivery.
- FIGURE 28: Signal transduction inhibitors promote maintenance of colonies established by mi-302a-d & 372 delivery.
- FIGURE 29: Kinase inhibitors promote maintenance of colonies established by STEMcircles™.
- FIGURE 30: Co-transfection of STEMcircles™ and miR-302a-d & 372 affects ONSL expression.
- FIGURE 31: Repeated delivery of STEMcircles™ promotes maintenance of colonies.
- FIGURE 32: Induction of Sox2 in clones is mediated by STEMcircles™ and subsequent treatment with 6 small molecules.
- FIGURE 33: 3D biological matrices from porcine jejunum.
- FIGURE 34: 3D biological matrices are adequate to culture and differentiation of ES cells.
- FIGURE 35: Directed differentiation generates DE for 2D and 3D pancreatic differentiation.
- FIGURE 36: Induction of DE progenitors on 3D matrices without EB formation.
- FIGURE 37: Primary MVECs and HUVECs maintain natural characteristics *in vitro*.
- FIGURE 38: Maintenance of primary ECs in pancreatic differentiation media.
- FIGURE 39: Pluripotency makers expressed in iMR90 iPS cells.
- FIGURE 40: Differentiation of human iMR90 iPS cells into pancreatic progenitors.
- FIGURE 41: Co-cultures with HUVECs regulate pancreatic differentiation.
- FIGURE 42: Matrices preserve viability of co-cultured DE progenitors and MVECs.
- FIGURE 43: Strategy for the use of non-viral methods to reprogram human somatic cells.
- FIGURE 44: Strategy for the use of 3D biological matrices and co-culture conditions to generate insulin-producing cells.

LIST OF TABLES

TABLE 1: Different sets of small molecules regulating different signaling pathways.

TABLE 2: Epigenetic modulators applied in different sets.

TABLE 3: Different sources for the generation of iPS cells.

LIST OF APPENDICES

APPENDIX 1: Morphology and GFP expression after delivery of pEGFP-N1 by electroporation and lipofection.

APPENDIX 2: Morphology and GFP expression after delivery of pEGFP-N1 using competitor reagents.

APPENDIX 3: Optimization of STEMcircles™ delivery.

APPENDIX 4: Morphology after delivery of miRs using competitor reagents.

APPENDIX 5: Morphology after delivery of miRs using different concentrations.

APPENDIX 6: Morphology and after delivery of miR-302a-d & 372 in the presence of hypoxia.

APPENDIX 7: Morphology and GFP expression after delivery of STEMcircles™ in the presence of normoxia and hypoxia.

APPENDIX 8: Morphology after treatment with small molecule epigenetic modulators.

APPENDIX 9: Small molecule epigenetic modulators, miR-302a-d & 372, and hypoxia affect the morphology of L87 cells.

APPENDIX 10: Morphology after treatment with miR-302a-d & 372, small molecule epigenetic modulators, and ES cell-specific culture conditions.

APPENDIX 11: Small molecule epigenetic modulators promote maintenance of colonies derived after transfection with miR-302a-d & 372.

APPENDIX 12: Small molecule kinase inhibitors do not preserve proliferation of non-epithelial colonies established by STEMcircles™.

APPENDIX 13: Alkaline Phosphatase staining of pluripotent ES cells and somatic cells.

APPENDIX 14: Morphology after co-transfection of STEMcircles™ and miR-302a-d & 372.

APPENDIX 15: Characteristics of human ES cells are preserved in iPS cells by MEF-conditioned medium.

APPENDIX 16: Morphology and GFP expression after subsequent treatment with STEMcircles™, miR-302a-d & 372, and small molecules.

APPENDIX 17: List of human semi-quantitative PCR primers.

APPENDIX 18: List of mouse semi-quantitative PCR primers.

APPENDIX 19: List of human qRT-PCR primers.

APPENDIX 20: List of mouse qRT-PCR primers.

APPENDIX 21: Oligonucleotides for the generation of pmiRGLO-Dnmt1, pmiRGLO-nonsense, and pmiRGLO-302a.

APPENDIX 22: Composition of media applied for pancreatic differentiation.

LIST OF ABBREVIATIONS

2D	two-dimensional	exocr panc	exocrine pancreas
3D	three-dimensional	extraembr	extramebryonic
5-mc	5-methylcytosine	F12	Nutrient Mixture F12
5hmc	5-hydroxymethylcytosine	FCS	fetal calf serum
AKT	v-akt muine thymoma viral oncogene	FDA	Food and Drug Administration of the USA
ALK	activin receptor-like kinase	FGF2	fibroblast growth factor 2
AP	alkaline phosphatase	FIG	figure
APP	appendix	FSC	forward scatter detector
APS	ammonium persulfate	GFP	green fluorescence protein
ARP	<i>atonal</i> -related protein	GFP ⁺	GFP-positive cells
ASCL	<i>achaete scute</i> -like	GMEM	Glasgow Minimal Essential Medium
ATCC	American Type Culture Collection	GMP	good manufacturing practice
BayK	BayK8644	GSK3	glycogen synthase kinase 3
beta cell dev	beta cell development	HDAC	histone deacetylase
BIO	6-bromo-indirubin-3'-oxime	HDMEC	human dermal microvascular endothelial cell
BME	beta-mercaptoethanol	HE	hematoxylin and eosin stain
BMP	bone morphogenetic proteins	HGF	hepatocyte growth factor
BSA	bovine serum albumin	HIF	hypoxia-inducible factor
CDM	chemically defined medium	HMEC-1	human microvascular endothelial cell line 1
cDNA	complementary DNA	HMT	histone methyltransferase
CpG	C-phosphate-G site	HPDM	human pancreatic differentiation medium
CR	conserved region	HRP	horseradish peroxidase
DE	definitive endoderm	HUVEC	human umbilical vascular endothelial cell
DMEM	Dulbecco's Modified Eagle Medium	hyp	hypoxia
DMSO	dimethyl sulfoxide	ICM	inner cell mass
DNA	deoxyribonucleic acid	IDE1/2	inducer of definitive endoderm 1 and 2
DNase	deoxyribonuclease	IF	immunofluorescence
DNMT	DNA methyltransferase	IGF	insulin-like growth factor
dNTP	deoxyribonucleotides	IMDM	Iscoe's modified Dulbecco's medium
E	embryonic day in mice development	INR	initiator element
e.g.	<i>exempli gratia</i>	iPS cells	induced pluripotent stem cells
EB	embryoid body	JAK	Janus kinase
EC	endothelial cell	KAAD-cyclopamine	3-Keto-N-(aminoethyl-aminocaproyl-dihydrocinnamoyl)-cyclopamine
EC cells	embryonic carcinoma cells	KO-DMEM	Knockout DMEM
ECGM	endothelial cell growth medium	KOSR	Knockout Serum Replacement
ECM	extracellular matrix	LIF	leukemia inhibitory factor
EDTA	ethylene diamine tetra acetic acid	MAPK	mitogen activated protein kinase
ecto	ectoderm	MBD	methyl-CpG binding proteins
EGF	epidermal growth factor	MCS	multiple cloning site
EGTA	ethylene glycol tetra acetic acid	MEF	mouse embryonic fibroblast
EMT	epithelial to mesenchymal transition	MEF-cond.	MEF-conditioned culture conditions
en ONSL	endogenous ONSL	MEK	MAPK/ERK kinase
endocr	endocrine		
ERK	extracellular-signal-regulated kinase		
ES cells	embryonic stem cells		
ESchG	Embryo Protection Act		
EU	European Union		

LIST OF ABBREVIATIONS

MEM	Minimal Essential Medium Eagle	RPMI-1640	Rosswell Park Memorial Institute 1640 medium
mesendo	mesendoderm		
meso	mesoderm	RTK	receptor tyrosine kinase
MET	mesenchymal to epithelial transition	SAM	S-adenosyl methionine
		SB	SB431542
mock	mock transfection without miRs/vectors	SC	STEMcircles™
		SCR	seed complementary region
mRNA	messenger RNA	SD	standard derivation
miR	micro RNA	SDS	sodium dodecyl sulfate
MODY	maturity-onset diabetes of the young	SDS-PAGE	SDS-polyacrylamide gel electrophoresis
MSC	mesenchymal stem cell	SEM	standard error of the mean
MSRE	methylation-sensitive restriction enzyme	SEM	scanning electron microscopy
		siRNA	small interfering RNA
MVEC	human dermal microvascular endothelial cell from skin biopsy	SMAD	homolog to the <i>Caenorhabditis</i> protein SMA and the <i>Drosophila</i> protein MAD
NEAA	nonessential amino acid		
neg	negative	SNP	single nucleotide polymorphism
norm	normoxia	snoRNA	small nucleolar RNA
ORS	outer root sheath	Sox	SRY-related HMG-box
OSKM	Oct4, Sox2, Klf4, c-Myc	SSC	side scatter detector
ONSL	Oct4, Nanog, Sox2, Lin28	SSEA1	stage-specific embryonic antigen 1
PAF1C	RNA polymerase II-associated factor complex	SSEA4	stage-specific embryonic antigen 4
pancr prog	pancreatic progenitor		
PBS	phosphate buffered saline	STAT	signal transducer and activator of transcription
PCR	polymerase chain reaction		
PD	PD0325901	StZG	Stem Cell Act
PDGF	platelet-derived growth factor	T1DM	type 1 diabetes mellitus
PDM	pancreatic differentiation medium	T2DM	type 2 diabetes mellitus
PFA	paraformaldehyde	TAB	table
PI	propidium iodide	TAE	tris base, acetic acid, and EDTA
PI3K	phosphatidylinositol-4,5- bisphosphate 3-kinase	TALE	transcription activator-like effectors
pos	positive	TBS-T	tris-buffered saline and Tween20
pre-miR	precursor-miR	TE	tris-EDTA
pri-miR	primary-miR	TEMED	tetramethylethylene-diamine
qRT PCR	quantitative real-time PCR	TGFβ	transforming growth factor β
RA	retinoic acid	THIA	thiazovivin
RBD	RNA binding domain	USA	United States of America
RBP	ribosomal protein	UTR	untranslated region
RG	RG108	VEGFa	vascular endothelial growth factor A
RIPA	radioimmunoprecipitation assay		
RISC	miR-induced silencing complex	WB	western Blot
RNA	ribonucleic acid	WD	week of human development
RNase	ribonuclease	WNT	wingless-related integration site
ROCK	Rho-associated protein kinase		

LIST OF GENES, TRANSCRIPTS, AND PROTEINS

LIST OF GENES, TRANSCRIPTS, AND PROTEINS

18SrRNA	18S ribosomal RNA	Dnmt3l	DNA methyltransferase 3l
A1AT	alpha-1 antitrypsin alias Serpina1	Dppa2	developmental pluripotency associated 2
Aatk	apoptosis-associated tyrosine kinase	Dppa4	developmental pluripotency associated 4
Afp	alpha fetoprotein	Dppa5	developmental pluripotency associated 5
Ago2	argonaute RISC catalytic component 2	Drosha	Drosha ribonuclease type III
Amy2	amylase alpha 2A alias Amy2a	E2F2	E2F transcription factor 5
Aof2	amine oxidase 2 alias Kdm1a	Elavl1	ELAV-like RBP 1 alias HuR
Arx	areistaless related homeobox	Eng	endoglin
Atm	ataxia telangiectasia mutated	Ephb2	ephrin receptors B2
Bbc3	Bcl2-binding component 3 alias Puma	Ephb4	ephrin receptors B4
Bcl2	B cell CCL/lymphoma 2	Esg1	embryonal stem cell-specific gene 1 alias Dppa5
Bdnf	brain-derived neurotrophic factors	Fgf4	fibroblast growth factor 4
Bhlha15	basic helix-loop-helix transcription factor a15 alias Mist1	Fitm1	fat storage-inducing transmembrane protein 1
Bra	T-box transcription factor Brachyury alias T	Flk1	fetal liver kinase 1 alias Kdr or Vegfr2
Btg1	B cell translocation gene 1	Foxa2	forkhead box transcription factors A2
c-Myc	v-myc myelocytomatosis viral oncogene homolog	Foxf1	forkhead box transcription factors F1
CD9	cluster of differentiation 9	Gabbr3	gamma-aminobutyric acid (GABA) A receptor, beta 3
CD34	cluster of differentiation 34	Gal	galanin/GMAP prepropeptide
CD45	cluster of differentiation 45 alias Ptprc	Gata4	gata binding protein 4
CD90	cluster of differentiation 90 alias Thy1	Gcg	glucagon
Cdc25a	cell division cycle 25a	Gck	glucokinase
Cdk6	cyclin-dependent kinase 6	Gdf3	growth differentiation factor 3
Cdx2	caudal type homeobox 2	Gfap	glial fibrillary acidic protein
Ccna1	cyclin A1	Glut2	glucose transporter 2 alias Slc2a2
Cdh5	cadherin 5, type 2 alias VEcad	Grb7	growth factor receptor-bound protein 7
Cdkn1a	cyclin-dependent kinase inhibitor 1A alias p21	Gsc	gooscooid
Chd1l	chromodomain helicase DNA binding protein 1-like	Hif1a	hypoxia-inducible factor 1a
Cpa1	pancreatic carboxypeptidase A1	Hif2a	hypoxia-inducible factor 2a
Csxl12	chemokine CXC ligand 12 alias Sdf1	Hnf1b	hepatocyte nuclear factor 1 B
Cxcr4	transmembrane chemokine CXC receptor 4	HuR	Hu antigen R alias Elavl1
Derl2	derlin 2	Icam	intercellular adhesion molecule 1
Dgcr8	DiGeorge critical region 8	Ins	insulin
Dicer	Dicer1 ribonuclease type III	Jmjd1a	Jumonji domain 1a
Dnmt1	DNA methyltransferase 1	Jmjd2c	Jumonji domain 2c
Dnmt1s	Dnmt1 isoform s	Kat6A	KAT6A K (lysine) acetyltransferase 6A alias Myst3
Dnmt1o1	Dnmt1 isoform o1	Kdm1a	lysine (K)-specific demethylase 1a alias Aof2
Dnmt1o2	Dnmt1 isoform o2	Kdm3a	lysine (K)-specific demethylase 3a alias Jmjd1a
Dnmt2	DNA methyltransferase 2 alias Trdmt1	Kdr	kinase insert domain protein receptor alias Flk1 or Vegfr2
Dnmt3a	DNA methyltransferase 3a	Klf4	kruppel-like factor 4
Dnmt3a2	Dnmt3a isoform 2	Klf4wt	Klf4 transcript variant wild type
Dnmt3b	DNA methyltransferase 3b	Klf4α	Klf4 transcript variant α

LIST OF GENES, TRANSCRIPTS, AND PROTEINS

Klf4 β	Klf4 transcript variant β	Ptpcr	protein tyrosine phosphatase, receptor type C alias CD45
Klf4 γ	Klf4 transcript variant γ		
Klf4 δ	Klf4 transcript variant δ	Puma	p53 up regulated modulator of apoptosis alias Bbc3
Klf13	kruppel-like factor 13		
Lefty1	left-right determination factor 1	Rest	RE1-silencing transcription factor
Lefty2	left-right determination factor 2	Rex1	RNA exonuclease 1 alias Zfp42
Lin28	cell lineage abnormal protein 28 homolog to <i>C. elegans</i> A alias Lin28A	Sdf1	stromal cell-derived factor 1 alias Cxcl12
Lin28B	Lin28A paralog	Sele	selectin E
Lmo2	LIM domain only 2	Serpina1	serin peptidase inhibitor clad A member 1 alias A1AT
		Shh	sonic hedgehog
Map2	microtubule-associated protein 2	Slc2a2	solute carrier family 2 member 2 alias Glut2
Mbd2	methyl-CpG binding domain protein 2	Smad1	SMAD family member 1
Meox1	mesenchyme homeobox 1	Sox2	Sox family transcription factor 2
Mist1	muscle, intestine and stomach expression 1 alias Bhlha15	Sox2otA	Sox2 overlapping transcript A
		Sox2otB	Sox2 overlapping transcript B
Myst3	MYST histone methyltransferase 3 alias Kat6A	Sox7	Sox family transcription factor 7
		Sox17	Sox family transcription factor 17
Nanog	nanog homeobox	Sox18	Sox family transcription factor 18
NanogA	Nanog transcript variant A	T	T-box transcription factor Brachyury alias Bra
NanogB	Nanog transcript variant B		
NanogC	Nanog transcript variant C	Tcf3	transcription factor 3
Nes	nestin	Tek	endothelial TEK tyrosine kinase alias Tie2
Ngn3	neurogenin 3 alias Neurog3	Terc	telomerase RNA component
Nkx2.2	Nk2 homeobox transcription factor 2	Tert	telomerase reverse transcriptase
Nkx6.1	Nk6 homeobox transcription factor 1	Tcfap2c	transcription factor AP-2Yc
Nodal	nodal growth differentiation factor	Tdgf1	teratocarcinoma-derived growth factor 1
Nr2f2	nuclear receptor 2F2		
NRSF	neuronal-restrictive silencer factor alias Rest	Tgfbr2	TGF beta receptor 2
Oct4	octamer binding transcription factor 4 alias POUF1	Thy1	thymus cell antigen 1 alias CD90
		Tie2	tunica internal endothelial cell kinase 2 alias Tek
Oct4A	Oct4 transcript variant A	Trdmt1	tRNA aspartic acid methyltransferase 1 alias Dnmt2
Oct4B	Oct4 transcript variant B		
Oct4B1	Oct4 transcript variant B1	Tubb3	tubulin beta 3
Oct4B-164	Oct4 isoform B-164	Twf1	twinfilin actin-binding protein 1 alias Ptk9
Oct4B-190	Oct4 isoform B-190		
p21	tumor protein p21 alias Cdkn1a	Utf1	undifferentiated embryonic cell transcription factor 1
p53	tumor protein p53		
p57	tumor protein p57	Vcam	vascular cell molecule
Pax4	paired box 4	VEcad	vascular endothelial cadherin alias Cdh5
Pax6	paired box 6		
Pdx1	pancreatic and duodenal homeobox 1	Vegfr2	vascular endothelial growth factor receptor 2 alias Flk1 or Kdr
Pecam1	platelet/endothelial cell adhesion molecule 1	vWF	von Willebrand factor
Pfn2	profilin2	Wdr61	WD repeat domain 61
Podxl	podocalyxin-like	Wnt3a	wingless-type integration site family member 3a
POUF1	POU class 5 homeobox 1 alias Oct4		
Prox1	prosepero homeobox 1	Zfp42	zinc finger protein 42 alias Rex1
Ptf1a	pancreas-specific transcription factor 1a		
Ptk9	protein tyrosine kinase 9 alias Twf1		

TABLE OF CONTENT

ACKNOWLEDGEMENTS.....	i
LIST OF FIGURES.....	i
LIST OF TABLES	ii
LIST OF APPENDICES	ii
LIST OF ABBREVIATIONS.....	iii
LIST OF GENES, TRANSCRIPTS, AND PROTEINS.....	v
TABLE OF CONTENT	vii
1. INTRODUCTION.....	1
1.1. Pluripotent Stem Cells.....	2
1.1.1. Signaling Pathways Controlling Pluripotency.....	4
1.1.1.1. Major Signaling Pathways.....	4
1.1.1.1. Minor Signaling Pathways.....	7
1.1.1.2. Epigenetic Regulation of Gene Expression	7
1.1.2. Regulation of Pluripotency by micro RNAs (miRs)	8
1.1.2.1. Biogenesis of miRs	8
1.1.2.2. ES Cell-Specific miRs Mark ES Cell Identity	9
1.1.2.3. ES Cell-Specific miRs Regulate Induction and Loss of Pluripotency	9
1.2. Induction of Pluripotency for Reprogramming.....	11
1.2.1. Reprogramming Strategies	11
1.2.1.1. Viral Reprogramming	11
1.2.1.2. Culture Conditions and Media Supplements for Reprogramming	11
1.2.1.3. Non-Viral Reprogramming	12
1.2.2. Disease-/Patient-Specific iPS Cells for the Cure of Diabetes.....	13
1.3. Pancreatic Development and Pancreatic Differentiation.....	15
1.3.1. Pancreatic Development of Mouse and Human Pancreas	15
1.3.1.1. Formation of Primary Germ Layer Progenitors.....	15
1.3.1.2. Embryonic Development of Beta Cells	16
1.3.1.3. Relationship of Endothelial Cells and Pancreatic Progenitors.....	17
1.3.2. <i>In vitro</i> Differentiation into Insulin-Producing Beta-Like Cells	19
1.3.2.1. Differentiation into Primary Germ Layer Progenitors.....	20
1.3.2.2. Differentiation Mimicking Organogenesis	21
1.4. Aims of the Study.....	22
2. MATERIAL AND METHODS.....	23
2.1. Ethical Considerations	23
2.2. Cell Culture and Growth Conditions	23
2.2.1. Culture of Somatic Cell Lines.....	23
2.2.2. Isolation and Culture of Primary Keratinocytes.....	24
2.2.3. Isolation and Culture of Primary ECs.....	25
2.2.4. Culture of Human and Mouse Pluripotent Stem Cells	26
2.3. Analysis of Gene Expression.....	27
2.3.1. Statistical Analysis	27
2.3.2. Reverse Transcription	27
2.3.3. Semi-Quantitative Polymerase Chain Reaction (PCR).....	28

2.3.4. Quantitative Real-Time PCR (qRT PCR).....	28
2.3.5. Analysis of miR Expression Levels	29
2.3.6. Cell Sorting and Flow Cytometry.....	29
2.3.7. Immunocytochemistry	30
2.3.7.1. Immunocytochemistry Using Monolayer Cultures	30
2.3.7.2. Immunocytochemistry Using Matrices	31
2.3.7.3. Western Blot (WB) Analysis.....	32
2.4. Reprogramming.....	33
2.4.1. Transfection of Episomal Vectors	33
2.4.2. Transfection of Synthetic miRs	34
2.4.3. Analysis of DNA Methylation.....	34
2.4.4. Luciferase Assay	35
2.5. Pancreatic Differentiation Models	36
2.5.1. Production of Porcine Matrices	36
2.5.2. Generation of Mouse Pancreatic Progenitors	36
2.5.3. Generation of Human Pancreatic Progenitors	38
3. RESULTS.....	39
3.1. Acquisition of Human Donor Cells - Isolation of Primary Keratinocytes.....	39
3.2. Pluripotency Genes in Keratinocytes, L87 MSCs, and BJ-5ta Fibroblasts.....	40
3.3. Analysis of Non-Viral Reprogramming Methods	40
3.3.1. Efficient and Functional Delivery of STEMcircles™ Induces Reprogramming	42
3.3.1.1. Quantification of STEMcircles™ Delivery	42
3.3.1.2. Induction of ONSL, Klf4, and c-Myc by STEMcircles™	42
3.3.1.3. Induction of Endogenous ONSL Expression by STEMcircles™	43
3.3.2. Efficient and Functional Delivery of miR-302a-d & 372 Induces Reprogramming.....	45
3.3.2.1. Validation of the miR Transfection Procedure	45
3.3.2.2. Quantification of miR Delivery by Flow Cytometry.....	46
3.3.2.3. Prediction of miR-302a-d & 372 Target mRNAs	47
3.3.2.4. Validation of miR-302a-d & 372 Target mRNAs	48
3.3.2.5. Induction of Endogenous miR-302a-d & 372 Expression	49
3.3.2.6. Induction of Oct4 and Nanog by miR-302a-d & 372	51
3.3.3. Oct4 Expression is Regulated by miR-302a-d & 372 Target mRNA Dnmt1	52
3.3.3.1. Regulation of Dnmt1 Expression by miR-302a-d & 372	52
3.3.3.2. Luciferase Assay for Validation of miR-302a-d & 372 Target mRNA Dnmt1	53
3.3.3.3. Oct4 Promoter Methylation is Regulated by miR-302a-d & 372	54
3.3.3.4. Regulation of Dnmt3a/b Expression by miR-302a-d & 372	55
3.3.4. Hypoxia Promotes Reprogramming	56
3.3.4.1. Hypoxia Promotes Induction of Reprogramming by miR-302a-d & 372	56
3.3.4.2. Hypoxia Promotes Induction of Reprogramming by STEMcircles™	57
3.3.4.3. Hypoxia Promotes Proliferation in MSCs.....	58
3.3.5. Small Molecules Promote Reprogramming	59
3.3.5.1. Epigenetic Modulators Promote Reprogramming.....	59
3.3.5.2. Signal Transduction Inhibitors Promote Reprogramming.....	62
3.3.5.3. Kinase Inhibitors Promote Reprogramming.....	63
3.3.6. Subsequent Use of Non-Viral Methods Promotes Maintenance	64
3.3.6.1. Preservation of Oct4 by co-transfection of STEMcircles™ and miR-302a-d & 372	64
3.3.6.2. Culture Conditions Without Feeder Cells are Suitable for Reprogramming	65
3.3.6.3. Repeated Transfection of STEMcircles™ Does Not Enhance Reprogramming.....	65
3.3.6.4. Subsequent use of 6 Small Molecules Promotes Maintenance of ONSL Expression....	67

3.4. 3D Biological Matrices and ECs during Human Pancreatic Differentiation	69
3.4.1. Production of 3D Biological Matrices from Porcine Jejunum	69
3.4.2. 3D Differentiation of Mouse ES Cells into Pancreatic Progenitors	69
3.4.2.1. Stem Cell Culture and Spontaneous Differentiation on 3D Matrices	69
3.4.2.2. Directed Pancreatic Differentiation without 3D Matrices.....	70
3.4.2.3. 3D Differentiation into DE Progenitors with Co-Culture Media	72
3.4.2.4. Induction of DE Progenitors without EB Formation on 3D matrices	72
3.4.3. Primary Endothelial Cells are Preserved under Co-Culture Conditions	73
3.4.4. Pancreatic Differentiation of Human iPS Cells using Co-Cultures and 3D Matrices	75
3.4.4.1. Pancreatic Differentiation of IMR90 iPS Cells	75
3.4.4.2. Co-culture with ECs regulates pancreatic differentiation	77
3.4.4.3. 3D Biological Matrices Require Co-Culture with ECs for Pancreatic Differentiation	79
4. DISCUSSION	81
4.1. Primary Keratinocytes are Adequate Donors for the Generation of iPS Cells	81
4.2. Cell Type-Specific Expression of Pluripotency Markers	82
4.2.1. Core Network Reprogramming Factors	82
4.2.2. Pluripotency-Associated Markers	84
4.3. Non-Viral Reprogramming of L87 MSCs and BJ-5ta Fibroblasts	86
4.3.1. Non-Viral Reprogramming Induced by Episomal Vectors	88
4.3.1.1. Comparison of Different Transfection Procedures.....	88
4.3.1.2. Comparison of Lipofection Techniques.....	89
4.3.1.3. Impermanent Induction of ONSL, Klf4, and c-Myc by Episomal Vectors	90
4.3.2. Non-Viral Reprogramming Induced by miR-302a-d & 372	92
4.3.2.1. Comparison with other Lipofection Techniques.....	92
4.3.2.2. Pluripotency Requires Human ES Cell-Specific miRs	93
4.3.2.3. Reprogramming Requires miR-302a-d & 372	95
4.3.2.4. Target Genes of miR-302a-d & 372	95
4.3.2.5. Induction of Endogenous miR-302a-d & 372 by Autoregulation.....	98
4.3.2.6. Indirect Regulation of Oct4, Nanog, and Thy1.....	99
4.3.3. Dnmt1 Repression by miR-302a-d & 372 Regulates Oct4 Induction.....	100
4.3.3.1. Dnmt1 Regulation by miR-302a-d & 372	100
4.3.3.2. Oct4 Promoter Methylation is Regulated by Dnmt1.....	103
4.3.3.3. Dnmt3a and Dnmt3b are Not Essential for Oct4 Promoter Methylation	105
4.3.4. Hypoxia Facilitates Non-Viral Reprogramming	107
4.3.4.1. Hypoxia-Induced Oct4A and Nanog expression.....	108
4.3.4.2. Hypoxia Improves Induction of Oct4A and Nanog by miR-302a-a & 372.....	108
4.3.4.3. ES cell-Specific Conditions Improve Oct4A Induction by miR-302a-a & 372	109
4.3.4.4. Hypoxia Improves Induction of ONSL by STEMcircles TM	109
4.3.4.5. Hypoxia is Capable to Enhance Proliferation	110
4.3.5. Small Molecules Facilitate Non-Viral Reprogramming.....	111
4.3.5.1. Epigenetic Modulators Enhance Colony Formation.....	112
4.3.5.2. Signal Transduction Inhibitors Enhance Colony Formation.....	114
4.3.5.3. Kinase Inhibitors Enhance Colony Formation.....	115
4.3.5.4. STEMcircles TM and Small Molecules Preserve Colonies.....	116
4.3.5.5. Affords to overcome partial reprogramming	118
4.4. Pancreatic Differentiation of iPS Cells	119
4.4.1. Pancreatic Differentiation on 3D Matrices.....	120
4.4.1.1. Advantages of 3D Biological Matrices	120
4.4.1.2. 3D Matrices Allow Pancreatic Differentiation.....	121

TABLE OF CONTENT

4.4.1.3. <i>3D Matrices Promote DE Differentiation</i>	124
4.4.2. Pancreatic Differentiation of Human iPS Cells.....	125
4.4.2.1. <i>Differentiation of Pancreatic Endocrine Progenitors</i>	125
4.4.2.2. <i>Heterogeneity of the Pancreatic Endocrine Progenitors</i>	127
4.4.3. Co-Culture with ECs during Pancreatic Differentiation	129
4.4.3.1. <i>Primary ECs for Co-Cultures</i>	129
4.4.3.2. <i>Differentiation of Pancreatic Progenitors is Affected by Co-Culture with ECs</i>	130
4.4.4. Organotypic Pancreatic Differentiation of Human iPS Cells	131
4.4.4.1. <i>Organotypic Differentiation in 3D Biological Matrices with ECs</i>	131
4.4.4.2. <i>Pancreatic Differentiation is Affected by ECs in 3D Biological Matrices</i>	132
5. SUMMARY	134
6. ZUSAMMENFASSUNG	136
7. REFERENCES	138
8. APPENDICES	156
<i>CURRICULUM VITAE</i>	177
EIDESSTATTLICHE ERKLÄRUNG	180

1. INTRODUCTION

The energy homeostasis of the human body can be disrupted by impaired functionality of beta cells, which secrete insulin to regulate glucose levels in blood and the interstitial fluid. Beta cells reside in the pancreas, but loss of beta cells or functional defects result in impaired glucose homeostasis, which is well known as diabetes mellitus and affects many organs. There are different types of diabetes mellitus. Type 1 diabetes mellitus (T1DM) is caused by a destructive autoimmune process and one of most common diseases in childhood (Wild et al., 2004). Type 2 diabetes mellitus (T2DM) results from deficient beta cell function and subsequent loss of beta cells. T2DM has reached epidemic proportions. Worldwide, about 285 million people were estimated to suffer from diabetes in 2010 (Unwin et al., 2010) and more than 90% are patients with T2DM (Stumvoll et al., 2005). The prevalence of all types of diabetes is increasing worldwide and the total number of diabetes patients is proposed to reach up to 438 million in 2030 (Unwin et al., 2010).

Insulin is used to treat diabetes mellitus, but insulin therapy does not prevent long-term complications, notably cardiovascular disease and damage to the microvasculature and nerves, associated with elevated blood glucose levels (Tripathi and Srivastava, 2006; Coccheri, 2007). In 1923, the Nobel Committee awarded Sir Frederick Banting and John Macleod the Nobel Prize in Physiology or Medicine “for the discovery of insulin”. Sir Frederick Banting emphasized in his Nobel lecture in 1925 that „insulin is not a cure for diabetes; it is a treatment”, which remains true to this date (Roth et al., 2012). Treatment strategies need optimizing to prevent long-term complications. Cell replacement therapies are proposed to be a cure for patients, but there is no renewable source of glucose-responsive, insulin-secreting cells available for clinical application.

In 2012, the Nobel Committee awarded Shinya Yamanaka and Sir John Gurdon the Nobel Prize in Physiology or Medicine “for the discovery that mature cells can be reprogrammed to become pluripotent”. Shinya Yamanaka generated induced pluripotent stem (iPS) cells from somatic cells. This technique also allows generating disease-specific iPS cells, which offer the promising opportunity to study disease-specific development of beta cells *in vitro*. Such disease-specific models could be useful for drug testing (Gunaseeli et al., 2010). Moreover, iPS cells provide the possibility to derive patient-specific autologous beta cells for the cure of diabetes. Just like embryonic stem (ES) cells, iPS cells can be used for the differentiation into beta-like cells (D'Amour et al., 2006; Kroon et al., 2008; Zhang et al., 2009; Borowiak, 2010). However, cell cultures are exposed to a set of factors or conditions culminating in development of the desired cell type as a minor subset in a mixed population of cells (McKnight et al., 2010). Attempts failed to generate clinical relevant levels of insulin-producing cells (Matveyenko et al., 2010; Mfopou et al., 2010a).

The following introducing chapters will summarize the current knowledge on pluripotent stem cells and the iPS technology to explain the need for the establishment of non-viral reprogramming strategies. Further, the current state of knowledge on pancreatic differentiation will be reviewed to support the need for the establishment of organotypic 3D pancreatic differentiation models.

1.1. Pluripotent Stem Cells

Human development starts with the totipotent zygote, which forms the organism through hierarchical specification and determination of cell identities and their functional differentiation (Wobus and Boheler, 2005). The differentiation potential subsequently decreases during differentiation (FIG. 1). Blastomers at the morula stage lose the ability to form the organism. At the blastocyst stage, pluripotent cells from the inner cell mass (ICM) are capable to differentiate into about 200 cell types of the human body (Boyer et al., 2005). In parallel, oligopotent hypoblast cells become restricted to produce extraembryonic tissues. After implantation into the uterine wall, pluripotent cells form multipotent progenitors of the embryonic germ layers ectoderm, mesoderm and endoderm. A small population of pluripotent cells is restricted to become unipotent precursors of the gametes. During embryonic development, multipotent stem cells differentiate into several progenitors, which finally give rise to differentiated cells of specialized tissues (Wobus and Boheler, 2005).

ES cells from mouse blastocysts were first established in 1981 (Evans and Kaufman, 1981). These cells are capable to replicate indefinitely and to differentiate into any cell type of the mouse body (Wobus and Boheler, 2005). Accordingly, ES cells are suitable to mimic *in vivo* development by *in vitro* differentiation (FIG. 1).

Currently, several mouse ES cell lines are available. CGR8 mouse ES cells, obtained from day 3.5 male pre-implantation mouse embryos (Mountford et al., 1994), are applied for the generation of many cell types such as beta-like cells or cardiomyocytes (Lima et al., 2012; Ou et al., 2013). Genetic modification of mouse ES cells broadens the field of differentiation models. For instance, CGR8-S17 cells were applied to analyze Sox17 expression during *in vitro* differentiation into endoderm progenitors (Schroeder et al., 2012). Just like wild type CGR8 cells, CGR8-S17 grow as small and tightly packed colonies on gelatin-coated dishes (FIG. 2 A).

Human ES cells were first isolated in 1998 at the University of Wisconsin-Madison, United States of

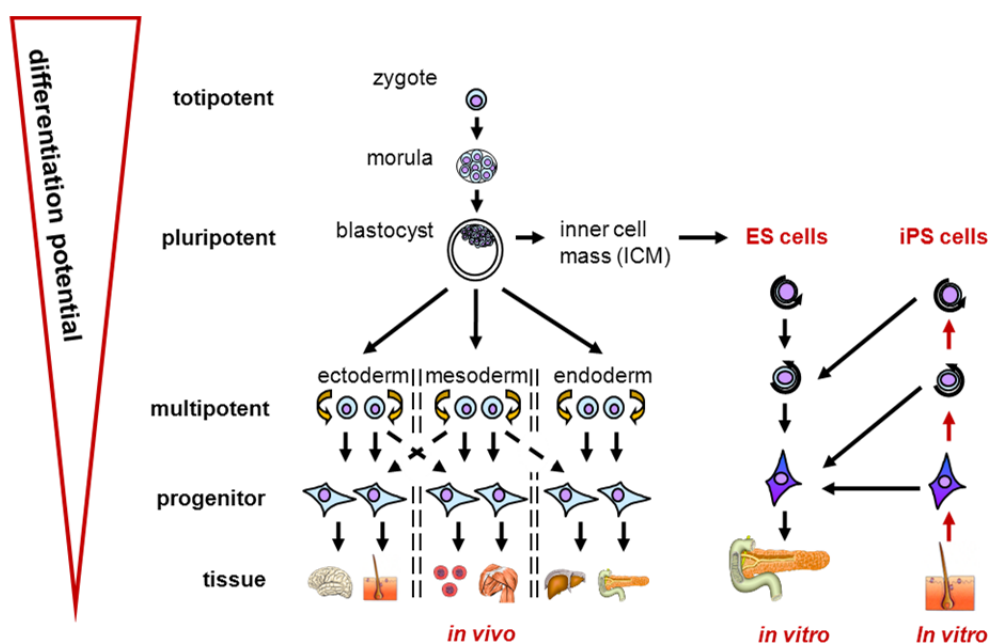


FIGURE 1: Potency of stem cells and progenitors during embryogenesis and reprogramming. The potential of stem cells and progenitors *in vivo* is illustrated. Differentiation of human ES cells and the induction of pluripotency in somatic cells is described *in vitro* (Wobus and Boheler, 2005; modified).

America (USA) (Thomson et al., 1998). Thomson and co-workers established 5 cell lines (including H9) from 5 d pre-implantation embryos that have been donated by patients undergoing *in vitro* fertilization. Human ES cells were characterized by a variety of differentiation models and teratoma assays (Gropp et al., 2012). Pluripotency of human ES cells is comparable to mouse ES cells, which could also be analyzed using chimerism and germ line transmission (Nagy et al., 1993). Like mouse ES cells, human ES cells are a well-established source of stem cells, which are applied in several *in vitro* differentiation models (**FIG. 1**). These differentiation models allow the analysis of organotypic and defective development of cells, tissues and organs (Schroeder et al., 2012). Importantly, beta-like cells can be obtained from *in vitro* differentiation of human ES cells (D'Amour et al., 2006; Kroon et al., 2008; Zhang et al., 2009; Borowiak, 2010).

Gene expression profile and the growth conditions of human ES cells differ from that of mouse ES cells (Mountford et al., 1994; Thomson et al., 1998; Hoffman and Carpenter, 2005). The differences are less likely to be species differences rather than a difference in the developmental stage. The same signaling pathways regulate early cell fate decisions in human and mouse ES cells (Vallier et al., 2009b). Importantly, H9 human ES cells do require fresh feeder cells weekly, because they are not able to grow on gelatin (**FIG. 2 B**). Feeder cells for human ES and iPS cell culture are predominantly primary mouse embryonic fibroblasts (MEFs) obtained from E13.5 CF1 mouse embryos (**FIG. 2 C**).

The discovery of human ES cells enables the generation of adequate cell material for cell replacement therapies (Thomson et al., 1998). In 2010, the Food and Drug Administration (FDA) of USA approved 2 clinical trials, which were applied human ES cell derivatives for replacement therapies. Oligodendrocyte progenitors were used to treat spinal cord injury (ClinicalTrials.gov identifier: NCT01217008) and retinal pigment epithelial cells were applied to treat dry age-related macular degeneration (ClinicalTrials.gov identifier: NCT01344993) (Schwartz et al., 2012; Grabel, 2012; Grabel, 2012). The trial analyzing spinal cord injury was discontinued in 2011. No official results have been published, but another company acquired the assets of the clinical trial in 2013. The trial analyzing macular degeneration expects to enroll 16 subjects by July 2014.

The generation of ES cells requires the destruction of fertilized eggs and therefore is ethically disputed (Lo and Parham, 2009). In Germany, the Embryo Protection Act (ESchG) and the Stem Cell Act (StZG) prohibit the generation of human ES cells (Kress, 2008). There is the possibility to import

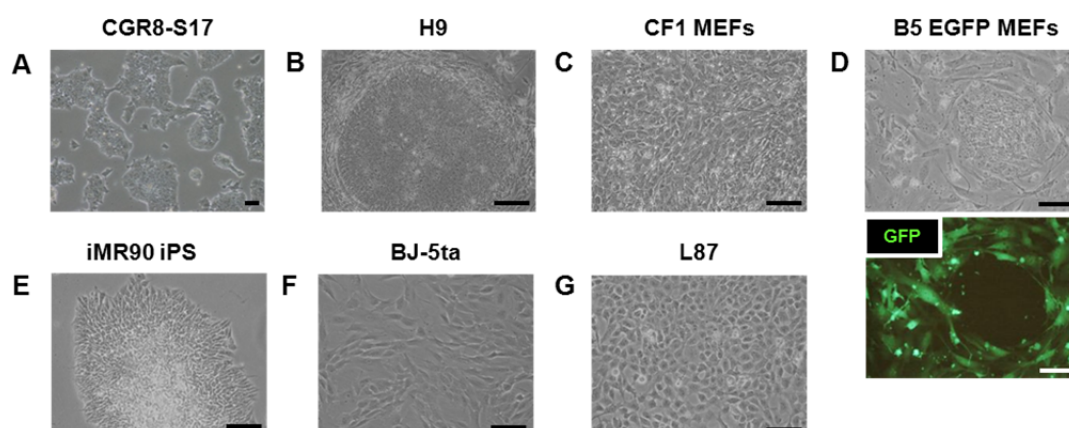


FIGURE 2: Cells for the analysis of induction and maintenance of pluripotency. Morphology of (A) murine CGR8-S17 ES cells, (B) human H9 ES cells on CF1 MEFs, (C) CF1 MEFs, (D) IMR90 iPS on B5 EGFP MEFs, (E) IMR90 iPS cells on Matrigel™, (F) BJ-5ta fibroblasts, and (G) L87 MSCs. Bars represent 100 μ m.

particular ES cell lines such as H9, which were generated prior to a cutoff date (May 1st, 2007).

In 2006, the group of Shinya Yamanaka generated a completely new source of pluripotent stem cells, the so-called induced pluripotent stem cells (iPS cells). In contrast to human ES cells, human iPS cells do not require the destruction of human blastocysts. The forced expression of POU class 5 homeobox 1 (POU5F1; also known as Oct4), SRY-related HMG-box (Sox) family transcription factor 2 (Sox2), kruppel-like factor 4 (Klf4), and v-myc myelocytomatosis viral oncogene homolog (c-Myc) (OSKM, Yamanaka factors) is sufficient to reprogram mouse fibroblasts into ES cell-like cells (Takahashi and Yamanaka, 2006). Human iPS cells were first generated in 2007 by the same group using an identical set of transcription factors (Takahashi et al., 2007). In parallel, the group of James Thomson successfully applied, Oct4, Sox2, nanog homeobox (Nanog) and cell lineage abnormal protein 28 homolog to *Caenorhabditis elegans* A (Lin28) (ONSL, Thomson factors) for the production of human iPS cells (Yu et al., 2007). Human iPS cells and human ES cells share almost all characteristics of pluripotent cells (**FIG. 1**). However, gene expression profiles of different iPS cell lines are very similar but not identical to human ES cell lines (Polouliakh, 2013). Differently expressed genes are retained from the somatic donor cell or induced during reprogramming (Muller, 2010). Importantly, iPS cells also require human ES cell-specific culture conditions including co-culture with MEFs (**FIG. 2 D**) or culture on Matrigel™ (**FIG. 2 E**). Many laboratories have successfully generated iPS cells from different cell types using different innovative methods (Mostoslavsky, 2012; Robinton and Daley, 2012). In the present study and in many other laboratories, fully differentiated fibroblasts (**FIG. 2 F**) and adult stem cells (**FIG. 2 G**) are used as donors for reprogramming. The choice of different cell types combined with the diversity of reprogramming procedures leads to different reprogramming efficiencies and varying iPS cell qualities.

1.1.1. Signaling Pathways Controlling Pluripotency

Several signaling pathways regulate induction, maintenance, and loss of pluripotency in human ES cells. Therefore, these signaling pathways are crucial for the generation of iPS cells as well. Pluripotency-associated genes, including OSKM, Nanog, and Lin28, regulate and are regulated by a few major signaling pathways namely FGF2/RTK, LIF/JAK-STAT, WNT/beta-catenin, TGFβ/activin A/nodal, BMP, and p53 (Walia et al., 2012; Pera and Tam, 2010). Further, there are several minor pathways, which regulate pluripotency including the Rho-associated protein kinase (ROCK) and Voltage gated Ca²⁺ channels. Likewise, pluripotency is regulated by epigenetics. On the one hand, OSKM, Nanog, and Lin28 are regulated by deoxyribonucleic acid (DNA) methylation and epigenetic modification of histones, on the other hand, pluripotency-associated genes themselves regulate the epigenetic status of the chromatin.

1.1.1.1. Major Signaling Pathways

Human ES cells need FGF2/RTK, which is one major signaling pathway for the preservation of pluripotency (**FIG. 3**). Interestingly, human ES cells produce fibroblast growth factor 2 (FGF2) and express the receptor for FGF2 as well. The FGF receptor is a receptor tyrosine kinase (RTK). FGF2 stimulates a signaling cascade through the MAPK/ERK kinase (MEK) and extracellular signal-regulated kinases (ERKs). FGF2/RTK signaling mediated by ERK1 and ERK2 (alias MAPK3 and MAPK1) induce the gene expression of pluripotency markers (Dvorak et al., 2005; Li et al., 2007a). However, MEK signaling is the most frequently disrupted pathway in human cancers

(Tommasi et al., 2012). MEK-mediated RTK signaling acts in a cooperative manner with FGF2-induced PI3K-AKT signaling (**FIG. 3**) supporting maintenance of pluripotency (Li et al., 2007b). Phosphatidylinositol-4,5-bisphosphate 3-kinase (PI3K) activates v-akt murine thymoma viral oncogene (AKT) and mitogen-activated protein kinase (MAPK). Importantly, RTK signaling mediated by insulin-like growth factors (IGFs) and platelet-derived growth factors (PDGFs) instead of FGF2 is also suitable for the maintenance of human ES cells. Detailed analysis of RTK signaling target genes is still required, because the FGF2/RTK signaling pathway is crucial for self-renewal (Pera and Tam, 2010).

Mouse ES cells do not require FGF2/RTK signaling for the maintenance of pluripotency, they require LIF/JAK-STAT signaling instead. Leukemia inhibitory factor (LIF) induces JAK-STAT signaling to stimulate subsequent activation of Klf4, Sox2, and octamer binding transcription factor 4 (Oct4) (Niwa et al., 2009). The JAK-STAT signaling pathway consists of cytokine receptors, Janus kinases (JAKs), and dimers of signal transducer and activator of transcription (STAT), which activate transcription of their target genes. In parallel, LIF activates PI3K-AKT signaling to induce Nanog expression (Niwa et al., 2009). In contrast to the human system, the FGF2/RTK signaling pathway induces differentiation of mouse ES cells (Burdon et al., 1999). MEK inhibition by PD0325901 (PD) (**FIG. 3**), accompanied by inhibition of glycogen synthase kinase 3 (GSK3), allows maintenance of mouse ES cells without LIF (Ying et al., 2008).

The WNT/beta-catenin signaling pathway is required for embryonic development and stem cell

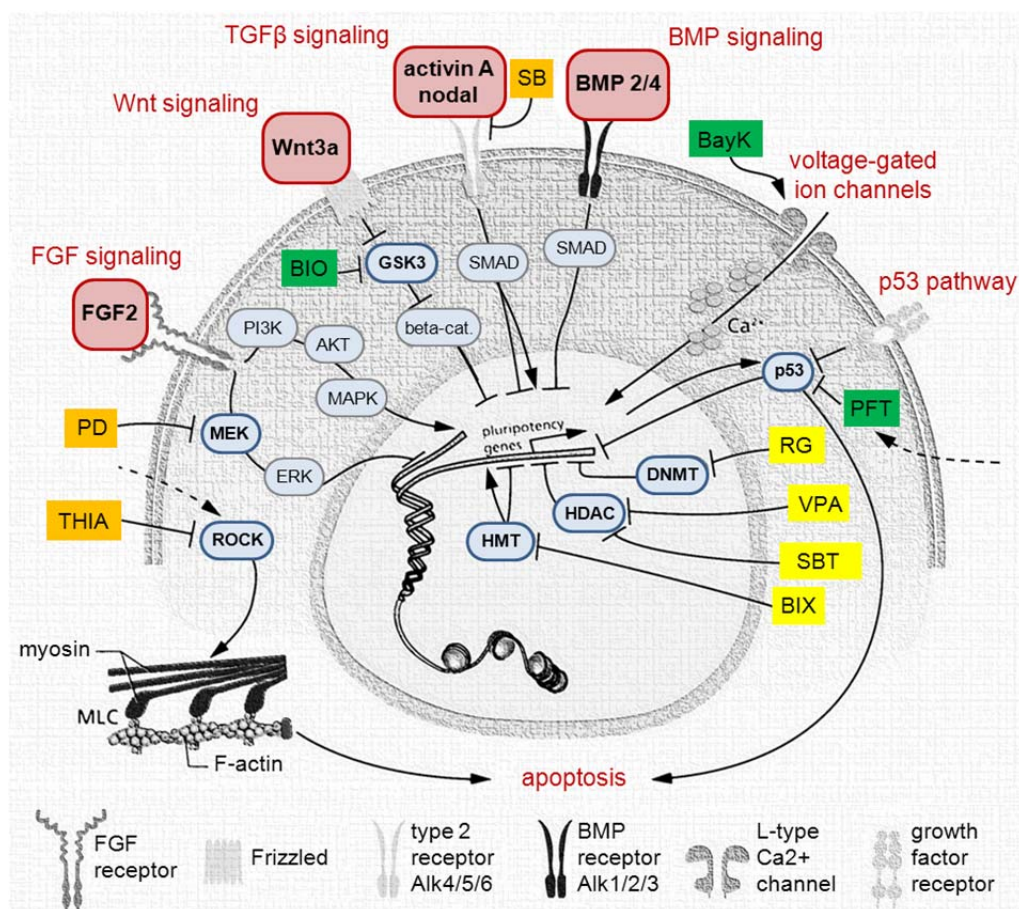


FIGURE 3: Signaling pathways for induction and maintenance of pluripotency. Signaling pathways and their impact on pluripotency genes in human pluripotent stem cells is denoted. Interaction of small molecules is indicated. The epigenetic modulators RG108 (RG), valproic acid (VPA), sodium butyrate (SBT), and BIX01294 (BIX) are indicated in yellow. Signal transduction inhibitors pifithrin alpha (PFT), BayK8644 (BayK), and BIO are shown green. Kinase inhibitors thiazovivin (THIA), SB431542 (SB), and PD032901 (PD) are indicated in orange.

maintenance as well. Wingless-type integration site family member 3a (Wnt3a) binds to the Frizzled receptor activating wingless-related integration site (WNT) signaling to down-regulate GSK3 (**FIG. 3**). GSK3 downregulation is needed to shuttle cytoplasmic beta catenin into the nucleus (Li et al., 2009). Beta catenin activates the expression of genes predominantly involved in differentiation. However, additional mechanisms are involved in the induction and maintenance of pluripotency. WNT signaling inhibits transcription factor 3 (Tcf3) in mouse ES cells, which responsible for Oct4 inhibition (Yi et al., 2011). Inhibiting differentiation, Oct4 hinders WNT signaling by binding to beta-catenin, which facilitates degradation of beta-catenin leading to the maintenance of mouse ES cells (Abu-Remaileh et al., 2010). The treatment with Wnt3a supports colony formation and survival of mouse iPS cells (Marson et al., 2008a). The repression of GSK3 by 6-bromo-indirubin-3'-oxime (BIO) mimics activation of the WNT signaling pathway (**FIG. 3**) promoting the generation of mouse and human iPS cells (Sato et al., 2004). Furthermore, inhibition of GSK3 can replace Sox2 during viral reprogramming of mouse fibroblasts using Oct4 and Klf4 (Li et al., 2009), but the mechanism is not clearly understood.

The balance between TGF β /activin A/nodal and BMP signaling pathways has a major impact on early cell fate decisions during differentiation of human ES cells (Vallier et al., 2009b). Bone morphogenetic proteins (BMPs) and other members of the transforming growth factor β (TGF β) superfamily such as activin A and nodal activate different sets of SMAD transcription factors, which in turn control the expression of other genes (**FIG. 3**). Activin A and nodal are also involved in maintenance of human ES cells (James et al., 2005). Both share ALK4, which is a type I TGF β receptor alias activin receptor-like kinase (ALK). Importantly, both growth factors are needed for Nanog gene expression in human ES cells (Vallier et al., 2009a). Activin A also supports feeder-free culture of human ES cells (Beattie et al., 2005). The ligand TGF β binds to the type I TGF β receptor ALK5. Interestingly, inhibition of ALK5 by SB431542 (SB) (**FIG. 3**) induces a rapid loss of Nanog expression and loss pluripotency (Chambers et al., 2009). SB blocks phosphorylation of ALK5 whereas ALK4 and ALK7 are inhibited less efficiently (Inman et al., 2002).

BMPs are also part of the TGF β superfamily, but BMPs bind to the type I receptors ALK1, ALK2, and ALK3 (**FIG. 3**) for maintenance of mouse, but not human ES cells (Ying et al., 2003; Xu et al., 2002). In human ES cells, Nanog blocks SMAD family member 1 (Smad1) activity to prevent signaling of BMPs towards trophoblast differentiation (Suzuki et al., 2006). SMAD are signaling-transducing proteins homologous to the *Caenorhabditis* protein SMA and the *Drosophila* protein MAD. Interestingly, another ligand of the TGF β superfamily growth differentiation factor 3 (Gdf3) inhibits BMP signaling in both murine and human ES cells (Levine and Brivanlou, 2006).

The signaling pathway of the tumor protein p53 (p53) restricts efficiency of reprogramming by the induction of cell cycle arrest or cell death in order to avoid formation of cancer cells (Oren, 2003). Accordingly, p53 is a tumor suppressor gene and a negative regulator of reprogramming (**FIG. 3**). During iPS cell generation, the forced expression of the oncogene c-Myc activates p53 signaling. The p53 dependent inhibition of iPS cell generation is mediated by tumor protein p21 (p21; alias Cdkn1a) leading to sustained cell cycle arrest in G1 phase (Hong et al., 2009) and the activation of Bcl2-binding component 3 (Bbc3; also known as Puma) inducing apoptosis (Li et al., 2013). Pifithrin alpha (**FIG. 3**) is a potent and well-established p53 inhibitor (Kawamura et al., 2009). However, repression of p53 signaling inhibits self-renewal of human ES cells (Abdelalim and Tooyama, 2012) demonstrating that p53 repression is crucial for reprogramming rather than for maintenance of pluripotency.

1.1.1.1. Minor Signaling Pathways

Even though minor signaling pathways do not appear to have a great impact on pluripotency, their modulation nonetheless results in the efficient generation of high quality iPS cells.

The ROCK signaling pathway regulates components of the cytoskeleton. During apoptosis, ROCK mediates cell contraction, membrane degradation, and nuclear disintegration (Coleman and Olson, 2002). In enzymatically passaged human ES and iPS cells, ROCK is responsible for cell cycle arrest and apoptosis (**FIG. 3**). Inhibition of ROCK by thiazovivin (THIA) promotes cell survival (Lin et al., 2009). ROCK inhibition by other molecules such as Y-27632 or HA-1077 generates similar effects. THIA directly targets ROCK and preserves human ES cells by regulating E-cadherin (Xu et al., 2010). However, ROCK inhibition leads to adverse effects on morphology and pluripotency genes in human ES cells, but these effects are in part reversible when cells are passaged mechanically again (Holm et al., 2013). Importantly, treatment with MEK inhibitor PD or ALK5 inhibitor SB alone affects pluripotency of human ES cells, but combined treatment with THIA drastically increased generation of iPS cells (Lin et al., 2009; Gross et al., 2013). Therefore, ROCK inhibition is important for reprogramming, but optimal treatment duration with ROCK inhibitors remains to be clarified.

Another minor signaling pathway includes voltage gated ion channels (**FIG. 3**). L-type Ca²⁺-channels can be activated by BayK8644 (BayK) leading to PI3K signaling and activation of cytosolic calcium (Chien et al., 1996). PI3K signaling is also stimulated by FGF2 in human ES cells (Li et al., 2007a) suggesting common downstream target genes. Interestingly, inhibition of L-type Ca²⁺-channels affects differentiation of ES cells (Nguemo et al., 2013). However, the mechanisms involved in regulation of pluripotency are currently not well understood. Importantly, reprogramming was achieved by Oct4 and Klf4 in the presence of BayK (Shi et al., 2008).

1.1.1.2. Epigenetic Regulation of Gene Expression

The epigenetic modification of DNA and histones changes dynamically during embryonic development, which broadly regulates genes across the whole genome. In ES cells, pluripotency gene expression is regulated by DNA methylation and histone modification as well (Altun et al., 2010). Accordingly, the understanding of epigenetic gene regulation is crucial for the understanding of reprogramming processes.

DNA methylation patterns are established during early embryonic development. Genome-wide methylation levels rapidly increase in the ICM of the blastocyst and methylation patterns established around this developmental period are found in the adult. Accordingly, increasing DNA methylation down-regulates pluripotency gene expression (**FIG. 3**). DNA methyltransferases (DNMTs) establish and maintain the cell-specific epigenetic DNA status. In human cells, DNA methyltransferase 1 (Dnmt1), Dnmt3a, and Dnmt3b, but not Dnmt2 (also known as Trdmt1) are responsible for DNA methylation. Dnmt1 predominantly controls maintenance of DNA methylation during cell division (Choi et al., 2011). In contrast, Dnmt3a and Dnmt3b are essential for the *de novo* DNA methylation during embryogenesis (Choi et al., 2011). DNA methylation occurs at CpGs, which are often clustered in so-called CpG islands. About 60% of human gene promoters contain CpG islands (Bird, 2002). They reside predominantly within the 5' region of genes, contain at least 200 nt with a G+C content of at least 50%, and exhibit CpG frequency of at least 60% (Bernstein et al., 2007). Interestingly, non-CpG methylation is observed in human ES cells and the early embryo, but with very low frequency and unclear biological function (Ramsahoye et al., 2000). Importantly, DNA methylation inhibitor RG108

(RG) enables iPS cell generation from mouse fibroblasts (**FIG. 3**) in the presence of the small molecule BIX01294 (BIX) and viral induced Oct4 and Klf4 (Stresemann et al., 2006; Shi et al., 2008).

DNA is tightly packed and coupled with octamers of 4 histones (H3, H4, H2A, H2B). These nucleosomes contain 147 base pairs. Interestingly, H3 and H4 modifications are more frequent in comparison to H2A and H2B. Histone modifications ensure open or closed chromatin. There are about 100 epigenetic histone modifications, which occur at specific sites within the histone proteins (Kouzarides, 2007). The vast majority of posttranslational modifications are caused by methylation, acetylation, phosphorylation, and ubiquitination, but the biological function of these modifications is often poorly understood. However, histone methylation and acetylation are thought to be powerful regulators of pluripotency gene expression. Histone methyltransferases (HMTs) add tri-methylation to lysines to open and close chromatin as well (**FIG. 3**). For example, methylation of H3 lysine 4 or 36 (H3K4me3, H3K36me3) is associated with transcribed chromatin (Bernstein et al., 2007). In contrast, methylation of H3 lysine 9 or 27 (H3K9me3, H3K27me3) and H4 lysine 20 (H4K20me3) is correlated with closed chromatin (Bernstein et al., 2007). The HMT inhibitor BIX (**FIG. 3**) enables iPS cell generation from mouse fibroblasts in the presence of the small molecule BayK and viral induced Oct4 and Klf4 (Kubicek et al., 2007; Shi et al., 2008).

Acetylation usually is associated with transcribed chromatin. Importantly, deacetylation mediated by 18 mammalian histone deacetylase (HDAC) genes broadly represses open chromatin during embryogenesis (Kretsovali et al., 2012). Pluripotency genes are downregulated in the absence of histone acetylation. Therefore, inhibition of HDACs is suitable to promote reprogramming (**FIG. 3**). The HDAC inhibitor sodium butyrate (SBT) when combined with TGF- β signaling inhibitor SB improves Sendai virus vector-mediated iPS cell generation (Trokovic et al., 2012). Additionally, viral reprogramming is more efficient in the presence of the HDAC inhibitor valproic acid (VPA) (Huangfu et al., 2008). HDAC inhibition acts through histone lysine 9 acetylation (H3K9ac) to enhance the activity of target genes involved in extracellular matrix (ECM) production supporting pluripotency (Hezroni et al., 2011).

1.1.2.Regulation of Pluripotency by micro RNAs (miRs)

The human genome encodes at least 800 miRs (Bentwich et al., 2005), which regulate approximately 30-60% of the human genome via multiple biological pathways (Friedman et al., 2009; Yang and Lai, 2011). Accordingly, miRs are a potent tool for the manipulation of the transcriptome towards a pluripotent state.

Small non-coding miRs (~22 nt) are abundant and capable of impairing or preventing translation by binding to hundreds of messenger ribonucleic acid (mRNA) molecules (Treiber et al., 2012). Accordingly, miRs are thought to regulate numerous signaling pathways including the epigenome. For example, miRs are strongly induced in the blastocyst, which is crucial for regulating the epigenome during embryonic growth (Ohnishi et al., 2010; Grandjean et al., 2009).

1.1.2.1.Biogenesis of miRs

The biogenesis of miR has been comprehensively reviewed elsewhere (Jung and Schroeder, 2013) and therefore the biogenesis is briefly described in this paragraph. Mature miRs are derived from long single-stranded primary miRs (pri-miRs). These originate from miR genes, intronic sequences of protein-coding ribonucleic acids (RNAs), intronic or exonic regions of non-coding RNAs

or intergenic regions. Similar to protein-coding genes, miR expression can be regulated (Ozsolak et al., 2008; Lee and Dutta, 2009). The precursor pri-miR is 3'poly-adenylated and carries a 5' cap (Lee et al., 2004). The pri-miR transcript is cleaved by the ribonuclease III enzyme Drosha to generate 70-80 nt long precursor-miRs (pre-miRs), which are transported to the cytoplasm (Katahira and Yoneda, 2011). Cleavage by Drosha requires the co-factor DiGeorge critical region 8 (Dgcr8), but many other proteins regulate pri-miR processing.

In the cytoplasm, pre-miRs are cleaved by the ribonuclease III-like enzyme Dicer (Koscianska et al., 2011). Cleavage generates 19-22 nt ds miRs, which contain the mature miR (leading strand) and the star miR (passenger strand, miR*). Upon maturation, the mature miR is loaded into the miR-induced silencing complex (RISC). In humans, recruitment of Argonaute RISC catalytic component 2 (Ago2) is necessary for mRNA cleavage (Hock and Meister, 2008). While attached to the RISC complex, miRs bind to the target mRNAs. The seed region of miRs (5' nucleotide 2-7), binds to the seed complementary region (SCR) within the 3' untranslated region (UTR) of mRNAs. Subsequently, miRs induce inhibition of translation or mRNA degradation (Fabian et al., 2010).

1.1.2.2. ES Cell-Specific miRs Mark ES Cell Identity

Importantly, mouse and human ES cells have a distinct miR expression profile, which is specific to pluripotency. Accordingly, a major miR impact on reprogramming is most likely.

ES cell-associated miRs are involved in a variety of signaling pathways to control the state of pluripotency and their proper differentiation (**FIG. 4**). Analyses of miRs in human ES cells revealed that the majority of them is specific to human ES cells and not present in adult tissues and cell lines (Suh et al., 2004). Interestingly, miRs expressed in ES cells do share the same or a similar seed sequence, which suggests a common set of target genes. In contrast, only a small set of miRs in tissues and cell lines is associated with a distinct cell type (Lagos-Quintana et al., 2003). However, mouse and human ES cells do have a different expression profile of miRs (Suh et al., 2004; Goff et al., 2009). This contributes to the different signaling pathways involved maintenance of pluripotency rather than to evolutionary differences. There are more similarities between the miR expression profiles of human ES cells and mouse epiblast stem cells, which contributing to the idea that human ES cells in general are more similar to mouse epiblast stem cells (Stadler et al., 2010; Jouneau et al., 2012).

Human ES cells abundantly express 14 miRs (**FIG. 4**) in a human ES cell-specific manner of which 11 miRs are processed from 2 primary transcripts the miR-371-373 and miR-302a-367 cluster, respectively (Suh et al., 2004). The miR-371-373 cluster is the human homologue to the mouse ES cell-specific miR-290-295 cluster. Human ES cell-specific miR-200c, miR-368, and miR-154* are transcribed from different clusters.

1.1.2.3. ES Cell-Specific miRs Regulate Induction and Loss of Pluripotency

In ES cells, miRs negatively (directly) and positively (indirectly) regulate many target genes to preserve pluripotency (**FIG. 4**). One mechanism of ES cell-associated miR action is to directly down-regulate or prevent expression of genes, which are responsible for the loss of pluripotency. Accordingly, pluripotency genes are indirectly up-regulated. ES cell-associated miRs interfere with signaling pathways such as DNA methylation or induction of epithelial to mesenchymal transition (EMT). EMT is necessary for several stages of the early development such as gastrulation and miR-200c-429 is involved in prevention of EMT in mouse ES cells (Gill et al., 2011). DNA methylation

by Dnmt1 is thought to broadly repress the expression of pluripotency genes during early differentiation of human ES cells. The miR-302a-367 cluster targets lysine (K)-specific demethylase 1a (Kdm1a; also known as Aof2), which is responsible for proper Dnmt1 function (Lin et al., 2011). Further, the miR-302a-367 cluster inhibits nuclear receptor 2F2 (Nr2f2), which is responsible for the induction of neuronal ectoderm (Rosa and Brivanlou, 2011).

Pluripotency-associated transcription factors in turn induce or repress the expression of several miRs. In ES cells, Oct4, Nanog, and Sox2 predominantly bind to miR promoters, which are abundantly expressed in ES cells including the miR-302a-267 cluster (Marson et al., 2008b; Barroso-delJesus et al., 2008; Card et al., 2008). Another crucial pluripotency factor Lin28 inhibits the pri-miR structure and pre-miR processing of let-7 (**FIG. 4**), which is strongly associated with early differentiation (Piskounova et al., 2011; Mayr et al., 2012).

Interestingly, there are miRs, which target mRNAs of pluripotency genes. For example, ribosomal proteins (RBPs) also regulate c-Myc expression. RBP L11 binds to the c-Myc mRNA and recruits a miR-24-loaded RISC (Challagundla et al., 2011). Subsequently, c-Myc translation is inhibited by miR-24 implicating that miR-24 counteracts reprogramming (**FIG. 4**).

Differentiation of pluripotent cells is influenced by miRs, which are not abundantly expressed in human ES cells. There are sets of miRs, which are related to ectoderm, mesoderm, and endoderm (**FIG. 4**) (Berardi et al., 2012). For example, myocardial precursors arise from mesoderm progenitors. The differentiation into cardiomyocytes depends on miRs such as miR-1 or miR-125b, which target the Lin28 mRNA (Glass and Singla, 2011; Wong et al., 2012). Neurogenesis from ectoderm progenitors is regulated by miRs such as miR-124 and miR-128 (Smirnova et al., 2005; Krichevsky et al., 2006). However, miR-124a is also involved in beta cell development (Joglekar et al., 2011). Adipocytes differentiate from mesodermal precursors regulated by several miRs including miR-140 and miR-375 (Ling et al., 2011; Liu et al., 2013), but miR-375 is also involved in the beta cell relevant development (Joglekar et al., 2011). Together, it is currently it is not clear whether miRs have a tissue-related or tissue-specific impact on the differentiation of ES cells.

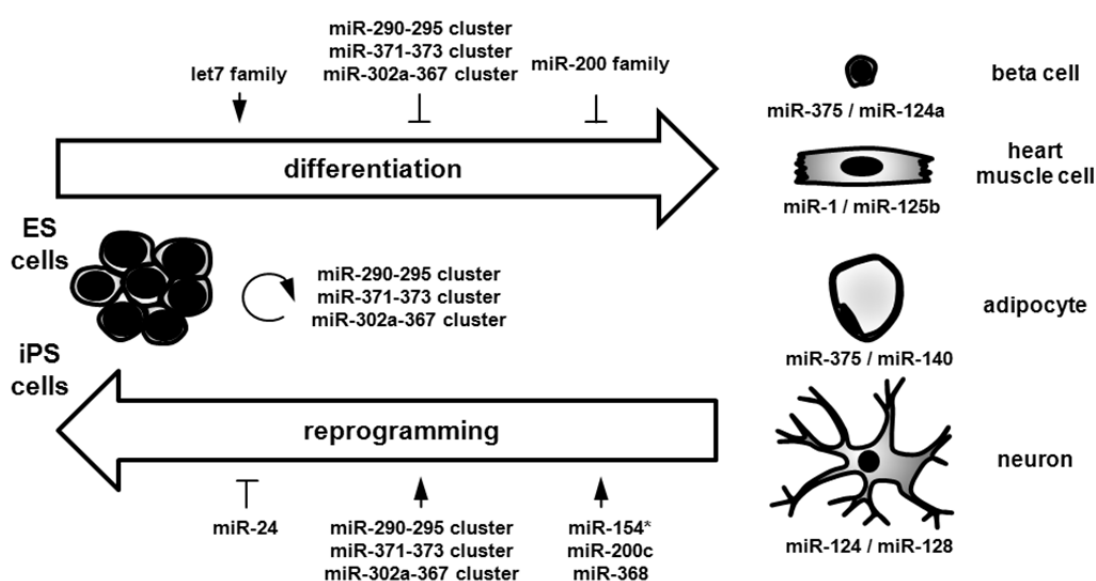


FIGURE 4: Induction, maintenance, and loss of pluripotency and involved miRs. Essential human and mouse miRs regulate reprogramming, self-renewal, and early differentiation. There are 14 miRs, which are expressed in a human ES cell-specific manner including miRs from the miR-302a-367 and the miR-371-373 cluster. These miRs are most important for reprogramming (modified from Jung and Schroeder, 2013).

1.2. Induction of Pluripotency for Reprogramming

Pluripotency of ES cells is predominantly preserved by growth factors, epigenetic chromatin modifications, and ES cell-specific miRs as described above. It is important to highlight that the same mechanisms are suitable for the induction of pluripotency in somatic cells.

1.2.1. Reprogramming Strategies

The development of a new strategy for non-viral reprogramming requires well-grounded knowledge of already described reprogramming approaches. Almost all somatic donors are suitable for reprogramming. For example, keratinocytes were obtained from diseased and healthy diabetes patients for efficient retroviral reprogramming (Ohmine et al., 2012). However, kinetics and efficiency differ dramatically among various cell types (Polo et al., 2010).

Fibroblasts, the cell type most often used as a starting material for reprogramming studies, are of mesenchyme origin and harbor two disadvantages that hamper reprogramming: They are fully differentiated and due to their mesenchymal nature have to undergo mesenchymal to epithelial transition to become pluripotent (Polo and Hochedlinger, 2010).

Mesenchymal stroma cells (MSCs) pose a valuable alternative for non-viral reprogramming. Even though also being of mesenchymal origin, MSCs are immature multipotent stem cells capable of differentiating into any mesenchymal cell type. Currently, MSCs are one of the most promising candidates for tissue engineering and applications in regenerative medicine (Caplan, 2007), mostly due to their differentiation potential and their immunological properties (Tae et al., 2006). The immaturity of multipotent MSCs is reflected in the expression of several genes found in pluripotent ES and iPS cells, which in turn facilitates the generation of iPS cells.

1.2.1.1. Viral Reprogramming

Human iPS cells are usually generated by transfection with retroviral vectors, which integrate into the host genome carrying reprogramming factors responsible for the induction of pluripotency (Takahashi and Yamanaka, 2006; Takahashi et al., 2007; Wernig et al., 2007; Park et al., 2008; Lowry et al., 2008). Meanwhile, this method has been shown to be also successful when other transcription factor combinations or fewer factors are used.

However, the efficiency is very low (0.01-0.001%) and media supplements (Huangfu et al., 2008; Shi et al., 2008) or small interfering RNAs (siRNAs) (Zhao et al., 2008) only slightly enhance reprogramming efficiency. Moreover, retroviral reprogramming results in massive gene-toxicity in host cells. For example, Kane and co-workers demonstrated that even integration of empty viral vectors can lead to uncontrollable reprogramming effects associated with gene and miR alterations and detrimental karyotype changes (Kane et al., 2010). The choice of other viral vectors such as the loxP-flanked lentivirus, non-integrating adenovirus, or DNA-free Sendai virus led to protocols bearing other side effects and did not result in improved efficacy (Somers et al., 2010; Zhou and Freed, 2009; Gonzalez et al., 2011; Nakanishi and Otsu, 2012). While viral reprogramming is well established and reproducible, non-viral reprogramming would overcome the above-mentioned disadvantages.

1.2.1.2. Culture Conditions and Media Supplements for Reprogramming

More suitable culture conditions and media supplements are potent parameters for proper regulation of pluripotency. *In vivo*, ES cells reside in the blastocyst, which provides an adequate microenvironment with hypoxic (<5%) conditions (Mitchell and Yochim, 1968; Yochim and Mitchell,

1968). Analysis of embryonic and adult cells revealed that the physiological oxygen tension lies in a range of 2-9% (Simon and Keith, 2008). Accordingly, hypoxia prevents differentiation of human ES cells *in vitro* (Ezashi et al., 2005). Current reprogramming strategies often disregard the physiologic correct milieu for pluripotent stem cells.

In vitro, the required substratum for ES and iPS cells is provided by MEFs, which are stimulated by FGF2 to release signaling molecules for the maintenance of human iPS and ES cells (Greber et al., 2007a). FGF2 induces differential expression of members of the TGF β superfamily. Thus, upregulation of TGF β 1, activin A (TGF β ligand), and gremlin1 (BMP4 inhibitor) as well as downregulation of BMP4 provoke Oct4, Nanog, and Sox2 expression (Greber et al., 2007b). Hypoxia and FGF2 treatment are sufficient to induce but not to preserve the expression of Oct4, Nanog and Sox2 in primary fibroblasts (Page et al., 2009). While hypoxia does not directly reprogram somatic cells, it promotes viral reprogramming of primary fibroblasts (Yoshida et al., 2009). Recently, proteomic analysis of human blastocoel fluid and blastocyst cells revealed about 1500 proteins that cells from the ICM are exposed to (Jensen et al., 2013). Further analysis will elucidate whether certain components are essential for improved ES and iPS cell culture.

However, chemical screens already provide media supplements termed as small molecules. Importantly, MEFs have been reprogrammed by staggered supplementation of 7 small molecules (Hou et al., 2013). There is a need to investigate efficiency and quality of small molecules-mediated reprogramming. Importantly, human and mouse ES cells correspond to different embryonic stages, suggesting that the chemical cocktail needs to be modified for human iPS cell generation. However, there is evidence that human chemically reprogrammed cells will be generated in the near future. Nevertheless, a combination of small molecules with other non-viral methods and/or culture conditions probably is the most efficient reprogramming strategy.

It is important to highlight that pluripotency is sensitive to alteration of epigenetic DNA and histone modifications, signaling pathways, ES cell-specific miRs, and oxygen supply. Therefore, non-viral reprogramming is suggested to be more efficient when more suitable culture conditions and media supplements are applied. Further, inappropriate culture conditions enable accumulation of chromosomal aberration, defective epigenetic modification, single nucleotide polymorphisms (SNPs), mitochondrial DNA aberrations, and elongation of telomeres (Ronen and Benvenisty, 2012).

1.2.1.3. Non-Viral Reprogramming

The reprogramming of somatic cells offers a promising opportunity for the generation of iPS cells that take the patients genetic background into account (Hankowski et al., 2011; Herder and Roden, 2011; Valdes and Spector, 2010; Norton et al., 2010). These iPS cells provide the opportunity to sustain the genetic background of a certain donor, who for example suffers from T2DM (**FIG. 5**). Generation of iPS cells and further differentiation into beta-like cells offers the opportunity to study diabetes more intensively on a molecular basis.

Viral reprogramming generates insertions, which disturb the integrity of the genome. Accordingly, it is controversial whether iPS cell generation by viruses is meaningful when the patient-specific background needs to be left unmodified. To protect the integrity of the host genome, non-viral reprogramming was established using episomal vectors, recombinant proteins or mRNAs, but these strategies were even more inefficient and challenging than retroviral approaches (Yu et al., 2009; Kim et al., 2009; Warren et al., 2010). Recently, non-viral delivery of miRs and a combination of

transposons and miRs were successfully applied for reprogramming (Miyoshi et al., 2011; Grabundzija et al., 2013), which is more clinically relevant than viral approaches. Yet, even these non-viral approaches for the delivery of miRs are inefficient and restricted to a certain donor cell type. Therefore, there is still the need to improve such non-viral reprogramming strategies to allow the development of clinically applicable stem cell therapies and *in vitro* test systems (**FIG. 5**).

Episomal vectors ectopically express reprogramming factors but do not integrate into the host genome. Further, episomal vectors are diluted out of the host cells during replication. These properties are ideal for the generation of high quality iPS cells. For example, retroviruses are needed to be silenced for successful reprogramming and subsequent differentiation.

There are a few episomal vectors, which are used to generate iPS cells. STEMcircles™ are popular reprogramming plasmids, which were first described by Jia and co-workers in 2010 (Jia et al., 2010; Narsinh et al., 2011). STEMcircles™ are minicircle DNA vectors free of bacterial DNA and thereby capable of consistent expression of ONSL. Further, oncogenes c-Myc and Klf4 are not encoded, because they are not necessary for episomal reprogramming. However, comparable to the miR approach, application of STEMcircles™ is not efficient and restricted to a certain cell type. Therefore, there is a need to further develop established non-viral reprogramming strategies, which use miR and/or episomal vectors. There is promising evidence that more suitable culture conditions and media supplements could improve reprogramming in general.

1.2.2. Disease-/Patient-Specific iPS Cells for the Cure of Diabetes

The International Diabetes Federation estimates that there will be about 438 million diabetes patients in 2030 including about 90-95% patients suffering from T2DM (Herder and Roden, 2011). T2DM is an epidemic disease, whose onset, progression, and treatment is regulated by about 100-1000 genes (Herder and Roden, 2011; Glamoclija and Jevric-Causevic, 2010). T2DM is caused by a combination of life style and genetic predisposition.

DNA variations in more than 50 loci have been predisposed with the onset of T2DM (McCarthy, 2010). These loci are predominately linked to insulin secretion and glucose sensing (Muller, 2010). Almost all variations result from SNPs, but one SNP moderately predisposes to T2DM (Weedon et al., 2006). T2DM is a complex disease and risk genes occur in a polygenic manner. Possibly, DNA variations influence certain genes involved in onset, progression, and treatment of T2DM. There are 36 T2DM risk genes carrying SNPs such as glucokinase (Gck) (Herder and Roden, 2011). Interestingly, monogenic defects related to the maturity onset diabetes of the young (MODY) affect essential pancreatic regulators such as Gck (MODY2), which is also predisposed to T2DM (Kim et al., 2004; Stumvoll et al., 2005; Edghill et al., 2008; Nyunt et al., 2009). Therefore, disease-specific iPS

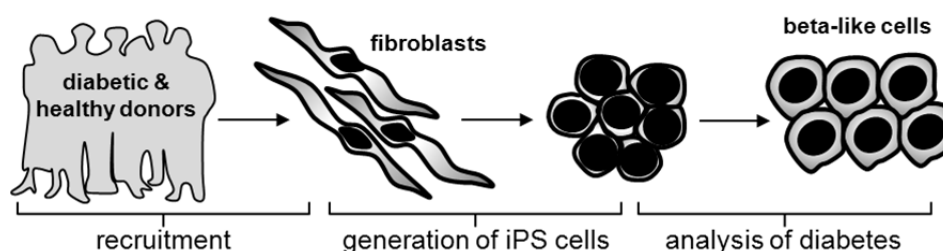


FIGURE 5: Procedure of patient- and disease-specific iPS cell generation. For example, fibroblasts are suitable to generate iPS cells. Pancreatic differentiation aims at the analysis of the beta cell development in diabetic and healthy individuals. Beta-like cells will allow stem cell therapies and *in vitro* test systems.

cells, which carry MODY- and T2DM-related genomic variations, are essential to further analyze the impact of T2DM-associated genetic variations (**FIG. 5**). Recently, T2DM-specific iPS cells have been generated by retroviral reprogramming (Ohmine et al., 2012; Park et al., 2008; Maehr et al., 2009). T2DM-specific iPS cells exclusively allow answering the question how genetic variations in T2DM risk genes impair beta cell development or function at a molecular level.

Treatment of diabetes by the routine use of recombinant insulins, continuous glucose monitoring, and use of pharmaceuticals improves the lives of millions of patients. Currently, 5 major classes of pharmaceuticals are available namely Sulfonylureas, Metformin, Thiazolidinediones, and alpha-glucosidase inhibitors (Glamoclija and Jevric-Causevic, 2010). Nevertheless, control of glucose levels is usually imperfect and dangerous long term side effects can hardly be prevented. Long-term complications are retinopathy, nephropathy, and neuropathy caused by defective microvasculature. Cardiovascular, cerebrovascular, and peripheral vascular diseases occur in response to damaged macrovasculature (Daneman, 2006). The understanding of pathways, which are involved in drug efficacy, is necessary to improve treatment. T2DM-specific iPS cells provide the opportunity to analyze drugs or to test new drugs in disease-specific differentiation models (Gunaseeli et al., 2010). Importantly, SNPs in drug-metabolizing genes were linked to different efficacy and toxicity (Evans and McLeod, 2003; Amani et al., 2008). Further, patient-tailored treatment would be possible but unaffordable for almost all diabetes patients.

Diabetes-specific iPS cells are also suitable to study beta cell regeneration. Studies in mice revealed that beta cells can derive from adult beta cells by replication after partial pancreatectomy (Dor et al., 2004; Nir et al., 2007). Further, studies in rodents demonstrated that beta cells are generated from duct cells after duct ligation (Inada et al., 2008; Solar et al., 2009). Human beta cell replication was observed during pregnancy (Van Assche et al., 1978) or autoimmune diseases (Willcox et al., 2010). However, the underlying mechanisms need to be clarified in diabetes-specific iPS cells for the discovery of treatment strategies including beta cell replication.

Finally, transplantation of beta cells would be the cure for diabetes. However, transplantation is worldwide limited by inadequate supply of human cadaver donors (Baiu et al., 2011). The generation of autologous beta cells from patient-specific iPS cells is one approach to overcome the inadequate supply of beta cells. Another approach describes the transdifferentiation (also termed as direct reprogramming) aiming at the generation of beta cells out of somatic cells without passing through a pluripotent state. For example, alpha cells can be converted into beta cells (Yang et al., 2011), quality of directly generated beta cells remains to be clarified. The successful delivery of pancreatic islets for human T1DM patients was first established in 2000 (Shapiro et al., 2000; Borowiak, 2010). In most cases, recipients of transplants achieved normal blood glucose levels, but in all cases beta cell function declined after some years. Islet encapsulation could preserve transplanted beta cells (Vaithilingam et al., 2010). Nevertheless, replacement therapies using autologous beta cells are still under investigation. Importantly, studies generally agree upon the fact that there will be no replacement therapies available for diabetes patients within the next 10 years.

1.3. Pancreatic Development and Pancreatic Differentiation

Importantly, pancreatic differentiation of diabetes-specific iPS cells provides a sophisticated tool to analyze the function of diabetes risk genes. Pancreatic differentiation of mouse and human ES and iPS cells *in vitro* is most efficient by mimicking the embryonic organ development. Thus, pancreatic development will be described briefly.

1.3.1. Pancreatic Development of Mouse and Human Pancreas

Until gastrulation, the earliest stages of vertebrate development are strongly regulated by the pluripotency gene Oct4. Within the pre-implantation embryo, Oct4 is required for the formation of the ICM (Campbell et al., 2007). After implantation, the ICM generates 3 primary germ layers endoderm, mesoderm and ectoderm (**FIG. 6 A**) for which downregulation of Oct4 is required (Campbell et al., 2007). The ICM differentiates embryonic and extraembryonic tissues as well. Primary germ layers are formed between 6.5 and 7.5 embryonic day in mice development (E) and within the second week of human development (WD) (Van et al., 2009). Importantly, endoderm progenitors generate the pancreas.

1.3.1.1. Formation of Primary Germ Layer Progenitors

Differentiation towards the pancreatic lineage requires formation of mesendoderm precursors, which are generated during gastrulation. Mesendoderm is particularly characterized by the expression of T-box transcription factor Brachyury (Bra, officially termed as T) (Van et al., 2009). Subsequently, bipotential mesendoderm generates mesoderm and endoderm progenitors (**FIG. 6 A**). The endoderm progenitors are also referred to as definitive endoderm (DE), because the ICM also generates extraembryonic endoderm contributing to the placenta. DE formation is governed by co-expression of Sox family transcription factor 17 (Sox17), forkhead box transcription factors A2 (Foxa2), and transmembrane chemokine CXC receptor 4 (Cxcr4) (Van et al., 2009; Schroeder et al., 2012). Sox17 expression is also present in extraembryonic endoderm cells. However, extraembryonic endoderm development depends on the expression of essential extraembryonic genes such as Sox family transcription factor 7 (Sox7) (Kanai-Azuma et al., 2002) and stromal cell-derived factor 1 (Sdf1, also known as chemokine CXC ligand 12) (Schroeder et al., 2012), which are not present in DE.

Endoderm progenitors give rise to the pancreas, but also to several other organs such as the liver (**FIG. 6 A**). Thereby, endoderm differentiates into certain organ-committed precursors. These precursors can be characterized by the expression of distinct markers such as the alpha fetoprotein (Afp), which is induced in the liver anlagen at E8.25 (Lee et al., 2012).

The formation of mesoderm within mesendoderm progenitors is characterized by continuous Bra expression (**FIG. 6 A**). Further, there is the induction of other mesoderm markers such as extraembryonic and/or lateral plate mesoderm gene forkhead box transcription factors F1 (Foxf1) and paraxial mesoderm gene mesenchyme homeobox 1 (Meox1) (Cao et al., 2008; Schroeder et al., 2012; Umeda et al., 2012).

Differentiation into ectoderm towards neural cell fates (**Fig. 6 A**) is ruled by the induction of paired box gene 6 (Pax6) and sonic hedgehog (Shh). Pax6 as well as Shh are crucial for proliferation and differentiation into the developing and adult vertebrate brain (Kayam et al., 2013; Martinez et al., 2013). Subsequently, the generation of neural cells reveals expression of glia- and neuron-associated genes. Glial fibrillary acidic protein (Gfap) is predominantly expressed in astrocytes. The expression of

microtubule-associated protein 2 (Map2) and tubulin beta 3 (Tubb3) indicates differentiation into neurons. Map2 encodes a neuron-specific cytoskeletal protein, which is enriched in dendrites to determine neuron development (Terabayashi et al., 2007). Tubb3 is involved in neurogenesis and axon development (Singh and Tsai, 2010). Interestingly, neural and pancreatic endocrine share signaling pathways including common transcription factors such as Pax6, which is responsible for ectoderm formation and maturation of alpha and beta cells (Van et al., 2009).

1.3.1.2. Embryonic Development of Beta Cells

DE progenitors give rise to primitive gut epithelial cells, which form ventral and dorsal buds to induce pancreas organogenesis within the foregut. In mice, the pancreas development starts between E8.5 and E9.0 from a dorsal and a ventral bud at the primitive gut. A dorsal evagination first occurs at the level of the liver during the 22-25 somite stage. Afterwards, the ventral bud is formed. The ventral bud is surrounded by cardiac mesenchyme, the dorsal bud is surrounded by the notochord and later by dorsal aorta. In humans, the pancreas originates within the 3WD (Van et al., 2009). Bud formation is regulated by its surrounding tissues (Oliver-Krasinski and Stoffers, 2008). Pancreatic buds contain pancreatic epithelium expressing duodenal homeobox 1 (Pdx1). Pdx1 is the first pancreas-specific marker during pancreatic development (**FIG. 6 A**). Pdx1-expressing progenitors give rise to all pancreatic cell types (Jonsson et al., 1994; Offield et al., 1996). Heterozygous mutations are responsible for maturity onset diabetes of the young type 4 (MODY4) in humans and Pdx1 knockout mice fail to generate the pancreas (Jonsson et al., 1994; Stoffers et al., 1997). Cells at the distal tip of the pancreatic epithelium are multipotent progenitors, which express Pdx1, pancreas-specific transcription factor 1a (Ptf1a), the stem cell marker c-Myc, and pancreatic carboxypeptidase A1 (Cpa1) (Zhou et al., 2007). Multipotent progenitors appear between E8.5 and 11.5 and their number at

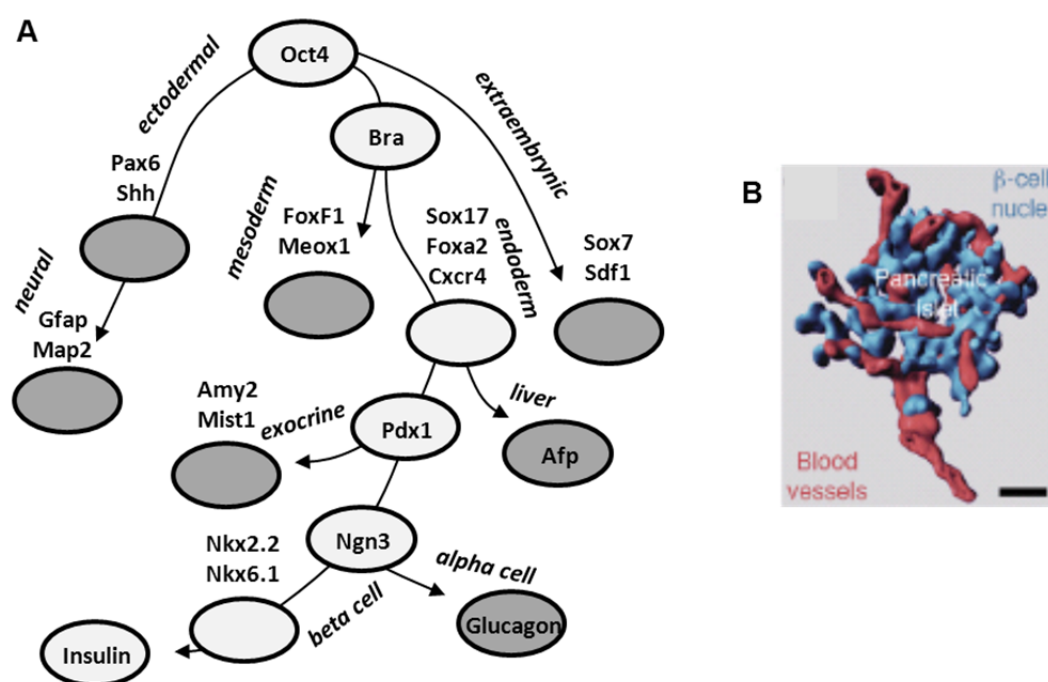


FIGURE 6: Pancreas development *in vivo* and pancreatic differentiation *in vitro*. (A) Pluripotent stem cells develop into ectodermal, mesodermal, and endodermal progenitors. Endoderm generates pancreatic progenitors, of which exocrine and endocrine progenitors derive. Besides pancreatic development pluripotent stem cells differentiate into other lineages and cell types. Extraembryonic tissues are derived alongside the 3 primary germ layers. (B) The computed 3D model of beta cells and blood vessels demonstrates the high amount of blood supply in adult islets of Langerhans (Nikolova et al., 2007). Scale bar represents 10 μ m.

that time ultimately determines the final size of the pancreas (Stanger et al., 2007). In mice at E12.5, in humans within 5WD, the gut rotates to bring the pancreatic rudiments in closer proximity (Van et al., 2009). Multipotent progenitors disappear after E14.9. Subsequently, Pdx1-expression becomes restricted to endocrine progenitors at E16.5. At E19.0, Pdx1 is limited to beta cells and a subset of delta cells. Pdx1-expressing cells also give rise to the exocrine pancreas (**FIG. 6 A**). Muscle, intestine and stomach expression 1 (Mist1; also known as Bhlha15) is responsible for remodeling of pancreatic acinar cells (Direnzo et al., 2012). Amylase alpha 2A (Amy2; also known as Amy2a) encodes a digestive enzyme in adult exocrine cells.

After branching of the pancreatic buds, endocrine precursors detach from the pancreatic epithelium at E15.5 (Oliver-Krasinski and Stoffers, 2008; Puri and Hebrok, 2010). Neurogenin 3 (Ngn3; also known as Neurog3) marks endocrine cell identity (**FIG. 6 A**), because Ngn3 knockout mice fail to generate islets of Langerhans (Gradwohl et al., 2000; Schwitzgebel et al., 2000). Ngn3-expressing progenitors give rise to all endocrine pancreatic cells (Herrera et al., 2002). Ngn3 controls the expression of many genes involved in endocrine differentiation (Van et al., 2009). The expanding pancreatic epithelium is characterized by Nk2 homeobox transcription factor 2 (Nkx2.2) and Nk6 homeobox transcription factor 1 (Nkx6.1) expression (Van et al., 2009). Nkx2.2 is sustained in alpha, beta, delta, and PP cells, while Nkx6.1 becomes restricted to beta cells (Van et al., 2009).

The human pancreas contains exocrine and endocrine compartments, but, the endocrine pancreas is small and represents about 1-2% of the total pancreas. About 1 million islets of Langerhans reside within the human pancreas and about 75% are beta cells (Butler et al., 2003). In contrast to mice, human beta cells are also located outside of the islets of Langerhans (Butler et al., 2003). The adult pancreas consists of head, body, and tail and differentiation of these compartments is differently regulated. For example, MODY5-related monogenic defects in hepatocyte nuclear factor 1 B (Hnf1b) disturb the formation of body and tail (Haldorsen et al., 2008). Interestingly, human islet of Langerhans distribution is not constant, islet density is 2-fold higher in the tail region (Wang et al., 2013). Human islets typically are composed of 10-65% glucagon-producing alpha cells, 28-75% insulin-producing beta cells, 1-22% somatostatin-producing delta cells, 3-5% pancreatic polypeptide-producing PP cells, and <1% ghrelin-producing delta cells (Brissova et al., 2005). It is important to highlight that the capillary network within an adult islet of Langerhans is enormous (**FIG. 6 B**). The adult pancreas depends on crossing blood vessels, which are needed for insulin release as will be described in the following chapter.

1.3.1.3. Relationship of Endothelial Cells and Pancreatic Progenitors

Importantly, the induction and development of pancreatic endocrine cells strictly depends on co-development of a capillary network (**FIG. 6 B**). Blood vessels support pancreas development not only by establishment of the tissue homeostasis. ECs from blood vessel cells are capable to regulate growth and maturation of pancreatic endocrine cells in addition to their nutritional function. Importantly, mouse pancreatic development starts under hypoxic conditions at E8.25, but blood flow responsible for normalization of the oxygen level is induced later at E14.5-15.0 (Shah et al., 2011). Moreover, mice embryos lacking kinase insert domain protein receptor (Kdr; also known as Flk1 or Vegfr2) fail to induce dorsal bud formation (Yoshitomi and Zaret, 2004). Vascular endothelial growth factor receptor 2 (Vegfr2) is essential for the development of endothelial cells (ECs). Further, Vegfr2 knockout is lethal in mice, because ECs are required for vascularization of the developing mouse

embryo. In all probability, vessels provide varying signals as their relationship to pancreatic cells differs within organogenesis (Cleaver and Dor, 2012). Pancreatic progenitors probably become less or more sensitive to EC signals during development (Cleaver and Dor, 2012). ECs are thought to provide regionally and temporally different tissue- and time-dependent differentiation signals.

Interestingly, early organogenesis is also regulated by differentiation signals from the surrounding mesoderm (Cleaver and Dor, 2012). Later on, growth and specification of pancreatic cells is regulated by the mesenchyme, which contains a variety of cell types such as neurons, smooth muscles, stroma and of course ECs. While the specific impact of distinct cell types remains to be clarified, the whole mesenchyme is necessary for establishment of the pancreatic epithelium (Landsman et al., 2011).

Expression of the pancreatic epithelium markers Pdx1 and Ptf1a during bud formation (around E8.25) depends on the presence of ECs before blood flow is initiated (Yoshitomi and Zaret, 2004). EC signals are potent inducers of Pdx1 expression, but it remains unclear whether toggled LIM domain only 2 (Lmo2) and/or retinoic acid (RA) mediates Pdx1 induction (Cleaver and Dor, 2012).

Human and mouse pancreatic endocrine cells are generated in 2 waves of differentiation (also termed as 2 transitions) identified by changes in organ morphology (Herrera, 2000). In humans, knowledge about the pancreatic development is mostly descriptive. In mice, the 2 transitions have been characterized more intensively. The first wave of differentiation around E9.5 generates immature endocrine cells, which produce insulin, but also several other hormones. Almost no endocrine cells, which are generated during that first wave, contribute to the adult islets of Langerhans. The formation of immature endocrine cells in the dorsal bud is regulated by fusing aortae between E8.75 and E9.5. Thus prevention of aortae signaling inhibits beta cell development (Cleaver and Dor, 2012). The second wave of differentiation at E12.5 generates mature hormone-producing cells. Importantly, the second transition is linked to growing blood vessels, which control endocrine and exocrine specification by Notch signaling (Murtaugh et al., 2003).

Maturation of beta cells occurs within the pancreatic epithelium, but cells need to leave the epithelium to generate certain islets of Langerhans within the exocrine compartment. Therefore, maturation of beta cells followed by islet formation requires cell-cell interaction between beta cells and ECs (Murtaugh et al., 2003; Nikolova et al., 2006; Nikolova et al., 2007). Interestingly, Sdf1-expressing pancreatic progenitors attract Cxcr4-expressing endothelial progenitors (angioblasts) prior to vessel formation to induce vascularization (Katsumoto and Kume, 2011). Subsequently, pancreatic bud formation is regulated by ECs, which restrict branching of buds to guide the final pancreas size (Magenheim et al., 2011). During late pancreatic development, proliferation of beta cells is supported by ECs as well (Nikolova et al., 2006). Beta cells communicate with fenestrated capillaries, which are abundant within the islet of Langerhans. Most probably, vascular endothelial growth factor A (VEGF_A) signaling by beta cells induces vascularization. Accordingly, deletion of VEGF_A in beta cells lowered (up to -90%) capillary density leading to many defects *exempli gratia* (e.g.) in glucose homeostasis (Lammert et al., 2003). According to the architecture of the adult pancreas, it is reasonable that the adult as well as the developing pancreas requires the presence of blood vessels. Studies from pancreas expansion during pregnancy revealed that islet capillaries were shown to proliferate and express high levels of hepatocyte growth factor (HGF) just prior to beta cell proliferation suggesting a positive correlation (Johansson et al., 2006). Moreover, *in vitro* co-culture of islets with ECs improves their function and survival (Pan et al., 2011).

There is a set of ECM compartments, which are involved in beta cell development and maturation. In mice, capillaries within islets of Langerhans supply a vascular basement membrane, which is crucial for beta cell development and insulin production. Laminin and collagen IV are part of the vascular basement membrane. Beta cells generate alpha-6-beta-1-integrin, which interacts with laminin for insulin (Ins) expression and beta cell proliferation (Nikolova et al., 2007). Vascular collagen IV is known to signal via beta cell alpha-1-beta-1-integrin to enhance both endocrine cell motility and secretory efficiency (Kaido et al., 2004; Nikolova et al., 2007). Mouse beta cells are in direct contact to the vascular basement membrane whereas human beta cells generate their own ECM to create a doubled basement membrane (Virtanen et al., 2008). The importance of ECM compartments suggests that organotypic 3D architecture of developing pancreatic buds and islets is necessary for beta cell development. Importantly, ECs start to shape the 3D architecture early during development of the pancreatic epithelium.

1.3.2. *In vitro* Differentiation into Insulin-Producing Beta-Like Cells

It is important to acknowledge that a variety of differentiation protocols have been established, but attempts failed to achieve efficient and functional *in vitro* differentiation into mature pancreatic beta cells. Generation of insulin-producing cells from mouse ES cells was first reported in 2000 (Soria et al., 2000). Soria and colleagues applied transgenic ES cells that expressed a hygromycin resistance gene under the control of the Ins promoter for a spontaneous differentiation model. DE progenitors were induced by embryoid body (EB) formation in suspension cultures. Soria and co-authors applied selective culture media containing hygromycin after differentiation into pancreatic progenitors at day 10 and a population of Ins-expressing cells was observed around day 23. Finally, insulin-producing cells were implanted into the mouse spleen, which was sufficient to normalize the blood glucose level of hyperglycemic mice. Pancreatic differentiation of human ES cells was first demonstrated in 2001 (Assady et al., 2001). Assady and co-workers successfully applied adherent as well as suspension culture for induction of DE enabling the generation of insulin-producing cells. However, even though beta cell markers like Pdx1, Gck, glucose transporter 2 (Glut2), and Ins were expressed, glucose-dependent insulin secretion was inefficient and time-consuming. Attempts by other authors failed to overcome poor efficiency and ineffective maturation (Kahan et al., 2003; Xu et al., 2006; Tsai et al., 2010). In mouse ES cells, another strategy based on the generation of DE progenitors by EB formation and subsequent enrichment of pancreatic progenitors expressing nestin (Nes) (Lumelsky et al., 2001). Nes is expressed in mouse and human pancreatic progenitors, but further studies revealed that Nes is also expressed in neural progenitors. Therefore, the selection of Nes-expressing cells is not applicable for the specific generation of pancreatic progenitors. Another important study in mouse ES cells applied PI3K inhibitor LY294002 after EB formation for more efficient generation of insulin-producing cells (Hori et al., 2002). However, insulin-immunoreactive cells generated according to the protocol of Hori and co-workers did not contain C-peptide, which is the by-product of *de novo* insulin synthesis (Hansson et al., 2004). Hansson and co-authors suggest that at least a subset of cells underwent apoptosis or necrosis followed by uptake of insulin, which is added to the culture medium to support the pancreatic differentiation. Use of conditioned medium from E16.5 pancreatic buds for the differentiation of mouse ES cells led to derivatives that co-expressed insulin and C-peptide, showed glucose-dependent release of insulin and C-peptide, and normalization of blood

glucose levels in diabetic mice (Vaca et al., 2006). However, such approaches are less applicable for differentiation studies in human ES cells and unsuitable for clinical applications.

1.3.2.1. Differentiation into Primary Germ Layer Progenitors

EB formation is a well-established tool for the *in vitro* generation of primary germ layer derivatives first established in the lab of Anna Wobus (Schroeder et al., 2012). EBs are blastocyst-like three-dimensional (3D) agglomerations of differentiating ES cells, which differentiate into derivatives of all 3 primary germ layers representing multi-lineage progenitors. Suspension cultures as well as hanging drops are suitable to generate EBs from mouse and human ES cells. Interestingly, size and culture duration can be optimized for more efficient generation of desired primary germ layer derivatives (Schroeder et al., 2009). The rationale of this approach is based on the knowledge that generation of multi-lineage progenitor cells release differentiation molecules of ectodermal and mesodermal precursor cells known to be required for successful pancreatic differentiation (Schroeder et al., 2006). EB formation of mouse and human ES cells was demonstrated by spontaneous differentiation using fetal calf serum (FCS) supplementation and directed differentiation in the presence of chemically defined media (CDM). Importantly, CDM contains activin A, which is responsible for enhanced differentiation into DE progenitors during EB formation (Kroon et al., 2008; Schroeder et al., 2012). Growth and extracellular matrix factors such as nicotinamide and laminin are supplemented for further pancreatic differentiation of endoderm progenitors.

Today, it is generally accepted that the initial differentiation of ES cells into DE progenitors is one of the most important steps for the successful and efficient generation of functional insulin-producing beta-like cells. *In vivo*, it requires nodal signaling from the most anterior region of the primitive streak (Tam and Loebel, 2007). However, access to biological active nodal for *in vitro* cultures is limited. Activin A can act as a surrogate of nodal. Several studies have proven that activin A promotes mouse and human ES cell differentiation into DE (D'Amour et al., 2006; Kroon et al., 2008; Schroeder et al., 2012). Yet, there is evidence that endogenous induction of nodal is more efficient than application of exogenous activin A (Takenaga et al., 2007).

A disadvantage of most pancreatic differentiation protocols is undesired cell heterogeneity. Hence, ways of improving the quality of stem cell progeny are the selection or enrichment of progenitors with stage-specific markers on the basis of flow cytometry or drug resistance. One promising study by Schroeder and co-workers aimed at the differentiation of mouse CGR8-S17 ES cells carrying a homologous dsRed-IRES-puromycin knock-in within the Sox17 locus (Schroeder et al., 2012). Selection of Sox17-positive cells enables detailed characterization of activin A-induced DE progenitors. Schroeder and co-authors reported that Sox17-expressing cells exhibited markers of the DE, primitive gut, posterior foregut, and endocrine progenitors (Schroeder et al., 2012). Notably, similar results were obtained selecting Sox17-positive progeny in human ES cells (Wang et al., 2011).

Interestingly, ablation of heterogeneity is also suggested by permanent expression of pancreatic developmental control genes. For example, mouse ES cells with the constitutive expression of the pancreatic developmental control genes Pdx1 and paired box 4 (Pax4) were analyzed during pancreatic differentiation (Blyszczuk et al., 2003). The differentiated insulin- and C-peptide-positive cells normalized blood glucose levels *in vivo* after transplantation into diabetic mice (Blyszczuk et al., 2004; Boyd et al., 2008). Nonetheless, the differentiation procedure was inefficient and cells failed

stable normalization of the blood glucose level. However, constitutive expression of Pdx1 and Pax4 is a promising tool to analyze their function during pancreatic differentiation.

1.3.2.2. Differentiation Mimicking Organogenesis

Differentiation by mimicking pancreatic organogenesis is more promising. Applying growth factors, extracellular matrix factors, and small molecules in differentiation protocols in the order that they would appear and function *in vivo* is suitable to obtain directed pancreatic differentiation. In contrast to spontaneous differentiation, application of FCS responsible for broad differentiation is restricted or avoided. Directed pancreatic differentiation first generates activin A-induced DE within EBs or within adherent cultures (Assady et al., 2001; D'Amour et al., 2006). Afterwards, organogenesis is mimicked by sequential treatment of pluripotent stem cells with defined growth and differentiation factors.

Activin A and Wnt3a are used for induction of DE progenitors (D'Amour et al., 2006). Subsequently, treatment with FGFs, hepatocyte growth factor, and epidermal growth factor (EGF) induce primitive gut tube-like cells. FGFs, HGF, and EGF play a central role during prenatal development promoting proliferation and differentiation of a variety of organs including the pancreas (D'Amour et al., 2006; Zhang et al., 2009). Afterwards, inhibition of Shh signaling and RA treatment up regulate Pdx1 expression and induce differentiation into posterior foregut-like cells (D'Amour et al., 2006). Knockout of the RA receptor in mouse ES cells impairs pancreatic endocrine development (Perez et al., 2013). Exendin 4 up regulates Pdx1 expression and maturation of pancreatic progenitors (Movassat et al., 2002). Nicotinamide preserves homeostasis of differentiating pancreatic endocrine progenitors (Vaca et al., 2006). It is a form of vitamin B3 and participates in diverse biological processes including production of energy, nutrient metabolism, signal transduction, and maintenance of genome integrity (Jung et al., 2009). Finally, the B27 supplement mix initiates differentiation of the pancreatic epithelium (D'Amour et al., 2006). B27 contains several components including insulin, transferrin, or progesterone suitable to orchestrate differentiation and maturation of pancreatic endocrine progenitors (Wachs et al., 2003). Generally, growth factor based protocols are rather complex differing in growth factor assembly, exposure durations and supplement concentrations (Mfopou et al., 2010b).

Interestingly, differentiation protocols for human ES cells have been adapted to the new class of iPS cells. Notably, pancreatic differentiation of iPS cells was reported to be less efficient compared to ES cells (Hu et al., 2010). Fortunately, differentiation of reprogrammed cells into the pancreatic lineage is comparable to human ES cells. Analysis of pancreatic iPS cell-derived insulin-producing cells secreted C-peptide (Kunisada et al., 2012), showed glucose-responsiveness (Thatava et al., 2011), or improved blood glucose levels in hyperglycemic mice (Saito et al., 2011). Recent data showed a preferential differentiation of iPS cells generated from pancreatic beta cells into insulin-producing cells (Bar-Nur et al., 2011). Beta cell-derived iPS cells apparently maintained open chromatin structures in key beta cells genes and a unique DNA methylation signature that distinguished them from other iPS cells. Accordingly, effective generation of pancreatic hormone-producing cells thus may depend more strongly on the method of pluripotency induction and the origin of the reprogrammed cells than on the applied differentiation protocol.

1.4. Aims of the Study

The overall aim of the study was to establish non-viral iPS cells and an organotypic 3D pancreatic differentiation model. These two strategies combined will allow analyzing pancreatic differentiation of human iPS cells within a healthy and disease context. For this purpose, isolation and culture of primary human donor cells was a mandatory first step. The study included the development of various non-viral reprogramming methods and the combination of the most potent methods aimed at the establishment of a non-viral reprogramming strategy. Organotypic pancreatic differentiation as an improvement over already existing differentiation protocols required the establishment of 3D co-cultures. Therefore, the specific work packages comprised of

the establishment of patient-specific primary keratinocytes,

the development and analysis of non-viral reprogramming methods for assembly within a non-viral reprogramming strategy,

and the development of a 3D pancreatic differentiation model including ECs.

2. MATERIAL AND METHODS

2.1. Ethical Considerations

Ethical approval for the use of human skin biopsies for the isolation of ECs was obtained from the ethics committee of the Medical Faculty, Martin Luther University Halle-Wittenberg, Germany. Vita34 held appropriate permits for the use of human umbilical cords. The central ethics committee for stem cell research, Robert Koch Institute, Berlin, Germany, evaluated and approved studies with H9 cells.

2.2. Cell Culture and Growth Conditions

Nunc™ cell culture dishes and well plates for the culture of CGR8-S17 ES cells, IMR90 iPS cells, H9 ES cells, and primary keratinocytes were obtained from Thermo Fisher Scientific, Karlsruhe, Germany. Tissue culture flasks for the culture of L87 MSCs, primary MSCs, and BJ-5ta fibroblasts were obtained from TPP, Klettgau, Germany. Bacteriological dishes for the culture of hanging drops were supplied by Greiner Bio-One, Frickenhausen, Germany. Cells were grown in at 37°C in a humidified environment of 20% O₂ and 5% CO₂ (normoxia) or 5% O₂, 5% CO₂, and 90% N₂ (hypoxia). Cell morphology was documented using a Nikon Eclipse TS100F inverted microscope (Nikon, Düsseldorf, Germany). If not mentioned otherwise, media contained 4.5 g/l glucose (high glucose) and 1.0 g/l sodium bicarbonate. FCS was heat inactivated at 56°C for 30 min. The absence of mycoplasma contaminants was routinely verified using the Venor®GeM Classic Kit (Minerva, Berlin, Germany). Cell suspensions were stained with trypan blue and counted in a Neubauer chamber (VWR, Darmstadt, Germany).

The procedure to freeze of cells was identical for all primary cells and cell lines used in the present study. Cell suspensions were prepared according to the cell line specific splitting procedures. Suspensions were centrifuged at 200 g for 5 min. Cells were reconstituted in 1.0 ml medium containing (6:3:1 v/v/v) cell type-specific medium, FCS, and dimethyl sulfoxide (DMSO). Slow freezing was performed in a freezing box containing isopropanol. Cells were frozen at -80°C for 1 d. Finally, vials were stored at -196°C in the gas phase of liquid nitrogen.

Thawing of cells was equally performed for all primary cells and cell lines. Frozen cells were quickly thawed in a 37°C water bath leaving an ice crystal inside. 1.0 ml pre-warmed cell type-specific medium was added dropwise to the 1.0 ml thawing cell suspension. The 2.0 ml cell suspension was transferred into a conical tube with 8.0 ml pre-warmed cell type-specific medium and centrifuged at 200 g for 5 min. The cells were reconstituted in pre-warmed cell type-specific medium and cultured under cell-specific conditions.

2.2.1. Culture of Somatic Cell Lines

The human MSC line L87 was provided by Prof. Dr. Stefan Burdach, Department of Pediatrics, Technische Universität München, Germany. L87 cells were cultured in Rosswell Park Memorial Institute 1640 medium (RPMI-1640; Life Technologie, Darmstadt, Germany) supplemented with 10% FCS (Lonza, Köln, Germany), 2 mM L-glutamine, and 1% 10 000 U/10 000 µg penicillin/streptomycin (Life Technologies, Darmstadt, Germany). The cells were seeded in a range of 1000-2000 cells/cm² and passaged at 70-80% confluence by exposing cells to 0.1 M ethylene diamine tetra acetic acid (EDTA; Carl Roth, Karlsruhe, Germany) for about 1 min and rinsing once with L87 medium. The cell

suspension was centrifuged at 200 g for 5 min. L87 cells were reconstituted in L87 medium and seeded in a 1:5 split ratio in a 4-10 d interval.

Primary MSCs, obtained from human bone marrow aspirates, were provided by Dr. Lutz Müller, Department of Internal Medicine IV, Medical Faculty, Martin Luther University Halle-Wittenberg, Germany. The cells were cultured in Minimal Essential Medium Eagle (MEM; PAA, Cölbe, Germany) supplemented with 15% FCS (Lonza, Köln, Germany), 1% nonessential amino acids (NEAA), 2 mM L-glutamine, 1% sodium pyruvate, and 1% 10 000 U/10 000 µg penicillin/streptomycin (all from Life Technologies, Darmstadt, Germany). Cells were seeded in a range of 200-400 cells/cm² and passaged at 60% confluence by exposing cells to 0.1 M EDTA (Carl Roth, Karlsruhe, Germany) for about 1 min and rinsing once in MSC medium. The cell suspension was centrifuged at 200 g for 5 min. The cells were reconstituted in MSC medium and seeded in a 1:2 split ratio in a 7-10 d interval.

The fibroblast line BJ-5ta was obtained from the American Type Culture Collection (ATCC; Wesel, Germany). The cells were cultured in a 4:1 (v/v) mixture of Dulbecco's Modified Eagle Medium (DMEM) and Medium 199 (PAA, Cölbe, Germany) supplemented with 10% FCS (Lonza, Köln, Germany), 4 mM L-glutamine, 1% 10 000 U/10 000 µg penicillin/streptomycin, and 0.01 mg/ml hygromycin B (all from Life Technologies, Darmstadt, Germany). BJ-5ta cells were seeded in a range of 3000-5000 cells/cm² and passaged at 70-80% confluence by exposing cells to 0.25% trypsin/0.53 mM EDTA (PAA, Cölbe, Germany/Carl Roth, Karlsruhe, Germany) for about 1 min and rinsing once in BJ-5ta medium. The cell suspension was centrifuged at 200 g for 5 min. The cells were reconstituted in BJ-5ta medium and seeded in a 1:2-1:3 split ratio in a 7 d interval.

2.2.2. Isolation and Culture of Primary Keratinocytes

Primary human keratinocytes were isolated as described by Savkovic and co-authors (Savkovic et al., 2012) with minor modifications. In brief, primary keratinocytes were isolated from anagen hairs that were plucked from the temporal scalp region and shortened at the proximal end. They were washed with phosphate buffered saline (PBS) containing 625.0 ng/ml amphotericin B (PAA, Cölbe, Germany) and 1% 10 000 U/10 000 µg penicillin/streptomycin (Life Technologies, Darmstadt, Germany). Subsequently, hairs were treated with sterile filtered collagenase IV/V solution at a concentration of 5.0 mg/ml PBS (Sigma-Aldrich, Taufkirchen, Germany) at 37°C for 15 min. At least 10 hair roots were lined up parallel in ThinCert™ cell culture inserts (Greiner Bio-One, Frickenhausen, Germany). Inserts were put into wells seeded with 3T3-L1 feeder cells. Hairs were cultured under hypoxic conditions using a medium-air-interface. Keratinocyte growth medium contained a 1:1 (v/v) mixture of DMEM and Ham's Nutrient Mixture F12 (F12) supplemented with 10% FCS (Lonza, Köln, Germany), 10.0 ng/ml EGF (Peprotech, Hamburg, Germany), 0.4 mM ethylene glycol tetra-acetic acid (EGTA), 0.4 µg/ml hydrocortisone, 0.1 nM cholera toxin, 180 µM adenine, 5.0 µg/ml insulin, 5.0 µg/ml transferrin (all from Sigma-Aldrich, Taufkirchen, Germany), 1% NEAA, 2 mM L-glutamine, 1% 10 000 U/10 000 µg penicillin/streptomycin (all from Life Technologies, Darmstadt, Germany), and 625.0 ng/ml amphotericin B (PAA, Cölbe, Germany). After 2-3 weeks, primary keratinocytes were obtained by exposing hairs to 0.1% trypsin/0.53 mM EDTA (PAA, Cölbe, Germany/Carl Roth, Karlsruhe, Germany) at 37°C for 10 min and rinsing once in keratinocyte growth medium. The cell suspension was centrifuged at 200 g for 5 min. The cells were reconstituted in keratinocyte growth medium and seeded onto feeder cells, which were changed once a week. Medium was changed thrice weekly. The cells were passaged at 70-80% confluence by exposing cells to 0.1% trypsin/0.53 mM EDTA (PAA,

Cölbe, Germany/Carl Roth, Karlsruhe, Germany) at 37°C for 10 min and rinsing once in keratinocyte growth medium. The cell suspension was centrifuged at 200 g for 5 min. The cells were reconstituted in keratinocyte growth medium and seeded in a 1:2-1:3 split ratio in a 7 d interval.

3T3-L1 MEFs served as feeder cells for hairs (indirectly) and primary keratinocytes (directly). Prof. Dr. Matthias Blüher (Department of Medicine, University of Leipzig, Germany) provided the 3T3-L1 MEF line. 3T3 spontaneously immortalized MEFs were established in 1962 from swiss mouse embryos. These cells are applied as feeder cells for primary keratinocytes (Rheinwald and Green, 1975). 3T3-L1 is a substrain of 3T3 developed through clonal isolation. Cells were mitotically inactivated by treatment with 3T3-L1 medium supplemented with 10.0 µg/ml mytomycin C (Sigma-Aldrich, Taufkirchen, Germany) for 2-3 h and rinsing once in 3T3-L1 medium. The cells were seeded in a range of 40 000-60 000 cells/cm².

Rhodamine B staining for the detection of keratinocytes was carried out according to a protocol previously described by Islam and co-workers (Islam and Zhou, 2007). Briefly, the cells were fixed in 4% paraformaldehyde (PFA) for 20 min and washed in PBS. Subsequently, cells were treated with 1.0 mg/ml rhodamine B (Sigma-Aldrich, Taufkirchen, Germany) in deionized water for 30 min and washed with PBS.

2.2.3. Isolation and Culture of Primary ECs

Commercially available primary human dermal microvascular endothelial cells (HDMECs) were obtained from Promocell, Heidelberg, Germany. Cell culture was performed according to manufacturer's instructions.

Primary human dermal microvascular endothelial cells (MVECs) were obtained from skin biopsies provided by PD. Dr. med. Michael Steen, Department of Hand and Plastic Surgery, BG-Kliniken Bergmannstrost, Germany. Cells were isolated according to the protocol by Moll and co-workers with minor modification (Moll et al., 2013). In brief, skin biopsies were collected in DMEM (PAA, Cölbe, Germany) supplemented with 10% FCS (Lonza, Köln, Germany), 2 mM L-glutamine (Life Technologies, Darmstadt, Germany), and 1% gentamycin (Biochrom part of Merck Millipore, Berlin, Germany). The skin was cut into small pieces of approximately 2-3 mm, washed in PBS, and covered with 2.0 mg/ml dispase at 4°C overnight. The epidermis was separated from the dermis, washed in PBS with Mg and Ca, and treated with 0.05% Trypsin/0.53 M EDTA in Versene (Life Technologies, Darmstadt, Germany) at 37°C for up to 1 h. Epidermis pieces were transferred to EC media and scraped out to separate ECs from the tissue. The cell suspension was filtered using sterile nylon meshes with a pore size of 100 µm (Corning, Kaiserslautern, Germany) and transferred to culture dishes. After 4 h, when ECs had attached, the medium was changed to remove unwanted cell types.

Primary human umbilical vascular endothelial cells (HUVECs) were kindly provided by Vita34, Leipzig, Germany. Umbilical cords were directly transferred to 4°C to preserve cell viability. The cord was cut into pieces of approximately 5 cm and washed in PBS and 1% gentamycin (Biochrom part of Merck Millipore, Berlin, Germany). Cord pieces were treated with 2.0 mg/ml dispase at 4°C overnight. Arteries and the vein were removed using a selfmade small hook comparable to a vein stripper. The vessel sections were washed in PBS with Mg and Ca, and treated with 0.05% Trypsin/0.53 M EDTA in Versene™ (Life Technologies, Darmstadt, Germany) at 37°C for up to 1 h. Vessel sections were transferred to EC media and scraped out to separate ECs from the tissue. The cell suspension was filtered using sterile nylon meshes with a pore size of 100 µm (Corning, Kaiserslautern, Germany) and

transferred to culture dishes. After 4 h, when ECs had attached, the medium was changed to remove unwanted cell types.

ECs were cultured in Endothelial Cell Growth Medium MV (ECGM; Promocell, Heidelberg, Germany) and 1% 10 000 U/10 000 µg penicillin/streptomycin (Life Technologies, Darmstadt, Germany). Primary ECs were seeded in a range of 10 000-20 000 cells/cm² and passaged at 70-90% confluence by exposing cells to 0.05% Trypsin/0.53 M EDTA (Carl Roth, Karlsruhe, Germany) for about 1 min and rinsing once in ECGM. The cell suspension was centrifuged at 200 g for 5 min. The cells were reconstituted in ECGM and seeded in a 1:2 split ratio every 7-10 d.

2.2.4. Culture of Human and Mouse Pluripotent Stem Cells

CGR8-S17 mouse ES cell line carrying a homologous dsRed-IRES-puromycin knock-in within the Sox17 locus was provided by Dr. Heinz Himmelbauer (Center for Genomic Regulation, Barcelona, Spain). Wild type CGR8 mouse ES cells can be obtained from Public Health England, Salisbury, UK. CGR8-S17 cells were cultured as describe previously (Schroeder et al., 2012) with minor modifications. In brief, cell grew on 0.1-1.0% gelatin-coated dishes (Sigma-Aldrich, Taufkirchen, Germany) in Glasgow Minimal Essential Medium (GMEM; PAA, Cölbe, Germany) supplemented with 10% FCS (Lonza, Köln, Germany), 0.05 mM beta-mercaptoethanol (BME), 2 mM L-glutamine, 1% sodium pyruvate, 1% 10 000 U/10 000 µg penicillin/streptomycin (all from Life Technologies, Darmstadt, Germany), and 1000 U/ml LIF (Peprotech, Hamburg, Germany). CGR8-S17 cells were seeded in a range of 2000-4000 cells/cm² and passaged at 70-80% confluence by exposing cells to 0.25% trypsin/0.01 M EDTA (Life Technologies, Darmstadt, Germany) for about 3 min and rinsing once in CGR8-S17 medium. The cell suspension was centrifuged at 200 g for 5 min. The cells were reconstituted in CGR8-S17 medium and seeded in a 1:4-1:10 split ratio every 3-5 d.

The WA09 (also known as H9) human ES cell line was obtained from the Wisconsin International Stem Cell Bank (WiCell Research Institute, Wisconsin, USA) and cultured according to manufacturer's instructions. In brief, the cells were cultured on inactivated feeder cells in Knockout™ DMEM (KO-DMEM) supplemented with 20% Knockout™ Serum Replacement (KOSR), 100 µM BME, 1 mM L-glutamine, 1% NEAA, 1% 10 000 U/10 000 µg penicillin/streptomycin (all from Life Technologies, Darmstadt, Germany), and 4.0 ng/ml FGF2 (Peprotech, Hamburg, Germany). Since human ES cells do not survive in single cell suspension, H9 cells were seeded as cell clumps and established colonies were passaged before they got into direct contact to each other by enzymatic and manual passaging. For enzymatic passaging, cells were treated with KO-DMEM supplemented with 1.0 mg/ml collagenase IV (Life Technologies, Darmstadt, Germany) for about 5-7 min at 37°C and rinsing once in KO-DMEM. The suspension was centrifuged at 200 g for 5 min. The cells were reconstituted in H9 medium. Manual passaging was required for long-term preservation of H9 cells. The cells were seeded in a 1:2-1:4 split ratio in a 4-10 d interval.

IMR90 iPS human pluripotent cells were obtained from the Wisconsin International Stem Cell Bank (WiCell Research Institute, Wisconsin, USA) and cultured according to protocols provided by the WiCell Research Institute. In brief, the cells were cultured on Matrigel™ using 0.5 mg in 6.0 ml KO-DMEM for coating of a 6-well plate (Fisher Scientific, Schwerte, Germany). Cells grew in mTeSR1™ (Stemcell Technologies, Köln, Germany) supplemented with 1% 10 000 U/10 000 µg penicillin/streptomycin (Life Technologies, Darmstadt, Germany). For distinct purposes, cells were also cultured on feeder cells in KO-DMEM supplemented with 20% KOSR, 100 µM BME, 1 mM

L-glutamine, 1% NEAA, 1% 10 000 U/10 000 µg penicillin/streptomycin (all from Life Technologies, Darmstadt, Germany), and 4.0 ng/ml FGF2 (Peprotech, Hamburg, Germany). Since human iPS cells do not survive in single cell suspension, IMR90 iPS cells were seeded as cell clumps and established colonies were passaged before they got into close contact to each other by enzymatic and manual passaging. For enzymatic passaging, cells were treated with DMEM/F12 supplemented with 2.0 mg/ml dispase (Life Technologies, Darmstadt, Germany) for about 3-5 min at 37°C and rinsing once in mTeSR1™. The suspension was centrifuged at 200 g for 5 min. The cells were reconstituted in mTeSR1™. Manual passaging was required for long-term preservation of IMR90 iPS cells. The cells were seeded in a 1:5-1:10 split ratio in a 4-10 d interval.

CF1 and B5 EGFP MEFs served as feeder cells for H9 and IMR90 iPS cells. MEFs were mitotically inactivated by treatment with MEF medium supplemented with 10.0 µg/ml mytomyacin C (Sigma-Aldrich, Taufkirchen, Germany) for 2-3 h and rinsing once with MEF medium. The cells were seeded on 0.1% gelatin-coated dishes (Sigma-Aldrich, Taufkirchen, Germany) in a range of 20 000-30 000 cells/cm². Primary CF1 MEFs were obtained from E13.5 embryos of pregnant CF1 mice (Charles River Laboratories, Wilmington, USA). Primary B5 EGFP MEFs were obtained from E13.5 embryos of pregnant B5 EGFP mice, which were provided by Prof. Dr. Anna M. Wobus (Department of Cytogenetics and Genome Analysis, Leibniz Institute of Plant Genetics and Crop Plant Research Gatersleben, Germany). MEFs were maintained until passage 3 cultured in DMEM (PAA, Cölbe, Germany) supplemented with 10% FCS (Lonza, Köln, Germany), 2 mM L-glutamine, 1% NEAA, and 1% 10 000 U/10 000 µg penicillin/streptomycin (Life Technologies, Darmstadt, Germany). MEFs were seeded in 3-5 10 cm dishes and passaged at 90% confluence by exposing cells to 0.25% trypsin/0.01 M EDTA (Life Technologies, Darmstadt, Germany) for 3-5 min and rinsing once in MEF medium. The cell suspension was centrifuged at 200 g for 5 min. The cells were reconstituted in MEF medium and seeded in a 1:3-1:5 split ratio in a 2-3 d interval.

MEF-conditioned medium was used for feeder-independent cultures and during reprogramming. Therefore, 10.0 ml H9 medium including 4.0 ng/ml FGF was given to mitotically inactivated CF1 MEFs seeded on 0.1% gelatin-coated 10 cm-dishes (Sigma-Aldrich, Taufkirchen, Germany) in a range of 50 000-60 000/cm². The media was collected after 24 h, filter sterilized, and stored at 4°C for up to 4 weeks.

2.3. Analysis of Gene Expression

2.3.1. Statistical Analysis

Variability of data following the normal distribution are presented as mean +/- standard deviation (SD) and differences were considered to be relevant with students T-test at $p < 0.05$ using Sigma Plot version 11.0 (Systat Software, Erkrath, Germany). A subset of data is presented as mean +/- standard error of the mean (SEM) describing the accuracy of the population mean rather than the variability of individual values.

2.3.2. Reverse Transcription

RNA isolation and deoxyribonuclease (DNase) treatment were performed using RNeasy® Mini Kit (Qiagen, Hilden, Germany) according to the manufacturer's protocol. When only a small sample size was available, RNA was isolated using the Dynabeads® mRNA Purification Kit (Life Technologies, Darmstadt, Germany) according to the manufacturer's manual. For RNA isolation from porcine 3D

biological matrices, these matrices were homogenized using a Precellys® 24 tissue homogenizer (Peqlab, Erlangen, Germany) according to manufacturer's instructions. RNA levels were quantified using a NanoVue™ spectrophotometer (GE Healthcare, München, Germany) and reverse transcribed into complementary DNA (cDNA). The reverse transcription reaction mix (20.0 µl) contained 0.5 µl ribonuclease (RNase) inhibitor, 1.0 µl 200 U/µl Revert Aid™ M-MuLV RT, 4.0 µl 5x buffer, 2.0 µl 10 mM deoxyribonucleotides (dNTPs), 1.0 µl 20 pmol/µl oligo (dt)₁₈ primers (all from Life Technologies, Darmstadt, Germany), and 11.5 RNase-free water including 2.0 µg RNA. The reaction was incubated at 65°C for 5 min, 42°C for 60 min, and 70°C for 10 min.

2.3.3. Semi-Quantitative Polymerase Chain Reaction (PCR)

The semi-quantitative PCR reaction mix (25.0 µl) contained 2.5 µl 10x buffer BD, 2.0 µl 25 mM MgCl₂, 2.0 µl 2.5 mM dNTPs, 0.25 µl 5 U/µl FIREpol® DNA polymerase (all from Solis Biodyne, Tartu, Estonia), 1.0 µl 10 pmol/µl forward and reverse primers (Biomers, Ulm, Germany) and RNase-free water including 1-3 µl template cDNA. PCR conditions were as follows: initial denaturation at 95°C for 5 min; 30-40 cycles of denaturation at 95°C for 45 sec, annealing at 57°C for 1 min, and extension at 72°C for 45 sec; final extension at 72°C for 10 min. Amplicons were separated in 1.5-2% agarose gels containing 0.5 µg/ml ethidium bromide. Electrophoresis was performed in a buffer solution with tris base, acetic acid, and EDTA (TAE). Amplicons were visualized by ultraviolet light. Semi-quantitative PCR primers (**APP. 17/18**) were designed using Primer3Plus online tool (<http://www.bioinformatics.nl>).

2.3.4. Quantitative Real-Time PCR (qRT PCR)

SYBR® Green-based qRT PCR was applied using the StepOnePlus™ Real-Time PCR System (Life Technologies, Darmstadt, Germany). Reaction plates, adhesive film, 8-tube stripes, and caps were also obtained from Life Technologies. Thermal cycling conditions were 95°C for 10 min, followed by 40 cycles of 95°C for 15 sec and 60°C for 1 min. A melt curve analysis was performed to ensure that the desired amplicon was detected. The specificity of the analyzed transcripts was also determined by gel electrophoresis using 2% agarose gels. The reaction mixture (20.0 µl) contained 4.0 µl 5x EvaGreen® reagent (Solis Biodyne, Tartu, Estonia), 10 pmol of each primer (Biomers, Ulm, Germany), RNase free water, and 1.0 µl template cDNA. All qRT PCR reactions were performed in triplicates and calculated relative to the endogenous control human 18S ribosomal RNA (18SrRNA) or mouse glyceraldehyde-3-phosphate dehydrogenase (Gapdh), whose expression did not change in the analyzed models. Template-free samples served as negative controls. Relative standard curve analysis was chosen for detection of transcript levels and standard deviation was calculated according to the StepOnePlus™ Real-Time PCR System manual (see manual appendix A-2 formulas). All qRT PCR primers (**APP. 19/20**) were designed using the software Primer Express® 3.0 (Life Technologies, Darmstadt, Germany).

TaqMan®-based qRT PCR was applied for more accurate analysis of the miR transfection protocol. TaqMan® Gene expression Assays (Life Technologies, Darmstadt, Germany) for the detection of Ptk9 (ID.Hs00702289_s1) and 18SrRNA (ID.Hs99999901_s1) are part of the Pre-miR™ miRNA Starter Kit (Life Technologies, Darmstadt, Germany), which was applied according to the manufacturer's protocol. Thermal cycling conditions were 50°C for 2 min, followed by 40 cycles of 95°C for 15 sec and 60°C for 1 min. The reaction mixture (20.0 µl) contained 10.0 µl 2x TaqMan® reagent, 1.0 µl 20x TaqMan® Gene expression Assay, RNase free water, and 1.0 µl template DNA.

2.3.5. Analysis of miR Expression Levels

Isolation of miRs and DNase treatment were performed using miRNeasy® MiniKit (Qiagen, Hilden, Germany) according to the manufacturer's protocol for purifying total RNA including miRs. Total RNA levels were quantified using a NanoVue™ spectrophotometer (GE Healthcare, München, Germany). For the detection of mature and pre-miRs, the miScript™ Reverse Transcription Kit (Qiagen, Hilden, Germany) allowed polyadenylation of miRs and subsequent template DNA synthesis with oligo (dt) priming. The reverse transcription reaction mix (20.0 µl) contained 1.0 µl miScript™ RT Mix, 4.0 µl 5x miScript™ RT Buffer, and RNase free water including 1.0 µg total RNA.

The miScript™ SYBR® Green PCR Kit (Qiagen, Hilden, Germany) was applied for SYBR® Green-based qRT PCR analysis according to the manufacturer's instructions. In brief, the StepOnePlus™ Real-Time PCR System (Life Technologies, Germany) was applied and a three-step-protocol was performed: 95°C for 15 min, followed by 40 cycles of 94°C for 15 sec, 55°C for 30 sec and 70°C for 30 sec. A melt curve analysis was performed to ensure that the desired amplicon was detected. The reaction mixture (20.0 µl) contained 10.0 µl miScript™ SYBR® Green, 1.0 µl universal forward primer, 1.0 µl specific reverse primer (specific for the respective miR/pre-miR), and RNase free water including 10.0 ng template cDNA. All qRT PCR reactions were performed in triplicates and calculated relative to the endogenous control small nucleolar RNA (snoRNA) U6B, which was shown to be unchanged in the analyzed models. Template-free samples served as negative controls. Specific reverse primers (miScript™ Primer Assays, miScript™ Precursor Assays) for the detection of miR-302a-d, pre-miR-302a-d, miR-372, pre-miR-372, and U6B were obtained from the Qiagen miScript™ Gene Globe online database (see www.qiagen.com/GeneGlobe). All reactions were performed in triplicate and normalized to the endogenous reference non-coding snoRNA U6B. Relative standard curve analysis and standard deviation were calculated according to the manufacturer's instructions (see miScript™ PCR System Handbook, Appendix B).

For the detection of pri-miRs, 5.0 µg of total RNA were applied for standard reverse transcription using a pri-miR-302-specific primer pair (**APP. 17**) for template DNA synthesis and subsequent semi-quantitative PCR as previously described by Suh and co-workers (Suh et al., 2004).

2.3.6. Cell Sorting and Flow Cytometry

Cell sorting of GFP-expressing L87 and BJ-5ta cells was performed after STEMcircles™ delivery. Cell suspensions were obtained by application of certain dissociation conditions also used for passaging of L87 and BJ-5ta cells. For cell sorting, about 1×10^6 cells/ml Hank's buffer containing 0.137 M NaCl, 5.4 mM KCl, 0.25 mM Na₂HPO₄, 0.44 mM KH₂PO₄, 1.3 mM CaCl₂, 1.0 mM MgSO₄, and 4.2 mM NaHCO₃ (all from Carl Roth, Karlsruhe, Germany) in deionized water were applied. Cells were filtered using sterile nylon meshes with a pore size of 100 µm (Corning, Kaiserslautern, Germany) and kept on ice until used. Cell sorting was carried out using a FACSVantage™ SE cell sorter (BD Biosciences, Heidelberg, Germany) operated by PD Dr. Dagmar Riemann, Department of Immunology, Medical Faculty, Martin Luther University Halle-Wittenberg, Germany. In every experiment, the forward scatter (FSC) was used to exclude events caused by cell debris. Cells were excited with a 488 nm argon ion laser. The GFP fluorescence (emission peak at 509 nm) was measured using a band pass filter at 530/30 nm. The sorting gates were set to sort GFP-positive cells. Sorted cells were centrifuged at 200 g for 5 min and reconstituted in the cell type-specific medium for further culture.

Flow cytometry for reliable quantification of STEMcirclesTM delivery and delivery of Cy3TM-labeled Anti-miRsTM into L87 and BJ-5ta cells was performed using a FACSCanto flow cytometer (BD Biosciences, Heidelberg, Germany). About 1×10^6 cells per ml were transferred to PBS. Cells were filtered using sterile nylon meshes with a pore size of 100 μm (Corning, Kaiserslautern, Germany) and kept on ice until use. The FSC was used to exclude events caused by cell debris. Non-viable cells were excluded by propidium iodide (PI) staining using 5.0 μg PI/ml cell suspension. The side scatter (SSC) was applied to exclude doublets. Cells were excited with a 488 nm argon ion laser to detect GFP and Cy3TM fluorescence. Cy3TM fluorescence intensity is lower than that of GFP, but Cy3TM is a small dye molecule suitable for conjugation with Anti-miRTM molecules. GFP fluorescence (emission peak at 509 nm) and the Cy3TM fluorescence (emission peak at 550 nm) were observed using the FL1 band pass filter at 530/30 nm. Data were processed using the CellQuest ProTM software provided by BD Biosciences, Heidelberg, Germany. The amount of positive cells was presented as % of vital gated cells. Additionally, data were presented in logarithmic values and the central tendency was measured by the geometric mean.

Flow cytometry of Ki67 stained L87 cells required staining of cell suspensions using mouse anti-Ki67 (Cat. No. 556003; BD Bioscience, Heidelberg, Germany) according to the manufacturer's instructions. Alexa Fluor® 488 chicken anti-mouse IgG (Cat. No. A-21200, Life Technologies, Germany) was used as a secondary antibody.

2.3.7. Immunocytochemistry

All immunocytochemical stainings were analyzed using a BZ-8100E fluorescence microscope (Keyence, Neu-Ilseburg, Germany).

2.3.7.1. Immunocytochemistry Using Monolayer Cultures

For immunofluorescence (IF) analysis of cells growing in monolayer cultures, these cells were seeded onto glass coverslips obtained from Menzel-Gläser part of Thermo Fisher Scientific, Braunschweig, Germany. The cells were fixed in 4% PFA (Appllichem, Darmstadt, Germany) for 20 min, washed in PBS, and permeabilized in 0.1% Triton® X-100 (Sigma Aldrich, Taufkirchen, Germany) and 1% mouse or goat serum (Life Technologies, Darmstadt, Germany) in PBS for 30 min. Non-specific binding was blocked with 5% serum for another 30 min. Primary antibodies were used at 4°C overnight. After washing three times in PBS, the secondary antibody was used at 37°C for 30 min. Cells were washed with PBS, stained for 5 min with 5.0 $\mu\text{g}/\text{ml}$ Hoechst 33342TM (Life Technologies, Darmstadt, Germany) in the dark and washed three times with PBS and once with distilled water. Afterwards coverslips were mounted upside down on glass slides using the Fluorescence Mounting Medium provided by Dako, Hamburg, Germany.

Pluripotency-associated antigens were detected using goat anti-Nanog (Cat. No. sc-30331, Santa Cruz, Heidelberg, Germany), mouse anti-Oct4 (Cat.No. sc-5279; Santa Cruz, Heidelberg, Germany), rabbit anti-Sox2 (Cat. No. AM09112PU-S; Acris, Herford, Germany) mouse anti-Tra-1-81 (Cat. No. ab16289; Abcam, Cambridge, UK), mouse anti-c-Myc (Cat. No. sc-40; Santa Cruz, Heidelberg, Germany), mouse anti-Lin28 (Cat. No. AM1485a; Biomol, Hamburg, Germany), rabbit anti-Rex1 (Cat. No. ab28141; Abcam, Heidelberg, Germany), mouse anti-SSEA4 (Cat.No. sc21704; Santa Cruz, Heidelberg, Germany), and mouse anti-SSEA1 (Cat. No. sc21702; Santa Cruz, Heidelberg, Germany).

The status of differentiation was characterized according to the presence of lineage-associated antigens detected using rat anti-Cxcr4 (Cat. No. MAB21651; R&D Systems, Wiesbaden, Germany), mouse anti-Tubb3 (Cat. No. MAB1637; Merck Millipore, Darmstadt, Germany) rabbit anti-Bra (Cat. No. ab20680; Abcam, Cambridge, UK), rabbit anti-Foxa2 (Cat. No. AB4125; Merck Millipore, Darmstadt, Germany), mouse anti-Sox17 (Cat.No. ab84990; Abcam, Cambridge, UK), and rabbit anti-Pdx1 (Cat.No. ab47267; Abcam, Cambridge, UK).

Primary ECs were characterized according to the presence of cell type-associated antigens using mouse anti- vWF (Cat. No. M0616; Dako, Hamburg, Germany), mouse anti-VEcad (Cat. No. AF1002; R&D Systems, Wiesbaden, Germany), goat anti-Pecam1 (Cat. No. sc-1506; Santa Cruz, Heidelberg, Germany), and goat anti-Vegfr2 (Cat. No. ab10972; Abcam, Cambridge, UK).

The secondary antibodies Alexa Fluor® 488 goat anti-mouse IgG (Cat. No. A11001; Life Technologies, Darmstadt, Germany), Alexa Fluor® 488 goat anti-rat IgG (Cat. No. A11006; Life Technologies, Darmstadt, Germany), Alexa Fluor® 488 chicken anti-rabbit IgG (Cat. No. A21441; Life Technologies, Darmstadt, Germany), Dylight® 488 donkey anti-goat IgG (Cat. No. 705485147; Dianova, Hamburg, Germany), and FITC goat anti-mouse IgM (Cat. No. sc-2082; Santa Cruz, Heidelberg, Germany) were used.

The Alkaline Phosphatase Detection Kit (Merck Millipore, Darmstadt, Germany) was used for alkaline phosphatase (AP) staining following the manufacturer's instructions.

2.3.7.2. Immunocytochemistry Using Matrices

Immunocytochemistry of cells grown on 3D biological matrices required the preparation of paraffin sections. Briefly, Matrices were fixed in 4% PFA (Applichem, Darmstadt, Germany) for 20 min and stored in 70% ethanol. Dehydration and paraffinization was processed using the automated Citadel™ tissue processor 2000 (Thermo Fisher Scientific, Karlsruhe, Germany). Matrices were dehydrated once in 70%, 80%, 90%, 96% ethanol for 2 h, twice in isopropanol for 1 h, and twice in Histo-Clear™ (Biozym, Hessisch Oldendorf, Germany) for 2 h. Subsequently, matrices were embedded into Paraplast® paraffin (VWR, Darmstadt, Germany) supplemented with 5% bees wax provided by a local beekeeper. Paraffin blocks were prepared using a DDM-P064 embedding center (Medim, Buseck, Germany). 5-10 µm thick tissue sections were obtained using a DDM-0013 rotary microtome (Medim, Buseck, Germany). Sections floating in a water bath were transferred onto microscope slides, and stored at RT. For deparaffinization, sections were placed in an oven at 60°C overnight. Rehydration was manually done by placing sections twice in Histo-Clear™ (Biozym, Hessisch Oldendorf, Germany) for 10 min, once in 96%, 90%, 80%, 70%, 60%, 50% ethanol for 5 min, and once in deionized water for 5 min. Rehydrated sections were applied for IF and cytological analysis.

IF analysis of paraffin-embedded sections required heat-mediated antigen retrieval at 90°C for 20 min in 10 mM citrate buffer pH6.0 or the commercially available citrate buffer Target Retrieval Solution (Dako, Hamburg, Germany). Sections were circled using a hydrophobic barrier Pen (Dako, Hamburg, Germany) and stained according to the procedure described for IF analysis as described earlier.

For cytological analysis of paraffin sections, a hematoxylin and eosin stain (HE) was performed without antigen retrieval. In brief, hemalum was produced according to the Mayer's protocol (0.5 g hematoxylin, 0.1 g sodium iodate, 25.0 g potassium aluminum sulfate, 25.0 g chloral hydrate, 0.5 g citric acid all obtained from Carl Roth, Karlsruhe, Germany in 500.0 ml deionized water) and sections

were placed for 5 min in hemalum. Afterwards, sections were washed with running tap water for 5 min. Sections were also stained with 1% eosin in deionized water for 10 min. After staining, sections were dehydrated again by placing them one time in 50%, 60%, 70%, 80%, 90%, 96% ethanol for 5 min and 2 times in Histo-Clear™ (Biozym, Hessisch Oldendorf, Germany) for 10 min. Sections were embedded with Histomount™ (Biozym, Hessisch Oldendorf, Germany).

Viable and dead cells on matrices were distinguished after staining with the Live/Dead Cell Staining Kit II (Promocell, Heidelberg, Germany) according to the manufacturer's instructions.

Scanning electron microscopy (SEM) was performed for the detailed analysis of cells within 3D biological matrices. Dehydration and fixation were done according to standard protocols, which were shown to be also suitable for SEM of embryonic cells (Vera et al., 2013). Briefly, matrices were fixed in modified Carnoy containing a 6:2:2 (v/v/v) mixture of ethanol, chloroform, and acetic acid for 15 min. Matrices were dehydrated once in 70%, 80%, 90%, 95%, 99.8% ethanol for 15 min. Next, matrices were dried with 1:1 (v/v) mixture of 99% hexamethyldisilazane and 99.8% ethanol (Sigma-Aldrich, Taufkirchen, Germany) for 5 min. Matrices were ion covered with 10 nm gold and examined using a scanning electron microscope operated by Angelika Steller, Department of Zoology, Faculty I of Natural Science, Martin Luther University Halle-Wittenberg, Germany.

2.3.7.3. Western Blot (WB) Analysis

Cells were harvested and washed in PBS. Cells were lysed in 860.0 µl radioimmunoprecipitation assay (RIPA) buffer containing 50 mM tris-HCl pH8.0, 150 mM NaCl, 1% NP40, 0.1% sodium dodecyl sulfate (SDS), and 0.5% sodium deoxycholate (all from Carl Roth, Karlsruhe, Germany) in deionized water supplemented with 40.0 µl 25x protease inhibitor and 100.0 µl 10x phosphatase inhibitor (both from Roche, Mannheim, Germany). Lysates were put on ice for 30 min and vortexed every 10 min. The resulting mixture was centrifuged and the supernatant was collected containing total protein. Protein was processed using the Protein Assay Dye Reagent Concentrate (Bio-Rad, München, Germany) according to manufacturer's instructions and concentration was determined using an Ultraspec™ 3300 Pro spectrophotometer (GE Healthcare, München, Germany).

30-60 µg protein was mixed with 2x Laemmli loading buffer containing 4% SDS, 10% BME, 20% glycerol, 0.004% bromophenol blue and 0.125 M tris-HCl pH6.8 (all from Carl Roth, Karlsruhe, Germany). The mixture was heated at 90°C for 5 min. Samples were separated in 10% acrylamide resolving gels by SDS-polyacrylamide gel electrophoresis (SDS-PAGE). The resolving gel was prepared by mixing 3.3 ml 30% acrylamide, 4.2 ml deionized water, 2.5 ml tris-SDS solution 2 (36.3 g tris base and 8.0 ml 10% SDS in 200.0 ml deionized water pH8.8, 20.0 µl tetramethylethylenediamine (TEMED), and 100.0 µl ammonium persulfate (APS; all from Carl Roth, Karlsruhe, Germany). The stacking gel was prepared by mixing 1.0 ml 99% acrylamide, 6.5 ml deionized water, 2.5 ml tris-SDS solution 3 (6.0 g tris base, 4.0 ml 10% SDS in 200.0 ml deionized water pH6.8), 20.0 µl TEMED, and 100.0 µl APS. Laemmli running buffer (10x buffer contained 30.25 g tris base, 144.25 g glycine, 10.0 g SDS in 1000.0 ml deionized water) was prepared and electrophoresis was performed using the XCell SureLock™ Mini-Cell Electrophoresis System (Life Technologies, Darmstadt, Germany) according to manufacturer's general protocol.

The proteins were electrotransferred from the gels onto Whatman Protran® nitrocellulose membranes (Sigma-Aldrich, Taufkirchen, Germany) using the XCell II™ Blot Module electroblotting apparatus (Life Technologies, Darmstadt, Germany) according to manufacturer's general instructions.

The blotting buffer was prepared by mixing 80.0 ml 12.5x blotting buffer stock solution (18.2 g tris base, 90.0 g glycine in 1000.0 ml), 2.0 ml 10% SDS, and 200.0 ml methanol in 1000.0 ml deionized water). Successful protein transfer was confirmed using 0.1% Ponceau S red staining solution in 5% acetic acid (Carl Roth, Karlsruhe, Germany) suitable for nitrocellulose membranes.

Non-specific binding was blocked with 5% Sucofin powdered milk (local drugstore) in tris-buffered saline and 1% Tween20 (TBS-T; Carl Roth, Karlsruhe, Germany) for 1 h on a vortex platform. Primary antibodies were used at 37°C for 1 h. The primary antibodies mouse anti-beta-Actin (Cat. No. A5441; Sigma-Aldrich, Taufkirchen, Germany), mouse anti-Dnmt3b (Cat. No. 211MG184; AMS Biotechnology, Wiesbaden, Germany) and mouse anti-Dnmt1 (Cat. No. H00001786M01; Abnova, Heidelberg, Germany) were used. After washing in TBS-T, membranes were incubated with the secondary antibody diluted in 1% bovine serum albumin in PBS (BSA; Applichem, Darmstadt, Germany) at 37°C for 2 h. As a secondary antibody, horseradish peroxidase (HRP) conjugated goat anti-mouse IgG (Cat. No. 115036003; Dianova, Hamburg, Germany) was used. After washing in TBS-T and TBS, Immobilon™ Western Chemiluminescent HRP Substrate (Merck Millipore, Darmstadt, Germany) was applied for chemi-luminescent detection of proteins according to manufacturer's instructions. Membranes were treated with a stripping-buffer containing 20.0 ml 10% SDS, 12.5 ml 1.0 M tris-HCl pH6.8, and 700.0 µl BME (Carl Roth, Karlsruhe, Germany) in 100.0 ml deionized water for the detection of the loading control beta-Actin. Densitometric analysis was done using a Fusion-FX7™ chemiluminescence detector (Peqlab, Erlangen, Germany).

2.4. Reprogramming

Non-viral reprogramming of L87 MSCs and BJ-5ta fibroblasts was attempted by single application or subsequent application of

- episomal reprogramming vectors carrying ONSL,
- human ES-cell specific miR-302a-d & 372,
- and/or treatment with small molecules

under human ES cell-specific culture conditions described earlier. Epigenetic modulators, signal transduction inhibitors, and kinase inhibitors were obtained from Biocat, Heidelberg, Germany. These molecules were applied according to manufacturer's instructions. For another approach, NutriStem™ iPS and ES cell medium was obtained from Miltenyi, Bergisch Gladbach, Germany.

2.4.1. Transfection of Episomal Vectors

For induction of reprogramming, STEMcircles™ episomal expression vectors (Stemcell Technologies, Köln, Germany) were transfected by lipofection using INTERFERRin™ (Peqlab, Erlangen, Germany) according to manufacturer's guidelines. Endogenous ONSL expression was analyzed using specific primers, which exclude STEMcircles™-derived, exogenous ONSL expression (**APP. 17**). Different transfection approaches for the delivery of STEMcircles™ were analyzed using a pEGFP-N1 reporter vector (Clontech, Heidelberg, Germany). Lipofection studies included Lipofectamine™ 2000 and Lipofectamine™ LTX & Plus™ transfection reagents (Life Technologies, Darmstadt, Germany) applied according to manufacturer's instructions. Electroporation was performed using a Gene Pulser® II electroporation system (Bio-Rad, München, Germany) and pulse duration and/or electric field strength were adjusted according manufacturer's instructions.

2.4.2. Transfection of Synthetic miRs

For the analysis of the transfection procedure, the Pre-miRTM miRNA Precursor Starter Kit (Life Technologies, Darmstadt, Germany) was applied according to the provided manual. The Kit includes siPORTTM and NeoFXTM transfection reagents, which were applied in competitive studies. The Kit also contains the Ambion Pre-miRTM miRNA Precursor of miR-1 (ID PM10617) and a negative control miR (ID AM17110) without any mouse or human mRNA target gene. Delivery of miR-1 was also performed using the TurbofectTM transfection reagent (Thermo Fisher Scientific, Karlsruhe, Germany) according to manufacturer's instructions.

For induction of reprogramming, Ambion Pre-miRTM miRNA Precursors of miR-302a-d & 372 (IDs PM10936, PM10081, PM10571, PM10927, PM10165) were transfected by lipofection using INTERFERInTM (Peqlab, Erlangen, Germany) according to manufacturer's guidelines. For repression of miR-302a, the mirVanaTM miRNA inhibitor of miR-302a (ID MH10936; Life Technologies, Darmstadt, Germany) was transfected also using INTERFERInTM (Peqlab, Erlangen, Germany).

2.4.3. Analysis of DNA Methylation

DNA methylation was quantified by real-time PCR using the OneStep qMethylTM Kit (Zymo Research, Freiburg, Germany) according to manufacturer's instructions. Human methylated and non-methylated DNA was applied in pilot studies to determine the accuracy of the OneStep qMethyl Kit procedure. Oct4 promoter methylation was analyzed using primers detecting a CpG-rich promoter region (**APP. 19**).

Genomic DNA was isolated using phenol-chloroform isoamyl alcohol DNA extraction. In brief, cells were harvested and washed in PBS. The cells were lysed in 400.0 µl extraction buffer containing 50 mM tris-HCl pH7.6, 25 mM EDTA disodium salt dehydrate, 0.5% NP40, and 0.5% SDS in deionized water (all from Carl Roth, Karlsruhe, Germany). The lysate was supplemented with 15.0 µl of a 20.0 µg/ml proteinase K solution (Thermo Fisher Scientific, Karlsruhe, Germany) and placed at 56°C for 3 h. Afterwards, the lysate was supplemented with an equal volume (400 µl) of phenol, gently mixed for 5 min, and centrifuged for 10 min at 13 000 rpm. The aqueous phase of approximately 400 µl was carefully removed and supplemented with a 25:24:1 (v/v/v) mixture of phenol, chloroform and isoamylalcohol. The obtained suspension was vortexed vigorously and centrifuged again. The aqueous phase of approximately 400 µl was carefully removed and supplemented with 400.0 µl chloroform. The obtained mixture was vortexed vigorously and centrifuged again. The supernatant was collected and DNA was precipitated with 1/10 volume of 3 M sodium acetate in deionized water and 1 volume isopropanol. The mixture was centrifuged and washed with 70% ethanol. The dried DNA pellet was resolved in 100.0 µl tris-EDTA buffer (TE) containing 10 mM tris-HCl pH7.5-8.0 and 1 mM EDTA in deionized water. Subsequently, the obtained DNA was treated with 2.0 µl of 10.0 mg/ml RNase (Thermo Fisher Scientific, Karlsruhe, Germany) at 37°C for 10 min.

DNA in 100.0 µl TE was processed using DNA Clean & ConcentratorTM Kit (Zymo Research, Freiburg, Germany) and diluted again in 100.0 µl deionized water. 20.0 ng of DNA were treated with restriction enzymes (test) or mock-digested (reference). DNA was digested with Hin6I und HpaII methylation-sensitive restriction enzymes (MRSEs; Thermo Fisher Scientific, Karlsruhe, Germany) at 37°C for 2 min. The test and reference samples were placed in a StepOnePlusTM Real-Time PCR System (Life Technologies, Darmstadt, Germany). The reaction mixture (20.0 µl) contained 5.0 µl test or reference DNA, 4.0 µl EvaGreen® reagent (Solis BioDyne, Tartu, Estonia), 10 pmol of each primer

(Biomers, Ulm, Germany), and RNase free water (Life technologies, Germany). All qRT PCR reactions were performed in triplicates. Template-free samples served as negative controls. Reaction plates, adhesive film, 8-tube stripes and caps were obtained from Life Technologies, Darmstadt, Germany. Thermal cycling conditions were 95°C for 10min, followed by 40 cycles of 95°C for 15 sec, 54°C for 1 min, and 72°C for 1 min. A melt curve analysis ensured that the desired amplicon was detected. The specificity of the analyzed transcripts was proven by gel electrophoresis using 2% agarose gels. Relative standard curve analysis was chosen for detection of ΔC_t values (C_t test – C_t reference) similar to calculating differences in a standard qRT PCR. The percentage of methylation (percentage = $100 \times 2^{-\Delta C_t}$) was calculated. The standard deviation was calculated according to manufacturer's manual of the StepOnePlus™ Real-Time PCR System (see appendix A-2 formulas).

2.4.4. Luciferase Assay

A luciferase assay was used to evaluate miR-302a-d & 372 by the insertion of an associated target site (present in Dnmt1) 3' of the firefly luciferase gene. Reduced firefly luciferase expression indicates the binding of miRs to the cloned miR target sequence.

The empty pmiRGLO Dual Luciferase miRNA Target Expression Vector, the Dual-Glo® Luciferase Assay System, and JM109 *Escherichia coli* cells (all from Promega, Mannheim, Germany) were applied according to manufacturer's protocols with minor modifications. Briefly, the pmiRGLO vector was isolated from JM109 cells using the peqGOLD Plasmid Miniprep Kit I (Peqlab, Erlangen, Germany). Oligonucleotides were synthesized as single stranded DNA by Biomers, Ulm, Germany. Both oligonucleotides (each 100 pM) were resuspended in TE buffer. For annealing of oligonucleotides, a mix at equimolar concentration (both 100 pM) was placed in a standard thermal cycler. Thermal cycling conditions were 95°C for 2 min followed by ramp cool to 37°C over a period of 45 min. This procedure generated double stranded DNA ready for ligation into the pmiRGLO vector. Approximately 1 µg of the empty pmiRGLO was linearized by MspI and XbaI restriction enzymes using the 10x recommended buffer (Thermo Fisher Scientific, Karlsruhe, Germany). Ligation was performed using 50.0 ng linearized vector, 4.0 ng annealed oligonucleotides, 1.0 µl 1-3 U/µl T4 DNA Ligase, and ligase buffer (both from Promega, Mannheim, Germany). For the analysis of Dnmt1, the pmiRGLO-Dnmt1, pmiRGLO-nonsense, and pmiRGLO-302a vectors (**APP. 21**) were generated and transferred into JM109 competent cells. Ampicillin-resistant clones were analyzed for successful ligation using the unique NotI restriction site within the designed oligonucleotides. L87 cells (3000/cm²) were transfected with pmiRGLO-Dnmt1 and miR-302a-d & 372 using jetPRIME™ transfection reagent (Peqlab, Erlangen, Germany) suitable for co-transfection of plasmids and miRs according to manufacturer's protocol. Transfection was performed in triplicates within an opaque and white 96-well plate (Greiner Bio-One, Frickenhausen, Germany). 24 h after transfection, cells were analyzed for luciferase activity measured by Dual-Glo® Luciferase Assay System (Promega, Mannheim, Germany) using a monochromator-based Tecan Infinite® M200 microplate reader (Tecan, Crailsheim, Germany). Firefly luciferase activity of pmiRGLO-Dnmt1-transfected cells was normalized (firefly luciferase/*renilla* luciferase) and compared to positive and negative controls.

2.5. Pancreatic Differentiation Models

Different pancreatic differentiation models were applied to study the impact of ECs and 3D biological matrices on mouse and human pluripotent stem cells. These models applied

- mouse ES cells on 3D matrices
- and human ES and iPS cells in the presence of ECs or a 3D co-culture environment

for the development of a 3D pancreatic differentiation model.

2.5.1. Production of Porcine Matrices

Porcine small intestines were obtained from suckling pigs or growth-restricted pigs kindly provided by a local slaughterhouse. Decellularized matrices were generated according to a protocol published by Schanz and co-workers with minor modification (Schanz et al., 2010). In brief, the porcine jejunum was separated from the intestine and flushed with PBS. The mesentery was removed. The jejunum was cut into segments of approximately 10 cm. Segments were turned inside out and the mucosa was scraped off manually. Segments were ligated at one end and filled with decellularization solution containing 4% sodium deoxycholate (Carl Roth, Karlsruhe, Germany) in PBS, ligated at the other end as well, and incubated in 1.0 l decellularization solution at 4°C for 1.5 h while being stirred constantly. Afterwards, tissues residues were removed. Segments were washed thrice in PBS containing 1% gentamycin (Biochrom part of Merck Millipore, Berlin, Germany) and kept at 4°C in PBS with 1% gentamycin overnight. Sterilization and inactivation of antibiotics were achieved by 20.1-30.3 kGy of electron-beam irradiation using an electron emitter operated by Dr. Wolfgang Knolle, Leibnitz-Institut für Oberflächenmodifikation, Leipzig, Germany. The matrices were stored at 4°C for several months.

2.5.2. Generation of Mouse Pancreatic Progenitors

CGR8-S17 mouse ES cells were differentiated into pancreatic progenitors according to the protocol recently provided by Schroeder and co-authors with minor modifications (Schroeder et al., 2012). Briefly, CGR8-S17 cells were differentiated by 3 different approaches. They were cultured in hanging drops or directly transferred onto matrices using media suitable for spontaneous and directed pancreatic differentiation (**FIG. 7**).

EB formation generating spontaneous pancreatic progenitors was initiated using spontaneous differentiation medium (see also **APP. 22**). This control medium is a 1:1 (v/v) mixture of Iscove's modified Dulbecco's medium (IMDM) and Ham's F-12 containing 2.5 mM L-glutamine (PAA, Cölbe, Germany) supplemented with 1% NEAA (Life Technologies, Darmstadt, Germany), 450 µM monothioglycerol (Sigma-Aldrich, Taufkirchen, Germany), and 20% FCS (Lonza, Köln, Germany). EB formation for the directed pancreatic differentiation was performed using a CDM (see also **APP. 22**) supplemented with by 50.0 ng/ml activin A (Peprotech, Hamburg, Germany). CDM is a 1:1 (v/v) mixture of IMDM and Ham's F12 containing 2.5 mM L-glutamine (Life Technologies, Darmstadt, Germany). The mixture was supplemented with 2 U/ml LIF (Peprotech, Hamburg, Germany), 1% chemically defined lipid concentrate (Life Technologies, Darmstadt, Germany), 450 µM monothioglycerol, 5.0 mg/ml BSA, 150.0 µg/ml transferrin, and 7.0 µg/ml insulin (Sigma-Aldrich, Taufkirchen, Germany).

EB formation was achieved in hanging drops containing 600 cells/20.0 µl CDM or control medium for 3 d. For the formation of EBs in CDM, CGR8-S17 cells were washed in CDM before use. Next, cells were cultured in bacteriological dishes using CDM or control medium for additional 5-7 d

depending on the occurrence of Sox17-DSred-positive cells. EBs were treated with Accutase® (Sigma-Aldrich, Taufkirchen, Germany) and dissected using a gentleMACS™ dissociator (Miltenyi, Bergisch Gladbach, Germany) according to the manufacturer's instructions for automated dissociation of up to 7 days old EBs.

For 2D culture conditions, DE progenitors obtained from EB dissociation at day 8-10 were replated onto poly-L-ornithine/laminin-coated dishes. For proper attachment of dissociated cells, 20% FCS supplementation was applied immediately after seeding for 1 d. Dishes were incubated with 0.1 mg/ml poly-L-ornithine in 10 mM sodium borate buffer pH8.4 (Sigma-Aldrich, Taufkirchen, Germany) for 3 h at 37°C, washed and dried at RT. Coating with 1.0 mg/ml laminin in PBS (Sigma-Aldrich, Taufkirchen, Germany) for 1 h was applied immediately prior to the use of the culture dishes.

DE progenitors were further differentiated into the pancreatic lineage using pancreatic differentiation medium (PDM; **APP. 22**) containing a 1:1 (v/v) mixture of IMDM and Ham's F12 containing 2.5 mM L-glutamine, 1% NEAA (Life Technologies, Darmstadt, Germany), 450 µM monothioglycerol (Sigma-Aldrich, Taufkirchen, Germany), and 2% FCS (Lonza, Köln, Germany). PDM1 was supplemented with 0.75 µM 3-Keto-N-(aminoethyl-aminocaproyl-dihydrocinnamoyl)-cyclopamine (KAAD-cyclopamine) (Merck Millipore, Darmstadt, Germany) and 300 nM indolactam V (Sigma-Aldrich, Taufkirchen, Germany) until day 12-14. Treatment with 0.75 µM KAAD-cyclopamine and 1 µM RA (Sigma-Aldrich, Taufkirchen, Germany) was applied in the presence of low glucose (1.0 g/l) until day 18-20 in PDM2. Terminal PDM3 was applied until day 30 containing a 1:1 (v/v) mixture of IMDM and Ham's F12 with 2.5 mM L-glutamine supplemented with 20 nM progesterone, 100 µM putrescine, 1.0 µg/ml laminin, 25.0 µg/ml insulin, 30 nM sodium selenite, 10 mM nicotinamide (Sigma-Aldrich, Taufkirchen, Germany), 50.0 µg/ml transferrin, B27® supplement (Life Technologies, Darmstadt, Germany), and 2% FCS (Lonza, Köln, Germany).

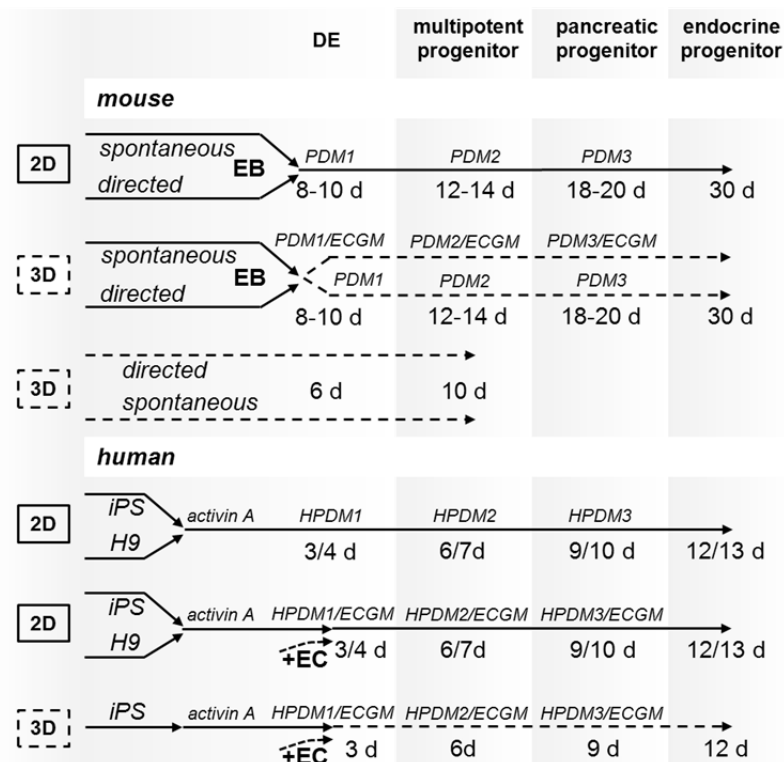


FIGURE 7: Mouse and human pancreatic differentiation models applied in the present study.

For 3D culture conditions, DE progenitors obtained from EB dissociation at day 8-10 were replated onto 3D biological matrices. Attachment in the presence of 20% FCS was not required. DE progenitors were differentiated in PDM or a 1:1 (v/v) mixture of PDM and ECGM as described for 2D culture conditions. Importantly, the PDM/ECGM medium contained PDM supplements in equimolar concentrations as described above.

For another approach of 3D culture conditions, ES cells were passaged onto matrices without EB formation. Cells were cultured in spontaneous differentiation medium or in CDM containing 50.0 ng/ml activin A (PeproTech, Hamburg, Germany), 100.0 ng/ml Nodal (R&D Systems, Wiesbaden, Germany), or 5 μ M inducer of definitive endoderm 1 and 2 (IDE1/2) (Miltenyi, Bergisch Gladbach, Germany).

2.5.3. Generation of Human Pancreatic Progenitors

Pancreatic differentiation of IMR90 iPS and H9 ES cells was performed without EB formation according to the protocols recently provided by D'Amour, Kroon, and co-authors with minor modifications (D'Amour et al., 2006; Kroon et al., 2008) and adjusted to 3D co-culture conditions (**FIG. 7**). Briefly, IMR90 iPS and H9 ES cells were seeded at a high density onto MatrigelTM-coated dishes (0.5 mg/6-well plate; Fisher Scientific, Schwerte, Germany) for 1 d prior to differentiation using mTeSR1TM (Stemcell Technologies, Köln, Germany) or MEF-conditioned media supplemented with 4.0 ng/ml FGF2 (PeproTech, Hamburg, Germany). Cells were treated with RPMI (Life Technologies, Darmstadt, Germany) supplemented with 2 mM L-glutamine, 1% 10 000 U/10 000 μ g penicillin/streptomycin (Life Technologies, Darmstadt, Germany), and 100.0 ng/ml activin A (PeproTech, Hamburg, Germany) for 1 d. Next, media was modified to contain 0.2% FCS (Lonza, Köln, Germany) in addition to the above mentioned components and applied for additional 2-3 d. Thus, DE progenitors were obtained at day 3-4.

For further differentiation, DE progenitors were cultured in human pancreatic differentiation medium (HPDM; **APP. 22**). HPDM1 was applied for another 3 d and comprised of RPMI-1640 (Life Technologies, Darmstadt, Germany) supplemented with 0.25 μ M KAAD-cyclopamine (Merck Millipore, Darmstadt, Germany), 50.0 ng/ml FGF10, 50.0 ng/ml human VEGFa (PeproTech, Hamburg, Germany), and 2% FCS (Lonza, Köln, Germany). Next, cells were cultured for 3 d in HPDM2 containing DMEM (PAA, Cölbe, Germany) supplemented with 0.25 μ M KAAD-cyclopamine, 50.0 ng/ml FGF10, 50.0 ng/ml human VEGFa, B27[®] supplement (Life Technologies, Darmstadt, Germany), 2 μ M RA (Sigma-Aldrich, Taufkirchen, Germany), and 10 μ M dorsomorphin (Miltenyi, Bergisch Gladbach, Germany). Finally, cells grew in until day 30 in HPDM3 containing DMEM supplemented with human VEGFa and B27[®] supplement. Medium was changed every third day.

For 2D differentiation under co-culture conditions, DE progenitors were removed from the culture dishes using 0.25% trypsin/0.53 mM EDTA (PAA, Cölbe, Germany/Carl Roth, Karlsruhe, Germany). About 1×10^6 DE progenitors were seeded with or without about 5×10^4 ECs onto 0.5% gelatin-coated dishes. Co-cultures were kept in a 1:1 (v/v) mixture of HPDM and ECGM as described for the further differentiation of DE progenitors. Importantly, the HPDM/ECGM medium contained HPDM and supplements in equimolar concentrations as described above.

For 3D culture and co-culture conditions, DE progenitors were removed from the culture dishes using 0.25% trypsin/0.53 mM EDTA (PAA, Cölbe, Germany/Carl Roth, Karlsruhe, Germany) and seeded onto 3D biological matrices. Cells were seeded and cultured as described for co-culture conditions.

3. RESULTS

The analysis of non-viral reprogramming methods and pancreatic differentiation in 3D biological matrices aimed at the establishment of an organotypic model examining onset, progress, and treatment of diabetes (predominantly of T2DM) *in vitro*. However, (i) isolation of human donor cells, (ii) creation of a non-viral reprogramming strategy, (iii) search for 3D biological matrices suitable to be used for pancreatic *in vitro* differentiation and (iv) the subsequent adjustment of differentiation protocols was required.

3.1. Acquisition of Human Donor Cells - Isolation of Primary Keratinocytes

Isolation of human donor cells was restricted to cell types, capable to be excised without surgery from human beings. According to that, isolation and propagation of keratinocytes from the outer root sheath (ORS) of plucked anagen hairs was desired to be an adequate method to obtain human donor cells. About 30-50 hairs were plucked from 6 healthy donors representing 3 groups of patients: (n=1) male <30 years, (n=4) female <30 years, and (n=1) female >30 years (**FIG. 8 A**). Plucking was repeated about 3 to 5 times for each subject. Hairs with outgrowing keratinocytes were successfully cultured using a liquid-air interface (**FIG. 8 B-D**). However, the number of outgrowing cells differed between donors (**FIG. 8 E-G**). This observation was independent of sex or age of the donors. There were 2 female donors (n=1 <30 and n=1 >30), which reproducibly showed less hairs with outgrowing

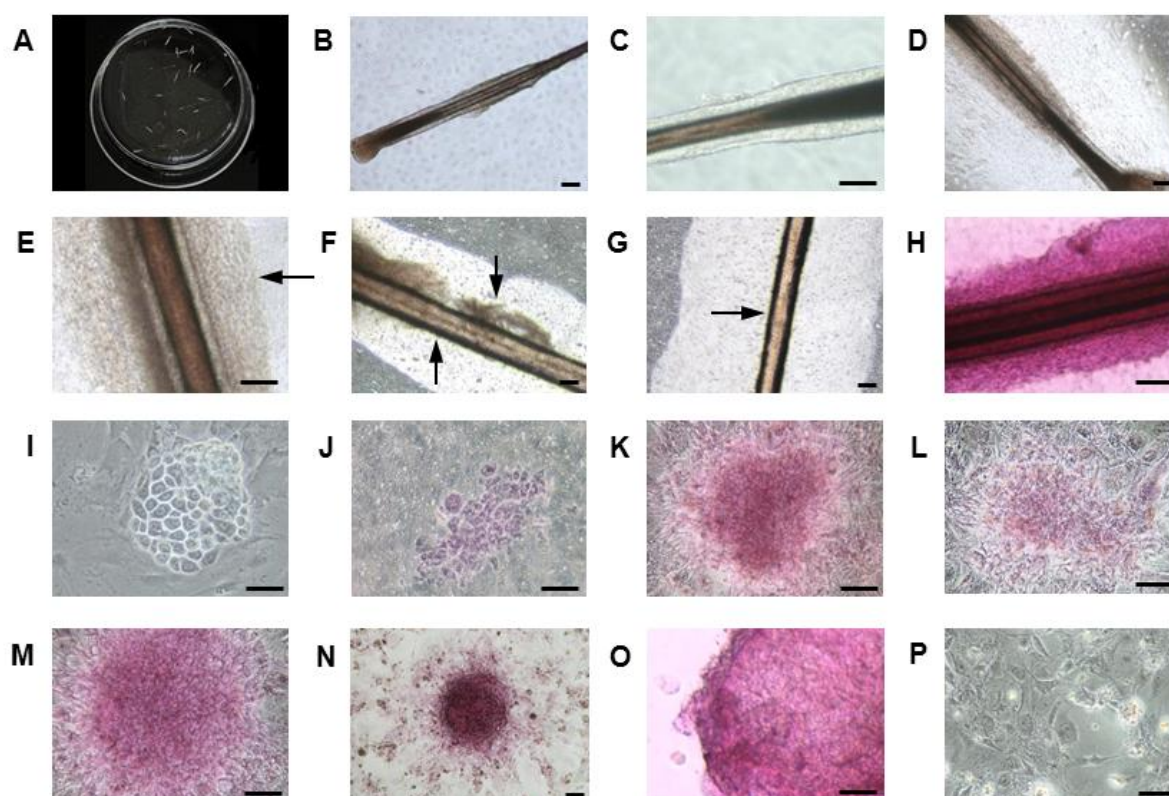


FIGURE 8: Primary keratinocytes obtained from human plucked hair. (A) Hairs are shown immediately after plucking. **(B/C)** Hairs are shown seeded on well plate inserts allowing the application of a medium-air-interface. **(D)** Proliferating keratinocytes are demonstrated at day 10. The picture shows a sample with prominent outgrowth of cells. **(E-G)** The number of ORS-derived keratinocytes differed between donors demonstrated at day 20 (arrows). **(H)** Rhodamine B staining of ORS-derived keratinocytes. **(I)** Primary keratinocytes are shown on 3T3-L1 feeder cells. The typical morphology is demonstrated one day after removal from hairs. **(J-N)** Morphological analysis of rhodamine B-stained colonies demonstrating the presence of keratinocytes with high and low proliferation potential. The morphology of proliferating holoclones (J) and growth-restricted meroclones (K, L, M) and paraclones (N) is shown. **(O-P)** Murine skin and 3T3-L1 MEFs served as controls. Bars represent 100 μm .

keratinocytes and a lower number of ORS-derived cells. Detection of keratins by rhodamine B staining demonstrated the presence of ORS-derived keratinocytes (**FIG. 8 H**) while hairs without proliferating keratinocytes were not stained. After 2 to 3 weeks, cells were transferred onto 3T3-L1 feeder cells. Keratinocytes were identified by their cobblestone morphology (**FIG. 8 I**). Rhodamine B staining confirmed the preservation of primary keratinocytes on feeder cells (**FIG. 8 J-N**). A culture of primary keratinocytes is composed of stem cells (holoclones) and cells with lower proliferation potential (meroclones and paraclones). The typical morphology of these different keratinocytes was observed. There were a few holoclonal colonies preserving the typical cobble stone morphology (**FIG. 8 J**). Thus, there were much more colonies of meroclones and paraclones showing diffuse cell aggregates and low proliferation potential. (**FIG. 8 K-N**). The ratio of stem cell-derived and low proliferating keratinocyte colonies was comparable between all donors at passage 1. Growth of primary cultures dramatically decreased during passage 2 and 3. Together, the procedure was sufficient to isolate keratinocytes but failed maintenance of these cells. Due to the low number of primary cells obtained, creation of a non-viral reprogramming strategy had to be studied without keratinocytes using L87 MSCs and BJ-5ta fibroblasts.

3.2. Pluripotency Genes in Keratinocytes, L87 MSCs, and BJ-5ta Fibroblasts

The analysis of pluripotency markers in somatic donor cells was necessary to evaluate the process of successful reprogramming. Therefore, a set of 30 common pluripotency markers was analyzed (**FIG. 9**). The mRNA expression profiles of BJ-5ta and L87 cells revealed 3 groups of markers. There was 1 group comprising of 12 markers, which were absent in somatic cells but thought to be crucial markers for successful reprogramming (**FIG. 9 A/B**). Among them were the pluripotency markers Oct4, Nanog, Sox2 and Lin28. A number of markers were already expressed either in BJ-5ta or L87 cells classified as ambivalent markers while some markers were expressed in both cell lines. Ambivalent and already expressed markers were thought to be less exclusive to elucidate pluripotency induction during reprogramming. The analysis of the mRNA expression profile of keratinocytes was necessary to estimate their applicability in a strategy for non-viral reprogramming. The mRNA was isolated from human skin. Interestingly, the expression of 6 crucial pluripotency markers including Nanog, Sox2, and Lin28 was observed (**FIG. 9 C**). The Oct4B mRNA was also detected but Oct4A transcripts were absent. Keratinocytes did express almost all pluripotency markers, which were detected in BJ-5ta and L87 cells. Further, several ambivalent markers were expressed in keratinocytes. In summary, the mRNA expression profiles of BJ-5ta and L87 cells were more similar to each other than to that of keratinocytes. Keratinocytes expressed additional pluripotency markers.

3.3. Analysis of Non-Viral Reprogramming Methods

To establish a non-viral reprogramming strategy, non-viral and non-integrative reprogramming methods were analyzed for their ability to induce pluripotency in L87 and BJ-5ta cells. Primary cells were not used, because those cells are more heterogeneous than cell lines, require more sophisticated culture conditions, and may not be continuously available. Further, reprogramming methods are more often described for cell lines such as BJ-5ta fibroblasts.

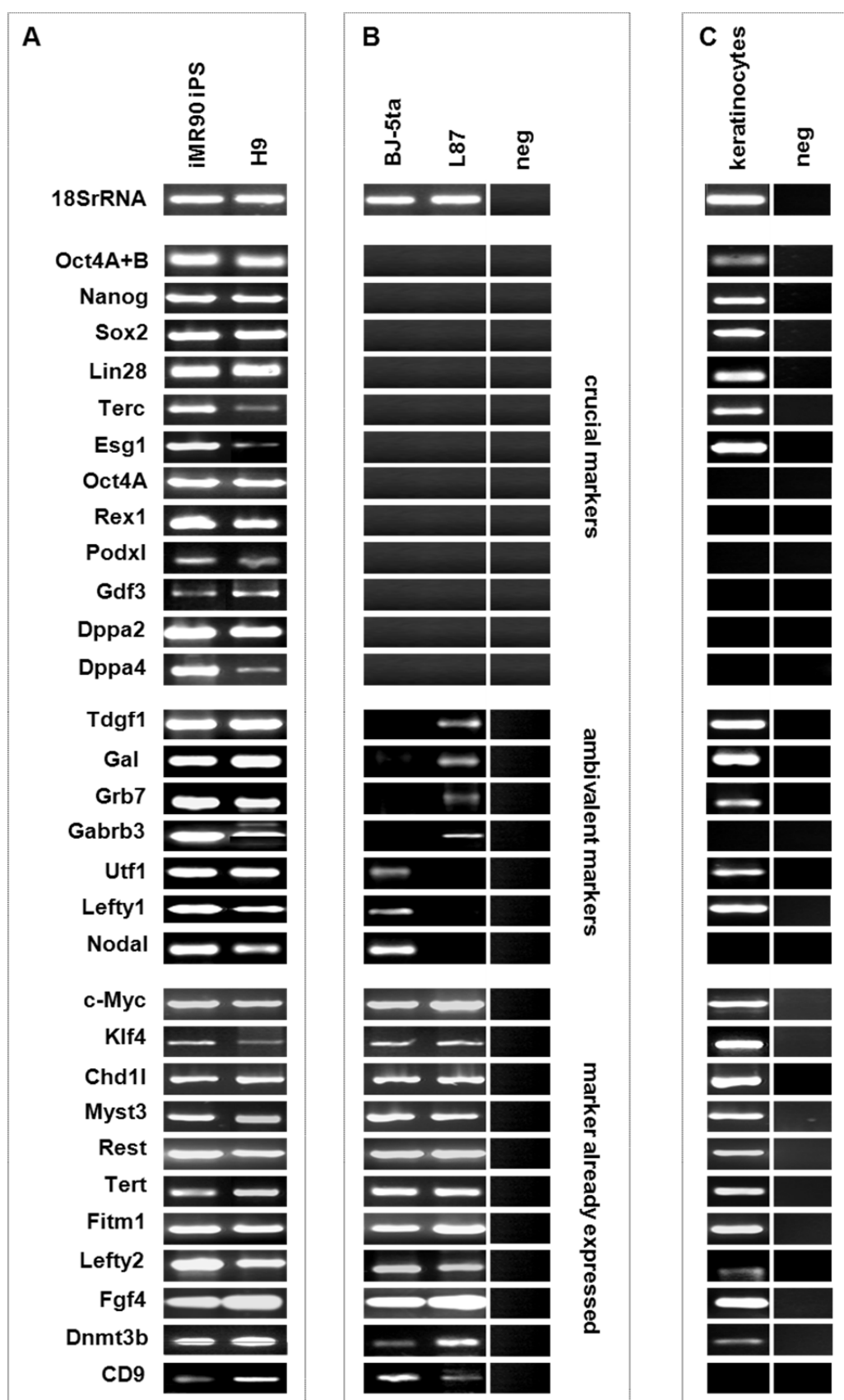


FIGURE 9: Analysis of pluripotency markers in BJ-5ta fibroblasts, L87 MSCs, and primary keratinocytes. (A) Expression of pluripotency genes is demonstrated in iMR90 iPS and H9 ES cells. (B) Expression of pluripotency genes in BJ-5ta and L87 cells. According to the presence or absence of gene expression, genes were classified as crucial, ambivalent, and already expressed. (C) Expression of pluripotency genes in primary keratinocytes obtained from human skin samples. Reactions without template served as a negative control (neg).

3.3.1. Efficient and Functional Delivery of STEMcircles™ Induces Reprogramming

STEMcircles™ are episomal vectors, which express the reprogramming factors Oct4A, Nanog, Sox2, and Lin28 for reprogramming of somatic cells. The vector also expresses GFP. Non-viral reprogramming of L87 MSCs and BJ-5ta fibroblasts was suggested to be induced by STEMcircles™.

3.3.1.1. Quantification of STEMcircles™ Delivery

STEMcircles™ are small plasmid derivatives of approximately 5 kb and plasmids usually are transfected by electroporation and lipofection. Therefore, both methods were analyzed by transfection of pEGFP-N1 (4.7 kb) to establish an efficient protocol in L87 MSCs. Standard protocols for the delivery of plasmid DNA by electroporation or lipofection varied between distinct specifications but several pilot studies revealed that lipofection was more applicable, more efficient, and gentler to L87 cells. Electroporation induced cell death in the majority of cells in contrast to lipofection by INTERFERin™ (**APP. 1**). Massive cell death was only observed after treatment with elevated amounts of the transfection reagent or increased amounts of the vector DNA (**APP. 1**). Importantly, the use of other transfection reagents less efficiently induced GFP expression after delivery of pEGFP-N1 (**APP. 2**). Therefore, INTERFERin™ was selected for lipofection of STEMcircles™.

However, previously described STEMcircles™-based reprogramming was inefficient. Sorting of GFP-positive cells was necessary to enrich the population of cells undergoing reprogramming. Thus, STEMcircles™-positive L87 and BJ-5ta cells were sorted. GFP expression was quantified by flow cytometry and PI-staining was applied to exclude non-viable cells. GFP expression was induced in up to 28.5% of L87 cells at day 3 (**FIG. 10 A**). The number of GFP-positive cells was lower at day 7 yielding up to 11.4 %. Flow cytometry verified that elevated amounts of INTERFERin™ transfection reagent or increased amounts of vector DNA did not increase the number of STEMcircles™-positive cells (**APP. 3**). Compared to L87 cells, GFP expression in BJ-5ta cells showed much lower transfection efficiencies of about 1.4% at day 3 (**FIG. 10 B**). However, the geometric mean of transfected BJ-5ta cells was more comparable to transfected L87 cells (**FIG. 10 C**). IF analysis demonstrated that GFP accumulated in cytoplasm of L87 cells and BJ-5ta cells (**FIG. 10 D-E**). Together, these data showed that efficient STEMcircles™ delivery was achieved by lipofection.

3.3.1.2. Induction of ONSL, Klf4, and c-Myc by STEMcircles™

Efficient delivery of STEMcircles™ was demonstrated suggesting the induction of ONSL in L87 and BJ-5ta cells. Accordingly, mRNAs levels and protein expression were analyzed from day 1 until day 7. Different primer pairs were used to distinguish between Oct4A and Oct4B expression. Real-time PCR analysis of L87 cells showed that Oct4A, Oct4B, Sox2, Nanog, Lin28, Klf4 and c-Myc were induced by STEMcircles™ at day 1, but expression decreased until day 3 (**FIG. 11 A**). Protein expression of Nanog and Oct4A was detected at day 3 in some but not all cells (**FIG. 11 B**). Sox2 and Oct4A protein was detected at day 7. Proteins were localized in the nucleus. In accordance to L87 cells, BJ-5ta cells showed strong induction of Oct4B, Nanog, and Lin28 mRNAs at day 1 (**FIG. 11 C**). In contrast, Oct4A and Sox2 were induced at day 3 and Klf4 and c-Myc were induced only insignificantly at day 5. While Nanog expression remained high until day 5, Lin28 expression slowly declined until day 5. Oct4A protein was rarely detected in transfected BJ-5ta cells at day 3 and day 7 (**FIG. 11 D**). Nanog and Sox2 proteins were not detected. The analysis of ONSL expression revealed differences between L87

and BJ-5ta cells. However, the expression of ONSL was induced in L87 and BJ-5ta cells demonstrating functionality of STEMcircles™.

3.3.1.3. Induction of Endogenous ONSL Expression by STEMcircles™

The ectopic expression of ONSL by STEMcircles™ aimed at the subsequent induction of endogenous ONSL transcripts. Endogenous and ectopic transcripts were distinguished by primers,

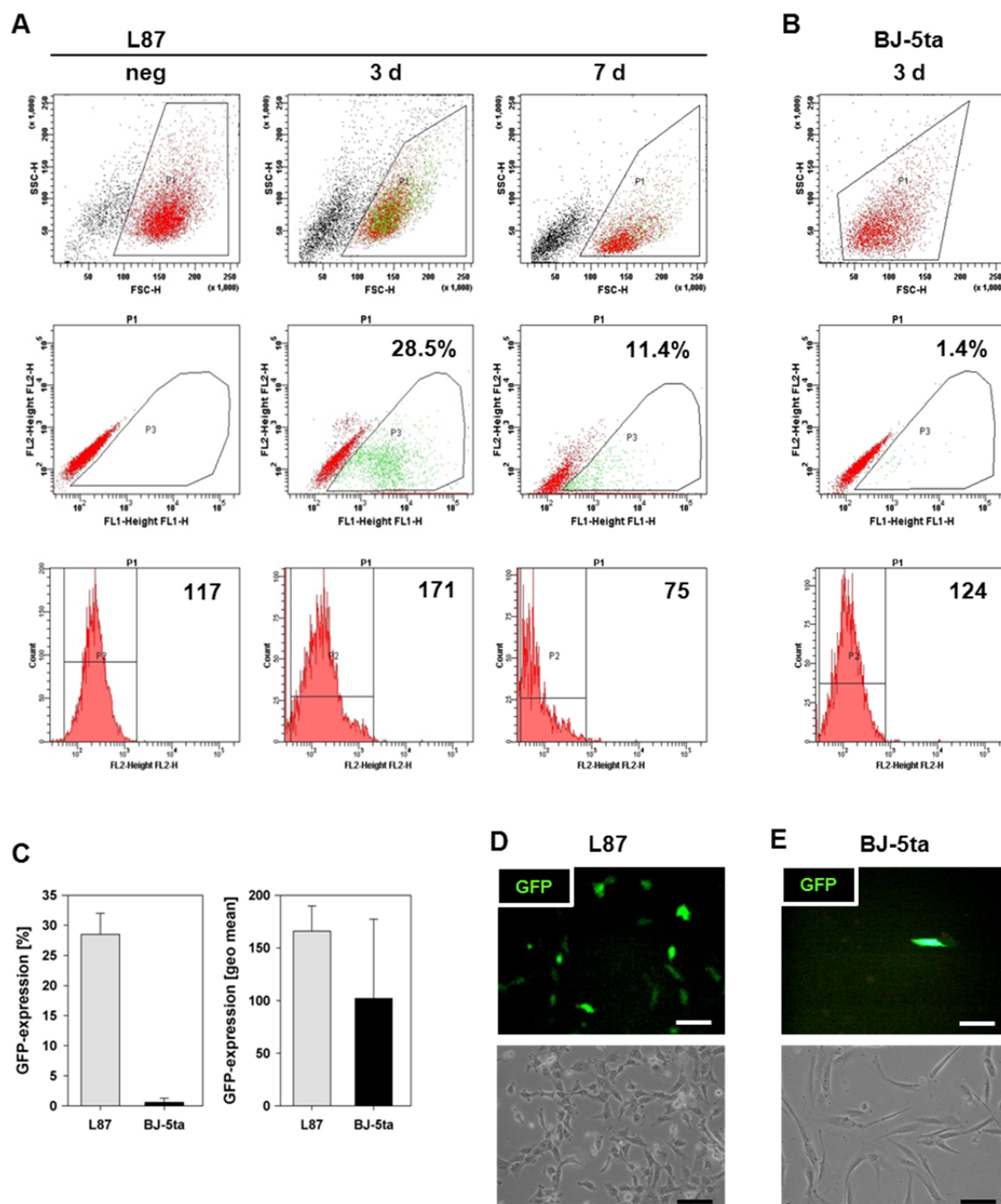


FIGURE 10: Delivery of STEMcircles™ into L87 and BJ-5ta cells. STEMcircles™ delivery was analyzed by GFP reporter gene expression in L87 and BJ-5ta cells. **(A)** Flow cytometry analysis of L87 cells at day 3 and day 7. Non-transfected L87 cells served as a control (neg). L87 cells were transfected with the standard amount of STEMcircles™ (1 µg/1.5 x 10⁶ cells). GFP expression is demonstrated by events (P3 in green, middle panel) and the geometric mean (lower panel). **(B)** Flow cytometry analysis of BJ-5ta cells at day 3. Representative data (n=3). **(C)** Comparison of GFP-expression using the parental population P3 (left) and the geometric mean (right) in L87 and BJ-5ta cells at day 3. Error bars represent SD (n=3). **(D)** IF analysis of L87 cells at day 3. **(E)** IF analysis of BJ-5ta cells at day 3. Bars represent 100 µM.

which included or excluded non-coding sequences of the analyzed mRNAs (FIG. 12 A). Oct4 primers for the detection of endogenous Oct4 expression did not differ between Oct4A or Oct4B transcripts.

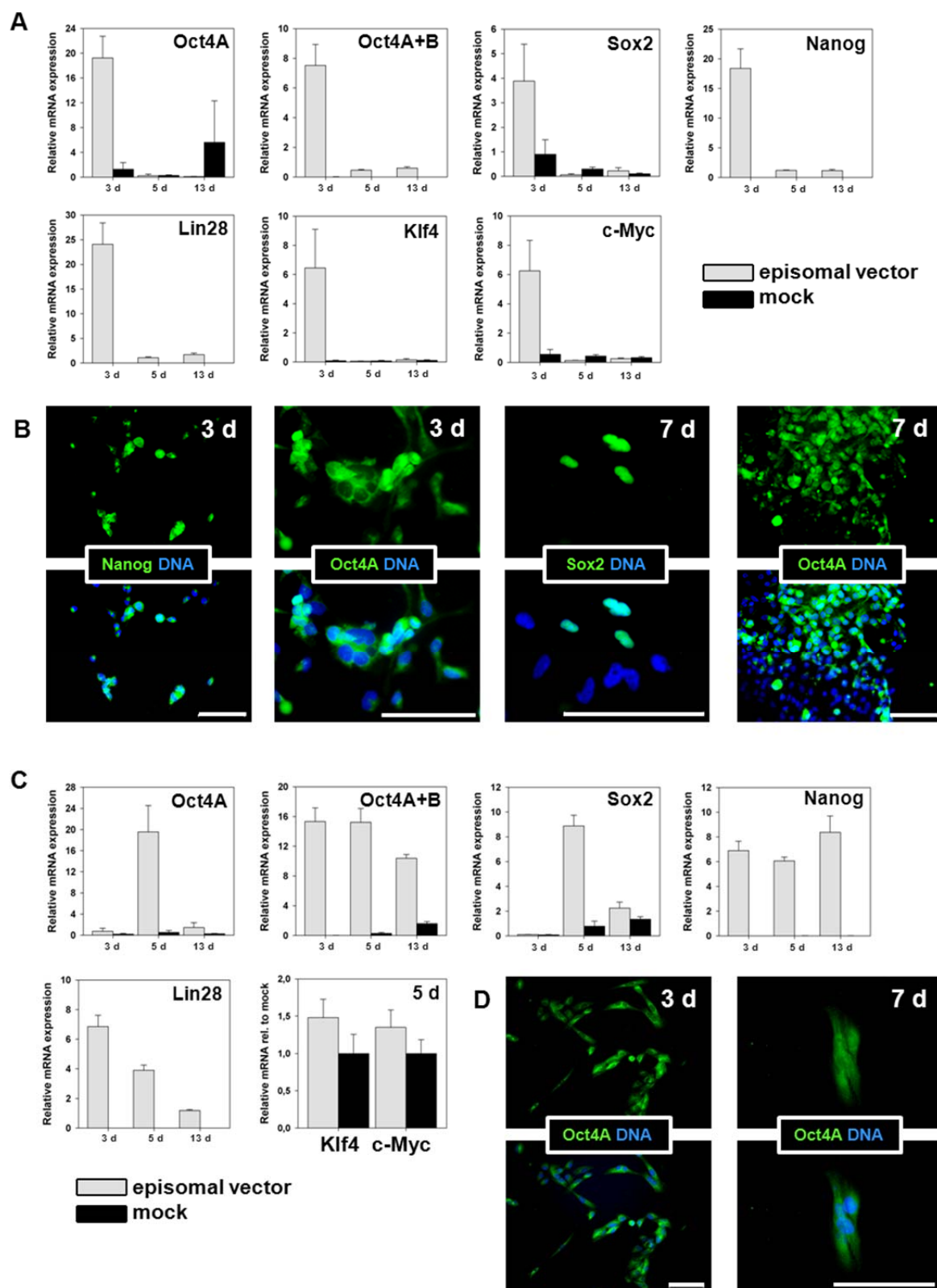


FIGURE 11: Induction of ONSL, Klf4, and c-Myc by STEMcircles™. L87 and BJ-5ta cells were transfected with STEMcircles™ or mock-transfected. Induction of pluripotency genes was analyzed from day 1 until day 7. **(A)** Real-time PCR analysis of L87 cells. **(B)** IF analysis of L87 cells demonstrating cellular localization of transcription factors. **(C)** Real-time PCR analysis of BJ-5ta cells. Expression of Klf4 and c-Myc is demonstrated at day 5 because insignificant induction was observed. Error bars represent SD (n=3). **(D)** IF analysis of BJ-5ta cells demonstrating cellular localization of Oct4A in L87 cells. Bars represent 100 μ m.

Semi-quantitative PCR analysis revealed that STEMcircles™ induced endogenous ONSL transcripts in L87 and BJ-5ta cells at day 3 (**FIG. 12 B**). Importantly, the induction of endogenous ONSL expression demonstrated the gain of pluripotency characteristics in L87 and BJ-5ta cells.

Altogether, the analysis of STEMcircles™ delivery showed efficient and functional vector delivery capable to induce pluripotency characteristics in L87 and BJ-5ta cells. Importantly, only transfection with STEMcircles™ is not capable to reprogram these cells. Enhancement of reprogramming was required. Accordingly, the application of additional non-viral reprogramming methods to create a non-viral reprogramming strategy was necessary.

3.3.2. Efficient and Functional Delivery of miR-302a-d & 372 Induces Reprogramming

Likewise reprogramming transcription factors, human ES cell-specific miRs are capable to shift the transcriptome of somatic cells towards pluripotency. Therefore, delivery of synthetic miR-302a-d & 372 into L87 and BJ-5ta cells was attempted as it offers the opportunity to manipulate the transcriptome of somatic cells. Again, a non-viral approach was favored. Lipofection of miR-302a-d & 372 was thought to induce and enhance pluripotency characteristics in L87 and BJ-5ta cells.

3.3.2.1. Validation of the miR Transfection Procedure

Transfection procedures usually are limited to a specific cell type. For delivery of miRs, a transfection protocol had to be established suitable for several cell types including BJ-5ta fibroblasts and L87 MSCs. Different transfection reagents were used according to manufacturer's instructions and analyzed in respect to the morphology of treated cells and the functionality of the delivered miRs.

Importantly, some reagents dramatically affected cell morphology (**APP. 4**). Lipofection using INTERFERin™ showed no obvious morphologic signs of cell death in BJ-5ta and L87 cells at day 3 after transfection (**FIG. 13 A**). Upon morphological analysis, the delivery of up to 50 nM miRs did not seem to affect the viability of transfected cells (**APP. 5**). To demonstrate functionality of the transfected miRs, miR-1 delivery was analyzed for the repression of the miR-1 target mRNA Ptk9. Downregulation of Ptk9 was analyzed by TaqMan®-based qRT PCR. Delivery of 50 nM miR-1 efficiently repressed Ptk9 mRNA after 36 h (to $15.4 \pm 4.7\%$ of its initial value) and 48 h ($14.8 \pm 7.9\%$)

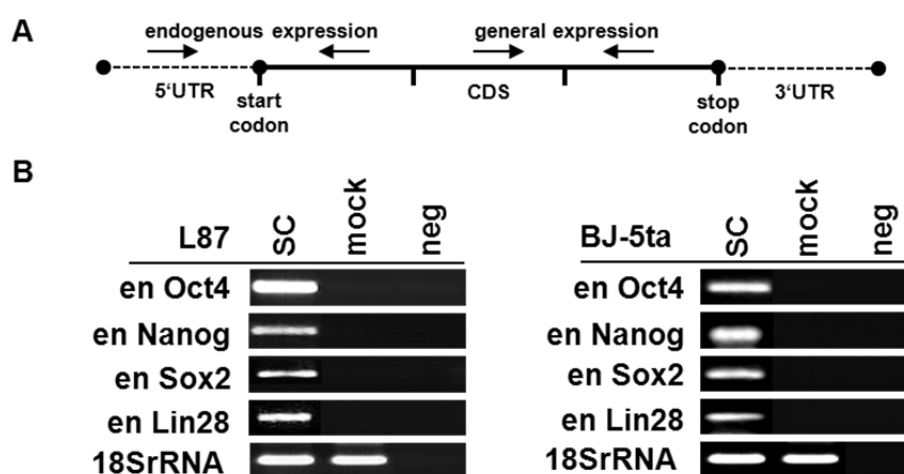


FIGURE 12: Induction of endogenous ONSL expression. L87 and BJ-5ta cells were analyzed for the induction of endogenous (en) ONSL expression by STEMcircles™ (SC). **(A)** Scheme of primer design for the discrimination of endogenous transcripts. The 5'UTR of mRNAs is not encoded on STEMcircles™ and therefore suitable to exclude mRNA expression derived from this vector. **(B)** Endogenous mRNA expression of ONSL at day 3. Cells were transfected with STEMcircles™ or mock-transfected (mock). Reactions without template served as a negative control (neg). Representative data (n=3).

(FIG. 13 B). Ptk9 mRNA was analyzed in response to different molarities of miR-1 in L87 cells at day 3 (FIG. 13 C). Downregulation was occurred in a dose dependent manner (5 nM 30.8%; 10 nM 21.6%; 25 nM 10.7%; 35 nM 8%; 45 nM 5.4%). Ptk9 repression was less efficient in BJ-5ta cells than in L87 cells (FIG. 13 B/C). Doubling the amount of transfection reagent for the delivery of 50 nM miR-1 increased repression of Ptk9 mRNA (from 22.6 % to 2.0 %, FIG. 13 D) without obvious effects on the morphology of BJ-5ta cells at day 3. In summary, the transfection procedure preserved morphology of treated cells and miR functionality was demonstrated in BJ-5ta fibroblasts and L87 MSCs.

3.3.2.2. Quantification of miR Delivery by Flow Cytometry

To further analyze the efficiency of miR delivery, BJ-5ta and L87 cells were transfected with Cy3-labeled Anti-miR Negative Control. Cy3 fluorescence was measured and quantified by flow cytometry in BJ-5ta and L87 cells from day 1 to day 3. At day 1, 97.4% of L87 cells were Cy3-positive (FIG. 14 A). In BJ-5ta cells, Cy3 was detected in up to 43.9% of cells (FIG. 14 B). The number of Cy3-positive L87 cells and BJ.5ta cells was increased until day 3 (FIG. 14 C/D). IF analysis localized Cy3 fluorescence in the cytoplasm of transfected cells (FIG. 14 E/F). In conclusion, the transfection

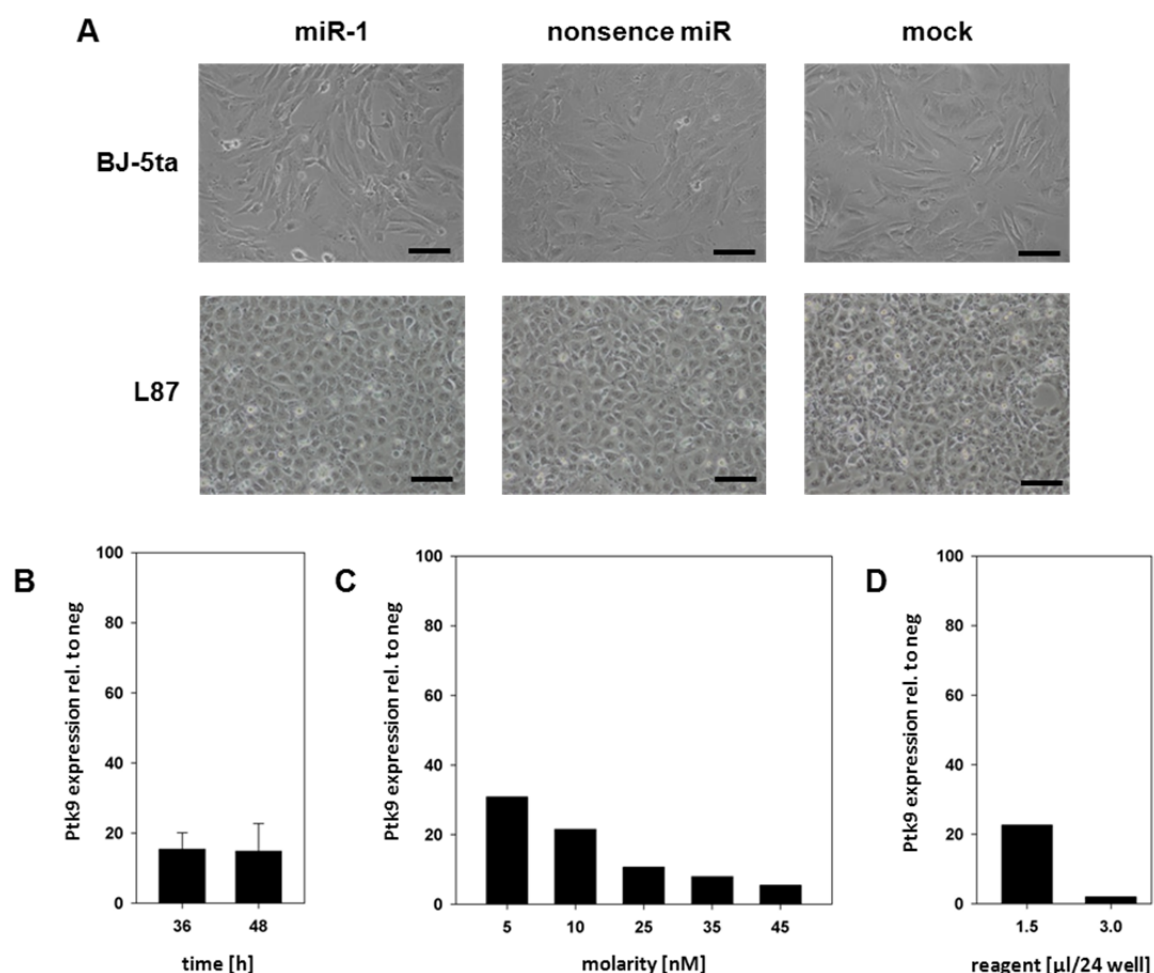


FIGURE 13. Analysis of the transfection procedure using novel miR-1. (A) Morphology of BJ-5ta cells and L87 cells is demonstrated after lipofection of 50 nM miR-1, 50 nM nonsense miR, and mock-transfection (mock) at day 3. Bars represent 100 µM. **(B)** TaqMan®-based qRT PCR analysis Ptk9, which is a target mRNA of miR-1. BJ-5ta were transfected using the standard concentration of INTERFERin™ (1.5 µl/24well) and 50 nM miR-1 or 50 nM nonsense miR (neg). Bars represent SD (n=3). **(C)** TaqMan®-based qRT PCR analysis of Ptk9 at day 3 using different molarities of miR-1. L87 cells were transfected with different molarities of miR-1 or 50 nM nonsense miR (neg). **(D)** TaqMan®-based qRT PCR analysis of Ptk9 using different amounts of the transfection reagent. BJ-5ta cells were transfected with 50 nM miR-1 or 50 nM nonsense miR and 1.5 µl/24 INTERFERin™.

procedure very efficient introduced miRs into BJ-5ta and L87 cells but efficiency was dependent on the cell type.

3.3.2.3. Prediction of miR-302a-d & 372 Target mRNAs

There are only few validated miR-302a-d & 372 targets, of which none are directly involved in reprogramming. Therefore, further target mRNA prediction was required. However, meaningful target prediction calls for more information in addition to the seed sequence (6-8 nt). Several data bases provide miR target mRNA prediction and 4 of them were chosen for further miR-302a-d & 372 target

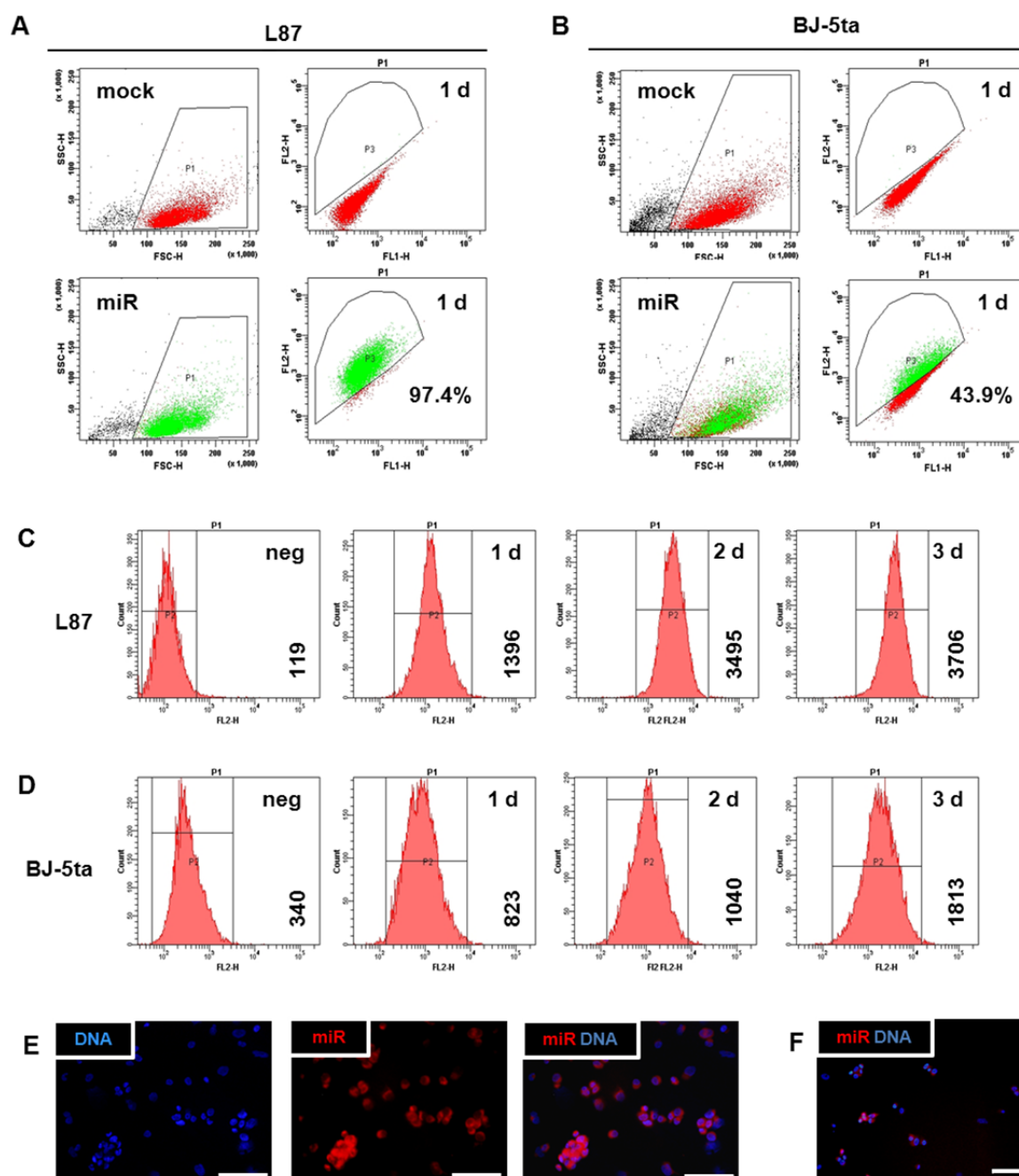


FIGURE 14: Flow cytometry and IF analysis of miR-delivery. L87 MSCs and BJ-5ta fibroblasts were transfected with 50 nM Cy3-labeled Anti-miR Negative Control (miR) and compared to mock-transfected cells (mock). **(A)** Flow cytometry after miR-delivery into L87 cells at day 1. Cy3-positive cells were quantified by events (P3 in green). **(B)** Flow cytometry after miR delivery into BJ-5ta cells at day 1. **(C)** Flow cytometry shows the geometric mean of Cy3-positive L87 cells at day 1 until day 3. Non-transfected L87 cells served as a control (neg). **(D)** Flow cytometry shows the geometric mean of Cy3-positive BJ-5ta cells. **(E)** IF analysis shows cellular localization of Cy3-labeled miRs in L87 cells. **(F)** IF analysis in BJ-5ta cells. Bars represent 100 μ m.

mRNA prediction (**FIG. 15 A**). Importantly, miR-302a-d and miR-372 share the same seed sequence but several predicted targets differ between miR-302a-d and miR-372. The SCRs of miR-302a-d & 372 were predicted to bind at the same locus within the 3'UTRs of the predicted target mRNAs (**FIG. 15 B**). The occurrence of compensatory and cooperative sites was variable (**FIG. 15 C**). Computing of target mRNAs also takes into account the conservation of the seed sequence between organisms in addition to other features, which leads to different sets of target mRNAs. Interestingly, targets provided one or more seed sequences in the 3'UTR of predicted mRNAs. Prediction in general led to a list of 500-1000 predicted genes differing between the target prediction tools. However, sets of target mRNAs were filtered according to signaling pathways involved in reprogramming such as early embryogenesis, apoptosis, epigenetic modification of DNA and histones, and cell cycle progression. A smaller set of predicted target mRNAs was obtained by combining high scores and possible biological function during induction or maintenance of pluripotency. According to this combination, cyclin A1 (Ccna1), kruppel-like factor 13 (Klf13), Dnmt1, and ED repeat domain 61 (Wdr61) were preferentially analyzed.

3.3.2.4. Validation of miR-302a-d & 372 Target mRNAs

The majority of miRs induce gene silencing via mRNA repression. Therefore, target mRNAs were analyzed in L87 and BJ-5ta cells after transfection to demonstrate functionality of miR-302a-d & 372. Ccna1, Klf13, Dnmt1, and Wdr61 were analyzed from day 3 to day 13 after transfection of miR-302a, miR-372, and in response to a cocktail of miR-302a-d & 372. Delivery of miR-302a or miR-372

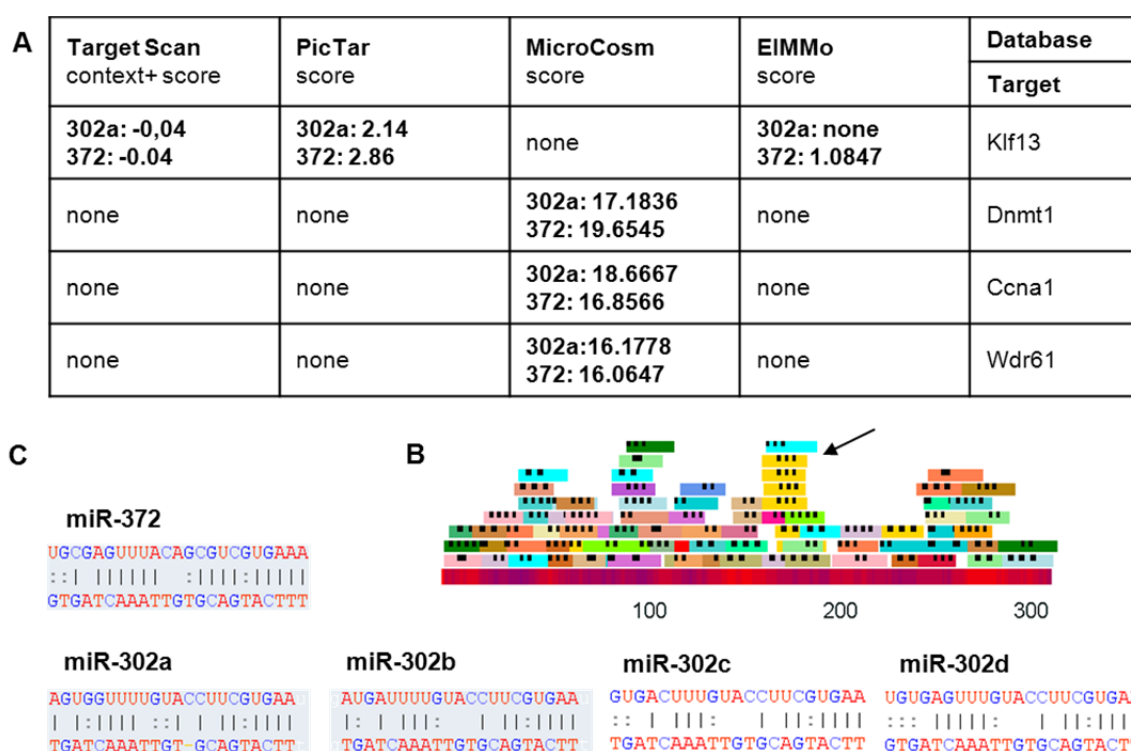


FIGURE 15: Prediction of target mRNA possibly involved in reprogramming. (A) For detection of targets of miR-302a-d & 372, 4 different data bases were used revealing different target predictions. The table shows predicted targets of miR-302a and miR-372. Targets of miR-302a-d were predicted to be the same by the data bases. (B) Scheme of the 3'UTR of human Dnmt1 containing predicted functional seed sequences of miR302a-d in yellow (arrow). Data are obtained from MicroCosm Targets version 5. (C) Seed sequence and SCR of miR-302a-d and miR-372. The pictures demonstrate binding of miRs (upper strand) to the same motive at the 3'UTR of Dnmt1 (lower strand, 168-190 bp).

strongly repressed mRNA levels of target mRNAs at day 3 (**FIG. 16 A/B**). *Ccna1* expression was retained at day 5 after transfection of miR-302a. In contrast to miR-302a, miR-372 was less efficient and all target mRNAs retained at day 5. Importantly, transfection of a cocktail of miR-302a-d & 372 was more efficient in target gene repression, which was preserved until day 13 (**FIG. 16 C**). However, this process was delayed starting only at day 5. Targets were also repressed by low concentrations of miRs, but with a significantly lower significance (**FIG. 16 D**). Taken together, the predicted targets *Ccna1*, *Klf13*, *Dnmt1*, and *Wdr61* were repressed verifying the functionality of the delivered miRs. Interestingly, validation of miR-302a-d & 372 target genes demonstrated repression of target genes until day 13, but it was questionable whether the transfected miRs were responsible for that observation. Further analysis required the detection of mature and precursor miR-302a-d & 372 to investigate whether induction of endogenous miR-302a-d & 372 expression was responsible for stable repression of the analyzed target mRNAs.

3.3.2.5. Induction of Endogenous miR-302a-d & 372 Expression

According to the analysis of target mRNAs, mature and precursor miR-302a-d & 372 were analyzed at day 1 until day 13 in BJ-5ta and L87 cells. Mature miR-302a-d & 372 are not detectable in BJ-5ta cells and L87 cells. In response to miR-302a transfection, mature miR-302a was detected at day 1 in L87 cells, but the mature miR-302a subsequently decreased until day 13 (FIG. 16 A). The cocktail of synthetic miR-302a-d & 372 induced mature miR-302a at a lower level than delivery of miR-302a alone. In accordance, mature miR-372 was detected at day 1 after delivery of synthetic

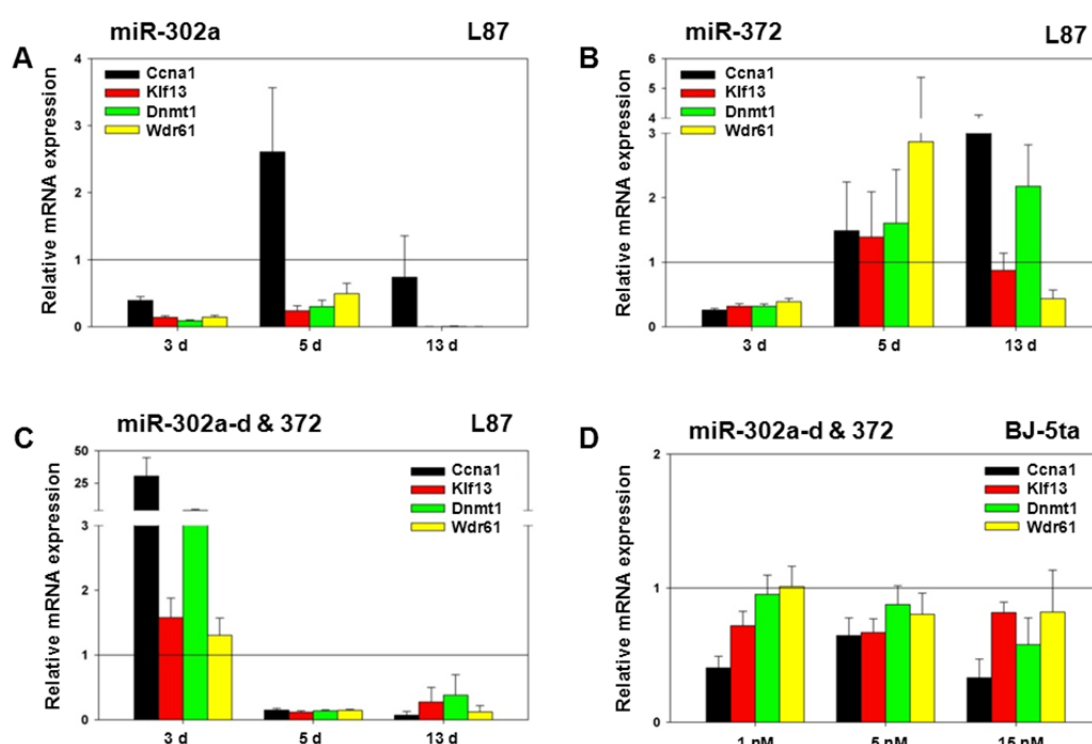


FIGURE 16: Expression analysis of predicted miR-302a-d & 372 target mRNAs *Ccna1*, *Klf13*, *Dnmt1*, and *Wdr61*. (A) qRT PCR analysis using 10 nM miR-302a. L87 cells were transfected with 10 nM miR-302a or 10 nM nonsense miR (neg=1) and analyzed for target mRNA expression from day 3 to day 13. (B) qRT PCR analysis using 10 nM miR-372 of target mRNA repression in L87 cells. (C) qRT PCR analysis after delivery of 10 nM miR-302a-d & 372. L87 cells were transfected with 10 nM of each miR and 50 nM nonsense miR (neg=1). (D) qRT PCR analysis after delivery of low concentrations of miR-302a-d & 372. BJ-5ta cells were transfected with 0.2 nM, 1 nM, or 3 nM of each miR (final concentration 1 nM, 5 nM, 15 nM) or mock-transfected (mock=1) at day 3. Bars represent SD, representative data.

miR-372 and mature miR-372 decreased until day 13 (**FIG. 17 B**). In contrast to miR-302a, miR-372 was more efficiently induced by the cocktail of miR-302a-d & 372 than by the delivery of synthetic miR-372 alone. Interestingly, synthetic miR-302a was not able to induce mature miR-372 (**FIG. 17 C**). Analysis in BJ-5ta cells validated that the cocktail of miR-302a-d & 372 induced all mature miR-302a-d & 372 at day 1, but highest levels were induced at day 6 (**FIG. 17 E**). The amount of each mature miR-302a-d & 372 differed between the single miRs, but all miRs were applied at the same concentration. However, mature miR-302a-d & 372 were detected until day 13 suggesting their endogenous expression.

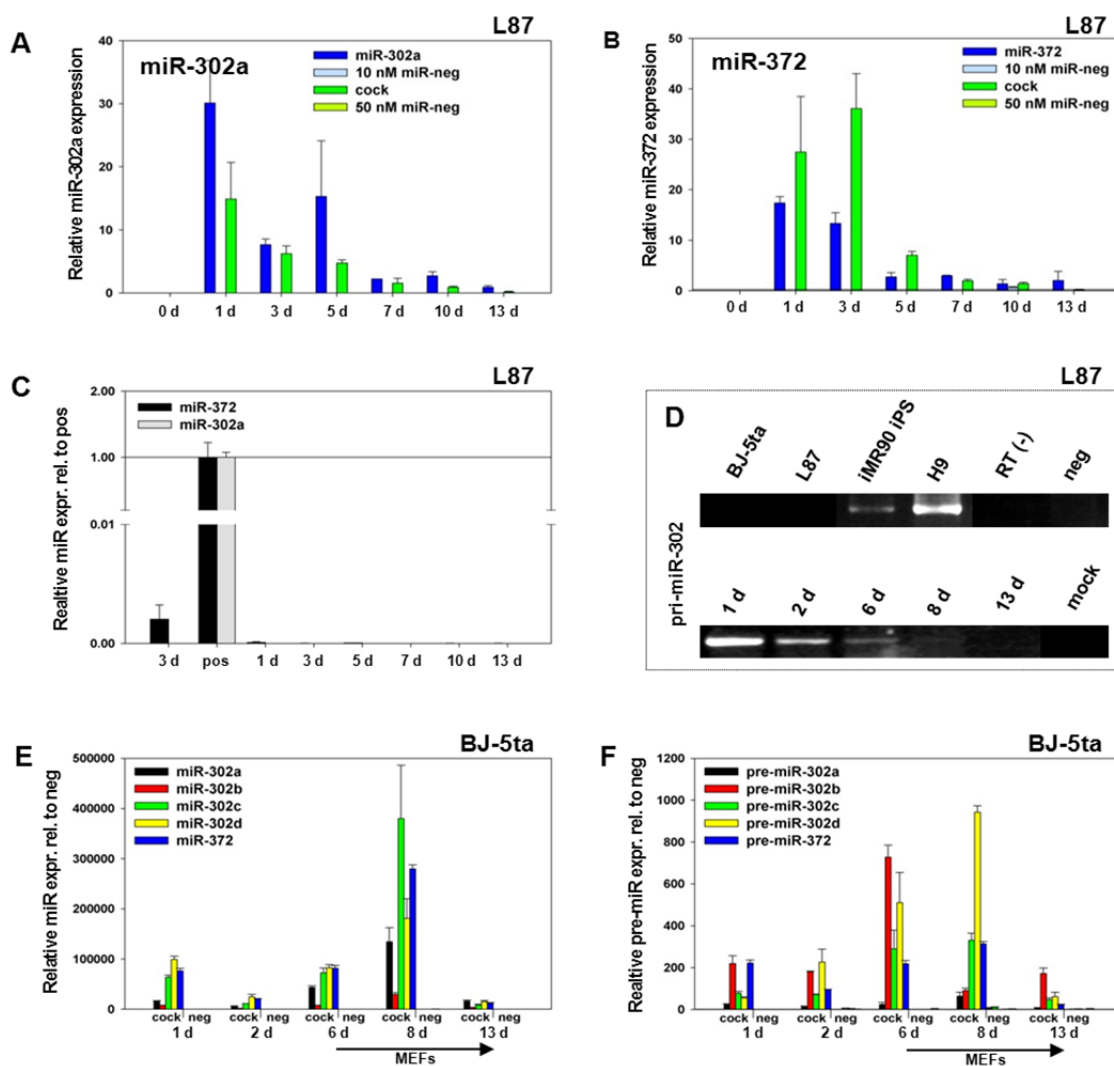


FIGURE 17: Induction of mature and precursor miR-302a-d & 372 expression. (A) qRT PCR analysis mature miR-302a expression in L87 cells after delivery of miR-302a. Cells were transfected with 10 nM miR-302a, 10 nM nonsense miR (miR-neg), cocktail of 10 nM miR-302a-d & 372 (cock) and 50 nM nonsense miR. Relative expression is compared to day 0 and shown from day 1 until day 13 after transfection. (B) qRT PCR analysis of miR-372 expression in L87 cells. (C) qRT PCR analysis of miR-302a or miR-372 expression after delivery of 50 nM miR-372 or miR-302a. Data are shown in comparison to miR-302a expression after miR-302a delivery (pos) and miR-372 expression after miR-372 delivery (pos). Bars represent SD (representative data). (D) Semi-quantitative PCR analysis of pri-miR-302 in L87 cells after transfection with 10 nM miR-302a-d & 372 from day 1 until day 13. H9 ES and iMR90 iPS cells are shown as a positive control. Samples from non-treated BJ-5ta and L87 cells served as a negative control. Reactions without template are shown from cDNA synthesis (RT(-)) and PCR (neg). (E) qRT PCR analysis of mature miR-302a-d & 372 in BJ-5ta cells after transfection of 5x 10 nM miR-302a-d & 372 (cock) and 50 nM nonsense miR (neg) from day 1 until day 13. Cells were seeded onto MEFs at day 6 (indicated by arrow). Relative expression of mature miR-302a-d & 372 after transfection of synthetic miR 302a-d & 372 (cock) is shown in comparison to miR-302a-d & 372 expression after delivery of nonsense miR (neg) at the indicated time points. (F) qRT PCR analysis of pre-miR-302a-d & 372 in BJ-5ta cells. Bars represent SD (representative data).

The expression of pri-miR-302 and pre-miR-302a-d & 372 was analyzed in L87 and BJ-5ta cells. L87 and BJ-5ta cells did not express pri-miR-302 in contrast to H9 ES cells and IMR90 iPS cells. The induction of pri-miR-302 by the cocktail of miRs was demonstrated at day 1 in L87 cells, but the pri-miR subsequently decreased until day 8 (**FIG. 17 D**). The induction of pre-miR-302a-d & 372 by the cocktail of miRs was also demonstrated at day 1 in BJ-5ta cells, but highest levels were induced at day 6 (**FIG. 17 E**). Again, BJ-5ta cells showed delayed response to the miR delivery.

Another approach combined delivery of miR-302a-d & 372 with human ES cell-specific culture conditions to preserve or enhance the induction of endogenous miR-302a-d & 372. Therefore, BJ-5ta cells were seeded onto MEFs at day 6 after transfection with miR-302a-d & 372. Mature miR-302a-d & 372 were enriched by feeder cells at day 8, but mature miRs decreased until day 13 (**FIG. 17 E**). The expression of pre-miR-302a-d & 372 was altered at day 8, but not all pre-miRs were increased (**FIG. 17 F**).

In summary, the preservation of mature and the induction of precursor miRs verified functionality of synthetic miR-302a-d & 372. Further, the endogenous expression of human ES cell-specific miR-302a-d & 372 demonstrated that the transfection of synthetic miR-302a-d & 372 induced pluripotency characteristics in L87 and BJ-5ta cells.

3.3.2.6. Induction of Oct4 and Nanog by miR-302a-d & 372

Because efficient and functional delivery of miR-302a-d & 372 was demonstrated, the regulation of the pluripotency markers Oct4 and Nanog was examined. Induction of Oct4 mRNA at day 3 was induced by miR-302a or miR-372 alone (**FIG. 18 A**). However, a cocktail of miR-302a-d & 372 more efficiently induced Oct4 mRNA expression. In contrast, Nanog mRNA was induced by miR-302a, but not by the cocktail. At day 7 and 10, the cocktail of miR-302a-d & 372 only slightly increased Oct4 mRNA levels (**FIG. 18 B**). Contrary, Nanog mRNA was increased at day 10 after miR delivery.

As a mesenchymal marker, thymus cell antigen 1 (Thy1) is expressed in L87 and BJ-5ta cells. Upon introduction of miR-302a-d & 372, Thy1 was strongly repressed at day 3 (**FIG. 18 C**). The Thy1 3'UTR did not contain SCRs necessary to bind miR-302a-d & 372 implicating the loss of mesenchymal characteristics. Taken together, functional miR-302a-d & 372 successfully induced Oct4 and Nanog mRNA expression, which demonstrated again that the transfection of synthetic miR-302a-d & 372

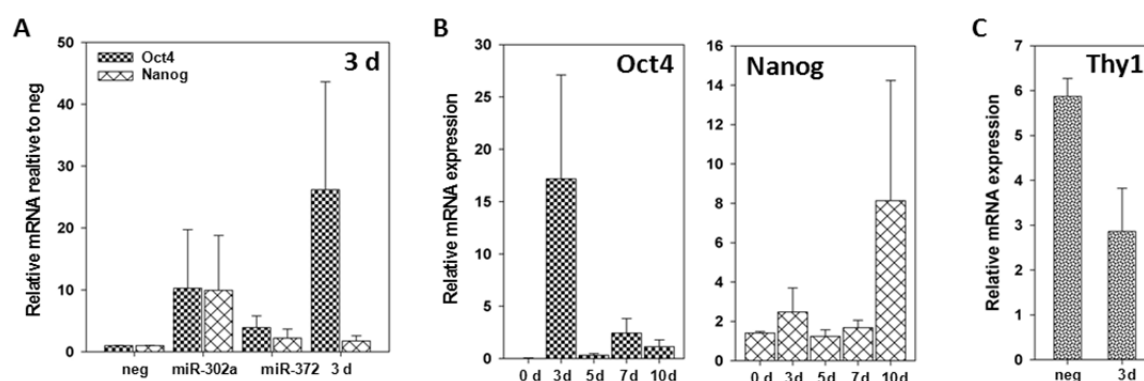


FIGURE 18: Regulation of Oct4 and Nanog by miR-302a-d & 372. (A) qRT PCR analysis of Oct4A+B and Nanog at day 3. L87 cells were transfected with 50 nM nonsense miR (neg), 50 nM miR-302a, 50 nM miR-372, and a cocktail of 5x 10 nM miR-302a-d & 372 (cock). (B) qRT PCR analysis of Oct4A+B and Nanog at day 0 until day 10. L87 cells were transfected with 5x 10 nM miR-302a-d & 372. Error bars represent SEM (n=3). (C) qRT PCR analysis of Thy1 at day 3. L87 cells were transfected with 5x 10 nM miR-302a-d & 372. Control cells were transfected with 50 nM nonsense miR (neg). Error bars represent SD (representative data).

induced pluripotency characteristics in L87 and BJ-5ta cells. Accordingly, it was interestingly to analyze how miR-302a-d & 372 regulated the expression of Oct4 and Nanog.

3.3.3. Oct4 Expression is Regulated by miR-302a-d & 372 Target mRNA Dnmt1

Interestingly, the validation of miR-302a-d & 372 target mRNAs revealed that Dnmt1 can strongly repressed by transfection of synthetic miR-302a-d & 372. Dnmt1 is key regulator of DNA methylation as described earlier. Further, Oct4 and Nanog gene expression are regulated by DNA methylation. Dnmt1 are responsible for the methylation of Oct4 and Nanog to inhibit their expression in somatic cells. Therefore, Oct4 induction was studied in response to the inhibition of Dnmt1.

3.3.3.1. Regulation of Dnmt1 Expression by miR-302a-d & 372

Dnmt1 expression in response to transfection of miR-302a-d & 372 was studied more intensively in L87 cells and BJ-5ta cells. To distinguish the impact of the miR-302 cluster and miR-372, miR-302a as a representative of the miR-302 cluster and miR-372 were analyzed in respect to their ability to repress Dnmt1 at day 3. Dnmt1 mRNA was significantly repressed by miR-302a (-69.1±5.3%) at day 3 (FIG. 19 A), but was not affected by miR-372. The cocktail of miR-302a-d & 372 slightly altered but not significantly lowered Dnmt1 transcript levels (FIG. 18 A). However, WB analysis of Dnmt1 protein

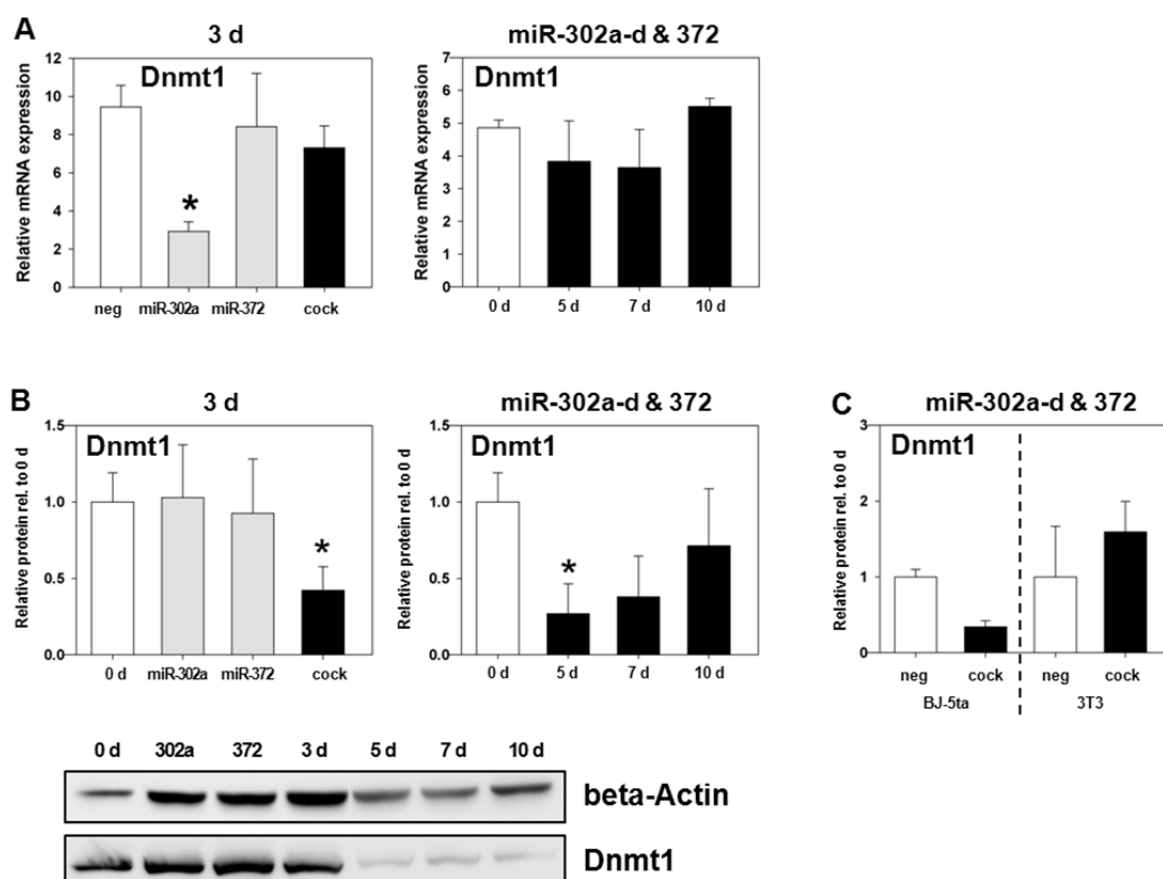


FIGURE 19: Regulation of Dnmt1 by miR-302a-d & 372. (A) qRT-PCR analysis of Dnmt1 expression after miR delivery. L87 MSCs were transfected with 50 nM nonsense miR (neg), 50 nM miR-302a, 50 nM miR-372, and a cocktail of 5x 10 nM miR-302a-d & 372 (cock). At day 3, Dnmt1 expression was compared to delivery of nonsense miR (neg) (left). Expression until day 10 was compared to day 0 (white). (B) WB analysis was used to examine Dnmt1 protein expression in response to miR delivery. Expression was compared to day 0. Error bars represent SEM (n=3). *p<0.05 versus neg/0d. Representative data are shown below. (C) WB analysis of human BJ-5ta and murine 3T3-L1 fibroblasts after transfection with 5x 10 nM miR-302a-d & 372 (cock). Dnmt1 protein expression was analyzed at day 3. Expression at day 0 served as a negative control (neg). Error bars represent SEM (n=2).

expression demonstrated significant repression ($-57.8 \pm 15.3\%$) by miR-302a-d & 372 at day 3 (FIG. 19 B). Dnmt1 protein level was not affected by miR-302a or miR-372 alone. The cocktail of miR-302a-d & 372 significantly reduced Dnmt1 protein level at day 5 ($-73.0 \pm 19.5\%$) and more slightly at day 7 to day 10. Dnmt1 protein was increasingly restored until day 10.

Regulation of Dnmt1 protein expression was additionally studied in human BJ-5ta and mouse 3T3-L1 fibroblasts. It was interestingly to analyze whether the way of action of human ES cell-specific miR-302a-d & 372 is restricted to the human system. The function of the miR-302 cluster is different in human and mouse pluripotent stem cells. Human ES cell-specific miR-302a-d & 372 strongly repressed Dnmt1 in human fibroblasts, but not in mouse fibroblasts (FIG. 19 C). Together, strong repression of Dnmt1 protein expression by miR-302a-d & 372 was demonstrated. Further analysis were required to elucidate whether the function of Dnmt1 was repressed, too.

3.3.3.2. Luciferase Assay for Validation of miR-302a-d & 372 Target mRNA Dnmt1

Studies intensively described Dnmt1 downregulation in response to miR-302a-d & 372. The 3'UTR of Dnmt1 mRNA was predicted to be a target of miR-302a-d & 372 containing a SCR. The luciferase assay was designed to demonstrate that miR-302a-d & 372 directly bind to the predicted binding site on the Dnmt1 mRNA. Modified pmiRGLO plasmids expressed *renilla* luciferase and firefly luciferase reporter genes. The 3'UTR of the firefly luciferase gene contained a multiple cloning site (MCS). The native Dnmt1 SCR of miR-302a-d & 372 was cloned into the MCS inside the 3'UTR of the firefly luciferase gene to obtain pmiRGLO-Dnmt1 (FIG. 20 A). Both, *renilla* and firefly luciferases, were

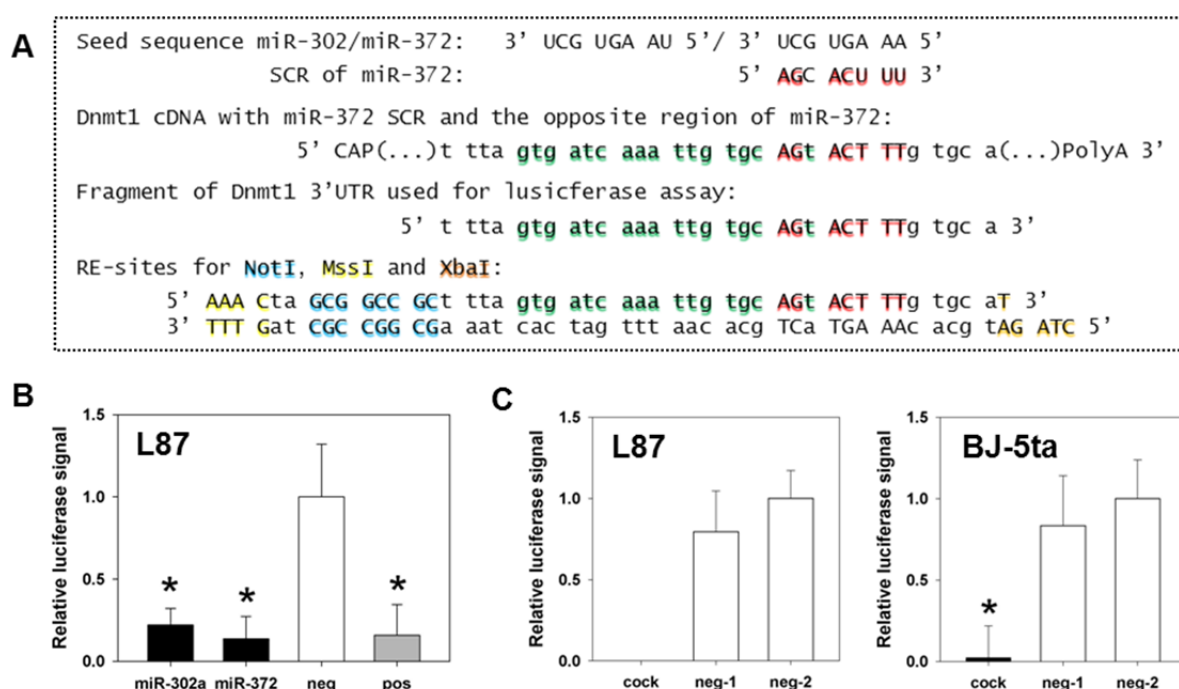


FIGURE 20: Direct interaction of mature miR-302a-d & 372 with the 3'UTR of Dnmt1 transcripts. (A) Design of pmiRGLO-Dnmt1 reporter plasmid carrying the SCR and the opposite region of miR-302a-d & 372 coupled with restriction enzyme sites for cloning. **(B)** Luciferase assay for Dnmt1 target gene verification. L87 cells were co-transfected with 50 nM miR-302a, 50 nM miR-372, and 50 nM nonsense miR (neg) and luciferase reporter pmiR-Dnmt1. As a positive control 50 nM miR-302a were co-transfected with pmiRGLO-302a (pos). One day after transfection, luciferase activity was measured and compared to co-transfected pmiR-Dnmt1 and nonsense miR (neg). Error bars represent SEM (n=3). *p<0.05 versus neg. **(C)** L87 and BJ-5ta cells were co-transfected with pmiR-Dnmt1 and 5x 10 nM miR-302a-d & 372 (cock) or 50 nM nonsense miR (control, neg-1). A second negative control was used by transfecting nonsense miRs and pmiRGLO-nonsense (neg-2). Luciferase activity was measured on day later and compared to controls. Error bars represent SEM (L87 n=2; BJ-5ta n=3). *p<0.05 versus neg-2.

constitutively expressed. Analysis of Luciferase activity was used to show whether the Luciferase mRNA was repressed after delivery of miR-302a-d & 372. *Renilla* activity was used to normalize firefly activity. L87 cells and BJ-5ta cells were co-transfected with miR-302a-d & 372 and pmiRGLO-Dnmt1, pmiRGLO-nonsense, or pmiRGLO-302a reporter vectors. A functional positive control was provided by co-transfection of miR-302a and pmiRGLO-302a, which carries a miR-302a complementary sequence to ensure most efficient binding. The pmiRGLO-nonsense plasmid carried a sequence not capable to bind miR-302a-d & 372. Co-transfection of pmiRGLO-Dnmt1 and miR-302a ($22.1 \pm 10.0\%$) or miR-372 ($13.6 \pm 13.6\%$) significantly reduced luciferase activity (**FIG. 20 B**). Interestingly, luciferase repression by miR-302a using pmiR-Dnmt1 or pmiRGLO-302a was comparable. More efficient downregulation of pmiRGLO-Dnmt1-driven luciferase activity ($0 \pm 21.5\%$) was demonstrated by a cocktail of miR-302a-d & 372 (**FIG. 20 C**). Therefore, Dnmt1 was verified as a direct miR-302a-d & 372 target mRNA.

3.3.3.3. Oct4 Promoter Methylation is Regulated by miR-302a-d & 372

As Dnmt1 protein repression by miR-302a-d & 372 was demonstrated, its impact on DNA methylation of the pluripotency marker Oct4 was analyzed. CpG methylation in the Oct4 promoter region was studied in L87 cells in response to miR-302a-d & 372 delivery. Therefore, a real-time PCR-based approach for the analysis of CpG methylation in the Oct4 promoter was designed (**FIG. 21 A**). DNA

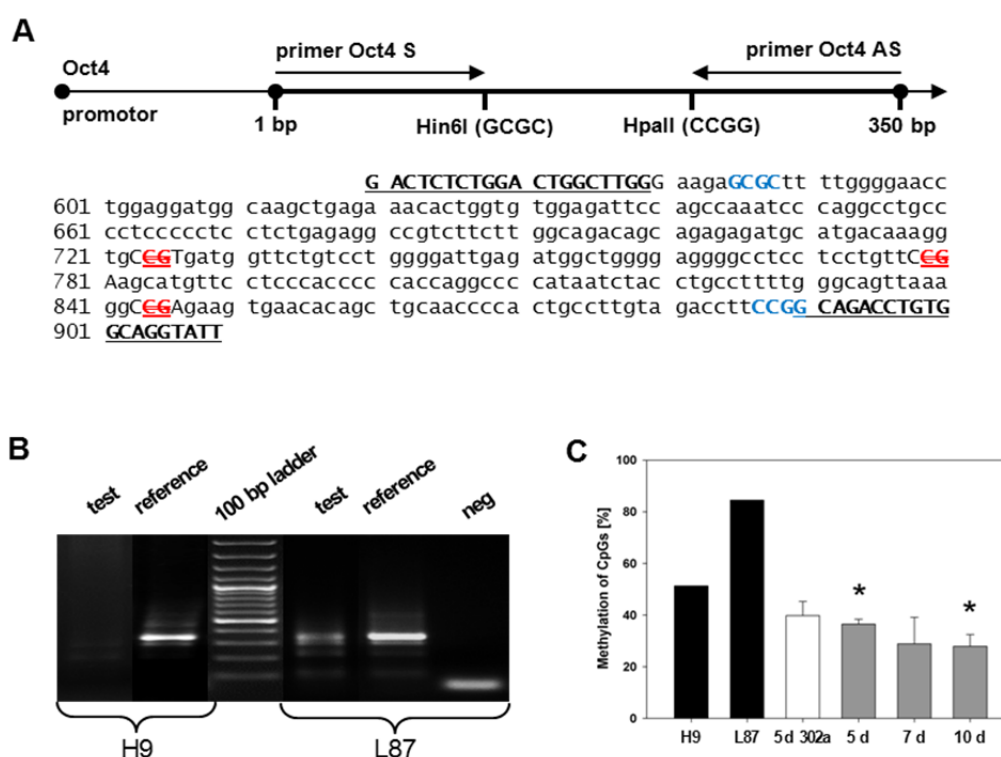


FIGURE 21: Regulation of the Oct4 promoter methylation by miR-302a-d & 372. (A) Scheme of primer design for the analysis of CpG methylation in the promoter region of Oct4 (upper part). The primer pair yields a 350 bp fragment, which is part of the Oct4 promoter (lower part, underlined letters). CpGs are shown in blue and red. For the red labeled CpGs no MSRE was available, which is indicated by crossed letters. Restriction sites of suitable MSREs are highlighted in blue bold letters (Hin6I GCGC and HpaII CCGG). **(B)** Analysis of CpG methylation in the Oct4 promoter of H9 ES cells and L87 MSCs (control cells). DNA was incubated with MSREs (indicated as test) and further analyzed using real-time PCR. Mock-digested DNA served as a reference (indicated as reference). Real-time PCR products were transferred on 1.5% agarose gel to confirm the PCR fragment of 350 bp using a 100 bp DNA ladder. Reactions without template served as a negative control (neg). **(C)** Quantification of CpG methylation after miR delivery using real-time PCR. L87 cells were transfected with 50 nM miR-302a and analyzed at day 5 (white bar). Further, cells were transfected with 5x 10 nM miR-302a-d & 372 (grey bars) and analyzed from day 5 to day 10. Quantification of CpG methylation in H9 and L87 cells served as a control. Error bars represent SEM (n=3). *p<0.05 versus L87 cells.

from H9 ES cells served as a control and carried hardly any methylated CpGs and no PCR fragment was detectable in the test reaction on the agarose gel (**FIG. 21 B**). H9 ES cells were not separated from feeder cells. This positive control sample therefore contained undifferentiated ES cells and differentiated MEFs. Accordingly, quantification revealed that the control sample contains cells with CpG methylation (51.3%) (**FIG. 21 C**). DNA from L87 cells carried methylated and not methylated CpGs, which was demonstrated by a moderate number of amplicons in the test reaction on the agarose gel (**FIG. 21 B**). Quantification revealed that CpG methylation in non-transfected L87 cells was high (84.5%) (**FIG. 21 C**). Delivery of miR-302a strongly repressed CpG methylation ($39.8 \pm 5.4\%$) at day 5. A cocktail of miR-302a-d significantly reduced CpG methylation at day 5 ($36.5 \pm 1.9\%$), day 7 ($28.9 \pm 10.3\%$), and day 10 ($27.9 \pm 4.5\%$). In summary, the percentage of methylated CpGs within the Oct4 promoter DNA was strongly repressed by miR-302a-d & 372 delivery.

3.3.3.4. Regulation of Dnmt3a/b Expression by miR-302a-d & 372

Oct4 demethylation by repression of the miR-302a-d & 372 target Dnmt1 was demonstrated, but DNA methylation is also achieved/regulated by other DNMTs and several co-factors. Therefore, a possible regulation of Dnmt3a or Dnmt3b in L87 cells after miR-302a-d & 372 delivery was examined. Dnmt3a/b mRNA levels were not significantly affected by miR-302a, miR-372, and the cocktail of miR-302a-d & 372 at day 3 (**FIG. 22A**). However, Dnmt3a mRNA was slightly lowered by miR-302a. Dnmt3a/b mRNA levels were analyzed until day 10 without any effect of the miRs on Dnmt3a/b transcription. WB analysis verified that Dnmt3b protein is not down-regulated by miR-302a-d & 372 (**FIG. 22 B**). Accordingly, these data underscore that absent maintenance methylation by Dnmt1 and not absent *de novo* methylation by Dnmt3a/b is responsible for DNA demethylation of Oct4.

Altogether, the analysis of miR-302a-d & 372 delivery showed efficient and functional miR delivery capable to induce pluripotency characteristics in L87 and BJ-5ta cells. Importantly, only transfection with miR-302a-d & 372 is not capable to reprogram these cells. Therefore, enhancement of reprogramming was required. Accordingly, the application of additional non-viral reprogramming methods to create a non-viral reprogramming strategy was necessary.

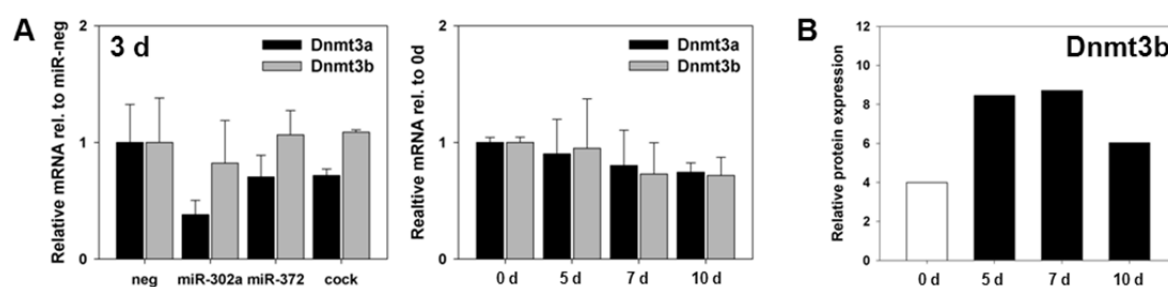
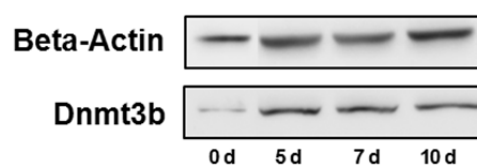


FIGURE 22: Regulation of Dnmt3a and Dnmt3b by miR-302a-d & 372. L87 MSCs were transfected with 50 nM nonsense miRs (neg), 50 nM miR-302a, 50 nM miR-372, and a cocktail of 5×10 nM miR-302a-d & 372 (cock) and analyzed for the mRNA expression of Dnmt3a and Dnmt3b. **(A)** qRT-PCR analysis of Dnmt3a/b mRNA after miR delivery. At day 3 (left) expression is shown in comparison to the delivery of nonsense miRs (neg). Expression until day 10 (right) is demonstrated in relation to the expression at day 0. Error bars represent SEM (n=3). **(B)** WB analysis of Dnmt3b expression in response to delivery of 5×10 nM miR-302a-d & 372 (n=1).



3.3.4. Hypoxia Promotes Reprogramming

STEMcircles™ and miR-302a-d & 372 were introduced into L87 and BJ-5ta cells, but permanent induction of ONSL was not achieved. Reprogramming by STEMcircles™ and miR-302a-d & 372 was adjusted to maintain pluripotency characteristics in L87 and BJ-5ta cells. Therefore, hypoxia and human ES cell-specific culture conditions were applied.

3.3.4.1. Hypoxia Promotes Induction of Reprogramming by miR-302a-d & 372

Induction of Oct4 transcription by miR-302a-d & 372 was achieved at day 3, but Oct4 expression was not stably induced (see also **FIG. 18 B**). In order to maintain Oct4 expression, cells were cultured under hypoxic and human ES cell-specific culture conditions including feeder cells, FGF2 treatment, and the use of human ES cell-specific medium. Morphologic analysis showed that cell viability was most probably not disturbed (**APP. 6**). Normoxia and ES cell-specific conditions maintained Oct4A expression in BJ-5ta cells until day 7 after transfection with miR-302a-d & 372 (**FIG. 23 A**). Interestingly, hypoxia induced Oct4A at day 7 with or without miR-302a-d & 372 delivery in the presence or absence of ES-cell specific conditions (**FIG. 23 B**). Further, Nanog expression was induced by hypoxia at day 7, but only in response to miR-302a-d & 372 delivery under standard conditions. Induction of reprogramming factors Sox2 and Lin28 was not detected. Another pluripotency-associated marker RNA exonuclease 1 (Rex1; alias Zfp42) was also not induced in BJ-5ta cells. However, other pluripotency-associated marker namely, MYST histone methyltransferase 3 (Myst3; also known as Kat6A) and c-Myc were detected in BJ-5ta cells, but these markers were already expressed in untreated cells (**FIG. 23 B**).

Together, the combination of miR-302a-d & 372 and ES cell-specific conditions preserved Oct4A mRNA expression until day 7. The combination of miR-302a-d & 372 and hypoxia preserved Nanog transcription until day 7. These data highlight the importance of both hypoxia and ES cell-specific conditions, but hypoxia and ES cell-specific conditions together did not preserve Nanog mRNA expression.

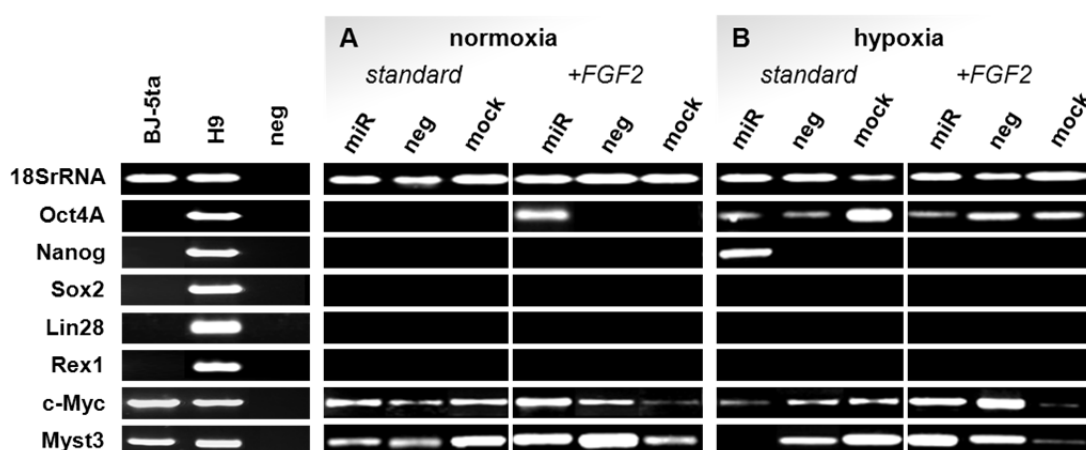


FIGURE 23: Induction of Oct4A and Nanog by miR-302a-d & 372 is regulated by ES cell-specific conditions and hypoxia. Semi-quantitative PCR analysis of growth condition during miR-mediated induction of Oct4 and Nanog in BJ-5ta cells. Further, expression of Sox2, Lin28, Rex1, c-Myc, and Myst3 was analyzed. Non-transfected BJ-5ta cells and H9 human ES cells served as control cells. Non-template reactions served as a negative control (neg). **(A)** BJ-5ta cells were transfected with 5x 10 nM miR-302a-d & 372 (miR), 50 nM nonsense miRs (neg), and mock-transfected (mock) and cultured under normoxic conditions. At day 3, cells were seeded on MEFs using standard medium (indicated as standard) and human ES cell-specific medium with FGF2 (indicated as +FGF2). At day 7, cells were analyzed. **(B)** BJ-5ta cells were analyzed in response to hypoxic conditions. Representative data (n=2).

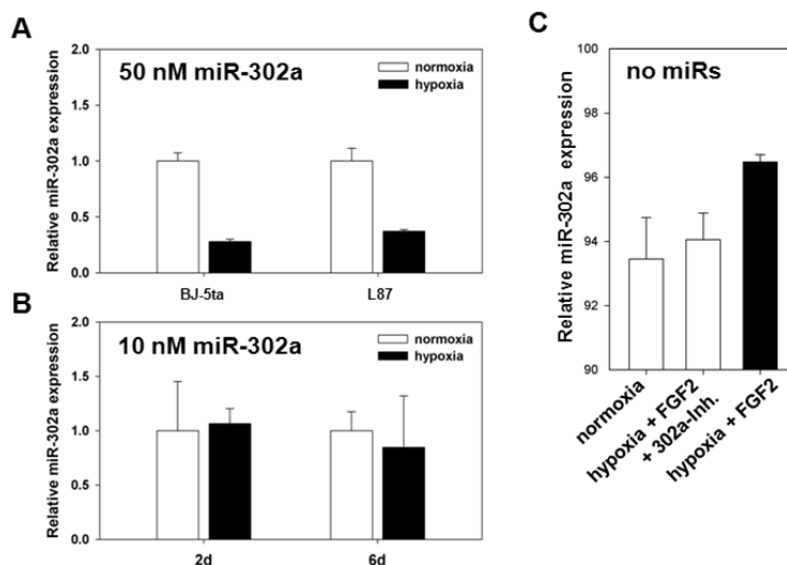
Additionally, the amount of detectable mature miR-302a after transfection of synthetic miR-302a was analyzed in the presence of hypoxia. The amount of mature miR-302a at day 3 was lower in the presence of hypoxia when 50 nM synthetic miR-302a were applied (**FIG. 24 A**). Treatment with lower concentration, namely 10 nM synthetic miR-302a was not affected by hypoxia (**FIG. 24 B**). Therefore, transfection of 5x 10 nM miR in a cocktail of miR302a-d & 372 was almost unaffected by hypoxia. Importantly, endogenous mature miR-302a was induced without miR delivery when hypoxia and ES-cell conditions were combined (**FIG. 24 C**).

Altogether, these data revealed that the combination of miR-302a-d & 372, hypoxia, and ES cell-specific conditions is challenging. However, application of hypoxia within a non-viral reprogramming strategy was preferred because hypoxic standard conditions maintained both Oct4A and Nanog mRNA expression induced by miR-302a-d & 372.

3.3.4.2. Hypoxia Promotes Induction of Reprogramming by STEMcircles™

ONSL expression was efficiently induced by STEMcircles™ in L87 MSCs and BJ-5ta fibroblasts, but only for short period of time. To preserve ONSL, hypoxia was applied in an approach for STEMcircles™-based reprogramming. L87 and BJ-5ta cells were treated with STEMcircles™ under hypoxic or normoxic conditions. Morphologic analysis indicated that their morphology was not affected by hypoxia and GFP expression by STEMcircles™ was sufficiently induced (**APP. 7**). Introduction of STEMcircles™ was sufficient to induce endogenous Oct4, Nanog, and Sox2 expression at day 3 after transfection using hypoxic conditions (**FIG. 25 A**). General and endogenous Lin28 mRNA expression was preserved in L87 cells, but decreased in BJ-5ta cells. In L87 cells, further qRT PCR analysis revealed that hypoxia positively regulated ONSL expression after vector delivery. To evaluate whether hypoxia could increase ONSL mRNA levels after STEMcircles™ delivery, the fold change of the expression induced by hypoxia in comparison to normoxia was determined at day 1 (**FIG. 25 B**). OCT4 induction remained to be very low and Sox2 was also induced at a very low level even under hypoxic conditions. However, Nanog expression dramatically increased in presence of low oxygen at day 1,

FIGURE 24: Induction of endogenous miR-302a expression by synthetic miR-302a-d & 372 is regulated by hypoxia. BJ-5ta and L87 cells were analyzed by real-time PCR whether endogenous miR-302a expression (induced by synthetic miR-302a-d & 372) is regulated by growth conditions. **(A)** qRT PCR analysis of miR-302a expression upon induction with 50 nM miR-302a in the presence of normoxia and hypoxia. BJ-5ta and L87 cells were transfected with 50 nM miR-302a, cultured using standard media, and analyzed at day 3. Data are represented compared to normoxia (normoxia=1). **(B)** qRT PCR



analysis of miR-302a expression upon induction with 5x 10 nM miR-302a-d & 372 in the presence of normoxia and hypoxia. L87 cells were transfected with 5x 10 nM miR-302a-d & 372 and analyzed at day 2 and day 6. Bars represent SD (representative data). **(C)** Induction of miR-302a by growth conditions without miR delivery. L87 cells were cultured in the presence of hypoxia and FGF2 (black bar) and analyzed at day 7. Control cells were grown under normoxia or hypoxia when a miR-302a inhibitor was added. Error bars represent SD (n=3).

while Lin28 levels were enhanced at a lower albeit until significant level. Further, hypoxia was shown to be relevant for maintenance of Oct4 and Nanog expression until day 5 (**FIG. 25 C**). Under normoxia, Oct4 mRNA was induced at day 1 and strongly reduced thereafter. In contrast, hypoxia led to the prolonged expression of Oct4 induced by STEMcircles™ until day 3. At day 5, hypoxia slightly increased Oct4 expression while an effect of STEMcircles™ could not be observed anymore. Nanog mRNA induction and maintenance until day 5 were strongly promoted by hypoxia. Interestingly, Nanog was decreased at day 3 and induced at day 5 under normoxia and hypoxia. Hypoxia improved or preserved ONSL expression induced by STEMcircles™ delivery.

In summary, application of hypoxia within a non-viral reprogramming strategy was underscored because hypoxia elevated/maintained both Oct4 and Nanog transcription induced by STEMcircles™.

3.3.4.3. Hypoxia Promotes Proliferation in MSCs

Preceding data suggested that hypoxia enhanced the reprogramming process and reprogramming is associated with triggered cell cycle progression. Additionally, proliferation of primary somatic cells is

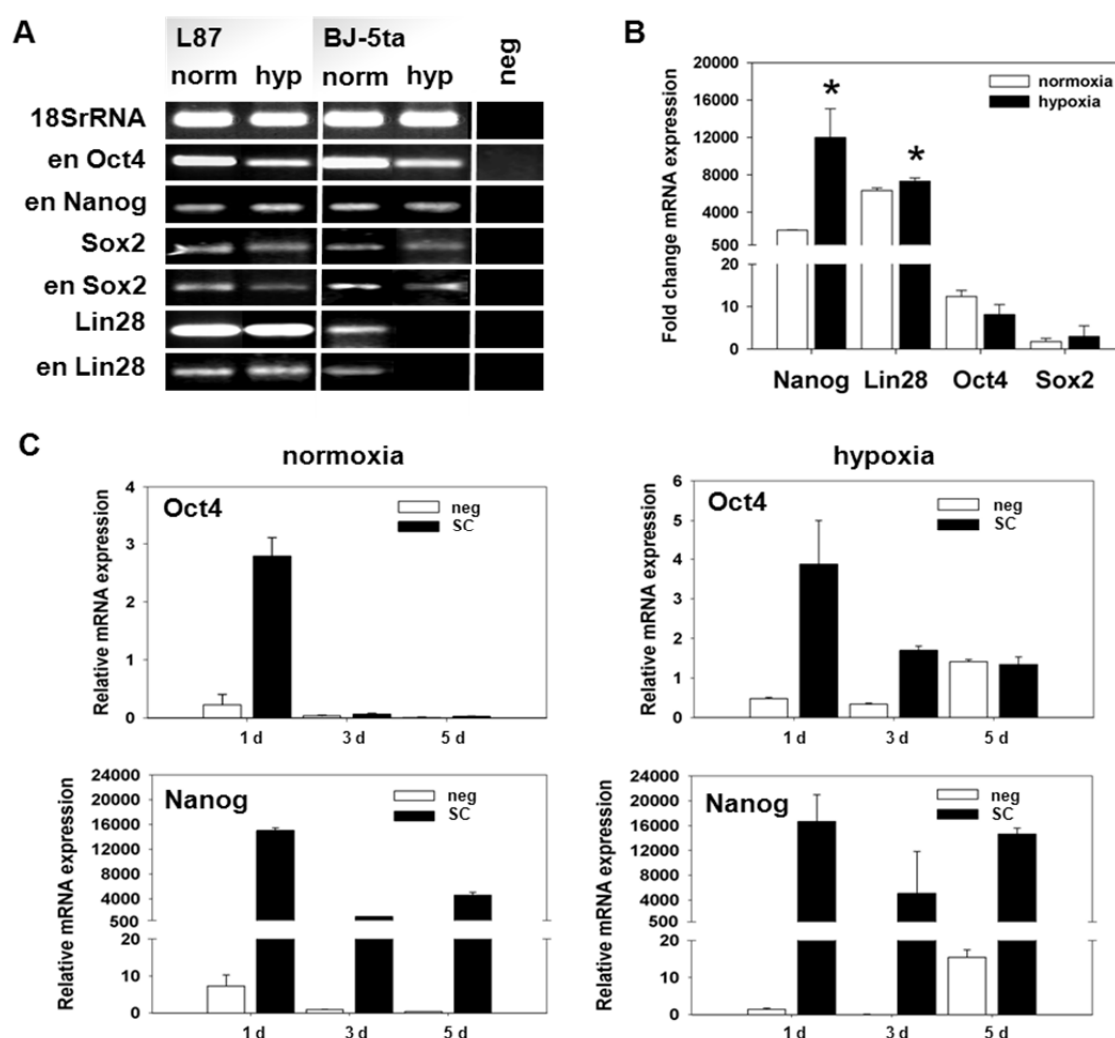


FIGURE 25: STEMcircles™-mediated induction of Oct4, Nanog, Sox2, and Lin28 is regulated by hypoxia. L87 and BJ-5ta cells were transfected with STEMcircles™ (SC) and cultured under normoxic and hypoxic conditions in standard media. **(A)** Semi-quantitative PCR analysis of general and the endogenous (en) ONSL expression at day 3. Reactions without template served as a negative control (neg). Representative data (n=3). **(B)** qRT-PCR analysis of ONSL expression in L87 cells at day 1. Data are shown as fold change in comparison to mock-transfected cells. Oct4A+B expression was examined. Error bars represent SD (n=3). *p<0.05 versus normoxia. **(C)** qRT-PCR analysis of Oct4A+B and Nanog expression from day 1 to day 5 after transfection with episomal vectors. Control cells were mock-transfected (neg). Error bars represent SD. Representative data (n=3).

often restricted to a few passages. Therefore, proliferation of L87 MSCs and primary MSCs was investigated in the presence of hypoxia. Proliferation was increased in L87 MSCs by hypoxia (**FIG. 25 A**). Ki67 staining detected mitotic divisions as a marker for proliferation. Correspondingly, increased proliferation of primary MSCs was reflected by elevated expression of Poli and Mcm5, two genes responsible for cell cycle progression (**FIG. 25 B**). Importantly, proliferation is an important characteristic of reprogrammed cells.

Altogether, the analysis of hypoxic condition after transfection with miR-302a-d & 273 or STEMcircles™ demonstrated strong effects on the induction and preservation of Oct4 and Nanog transcription. These effects were more stronger observed in L87 cells. Further, hypoxia enhanced proliferation, which highlights again that hypoxia is a potent tool within a non-viral reprogramming strategy. Nevertheless, hypoxia did not allow permanent induction of pluripotency characteristics necessary for successful reprogramming

3.3.5. Small Molecules Promote Reprogramming

In order to preserve and to further induce pluripotency characteristics given by miR-302a-d & 273 or STEMcircles™, small molecules were applied because they are potent modulators of signaling pathways involved in pluripotency and reprogramming (**FIG. 3**). Small molecules were applied in different sets according to their way of function namely, epigenetic modulators, signal transduction inhibitors, and kinase inhibitors (**TAB. 1**).

3.3.5.1. Epigenetic Modulators Promote Reprogramming

To study the effect of the above mentioned epigenetic modulators, first the appropriate concentrations of each small molecule namely, SBT, RG, VPA, and BIX were studied. This was important because epigenetic modulators are known to have cytotoxic side effects when they are applied in to high concentrations. Concentrations described in the literature varied depending on the cell type. Therefore, the morphology of L87 cells was intensively studied until day 12 after treatment with epigenetic modulators using standard culture conditions (**APP. 8**). Low and high doses of epigenetic modulators did not seem to affect L87 cell's viability until day 12, but morphologic changes were observed independently from normoxia and hypoxia (**APP. 8/9**). Cells accumulated and formed tight packed clusters in the presence of epigenetic modulators at day 6, but it was not analyzed whether this observation contributes to reprogramming. One important result was that L87 cells were

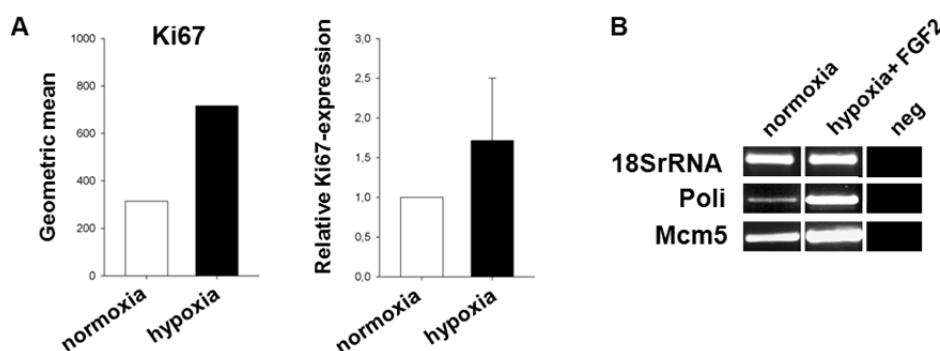


FIGURE 26: Proliferation is regulated by hypoxia and FGF2. (A) Proliferation of L87 MSCs under normoxic and hypoxic conditions. Proliferation was measured at day 7 by Ki67 staining and quantified using flow cytometry. The geometric mean is demonstrated from one representative experiment (left) and fold change of relative Ki67 expression is shown in comparison to normoxia (right). Error bars represent SD (n=3). **(B)** Semi-quantitative PCR analysis Poli and Mcm5. Primary MSCs were cultured under normoxia and hypoxia with FGF2 and analyzed at day 7. Reactions without template served as a negative control (neg).

Table 1: Different sets of small molecules regulating different signaling pathways

small molecule	abbreviation	way of action	single treatment	treatment by a set
RG108	RG ¹	DNMT inhibitor	2 - 20 μ M	0.5 μ M
BIX01294	BIX ¹	HMT inhibitor	0.5 - 2 μ M	1 - 2 μ M
valproic acid	VPA ¹	HDAC inhibitor	0.002 - 0.5 mM	0.5 mM
sodium butyrate	SBT ¹	HDAC inhibitor	0.3 - 3 mM	0.1 - 0.5 mM
BIO	BIO ²	GSK3 inhibitor	2 μ M	2 μ M
Pifithrin alpha	PFT ²	p53 inhibitor	10 μ M	10 μ M
BayK8644	BayK ²	L-type Ca ²⁺ channel activator	2 μ M	2 μ M
PD0325901	PD ³	MEK inhibitor	0.5 μ M	0.5 μ M
SB431542	SB ³	ALK5 inhibitor	2 μ M	2 μ M
Thiazovivin	THIA ³	ROCK inhibitor	2 μ M	2 μ M

¹epigenetic modulators, ²signal transduction inhibitors, and ³kinase inhibitors

Table 2: Epigenetic modulators were applied in different sets.

SBT without VPA	SBT and delayed VPA				VPA and SBT together	
set#1	set#2	set#3	set#4	set#5	set#6	set#7
0 d to 7 d	0 d to 7 d			7 d to 27 d	0 d to 5 d	5 d to 7 d
0.5 mM SBT	0.1 mM SBT	0.3 mM SBT	0.3 mM SBT		0.5 mM SBT	
8 μ M RG	0.5 μ M RG		0.5 μ M RG			0.5 μ M RG
2 μ M BIX	1 μ M BIX	1 μ M BIX				2 μ M BIX
				0.5 mM VPA	0.5 mM VPA	

much more sensitive to epigenetic modulators after transfection with miR-302a-d & 372 (**APP. 9**). Accordingly, epigenetic modulators were applied in 7 different sets, which were applied in different periods of time (**TAB. 2**).

L87 and BJ-5ta cells were transfected with miR-302a-d & 372 and treated with epigenetic modulator set#1–set#7 in the presence of hypoxia because hypoxia was demonstrated to support induction of Oct4 and Nanog subsequent miR-302a-d & 372 delivery in BJ-5ta and L87 cells (**FIG. 23/25**). ES cell-specific conditions were applied to maintain reprogrammed cells (**FIG. 27 A**). Application of set#1 (SBT without VPA) led to strong reduction of surviving cells in the presence or absence of hypoxia in L87 and BJ-5ta cells (**FIG. 27 B; APP. 10**). Modulator set#2–#5 (SBT and delayed VPA) preserved L87 and BJ-5ta cells transfected with miR-302a-d & 372 and supported the formation of colonies around day 27 (**FIG. 27 C**). These morphology of colonies was very similar to that of pre-iPS colonies. Small molecule set#2–#4 were applied until day 7. Cells were transferred to MEFs at day 7 and set#5 was applied until clones were picked at around day 27. Colonies were cut into pieces and seeded onto fresh MEFs (passage 1) without addition of small molecules (**FIG. 27 C**). The procedure was sufficient to generate 49 clones (**APP. 11**). However, 25 out of 49 clones (about 50%) lowered or stopped proliferating within passage 1. Finally, a few clones were preserved until passage 4 (**FIG. 27 D**) and AP staining demonstrated low AP activity in L87-derived colonies at day 60 (**FIG. 27 E**). AP activity was absent in non-treated L87 and BJ 5ta cells while human and mouse ES cells showed high AP activity (**APP. 12**). Application of set#6–#7 (VPA and SBT together) did not allow

the formation of colonies, but single cells harvested at day 26 showed AP staining (FIG. 27 F). Small molecule set#6 was applied until day 5 and set#7 was applied until day 7. In summary, treatment of L87 and BJ-5ta cells with epigenetic modulators was challenging, but treatment allowed the formation and maintenance of colonies with an epithelial morphology after miR-302a-d & 372 delivery. Further, hypoxia and ES cell-specific culture conditions were implemented to create a non-viral reprogramming strategy. It was demonstrated that these BJ-5ta- and L87-derived cells acquired several pluripotency characteristics, but permanent reprogramming was not achieved. Therefore, it was necessary to study other small molecules to create a non-viral reprogramming strategy.

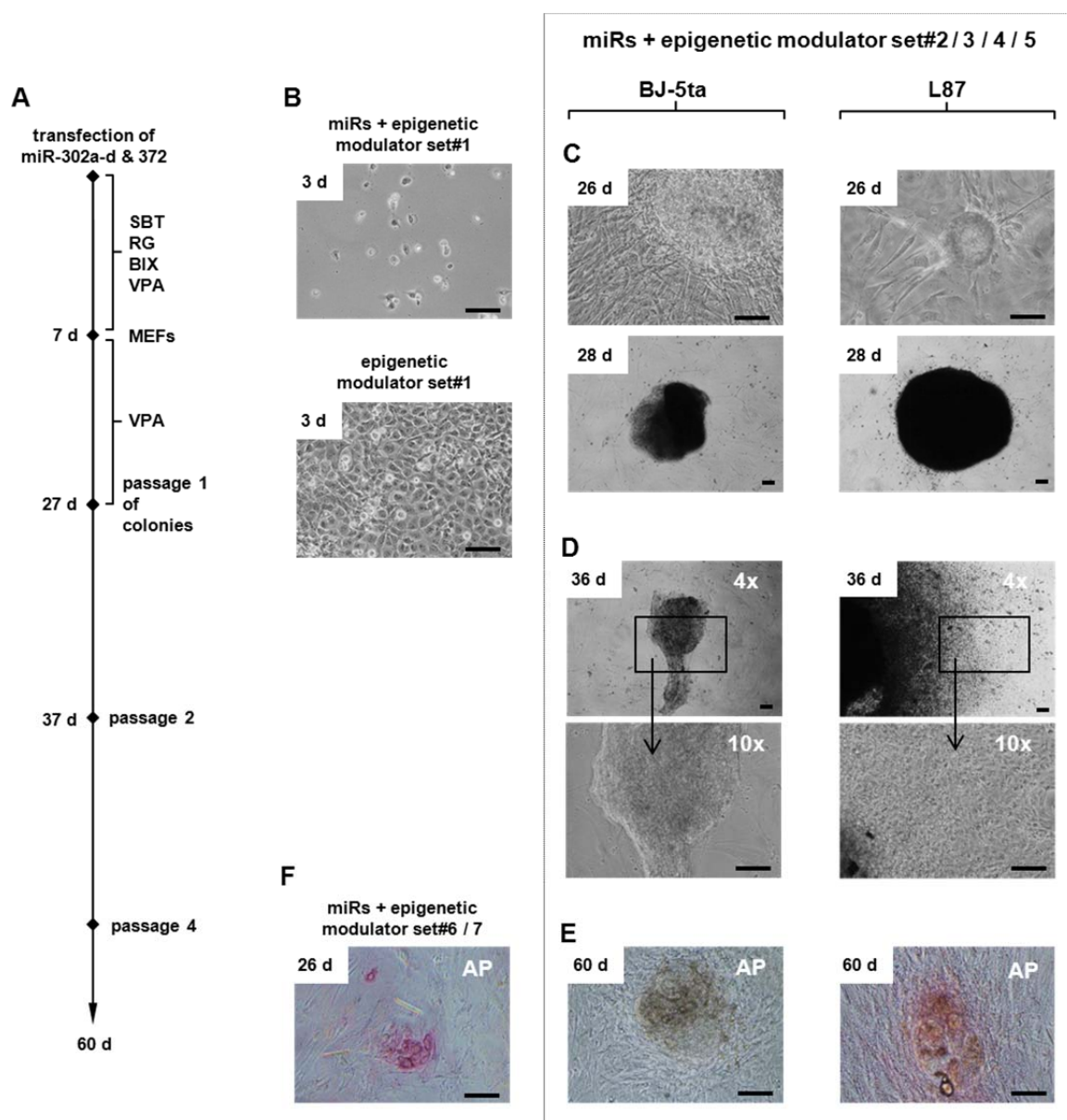


FIGURE 27: Epigenetic modulators promote maintenance of undergoing reprogramming by miR-302a-d & 372 delivery. L87 and BJ-5ta cells were transfected with 5×10^5 nM miR-302a-d & 372 and cultured in the presence of MEFs, ES cell medium with FGF2, and hypoxia. Cells were treated with different sets (set#1-7) of RG, BIX, VPA, and SBT. **(A)** Scheme of pre-iPS generation promoted by epigenetic modulators. **(B)** Analysis of morphology after treatment with epigenetic modulator set#1 (without VPA). L87 cells are shown at day 3. Control cells were not transfected. **(C-E)** Analysis of morphology and AP staining after treatment with epigenetic modulator set#2-#5 (delayed VPA treatment). Epigenetic modulator SBT, RG, and BIX were supplemented until day 7 using different concentrations. VPA treatment started at day 7. **(C)** Morphology of pre-iPS colonies obtained from L87 and BJ-5ta cells at day 26. Picked colonies are shown attached to fresh MEFs at day 28. **(D)** Morphology of pre-iPS clones at day 36. **(E)** AP staining of pre-iPS clones at day 60. **(F)** Analysis of epigenetic modulator set#6 and set#7 (SBT and VPA together). Single cells obtained from BJ-5ta cells are shown at day 26. Bars represent 100 μ m.

3.3.5.2. Signal Transduction Inhibitors Promote Reprogramming

Signal transduction inhibitors PFT, BayK, and BIO (TAB. 1) were analyzed because targeted signaling pathways were thought to be responsible for pluripotency (FIG. 3). Treatment did not seem to affect the morphology of L87 and BJ-5ta cells (FIG. 28 A). Again, a reduction of surviving L87 and BJ-5ta cells was observed after delivery of miR-302a-d & 372 (FIG. 28 B/C). Therefore, hypoxia was not applied aiming at the elevation of surviving cells. Signal transduction inhibitors were applied from day 1 to day 7. Subsequently, cells were cultured under ES cell-specific conditions (FIG. 28 D). Similar to epigenetic modulators, signal transduction inhibitors enhanced a given impulse by miR-302a-d & 372 allowing the formation of colonies at around day 27, but only BJ-5ta cells generated colonies with AP activity (FIG. 28 E). L87-derived cells did not generate distinct clones. BJ-5ta-derived colonies were picked around day 27, but obtained clones stopped growing after passaging.

Together, signal transduction inhibitors allowed the formation of colonies with pluripotency characteristics subsequent transfection with miR-302a-d & 372, but again treatment with small

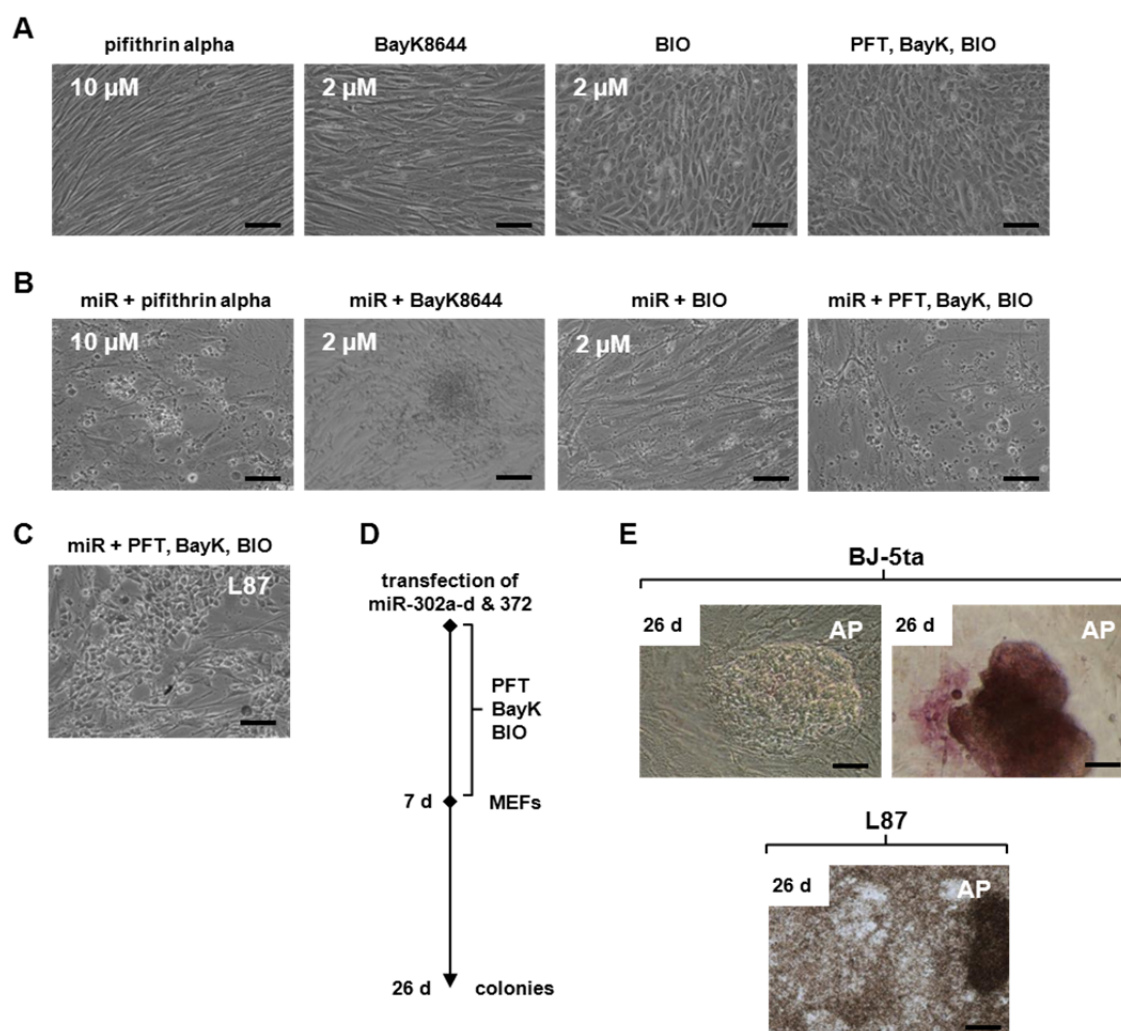


FIGURE 28: Signal transduction inhibitors promote maintenance of pre-iPS colonies established by mi-302a-d & 372 delivery. (A) Analysis of morphology after treatment with signal transduction inhibitors in BJ-5ta cells at day 6. Media were supplemented with PFT, BayK, and BIO as indicated. (B) Morphological analysis of BJ 5ta cells after treatment with signal transduction inhibitors and miR-302a-d & 372 at day 8. Cells were transfected with 5×10 nM miR-302a-d & 372 and cultured in the presence ES cell medium with FGF2 under normoxia. Cells were transferred onto MEFs at day 7. (C) Morphological analysis of L87 cells after treatment with signal transduction inhibitors and miR-302a-d & 372 at day 8. (D) Scheme of reprogramming promoted by signal transduction inhibitors. (E) AP staining of colonies is demonstrated at day 26 before clones were picked. Bars represent 100 μ m.

molecules was not capable to induce permanent reprogramming of L87 and BJ-5ta cells. Therefore, it was necessary to study the application of small molecules in combination with other non-viral reprogramming methods.

3.3.5.3. Kinase Inhibitors Promote Reprogramming

The induction of Oct4 and Nanog by miR-302a-d & 372 was demonstrated in the present work, but STEMcircles™ induced ONSL suggesting that these episomal vectors have a stronger initial impulse towards reprogramming. Accordingly, the kinase inhibitors THIA, SB, and PD (**TAB. 1**) were applied after STEMcircles™ delivery. THIA, SB, and PD are commercially provided as a set of molecules suitable for a variety of studies, but reprogramming was not described. Therefore, morphological analysis after single treatment or combined treatment was not addressed, but the set of kinase inhibitors did not seem to affect cell's morphology.

STEMcircles™ express a GFP reporter, which allowed sorting of transfected and GFP-positive L87 cells (GFP⁺) at day 3 (**FIG. 29 A**). BJ-5ta cells were not applied because STEMcircles™ delivery was shown to be inefficient (**FIG. 9 B**), which hindered enrichment by cell sorting. GFP-positive cells were reseeded onto feeder cells at day 3 and cultured under hypoxic and ES cell-specific culture conditions. Kinase inhibitors were supplemented to the media from day 1 to day 7. The set of kinase inhibitors maintained L87-derived cells and promoted the formation of colonies, which were picked at around day 27. The number of colonies was comparable to the treatment by epigenetic modulators and kinase inhibitors. Importantly, these colonies showed an epithelial morphology and a subset additionally showed AP activity (**FIG. 29 B**). These pluripotency characteristics were maintained in a subset of clones until passage 4 (**FIG. 29 C**). Morphological analyses demonstrated that clones lost their epithelial morphology, formed clumps, and stopped proliferating (**APP. 13**).

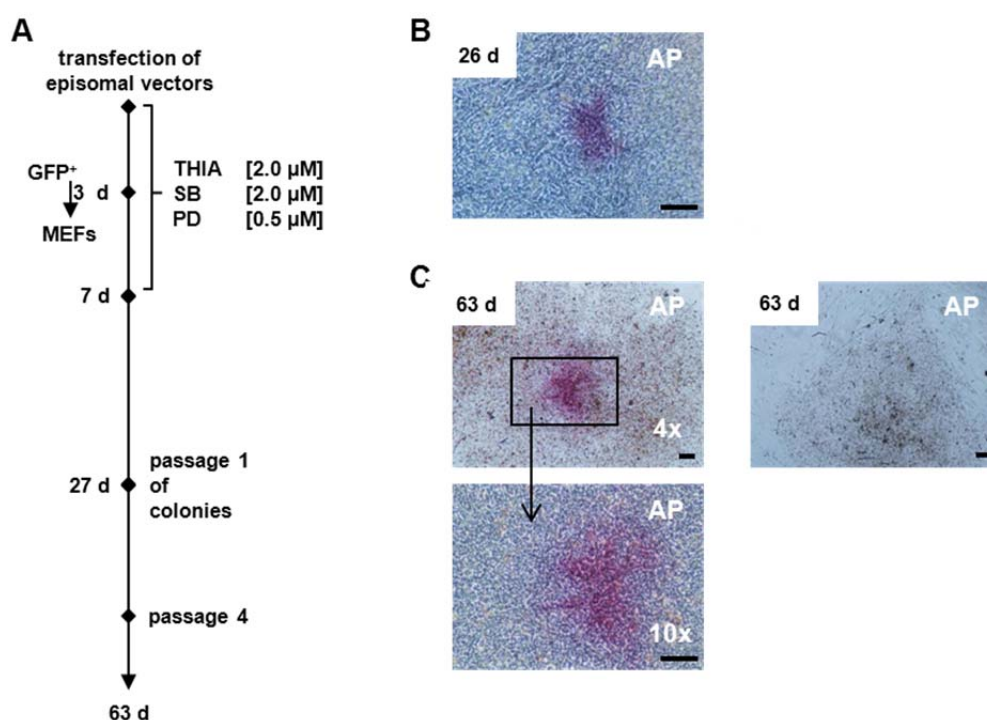


FIGURE 29: Kinase inhibitors promote maintenance of colonies established by STEMcircles™. (A) Scheme of reprogramming promoted by kinase inhibitors. L87 cells were transfected with episomal vectors and GFP-positive cells were cultured in the presence of hypoxic and ES cell-specific conditions. Media was supplemented with THIA, SB, and PD as indicated. (B) AP staining of colonies is demonstrated at day 26. (C) Positive and negative AP staining of L87-derived clones at day 63. Bars represent 100 μm.

In summary, kinase inhibitors allowed the formation of colonies with pluripotency characteristics subsequent transfection with STEMcircles™, but again treatment with small molecules was not capable to induce permanent reprogramming.

Altogether, the analysis of small molecules revealed that an impulse towards reprogramming given by miR-302a-d & 372 or STEMcircles™ can be preserved for a period of time by epigenetic modulators, signal transduction inhibitors, and kinase inhibitors. However, permanent induction of pluripotency characteristics implicating successful reprogramming was not achieved. Importantly, the obtained data recommended the study of subsequent application of all analyzed small molecules in combination with other reprogramming methods to create a non-viral reprogramming strategy.

Up to this point of this study, successful induction of pluripotency characteristics in L87 and BJ-5ta cells by STEMcircles™ or transfection of miR-302a-d & 372 was demonstrated, but these characteristics were not maintained. Further, subsequent application of hypoxic and ES cell-specific culture conditions and treatment with small molecules demonstrated that some of these characteristics can be preserved for a limited period of time, but again permanent maintenance implicating successful reprogramming was not achieved.

3.3.6. Subsequent Use of Non-Viral Methods Promotes Maintenance

Maintenance of L87- and BJ-5ta-derived clones was thought to be a necessary to complete reprogramming for establishment of permanent L87 and BJ-5ta iPS cell lines. Accordingly, subsequent combination of all described reprogramming methods was studied suggesting that additive effects of these methods would allow successful reprogramming.

3.3.6.1. Preservation of Oct4 by co-transfection of STEMcircles™ and miR-302a-d & 372

STEMcircles™ or miR-302a-d & 372 successfully induced endogenous expression of ONSL or miR-302a-d & 372 in L87 and BJ-5ta cells. To enhance an initial impact towards reprogramming, co-transfection aimed at elevating the induction of pluripotency factors, especially of Oct4.

Therefore, cells were co-transfected with both STEMcircles™ and miR-302a-d & 372 using the established protocols described earlier. Transfected cells were cultured under hypoxic and ES cell-specific conditions. Morphological analysis of co-transfected cells showed a strongly reduced number of surviving cells (**APP. 14**). This observation was due to IF analysis in L87 cells demonstrating that GFP expression was reduced at day 3 (**FIG. 30 A**). IF analysis of BJ-5ta cells is not shown because the number of GFP-positive BJ-5ta cells was low even without co-transfection as described earlier. Quantification by flow cytometry demonstrated that the number of GFP-expressing L87 cells was lowered (up to 6.3 %) but the number of GFP-expressing BJ-5ta was not decreased (**FIG. 30 B**). ONSL expression after co-transfection was demonstrated at day 3 under standard conditions. Again, Lin28 transcripts were absent in hypoxia-treated BJ-5ta cells (**FIG. 30 C**). Interestingly, Oct4 expression was elevated by co-transfection at day 7 when normoxic conditions were applied (**FIG. 30 D**). Hypoxia adversely affected Oct4 expression after co-transfection.

Together, miR-302a-d & 372 transfection additionally to STEMcircles™ reduced the efficiency of STEMcircles™, but Oct4 transcription was preserved in L87 and BJ-5ta cells suggesting a subsequent application of these reprogramming methods.

3.3.6.2. Culture Conditions Without Feeder Cells are Suitable for Reprogramming

The use of MEFs providing ES cell-specific culture conditions hampered the localization of establishing BJ-5ta-derived clones. Further, MEFs provide a hard to standardize component in a non-viral reprogramming strategy. Therefore, validation of feeder-free ES cell conditions suitable for maintenance of pluripotent cells was analyzed.

Cultures without feeder cells requires coating of the culture surfaces with ECM compounds such as Matrigel™. In addition, MEF-conditioned medium or media compositions specifically designed for the maintenance of ES and iPS cells are mandatory. The IMR90 iPS cell line was analyzed after 3 passages using Matrigel™ or growth factor reduced Matrigel™ combined with mTeSR1™ or Nutristem™ ES cell medium. The morphology of IMR90 iPS cells slightly varied between different media but not between the different types of Matrigel™ (APP. 15 A). The mRNA expression levels of common pluripotency factors were strongly affected (APP. 15 B). Interestingly, Oct4A and Sox2 mRNA transcripts were up regulated by MEF-conditioned medium, but it was not further analyzed whether this observation contributes to reprogramming. Importantly, IF analysis underscored that MEF-conditioned medium is suitable to replace mTeSR1™ (APP. 15 C). Together, MEF-conditioned medium provides an alternative to commercially available media.

3.3.6.3. Repeated Transfection of STEMcircles™ Does Not Enhance Reprogramming

To enhance the effect of STEMcircles™, repeated treatment with these episomal vectors was attempted to generate fully reprogrammed iPS cells. Transfection of STEMcircles™ was repeated

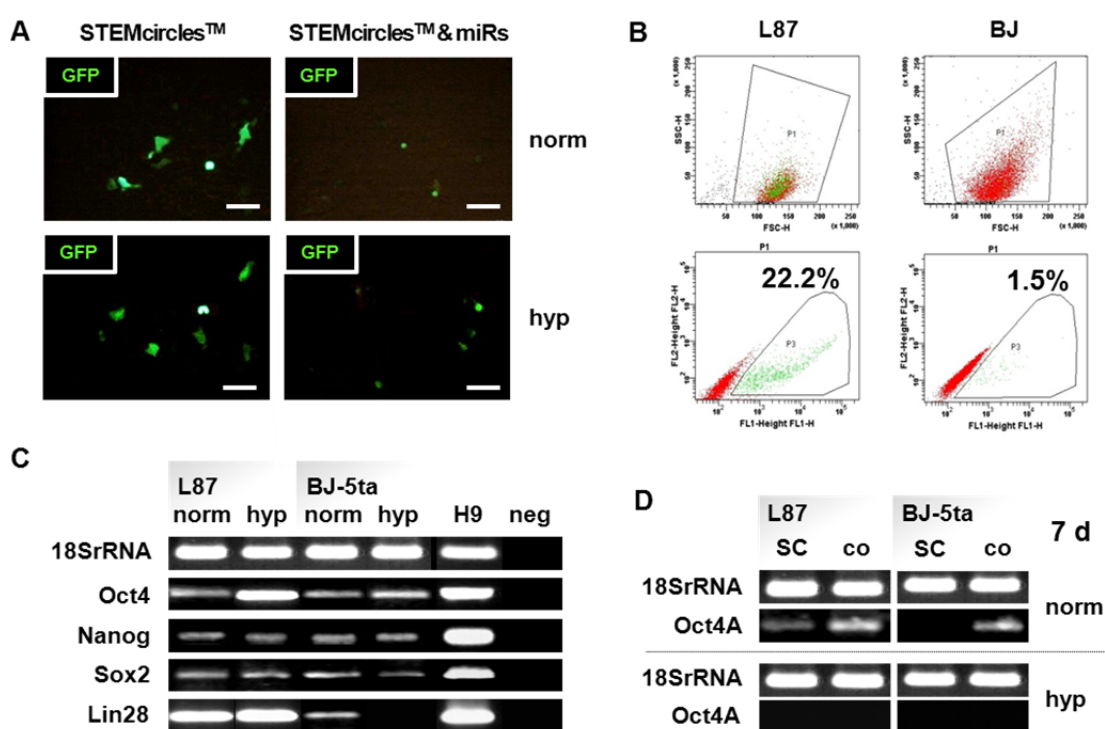


FIGURE 30: Co-transfection of STEMcircles™ and miR-302a-d & 372 affects ONSL expression. L87 and BJ-5ta cells were co-transfected with STEMcircles™ (SC) and miRs using standard procedures and cultured in presence of hypoxia (hyp) and normoxia (norm) using standard media. **(A)** IF analysis of episomal vector-derived GFP-expression in L87 cells at day 3. Bars represent 100 μ m. **(B)** Quantification of vector delivery by flow cytometry at day 3. The percentage of events in parental population P3 is shown. **(C)** Semi-quantitative PCR analysis of ONSL expression at day 3. H9 human ES cells served as a control. Reactions without template served as a negative control (neg). **(D)** Semi-quantitative PCR analysis of Oct4A expression at day 7 after co-transfection (co). GFP-positive cells were reseeded onto MEFs under ES cell-specific conditions and cultured with normoxia or hypoxia. Control cells were transfected only with episomal vectors. Representative data (n=2).

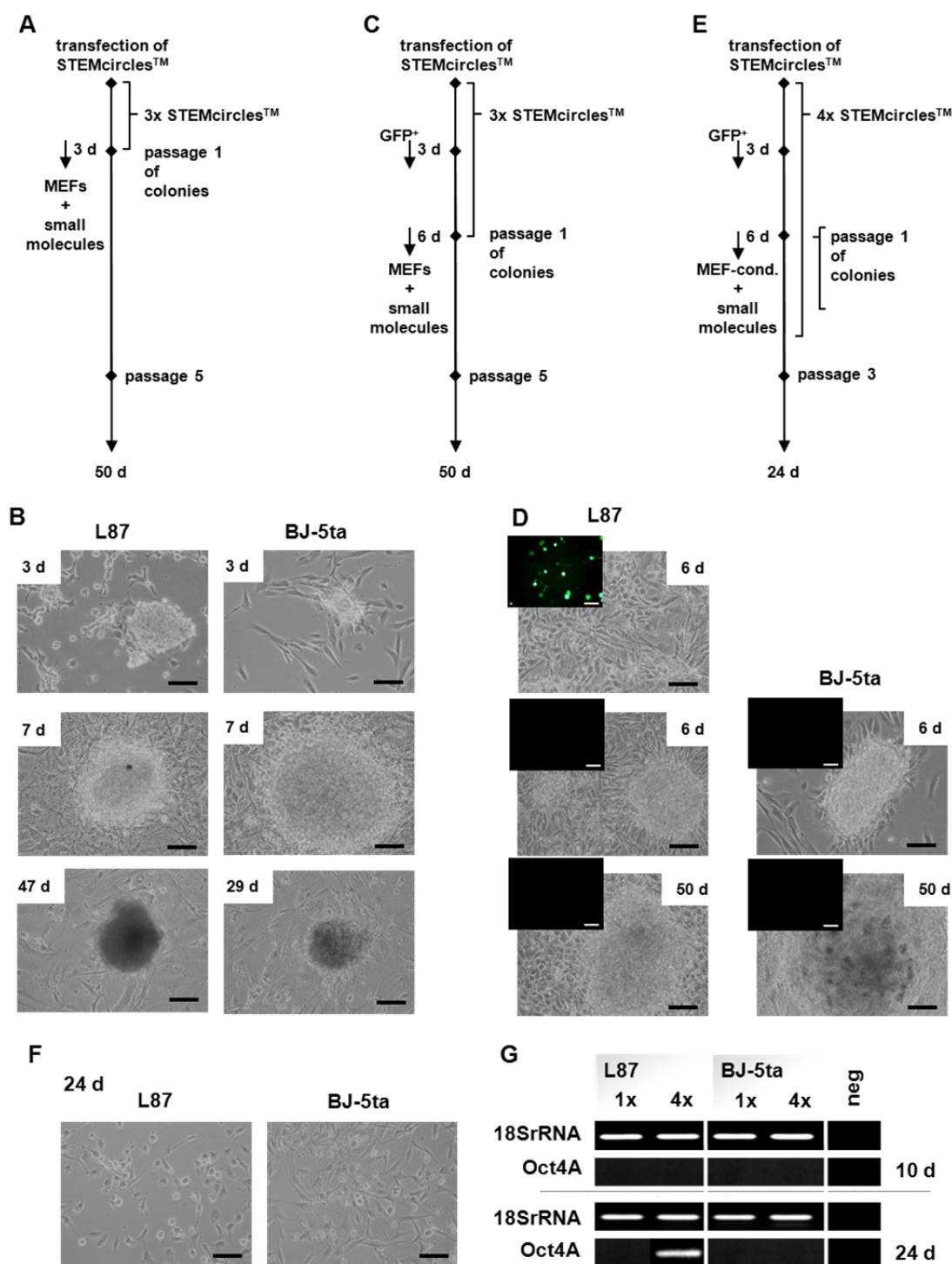


FIGURE 31: Repeated delivery of STEMcircles™ promotes maintenance of colonies. L87 and BJ-5ta cells were transfected with STEMcircles™. Maintenance of colonies was performed under normoxic and ES cell-specific culture conditions (indicated as MEFs) or MEF-conditioned culture conditions (indicated as MEF-cond.). Small molecules were applied using concentrations described earlier (see also FIG. 26-28). **(A)** Approach aiming at the induction of reprogramming by transfection at day 0, day 1, and day 3. Cells were subsequently treated with epigenetic modulator SBT (0.5 mM; 10 d-13 d), signal transduction inhibitors (BayK, BIO, PFT; 13 d-16 d), and kinase inhibitors (THIA, SB, PD; 16 d-19 d). **(B)** Morphological analysis of colonies obtained after transfection with STEMcircles™ at day 0, day 1, and day 3. L87- and BJ-5ta-derived colonies are shown from day 3 to day 47 or day 29. **(C)** Approach aiming at the induction of reprogramming by transfection at day 0, day 4, and day 6. At day 3, GFP-expressing L87 cells were enriched by flow sorting while BJ-5ta cells were not sorted for GFP. Kinase inhibitors were supplemented from day 3 to day 17 **(D)** Morphological and IF analysis of colonies obtained after transfection with STEMcircles™ at day 0, day 4, and day 6. GFP-expressing cells are demonstrated because they were not related to colonies. Maintenance of L87- and BJ-5ta-derived colonies is shown at day 50. **(E)** Approach aiming at the induction of reprogramming by transfection at day 0, day 5, day 12, and day 17. **(F)** Morphological analysis at day 24 and **(G)** semi-quantitative PCR analysis of Oct4A expression after transfection with STEMcircles™ at day 0, day 5, day 12, and day 17. Bars represent 100 μ m.

within a short (3 days), a medium (6 days), and a long time period (17 days). At day 3, ES cell conditions, normoxia, and treatment with small molecules were applied for maintenance of clones. Again, GFP-expressing L87 cells were enriched by flow cytometry, while BJ-5ta cell were not sorted due to their low transfection efficiency.

Transfections within 3 days changed the morphology of L87 and BJ-5ta cells (**FIG. 31 A**). Colony formation was observed at around day 7. Afterwards, treatment with epigenetic modulator SBT (0.5 mM; 10 d-13 d), signal transduction inhibitors (BayK, BIO, PFT; 13 d-16 d), and kinase inhibitors (THIA, SB, PD; 16 d-19 d) was applied. Propagation of L87-derived clones was achieved until passage 5 while BJ-5ta-derived clones stopped growing at passage 3 (**FIG. 31 B**).

Transfection of STEMcircles™ repeated within 6 days generated colonies at day 6 (**FIG. 31 C/D**). Interestingly, GFP expression was not localized in colonies but in single cells between the observed colonies indicating that colony-derived cells lost forced expression of ONSL by STEMcircles™ (**FIG. 32 D**). These colonies were picked and cultured under normoxic and ES cell-specific conditions. Treatment with kinase inhibitors until day 17 allowed propagation of L87- and BJ-5ta-derived clones for a few passages, but these clones underwent cell death within passage 5.

Transfection within 17 days did not generate colonies until day 24 (**FIG. 31 E**). Interestingly, semi-quantitative PCR analysis of these cells demonstrated that Oct4A was transcribed in L87 cells, but Oct4A was absent in BJ-5ta cells (**FIG. 31 G**). In summary, repeated delivery of STEMcircles™ was not sufficient to enhance an initial impulse towards reprogramming.

3.3.6.4. Subsequent use of 6 Small Molecules Promotes Maintenance of ONSL Expression

Data obtained from co-transfection of STEMcircles™ and miR-302a-d & 372 suggested that subsequent delivery of both would promote the preservation of Oct4A. Further, data obtained from repeated STEMcircles™ delivery showed that subsequent treatment with kinase inhibitors and transduction inhibitors is applicable during reprogramming, but another treatment strategy was suggest to be more suitable. Together, these results suggested application of a non-viral reprogramming protocol including (1) STEMcircles™, (2) miR-302a-d & 372, (3) kinase inhibitors, and (4) signal transduction inhibitors (**FIG. 32 A**). At day 5, hypoxic and ES cell-specific conditions were applied for maintenance of clones. Colonies of L87 cells were first observed at day 12 and clones were picked around day 27 (**APP. 16**).

Subsequent treatment with vectors, miRs, and small molecules did induce Sox2 mRNA expression at day 27 neither under normoxic nor under hypoxic conditions, but Oct4A, Nanog and Lin28 were detected (**FIG. 32 B**). Nonetheless, Sox2 was absent and due to this observation clones stopped proliferating at passage 3. Interestingly, cells studied under normoxia and without transfection of miR-302a-d & 372 preserved ONSL expression until day 27 (**FIG. 32 B**). However, these clones also stopped growing at passage 3. However, the subsequent combination of reprogramming methods revealed the accumulation of pluripotency characteristics in L87 derivatives analyzed by the expression of ONSL reprogramming factors. Unfortunately, the induction of permanent proliferating clones was not achieved. Due to the ONSL induction, one can conclude that partial reprogrammed cells were established.

Altogether, the analysis of non-viral reprogramming methods led to a protocol combining these methods for the creation of a non-viral reprogramming strategy. Reprogramming methods namely, delivery of STEMcircles™, delivery of miR-302a-d & 372, application of hypoxic and ES cell-specific

conditions, and treatment with small molecules successfully induced some pluripotency characteristics in L87 and BJ-5ta somatic donor cells.

Importantly, the generation of non-viral iPS cells aimed at their subsequent differentiation into the pancreatic lineage. Pancreatic differentiation requires pluripotent stem cells such as H9 human ES cells, but fully reprogrammed cells were not generated from L87 and BJ-5ta cells. Further, generated clones stopped growing after a few passages also preventing their use in pancreatic differentiation studies. Due to these results, creation of a 3D pancreatic differentiation model had to be studied without own generated iPS cells using human IMR90 iPS cells.

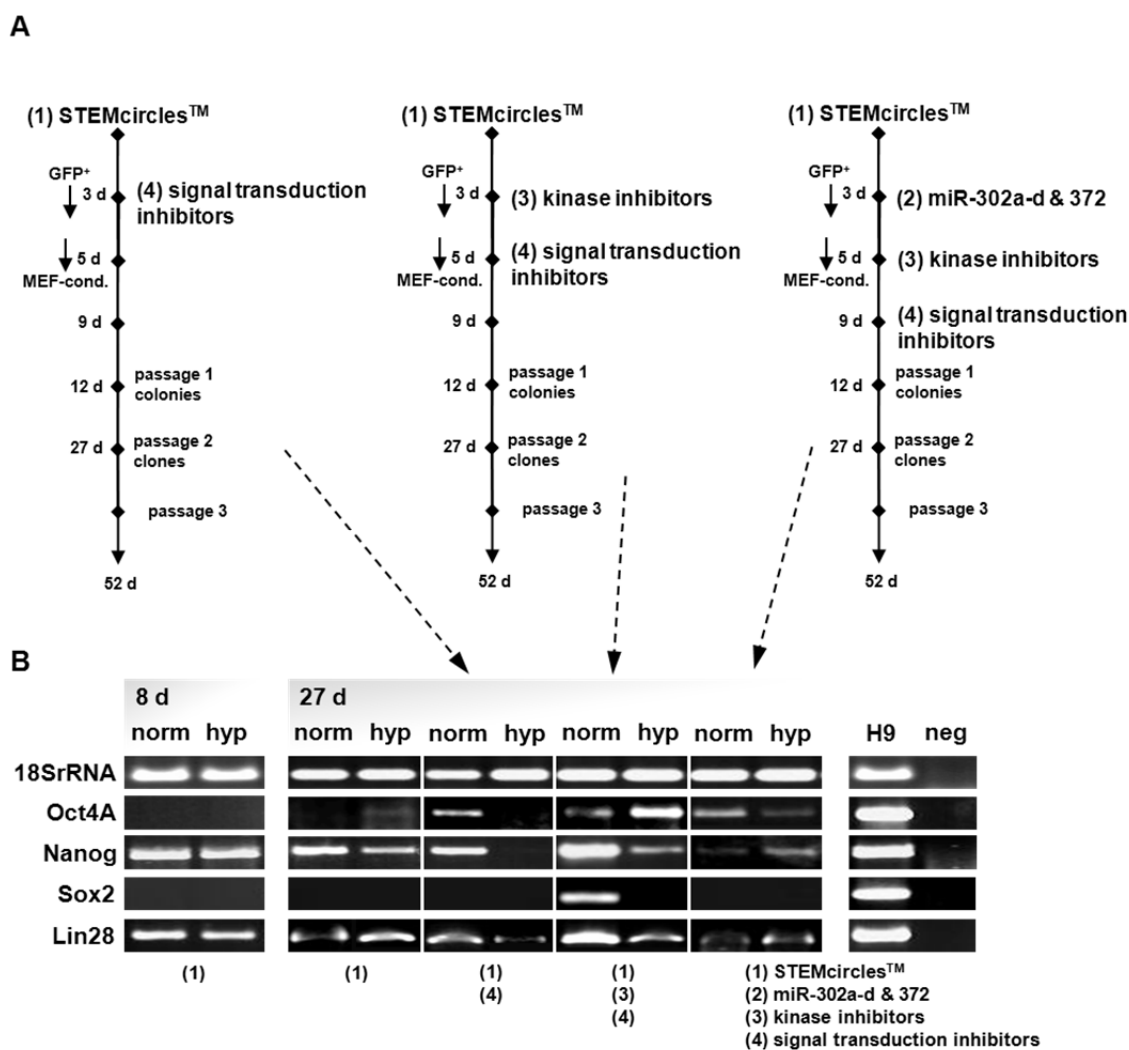


FIGURE 32: Induction of Sox2 in pre-iPS clones is mediated by STEMcircles™ and subsequent treatment with 6 small molecules. (A) Induction of Sox2 expression was analyzed in L87 using a protocol combining subsequent treatment with (1) STEMcircles™, (2) miR-302a-d & 372, (3+4) small molecules. Cells were cultured normoxic (indicated as norm) or hypoxic conditions (indicated as hyp) and human ES cell-specific culture conditions. GFP-positive L87 cells were sorted at day 3 and used in different protocols as indicated. ES cell-specific conditions (indicated as MEF-cond.) were achieved by MEF-conditioned medium with FGF2 and Matrigel™. **(B)** Semi-quantitative PCR analysis of ONSL expression in L87-derived colonies at day 27. H9 human ES cells (H9) served as a positive control. Reactions without template served as a negative control (neg).

3.4. 3D Biological Matrices and ECs during Human Pancreatic Differentiation

The establishment of a 3D pancreatic differentiation model required mimicking of organotypic properties of the endocrine pancreas *in vitro*. Therefore, a 3D biological scaffold and the co-culture with ECs were suggested to be appropriate. Accordingly, applicability and suitability of 3D scaffolds and co-cultures for 3D pancreatic differentiation models were studied intensively aiming at the creation of strategy for the use of 3D biological matrices and co-culture conditions to generate insulin-producing cells.

3.4.1. Production of 3D Biological Matrices from Porcine Jejunum

For the production of the 3D biological matrices, the donor material should have been (i) easy accessible, (ii) easy to produce, and (iii) suitable for pancreatic differentiation. Porcine jejunum satisfied these requirements. The donor material was obtained from suckling pigs or growth-restricted pigs. Jejunum segments were decellularized leaving the 3D biological matrices (**FIG. 33 A/B**). Sterilization and inactivating of antibiotics was achieved by electron-beams (20.1–30.3 kGy) because matrices were heat sensitive (**FIG. 33 C**). Obtained matrices showed a homogenous morphology (**FIG. 33 D**). Interestingly, extra cellular structures of blood vessels were sustained (**FIG. 33 E**). Applicability of 3D biological matrices from porcine jejunum was demonstrated suggesting their analysis during pancreatic differentiation.

3.4.2. 3D Differentiation of Mouse ES Cells into Pancreatic Progenitors

Mouse ES cells provided an appropriate model to study the general suitability of 3D biological matrices for the induction of pancreatic progenitors.

3.4.2.1. Stem Cell Culture and Spontaneous Differentiation on 3D Matrices

The fundamental question was whether 3D matrices allow the culture and differentiation of ES cells. Therefore, mouse CGR8-S17 ES cells were seeded onto 3D matrices and cultured in the presence of stem culture medium. HE staining and SEM showed that ES cell colonies attached to the surface of the 3D matrix, but immigrating cells was not observed (**FIG. 34 A**). The tight net of collagen fibers was visualized by SEM. IF analysis revealed that ES cells sustained the stage-specific embryonic antigen 1 (SSEA1), while endoderm marker *Cxcr4* was absent (**FIG. 34 B**). Accordingly, the undifferentiated status of CGR8-S17 cells was not affected by 3D culture conditions.

The spontaneous differentiation into derivatives of the 3 germ layers was achieved by the generation of EBs. CGR8-S17 ES cells expressed Sox17-DSred at day 9 implicating the generation of DE progenitors (**FIG. 34 C**). Further, the mRNA expression of endodermal, mesodermal, and

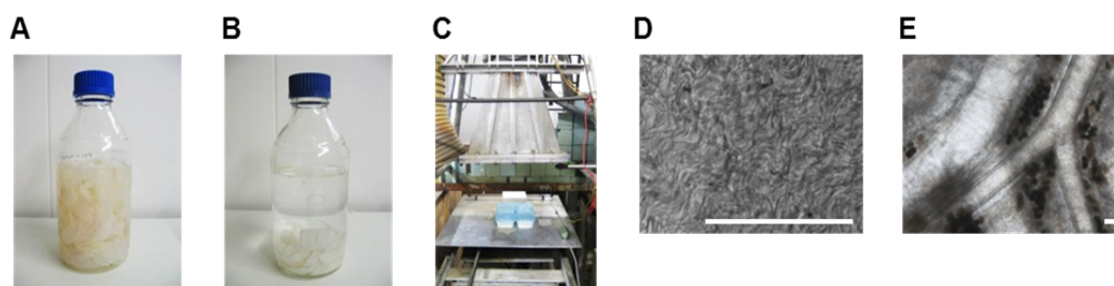


FIGURE 33: 3D biological matrices from porcine jejunum. (A) Porcine jejunum during the decellularization procedure. **(B)** Clean 3D biological matrices ready to use. **(C)** Electron-beam derived sterilization of 3D biological matrices. **(D)** Surface of 3D biological matrices shown by light microscopy. **(E)** Extra cellular structures of blood vessels. Matrices show structures of former venules and arterioles. Bar represents 100 μm .

ectodermal markers was demonstrated due to the spontaneous differentiation (**FIG. 34 D**). However, DE markers *Foxa2* and *Cxcr4* were not detected at day 9 indicating inefficient DE formation due to the spontaneously induced differentiation. Importantly, differentiating cells immigrate into matrices (**FIG. 34 E/F**). Together, these data suggest that 3D matrices are suitable for 3D ES cell differentiation. However, directed pancreatic differentiation had to be analyzed.

3.4.2.2. Directed Pancreatic Differentiation without 3D Matrices

The directed pancreatic differentiation into DE progenitors was achieved by the generation of EBs in the presence of activin A (**FIG. 35 A**). Control cells were spontaneously differentiated in the presence of FCS. EBs were seeded at around day 9 when *Sox17*-DSred was strongly expressed. Afterwards DE progenitors differentiated into the pancreatic lineage in the presence of a PDM. Morphological analysis at around day 14 revealed the presence of small epithelial clusters also known as islet-like clusters. Semi-quantitative PCR analysis at day 20 showed that the mesendoderm and

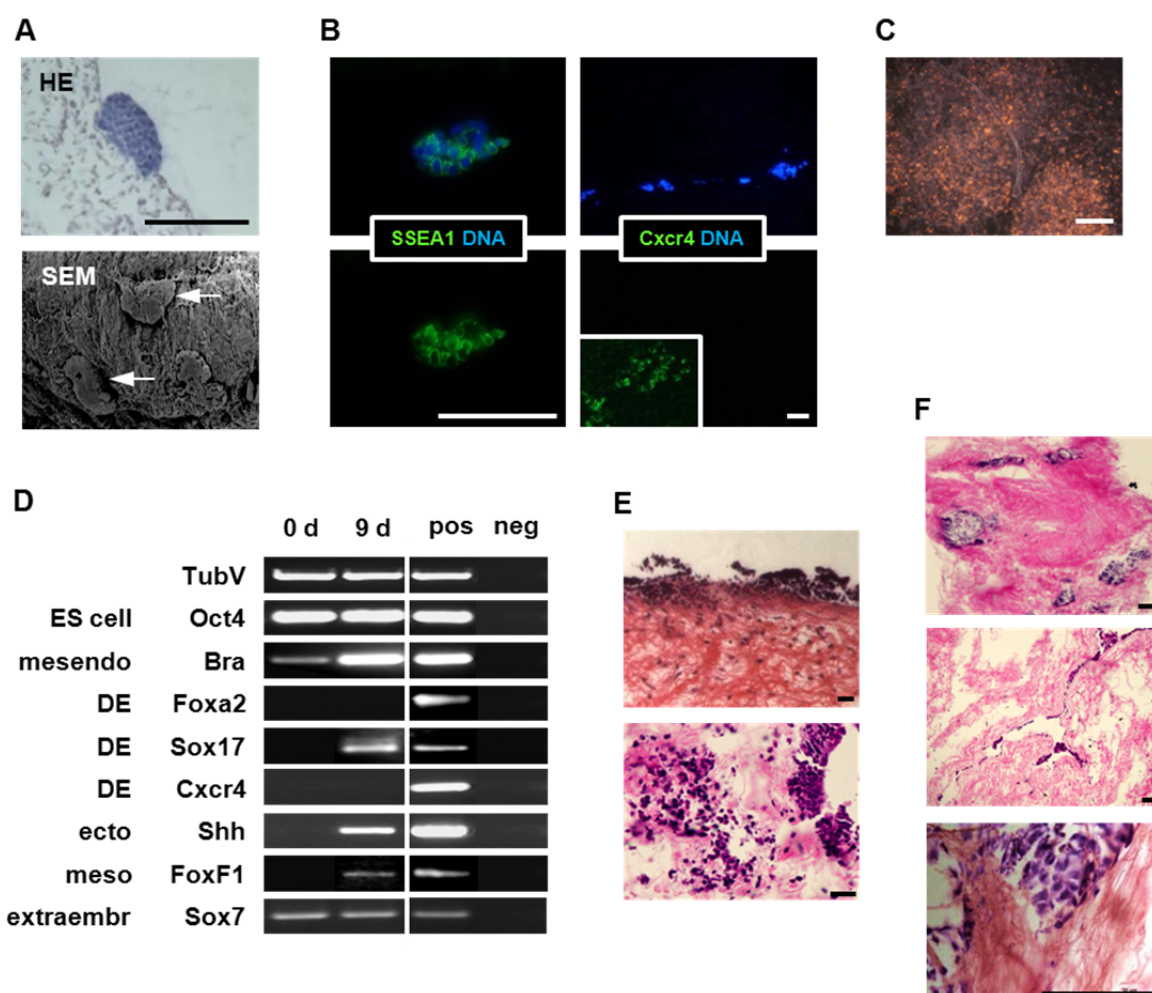


FIGURE 34: 3D biological matrices are adequate to culture and differentiation of ES cells. CGR8-S17 mouse ES cells were cultured on 3D matrices using stem culture medium or medium for spontaneous differentiation. **(A)** HE staining and SEM of ES cell colonies (arrows) on 3D matrices with stem culture medium. **(B)** IF analysis of undifferentiated ES cells. Murine pluripotency gene *SSEA1* and early differentiation gene *Cxcr4* (absent) are shown. Mouse spleen served as a positive control for *Cxcr4* (lower box). **(C)** IF analysis of spontaneously generated *Sox17*-DSred-positive DE progenitors at day 9. **(D)** Semi-quantitative PCR analysis of spontaneous differentiation at day 9. The mRNA expression of mesendoderm (mesendo), definitive endoderm (DE), ectoderm (ecto), mesoderm (meso), and extraembryonic (extraembr) was analyzed. RNA from mice tissues served as positive controls (pos). Reactions without template served as a negative control (neg). Representative data (n=3). **(E)** HE staining of vertical paraffin and **(F)** HE staining of horizontal paraffin sections at day 14 of spontaneous differentiation. Emigrating cells are demonstrated in different magnifications. Bars represent 100 μ m.

endoderm markers Bra and Cxcr4 were expressed after spontaneous and directed differentiation (FIG. 35 B). Importantly, the induction of Pdx1 mRNA indicated the presence pancreatic progenitors (FIG. 35 B). Pancreatic exocrine marker Amy2 was not detected after directed differentiation implicating a low number of pancreatic exocrine progenitors. However, pancreatic endocrine marker

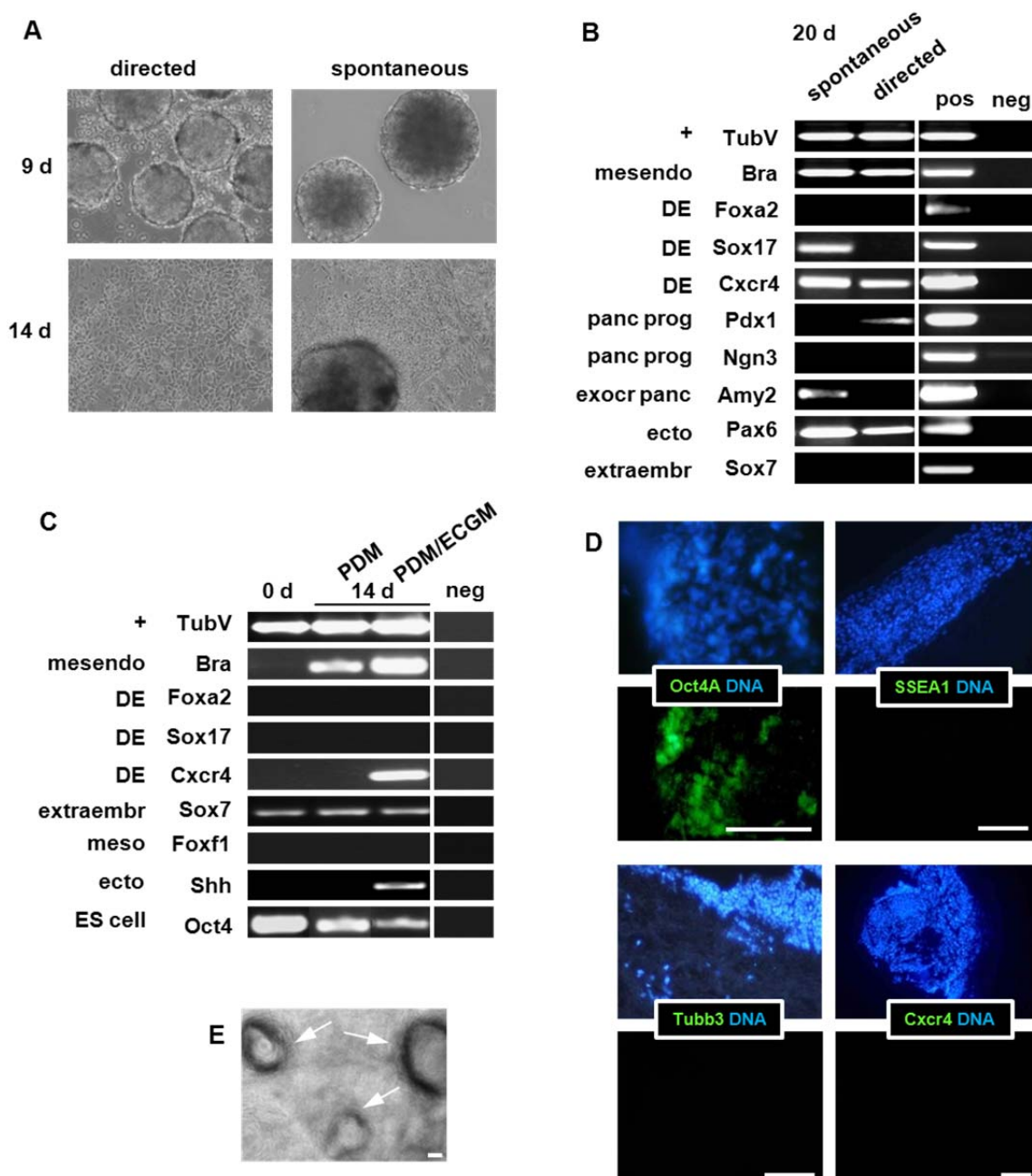


FIGURE 35: Directed differentiation generates DE for 2D and 3D pancreatic differentiation. CGR8-S17 cells were cultured in hanging drops in CDM with 50 ng/ml activin A for directed differentiation of DE progenitors. Control cells were spontaneously differentiated. **(A)** Morphology during 2D differentiation. At day 9, the formation of EBs is demonstrated for directed and spontaneous differentiation. At day 9, EBs were cultured in pancreatic differentiation medium (PDM). The morphology of outgrowing cells is demonstrated at day 14. **(B)** Semi-quantitative PCR analysis of directed and spontaneous pancreatic 2D differentiation at day 20. The mRNA expression of markers for mesendoderm (mesendo), definitive endoderm (DE), pancreatic progenitors (panc prog), exocrine pancreas (exocr panc), ectoderm (ecto), and extraembryonic tissue (extraembr) is shown. RNA from mice tissues served as positive controls (pos). Reactions without template served as negative controls (neg). **(C)** Semi-quantitative PCR analysis of directed pancreatic differentiation on 3D matrices. Activin A-induced EBs were seeded onto 3D matrices at day 9. Cells were cultured in PDM or a 1:1 mixture of PDM and ECGM until day 14. Cells were characterized by genes as indicated. Representative data (n=3). **(D)** IF analysis of directed pancreatic differentiation on 3D matrices. Paraffin sections were stained for pluripotency genes Oct4A and SSEA1, neuronal gene Tubb3, and DE gene Cxcr4 at day 14. Representative data (n=2). **(E)** Light microscopy shows cavities on 3D matrices after separation of EBs at day 14. Bars represent 100 μ m.

Ngn3 was absent at day 20. However, the differentiation of CGR8-S17 cells into Pdx1-expressing cells verified successful pancreatic progenitor formation under two-dimensional (2D) culture conditions. Therefore, this verified protocol had to be transferred to 3D culture conditions.

3.4.2.3. 3D Differentiation into DE Progenitors with Co-Culture Media

Particularly because the pancreatic induction was demonstrated in 2D cultures, this protocol was also applied for the 3D pancreatic differentiation of CGR8-S17 cells. EBs were transferred to matrices at around day 9 when Sox17-DSred was strongly expressed. At day 14, semi-quantitative analysis revealed that germ layer markers were down-regulated (**FIG. 35 C**). Albeit the expression of Oct4 and Bra was detected, loss of Foxa2, Sox17, Cxcr4, Foxf1, and Shh suggested continuing differentiation of germ layer progenitors on 3D matrices. IF analysis at day 14 demonstrated that a few Oct4A-expressing cells were sustained, but SSEA1 was absent in differentiated cells (**FIG. 35 D**). Differentiation on 3D matrices did not seem to induce formation of neuronal progenitors because Tubb3 protein was absent. Interestingly, attached EBs formed cavities on 3D matrices suggesting that these cells remodeled the structure of their surrounding ECM (**FIG. 35 E**).

Another fundamental question was whether co-culture conditions allow the pancreatic differentiation of ES cells. Accordingly, EBs were seed onto matrices and cultured in co-culture medium composed of 1:1 PDM and ECGM. Semi-quantitative PCR analysis at day 14 showed the induction of Shh while Foxf1 remained absent and Sox7 was not elevated (**FIG. 35 C**). Albeit the induction of ectoderm marker Shh was observed, the endoderm marker Cxcr4 was induced, too.

Together, these data provide evidence that differentiation of pancreatic endocrine cells can be performed using 3D biological matrices and co-culture media. However, differentiation towards the pancreatic lineage had to be studied more intensively in the human system.

3.4.2.4. Induction of DE Progenitors without EB Formation on 3D matrices

One basic idea was that DE progenitor formation can be achieved without EB formation, but

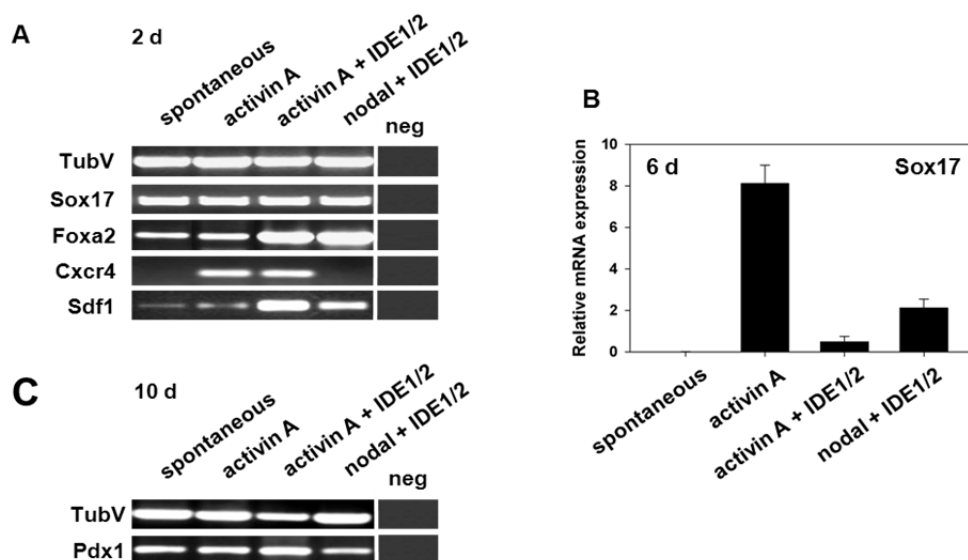


FIGURE 36: Induction of DE progenitors on 3D matrices without EB formation. Directed differentiation of CGR8-S17 ES cells on 3D matrices was analyzed. ES cells seeding on 3D matrices were treated with activin A, nodal, and IDE1/2 as indicated. Control cells were spontaneously differentiated. **(A)** Semi-quantitative PCR analysis of DE markers Sox17, Foxa2, Cxcr4, or extraembryonic endoderm marker Sdf1 at day 2. **(B)** qRT PCR analysis of Sox17 mRNA levels at day 6. **(C)** Semi-quantitative PCR analysis of pancreatic marker Pdx1 at day 10. Reactions without template served as a negative control (neg). Representative data (n=2).

efficiencies are very low when 2D culture conditions are applied. Therefore, it was interestingly to study the generation of DE progenitors from ES cells, which were already cultured on 3D matrices.

Treatment with activin A, IDE1/2, and nodal was analyzed because they are generally applied for the induction of DE progenitors. Interestingly, analysis of DE genes at day 2 demonstrated that Sox17, Foxa2, and Cxcr4 were present only by treatment with activin A (**FIG. 36 A**). Sdf1 mRNA indicating the presence of extraembryonic endoderm induced by spontaneous and directed differentiation. Interestingly, qRT PCR showed highest Sox17 mRNA levels by activin A alone (**FIG. 36 B**). Further differentiation revealed that the pancreatic progenitor marker Pdx1 was induced at day 10 only by the presence of 3D matrices. (**FIG. 36 C**). Taken together, these data raise evidence that 3D pancreatic differentiation might be successful without EB formation. However, this completely new approach had to be analyzed separately.

3.4.3. Primary Endothelial Cells are Preserved under Co-Culture Conditions

The establishment of a 3D pancreatic differentiation model required the generation of primary EC for the establishment of co-culture conditions during pancreatic differentiation. Primary MVECs were obtained from skin biopsies and HUVECs were obtained from human umbilical cords.

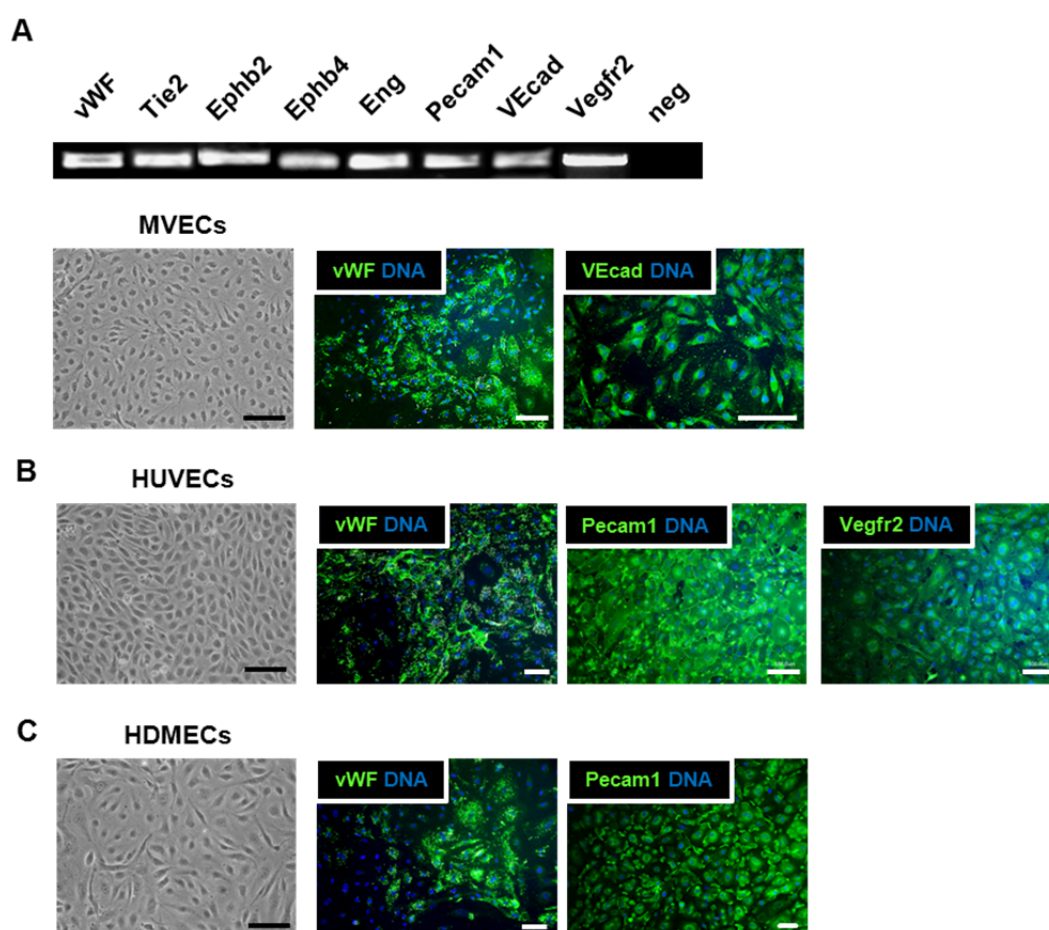


FIGURE 37: Primary MVECs and HUVECs maintain natural characteristics *in vitro*. ECs were characterized by morphology and the expression of EC genes (**A**) Characterization of primary MVECs at passage 3. Semi-quantitative PCR analysis shows the mRNA expression of EC markers. Reaction without template served as negative control (neg). The morphology is demonstrated. IF analysis shows the protein expression of vWF and VEcad. (**B**) Characterization of primary HUVECs at passage 3. The morphology is demonstrated. IF analysis shows the protein expression of vWF, Pecam1, and Vegfr2. (**C**) Characterization of commercially available primary HDMECs at passage 3. The morphology and the expression of vWF and Pecam1 protein are demonstrated. Bars represent 100 μ m.

For the isolation of MVECs, skin biopsies from palms and plantar or from surgical removal of excess skin were not suitable. Primary MVECs showed EC-like morphology and expressed several EC markers on the mRNA level namely, von Willebrand factor (vWF), tunica internal endothelial cell kinase 2 (Tie2; officially termed as Tek), ephrin receptors B2 (Ephb2) and B4 (Ephb4), endoglin (Eng), platelet/endothelial cell adhesion molecule 1 (Pecam1), vascular endothelial cadherin (VEcad; also known as Cdh5), and Vegfr2 (**FIG. 37 A**). Further, vWR, and VEcad protein expression was verified by IF analysis. During further passages, proliferation was continuously decreased and the EC-like morphology was getting lost related to the appearance of senescent cells. The age donors did not have a significant impact on the number of isolated ECs, but differences were observed. HUVECs showed a slightly different morphology, but morphology was typical for ECs (**FIG. 37 B**). The protein expression of the crucial EC markers vWF, Pecam1, and Vegfr2 was verified by IF analysis. Commercially available HDMECs were analyzed as a positive control (**FIG. 37 C**) to ensure the presence of natural characteristics in MVECs and HUVECs.

Primary ECs retained natural characteristics, but there was a need to analyze whether these characteristics were preserved in co-culture medium composed of 1:1 ECGM and HPDM. The mRNA expression of vWF, Pecam1, Vegfr2, and VEcad was not affected by treatment with high glucose, 1:1 HPDM and ECGM, and HPDM alone (**FIG. 38**). Importantly, HPDM almost abolished protein expression of vWF and Pecam1 demonstrated by IF analysis (**FIG. 38**). ECGM and high glucose slightly reduced the protein expression vWF and Pecam1. However, IF analysis of 1:1 ECGM and HPDM revealed that vWF and Pecam1 proteins were abundantly expressed. In summary, successful

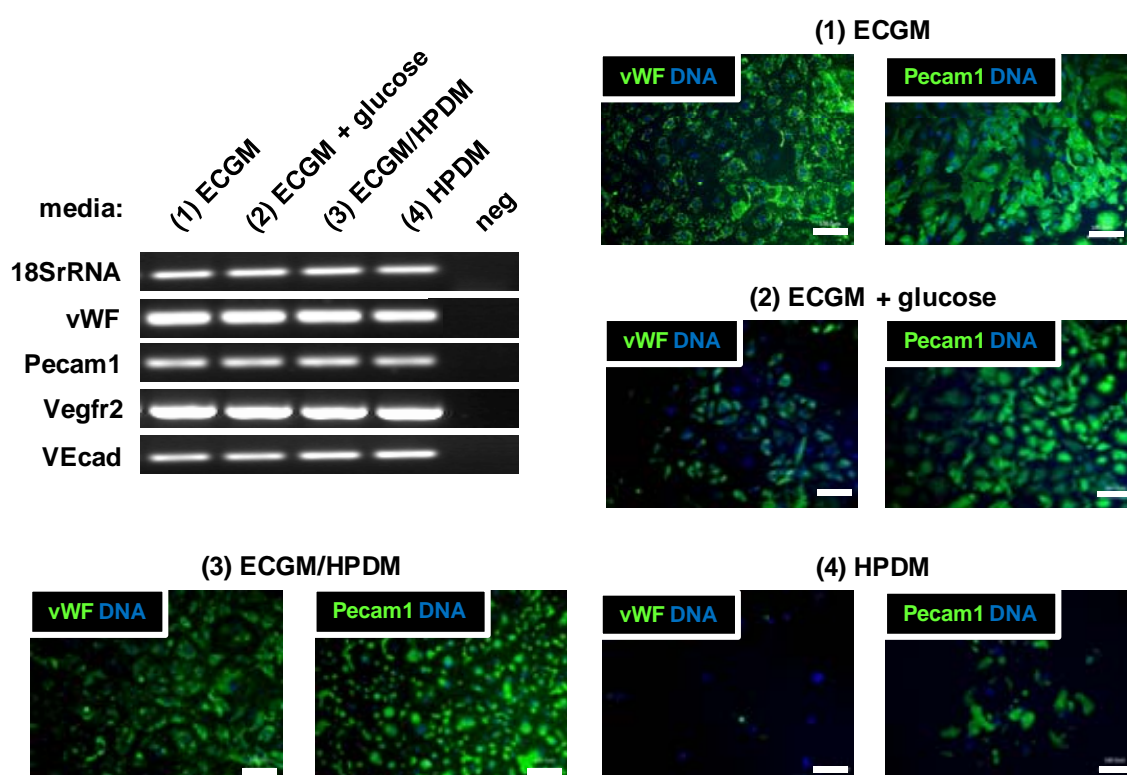


FIGURE 38: Maintenance of primary ECs in pancreatic differentiation media. Analysis of culture conditions of primary HDMECs at day 7. Cells were propagated using 4 different media: **(1)** Standard EC medium indicated as ECGM, **(2)** ECGM supplemented with 50 mM glucose, **(3)** 1:1 mixture of ECGM and HPDM. **(4)** Pancreatic differentiation medium indicated as HPDM. Semi-quantitative PCR analysis of EC gene expression is demonstrated. Reactions without template served as a negative control (neg). IF analysis shows the protein expression of vWF and Pecam1. Representative data (n=3). Bars represent 100 μm.

isolation and maintenance of primary ECs was demonstrated. Further, co-culture with ECs retaining their natural characteristics is possible using a 1:1 mixture of ECGM and HPDM.

3.4.4. Pancreatic Differentiation of Human iPS Cells using Co-Cultures and 3D Matrices

For the establishment of a 3D pancreatic differentiation model, primary ECs, co-culture medium, and 3D matrices were successfully established. Accordingly, co-culture with ECs and 3D matrices were analyzed using IMR90 iPS cells. Protein expression of pluripotency markers in IMR90 iPS cells was demonstrated verifying their pluripotency, which is a prerequisite for successful pancreatic differentiation (**FIG 39**). Importantly, as a positive control, the differentiation of IMR90 iPS into pancreatic progenitors using 2D cultures was analyzed.

3.4.4.1. Pancreatic Differentiation of IMR90 iPS Cells

Differentiation of commercially available IMR90 iPS cells into pancreatic progenitors was analyzed in 2D cultures to show that pancreatic progenitors can be derived from patient- and disease-specific iPS. Further, successful generation of pancreatic progenitors in 2D culture should serve as a positive control for the analysis of co-cultures with ECs and 3D differentiation on matrices.

In accordance with mouse pancreatic differentiation, directed pancreatic differentiation was induced by activin A. Spontaneous differentiation was induced by FCS. Albeit the principal differentiation protocol is very similar to that of mouse ES cells, human ES cells are generally differentiated without EB formation. The directed differentiation generated small epithelial clusters at day 3 thought to be DE progenitors (**FIG. 40 A**). In contrast, spontaneous differentiation generated cells with manifold morphology and few small epithelial clusters were rarely detected at day 3 (**FIG. 40 B**). Cells with a neuron-like morphology were observed at around day 7. The manifold morphology of spontaneously differentiated cells was sustained during the entire differentiation.

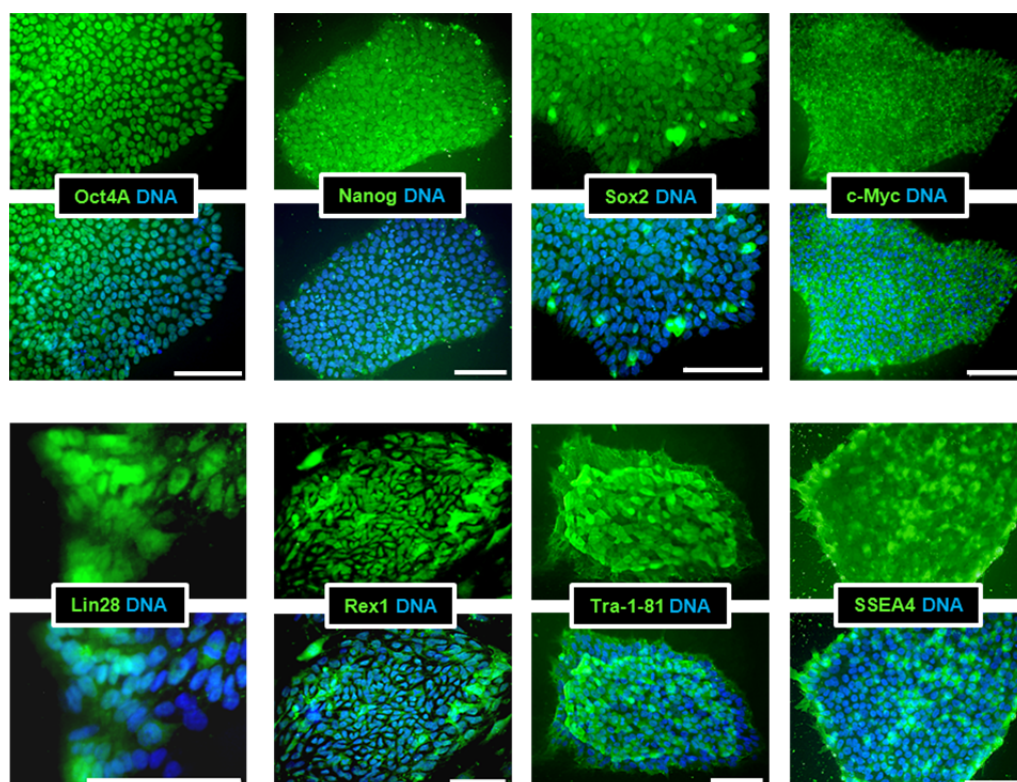


FIGURE 39: Pluripotency makers expressed in IMR90 iPS cells. IF analysis of transcription factors Oct4A, Nanog, Sox2, c-Myc, Lin28, Rex1 and surface proteins Tra-1-81, SSEA4. Bars represent 100 μ m.

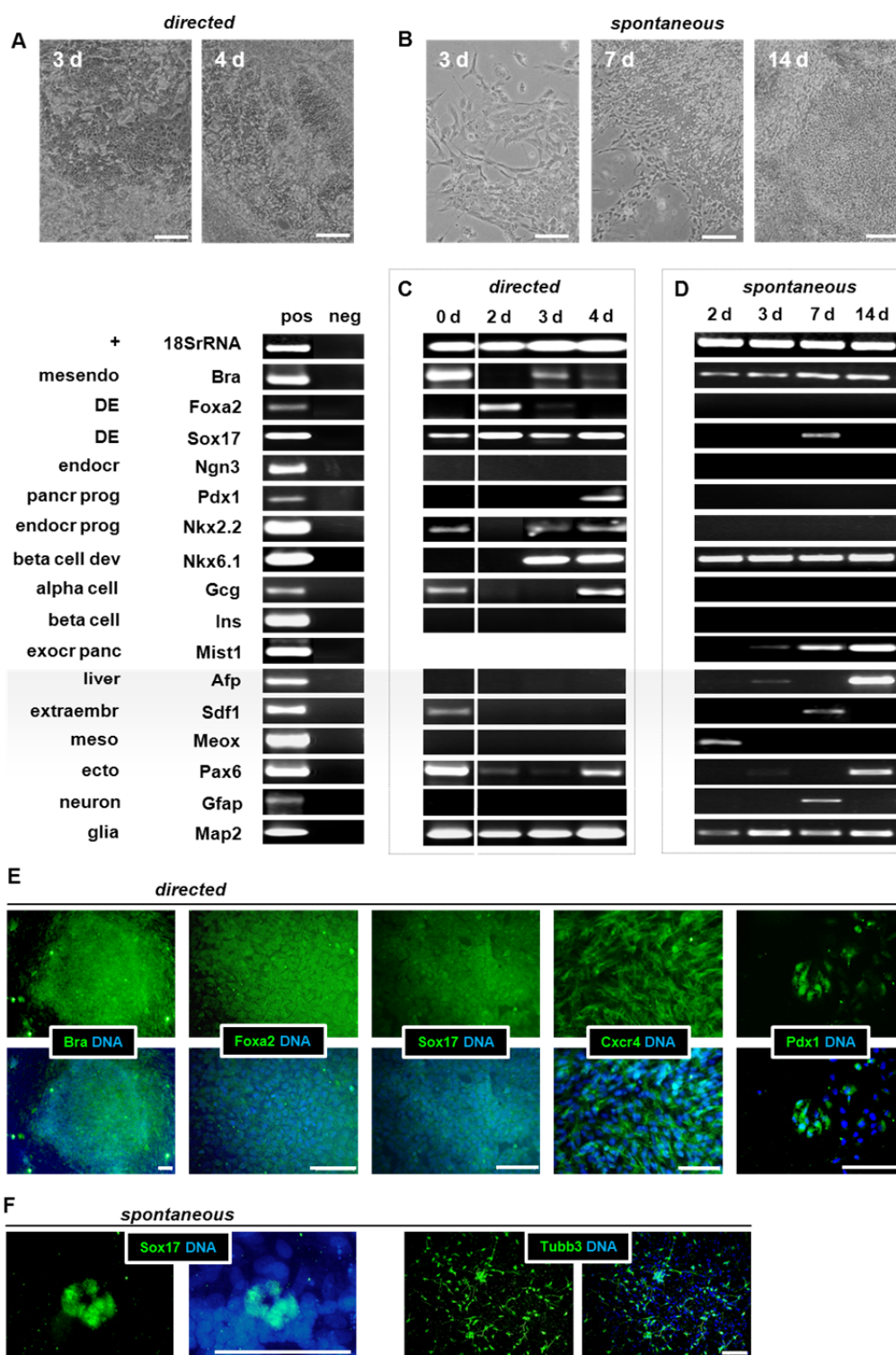


FIGURE 40: Differentiation of human IMR90 iPS cells into pancreatic progenitors. Cells were differentiated according to the pancreatic differentiation protocol and analyzed for their morphology and the expression of lineage specific genes. Control cells were spontaneously differentiated. (A) Morphology of DE progenitors during directed pancreatic differentiation. (B) Morphology of cells during spontaneous differentiation. (C) Semi-quantitative PCR analysis of directed pancreatic differentiation. RNA from human tissues served as positive controls (pos). Reactions without template served as a negative control (neg). Selected genes indicate the presence of mesendoderm (mesendo), definitive endoderm (DE), endocrine cells (endocr), pancreatic progenitors (panc prog), endocrine pancreatic progenitors (endocr prog), developing beta cells (beta cell dev), immature alpha cells (alpha cell), immature beta cells (beta cell), exocrine pancreatic progenitor (exocr panc), immature liver cells (liver), extraembryonic tissue (extraembr), mesoderm (meso), ectoderm (ecto), neuron progenitors (neuron), glia progenitors (glia). Representative data (n=3). (D) Semi-quantitative PCR analysis of spontaneous differentiation. (E) IF analysis of directed pancreatic differentiation. Staining of mesendoderm marker Bra and DE markers Sox17, Cxcr4, and Foxa2 is demonstrated at day 3. Pdx1 is shown at day 9. (F) IF analysis of spontaneous differentiation. Staining of Sox17 and neuronal marker Tubb3 is demonstrated at day 12. Bars represent 100 μ m.

Semi-quantitative PCR analysis of directed pancreatic differentiation until day 4 was used to describe the development of multipotent progenitors and their development towards the pancreatic lineage. Directed differentiation induced mRNA expression of the mesendoderm marker Bra and the DE markers Foxa2 and Sox17 were induced (**FIG. 40 C**). IF analysis of Bra, Foxa2, Sox17, and Cxcr4 at day 3 verified the generation of DE progenitors (**FIG. 40 E**). Importantly, the Pdx1 mRNA was induced at day 4 and Pdx1 protein was observed at day 9 by IF analysis (**FIG. 40 C/E**). Pdx1 expression indicates the formation of pancreatic progenitors. Accordingly, beta cell development markers Nkx2.2 and Nkx6.1 and alpha cell development marker glucagon (Gcg) were induced on the mRNA level at day 3 and day 4. These markers are necessary for the generation of pancreatic endocrine progenitors. Ngn3 and Ins transcripts were not detected until day 4, but they are generally associated with later stages of the pancreatic development. Pax6 and Map2 mRNA expression was induced until day 4 because directed pancreatic differentiation strongly promoted the pancreatic lineage, but other germ layer derivatives were also differentiated to a lower extent.

In contrast to the directed differentiation, spontaneous differentiation showed delayed and low induction of Sox17 transcripts at day 7 (**FIG. 40 D**). Albeit the Nkx6.1 mRNA expression was observed, the vast majority of lineage markers indicated the enhanced generation of mesoderm- and ectoderm-derived cells until day 14. IF analysis at day 12 verified that spontaneous differentiation barely generated Sox17-expressing cells (**FIG. 40 F**). Further, Tubb3 protein was strongly induced at day 12 indicating the presence of many ectoderm derivatives. However, the analysis of directed pancreatic differentiation successfully demonstrated the differentiation of IMR90 iPS cells into DE progenitors, which already expressed crucial pancreatic lineage markers. Accordingly, integration of co-cultures in the established pancreatic differentiation protocol had to be analyzed.

3.4.4.2. Co-culture with ECs regulates pancreatic differentiation

The recent chapter described the successful differentiation of IMR90 iPS into pancreatic multipotent progenitors. Further, this work described that the pancreatic differentiation of mouse ES cells was not disturbed by a co-culture medium containing a 1:1 mixture of PDM and ECGM. Additionally, this study demonstrated that the co-culture medium also preserved the natural characteristics of primary ECs. The co-culture medium contained the full amount of pancreatic differentiating agents and agents necessary for the maintenance of ECs. Together, obtained data suggested the co-culture of pancreatic differentiating cells and ECs using the established co-culture medium. The differentiation protocol aimed at the subsequent generation of multipotent progenitors at around day 6, pancreatic progenitors at around day 9, and endocrine progenitors at around day 12, which contributes to the *in vivo* development of pancreatic endocrine cells.

The morphology of co-cultures showed prominent clusters of small epithelial cells derived from IMR90 iPS cells surrounded by HUVECs at day 6 and day 12 (**FIG. 41 A**). Semi-quantitative PCR analysis of crucial pancreatic lineage markers at day 6 and day 12 showed that mesendodermal and endodermal markers Bra, Sox17, and Foxa2 were preserved or induced until day 12 (**FIG. 41 B**), which does not contribute to the differentiation into pancreatic progenitors. Further, non-pancreatic endoderm markers Afp and Sdf were also preserved by co-cultures. The mRNA analysis of ectoderm and mesoderm markers implicated that co-cultures generated ectodermal cells while mesodermal differentiated cells were not induced. However, this observation contributes to the data obtained from pancreatic differentiation without ECs. Interestingly, co-cultures induced Pdx1 mRNA expression at

day 6 indicating the differentiation of multipotent progenitors. However, Pdx1 was absent at day 12. Due to the downregulation of Pdx1 at day 12, Nkx6.1 expression was lowered, Gcg was down-regulated, and Nkx2.2 mRNA remained absent at day 12. Albeit the pancreatic endocrine marker Ngn3 was induced at day 12, its mRNA expression was induced at low level.

In co-cultures with H9 ES cells, semi-quantitative PCR analysis at day 7 and day 13 showed that mesendodermal and endodermal markers Bra, Sox17, and Foxa2 were not regulated (**FIG. 41 C**). This observation contributes to pancreatic differentiation process. Further, Ngn3, Nkx6.1, and Gcg transcripts were expressed at day 13, which contributes to the development of pancreatic endocrine progenitors. However, the most crucial pancreatic marker Pdx1 were not induced in co-cultures. Nkx2.2 mRNA remained absent while non-pancreatic markers including mesoderm marker Meox1

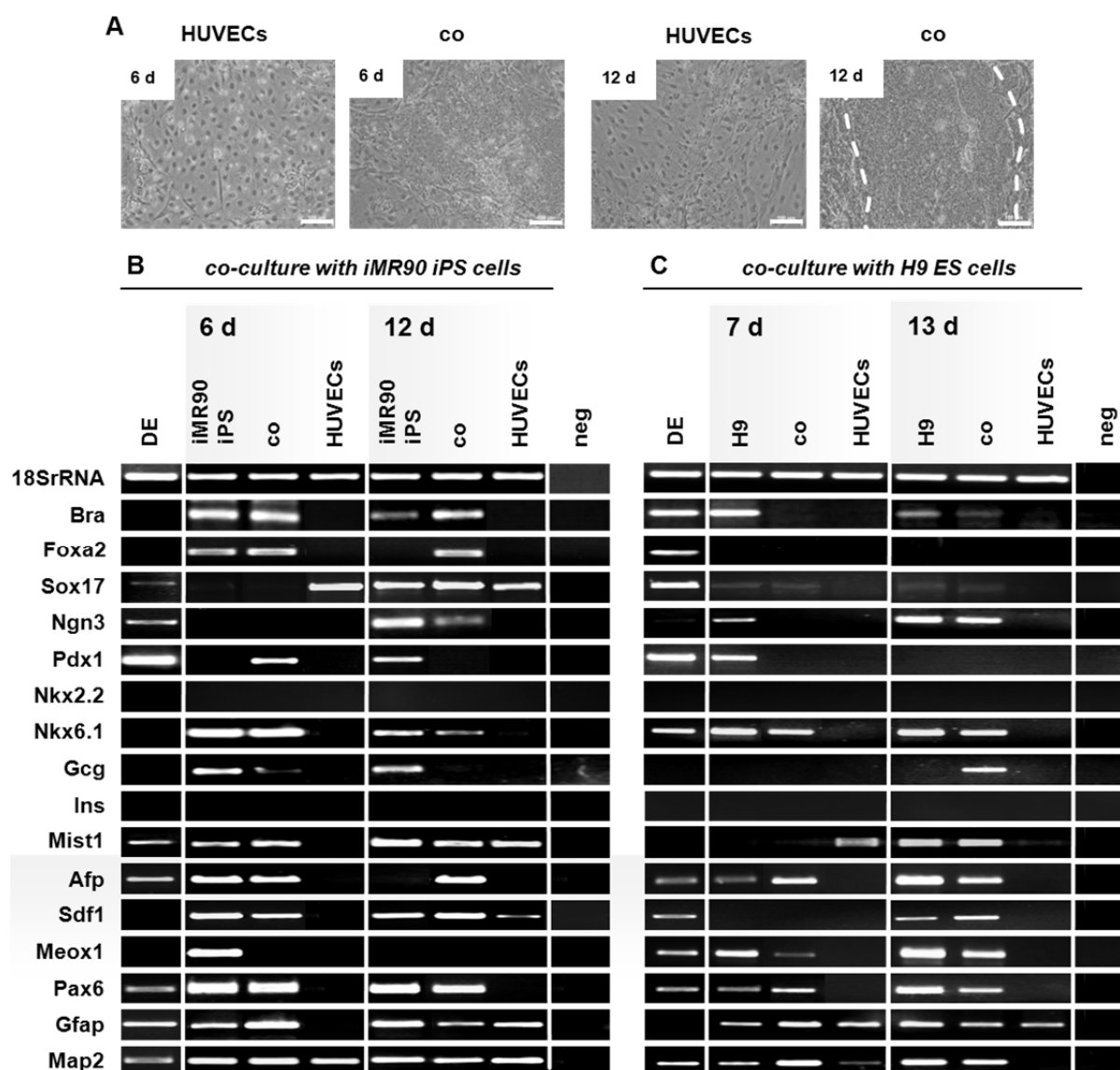


FIGURE 41: Co-cultures with HUVECs regulate pancreatic differentiation. IMR90 iPS and H9 ES cells were differentiated according to the same pancreatic differentiation protocol. Co-culture with HUVECs (indicated as co) started with the generation of DE progenitors at day 3 in iPS cells and at day 4 in ES cells. Differentiation without HUVECs is demonstrated. Culture of HUVECs without stem cells served as a control. **(A)** The morphology of HUVECs and co-cultures composed of IMR90 iPS cells and HUVECs is demonstrated at day 6 and day 12. Bars represent 100 μ m. Representative data (n=2). **(B)** Semi-quantitative PCR analysis of the co-culture containing IMR90 iPS cells and HUVECs. Cells were analyzed at day 6 and day 12. **(C)** Semi-quantitative PCR analysis of the co-culture containing H9 ES cells and HUVECs. Cells were analyzed at day 7 and day 13. Reactions without template served as a negative control (neg).

were preserved at day 7 and day 13. Together, the mRNA expression profile of IMR90 iPS cell and H9 ES cell co-cultures at day 12 and day 13 did not confirm efficient differentiation of pancreatic endocrine cells.

As a control, IMR90 iPS and H9 ES were differentiated in the presence of the co-culture medium. Semi-quantitative PCR analysis revealed the expression of Pdx1, Ngn3, Nkx6.1 in IMR90 iPS cells at day 12 and in H9 ES cells at day 7 (**FIG. 41 B/C**). Importantly, these markers were induced together in presence of the co-culture medium, but not in co-cultures.

The co-culture medium did not affect the morphology of HUVECs until day 6, but some cells showed morphological signs of senescence at day 12 (**FIG. 41 A**). The mRNA expression of lineage markers differed between different isolates of HUVECs applied in different co-culture studies. This is demonstrated in isolates used for the differentiation IMR90 iPS and H9 ES cells (**FIG. 41 B/C**).

Together, co-cultures including HUVECs induced or down-regulated mRNA expression levels of pancreatic lineage markers in IMR90 iPS and in H9 ES cells, which does neither prevented nor enhanced pancreatic differentiation. Accordingly, to improve the organotypic pancreatic differentiation, the application of 3D matrices combined with co-cultures was suggested.

3.4.4.3. 3D Biological Matrices Require Co-Culture with ECs for Pancreatic Differentiation

Data obtained from 3D differentiation of mouse ES cells into pancreatic progenitors raised evidence that these matrices would allow the further differentiation of IMR90 iPS cells into pancreatic endocrine cells. Additionally, 3D matrices were suggested to improve the pancreatic differentiation of co-cultures by mimicking a 3D organotypic scaffold. Therefore, 3D pancreatic differentiation of IMR90 iPS cell co-cultures including ECs was investigated. Cells were differentiated according to the pancreatic differentiation protocol using the co-culture medium.

The fundamental question was whether co-cultured cells do remain viability after reseeding (at day 3) onto 3D matrices. Therefore, the viability of co-cultures on 3D matrices was analyzed at day 12 (**FIG. 42 A-C**). 3D matrices were shown to be completely covered with cells. As a control, MVECs or DE progenitors were cultured in the presence of the co-culture medium, which demonstrated that 3D matrices preserved their viability due to a low number of dead cells (**FIG. 42 A**). Importantly, DE-derived cells generated clusters of cells similar to that observed in 2D cultures. These clusters were observed in DE-derived cells and in co-cultures (**FIG. 42 C**). Interestingly, extra cellular structures of vessels were also covered with viable cells, but no cell clusters were observed (**FIG. 42 B**). Together, cells obtained from 3D pancreatic differentiation with or without MVECs remained viable until day 12.

Semi-quantitative PCR analysis 3D pancreatic differentiation and 3D co-cultures revealed a different expression pattern (**FIG. 42 D**). Albeit Map2 was expressed in 3D pancreatic differentiation, other pancreatic and non-pancreatic lineage markers were absent at day 6. Therefore, it remains unclear, which direction of differentiation was induced. In contrast, 3D co-cultures induced the endodermal markers Sox17 and Afp and the pancreatic markers Nkx6.1, Gcg, and Mist1 at day 6. However, Pdx1 and Ngn3 mRNA expression was absent, which did not confirm efficient differentiation of pancreatic endocrine cells. At day 12, except of Map2, again no lineage markers were detected.

Altogether, the analysis of organotypic culture approaches led to a protocol combining these approaches in a strategy for the use of 3D biological matrices and co-culture conditions in an organotypic pancreatic differentiation model. Established culture methods namely, the production of a

3D biological matrix, the isolation of primary ECs, the establishment of 3D co-culture conditions, and the differentiation of pancreatic progenitors from mouse/human ES and human iPS cells were shown to be applicable and suitable for 3D pancreatic differentiation studies.

Importantly, the combination of organotypic culture methods aimed at the efficient differentiation of pancreatic endocrine cells, but the expression of beta cell development markers was hardly improved. Unfortunately, the obtained data indicate that the described combination of culture organotypic culture models were unsuitable for the efficient generation of mature insulin-producing cells.

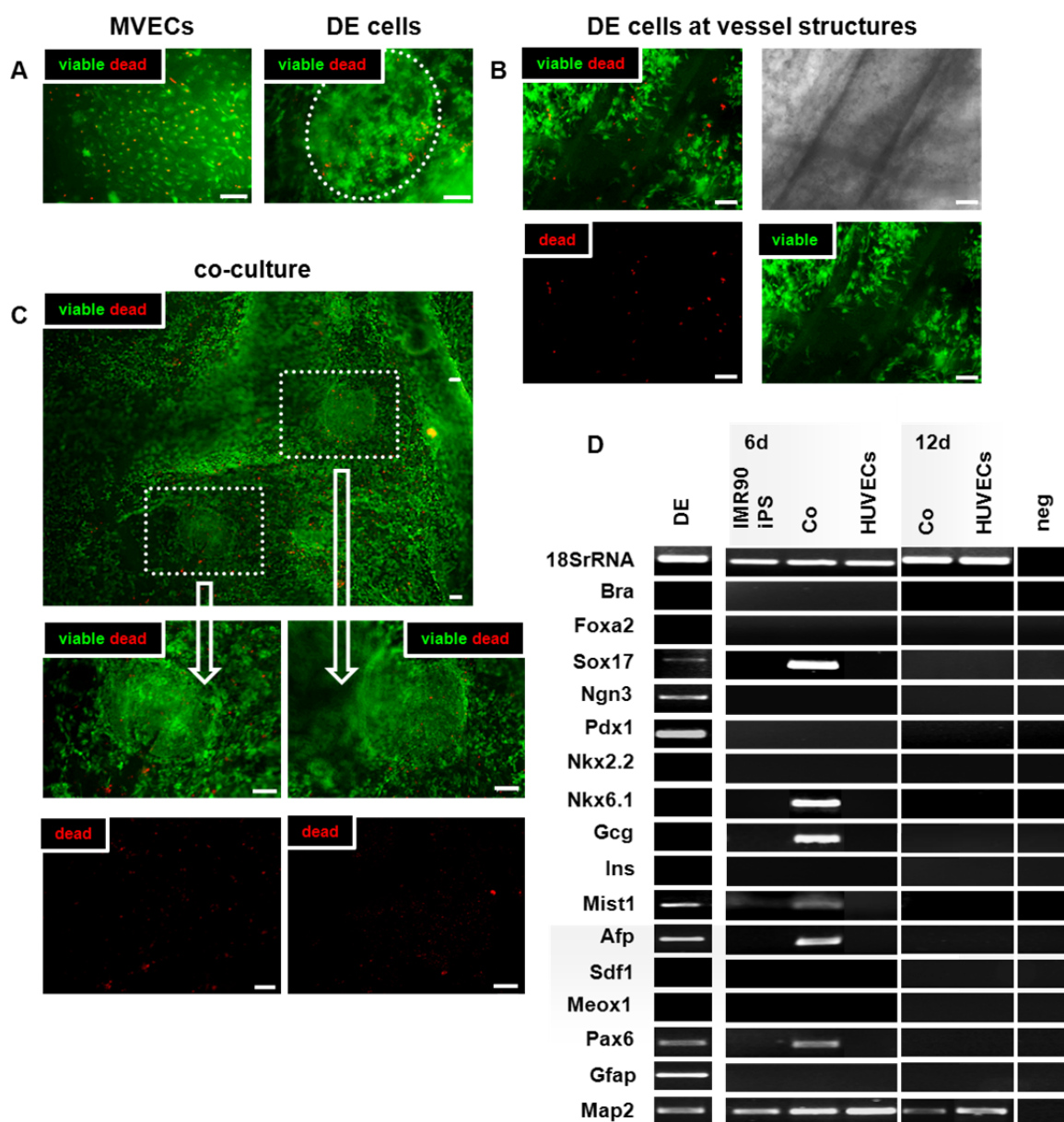


FIGURE 42: Matrices preserve viability of co-cultured DE progenitors and MVECs. Human IMR90 iPS cells were differentiated into DE progenitors until day 3. DE cells, primary MVECs, or both were seeded onto 3D biological matrices. Cells were treated according to the pancreatic differentiation protocol. Their viability was analyzed at day 12. Viable cells are stained by green fluorescence. Dying or dead cells are demonstrated by red staining of the nuclei. **(A)** Cell viability assay of primary MVECs or DE-derived differentiated cells. **(B)** Cell viability assay of DE-derived cells near to the extracellular structures of blood vessels. **(C)** Cell viability assay of co-cultures at day 12. Bars represent 100 μ m. Representative data (n=3). **(D)** Semi-quantitative PCR analysis of IMR90 iPS co-cultured with HUVECs on 3D matrices. Cells were differentiated according to the pancreatic differentiation protocol, but co-culture with HUVECs (indicated as co) started at day 3 after the generation of DE progenitors. Cells were analyzed at day 6 and 12. Differentiation without HUVECs in co-culture medium is demonstrated at day 6. Culture of HUVECs in co-culture medium served as a control. Reactions without template served as a negative control (neg). Representative data (n=2).

4. DISCUSSION

The invention of an organotypic model for the analysis of appearance, progress, and treatment of diabetes requires the generation of iPS cells and their differentiation into the pancreatic lineage. The present study demonstrated mandatory techniques for (i) the establishment of primary keratinocyte cultures, (ii) the non-viral generation of iPS cells, and (iii) the generation of pancreatic progenitors from iPS cells. Combining of these techniques represents one approach to mimic patient- and disease-specific pancreatic differentiation within a model for the analysis of diabetes.

4.1. Primary Keratinocytes are Adequate Donors for the Generation of iPS Cells

In the present study, efficient isolation and successful culture of primary keratinocytes was demonstrated (**FIG. 8**). Keratinocytes are adequate donors for the generation of iPS cells because reprogramming is 100-fold more efficient and 2-fold faster than reprogramming of fibroblasts (Aasen et al., 2008; Ohmine et al., 2012). Additionally, keratinocytes are easy accessible because they are obtained from hair follicles or skin biopsy without surgery. During reprogramming, keratinocytes do not need to undergo mesenchymal to epithelial transition (MET) such as fibroblasts because they are already epithelial. MET is a critical event during reprogramming of fibroblasts (Polo and Hochedlinger, 2010).

Isolation of primary keratinocyte from plucked hairs was demonstrated in the present study (**FIG. 8 A**). Plucked hairs were cultured using an air-liquid interphase and low calcium concentrations to obtain proliferating keratinocytes at the ORS. These culture conditions are also suitable to isolate melanocytes from plucked hair (Savkovic et al., 2012). Low calcium concentrations contribute to maintenance of undifferentiated epidermal progenitors (Vollmers et al., 2012). The use of an air-liquid interphase and high calcium is suitable to generate epidermal equivalents (Vollmers et al., 2012). Proliferating keratinocytes did not appear at the bulb region of plucked hairs (**FIG. 8 E-F**). Importantly, plucking of hairs isolates mainly transit-amplifying keratinocytes with short-term culture potential, whereas skin biopsies allow the isolation of bulge region-associated keratinocyte stem cells with longer culture potential (Aasen and Izpisua Belmonte, 2010).

Successful keratinocyte isolation was demonstrated in the present study using 30-50 plucked hairs from male and female healthy donors at the age of 22 to 41 years. At least 10 hairs are required to generate primary keratinocyte cultures from donors at the age of 18 to 35 (Aasen and Izpisua Belmonte, 2010). Successful isolation does not depend on the age of the donors (Sasahara et al., 2009; Ohmine et al., 2012). For example, Ohmine and co-workers obtained keratinocytes from skin biopsies of 56 to 78 year-old individuals. Keratinocytes are cultured using traditional feeder-dependent methods (Rheinwald and Green, 1975) and feeder-free methods that do require low-calcium chemically defined media (Tenchini et al., 1992). Feeder-free methods require more sophisticated techniques and cells grow less well without feeder. For example, high-calcium induces differentiation and loss of proliferation of keratinocyte stem cells. Therefore, ORS-derived keratinocytes obtained within the present study were expanded on 3T3 L1 feeder layer to ensure efficient propagation. Feeder-dependent keratinocyte cultures are well established (Reichelt and Haase, 2010). Interestingly, 3T3 L1, 3T3 J2, and several MEFs are suitable for maintenance of keratinocytes and pluripotent stem cells as well (Aasen and Izpisua Belmonte, 2010). However, Aasen and co-authors reported that iPS cell lines could be generated without any feeder cells.

Primary keratinocytes cultures generated in the present study grew in colonies (**FIG. 8 I**). According to their morphology, these colonies were mainly classified as meroclones with low growth potential. In accordance with the present results, Vollmers and colleagues also demonstrated a prevalent formation of meroclones (55%) after isolation of primary mouse keratinocytes even from the bulge region of hairs (Vollmers et al., 2012). In 1987, Brandon and Green first described that the morphology of primary keratinocyte colonies is associated with high, moderate, and low proliferation capacity (Barrandon and Green, 1987). According to their morphology, colonies were termed as holoclones, paraclones and meroclones. Meroclones and paraclones are derived from trans-amplifying cells. Holoclones have the largest growth potential because they are derived from Keratinocyte stem cells residing in bulb region of hairs or in the basal layer of stratified skin (Rochat et al., 2007). Notably, the epidermis contains several adult stem cells with different potentials to ensure the homeostasis of the skin barrier throughout the human life (Blanpain and Fuchs, 2009). In the present study, primary keratinocytes did proliferate until passage 3, which contributes to the idea that mainly trans-amplifying cells can be obtained from plucked hairs.

Importantly, feeder-dependent conditions are not applicable in clinical practice. Isolation and propagation of patient-specific cells as well as their application in regenerative treatment strategies requires GMP-suitable conditions (Zhou et al., 2012). Feeder-free procedures are described but obtained keratinocytes have a low proliferation capacity, which allows culture for up to 4 passages (Aasen and Izpisua Belmonte, 2010). Currently, feeder-dependent cultures provide a more efficient approach to study isolation, propagation and induction of reprogramming of primary keratinocytes.

The present study demonstrated successful isolation and propagation of primary keratinocytes suitable for reprogramming studies. Even small amounts of primary keratinocytes are suitable for iPS cells generation because one single hair was demonstrated to be enough for the generation of keratinocyte-derived iPS cells (Aasen et al., 2008). However, more efficient isolation and culture procedures would even improve the generation of iPS cells. Application of an air-liquid interface during propagation of primary keratinocytes could preserve the proliferation capacity of primary keratinocytes. Enhancement of proliferation is one critical step during reprogramming. Keratinocyte marker gene Krt15 is predominantly expressed in keratinocyte stem cells and analysis of Krt15 expression would offer a tool for the selection of keratinocytes with high proliferation potential (Tudor et al., 2007; Nowak et al., 2008). The need of more suitable keratinocyte culture conditions is supported by the fact that viral and non-viral reprogramming are very inefficient procedures.

4.2. Cell Type-Specific Expression of Pluripotency Markers

The expression of 30 human ES cell-specific markers was analyzed in accordance with other reports, which included all or some of these markers for the characterization of iPS cells (Takahashi and Yamanaka, 2006; Takahashi et al., 2007). The set of markers included 6 core network reprogramming factors. Currently, reprogramming is achieved by delivery of Oct4 in conjunction with Sox2, Nanog, Lin28 (Thomson factors) or Sox2 Klf4, c-Myc (Yamanaka factors). Oct4 is the most important marker, which is not exchangeable for reprogramming (Kim et al., 2009c).

4.2.1. Core Network Reprogramming Factors

In the present study, Oct4A and Oct4B expression was not detected in BJ-5ta cells and L87 cells (**FIG. 9 B**). Oct4A and Oct4B detection by specific primers excluded Oct4 pseudogenes, which share

high similarities (Pain et al., 2005; Suo et al., 2005). Pluripotent stem cells express both Oct4A and Oct4B, but Oct4A expression is absent in several primary and permanent cells derived from cancer, mononuclear cells, and adult stem cells (Campbell et al., 2007; Atlasi et al., 2008; Cantz et al., 2008). Interestingly, Oct4 expression was reported in comparable primary and permanent cells (Tai et al., 2005; Webster et al., 2007; Zangrossi et al., 2007), but not all studies differed between splice variants (Cauffman et al., 2006; Tai et al., 2005; Liedtke et al., 2007). Oct4 can potentially encode 3 spliced variants (Takeda et al., 1992; Atlasi et al., 2008). Oct4A, Oct4B, and Oct4B1 differ within their N-terminal region resulting in at least 4 protein isoforms (Oct4A, Oct4B, Oct4B1-164, Oct4B-190) (Cheong and Lufkin, 2011). Oct4A expression is restricted to pluripotent ES and embryonic carcinoma cells (EC cells) (Scholer et al., 1990; Rosner et al., 1991; Matin et al., 2004; Campbell et al., 2007). Further, Oct4A is present in human cancers such as benign and malignant prostate glands (Sotomayor et al., 2009). The transcript variants B and possibly B1 are not able to sustain ES cell self-renewal (Mueller et al., 2009; Wang and Dai, 2010). Interestingly, the mRNA sequence of Oct4B1 is more similar to Oct4B but expression is also restricted to ES and EC cells (Atlasi et al., 2008). Further studies are needed to elucidate the function of Oct4B1 in pluripotent stem cells. In contrast to Oct4A, the N-terminal domain of Oct4B has an inhibitory effect on the binding of Oct4B to Oct4-dependent promoters (Cauffman et al., 2006; Lee et al., 2006) suggesting a different function of Oct4B. Accordingly, Oct4B is expressed in progenitor and somatic cells (Mueller et al., 2009; Wang and Dai, 2010). In contrast to the human system, mouse ES and adult stem cells do express only one Oct4 transcript which is orthologous to human Oct4A (Atlasi et al., 2008). Accordingly, murine adult stem cells express Oct4 (De et al., 2007; Ling et al., 2006). However, Oct4A is thought to be absent in human adult stem cells. Therefore, the expression of Oct4A in human adult stem cells including MSCs needs to be clarified when Oct4 expression is analyzed. Oct4 is the most important regulatory molecule in totipotent and pluripotent stem cells. The analysis of Oct4A represents the most reliable approach to analyze Oct4 expression in the context of pluripotency.

Interestingly, the present study demonstrated that the Yamanaka factors c-Myc and Klf4 were already expressed in L87 MSCs, BJ-5ta fibroblasts, and keratinocytes (**FIG. 8**). BJ-5ta and L87 immortalized cell lines were obtained by transformation of primary cells, which explains c-Myc and Klf4 expression (Thalmeier et al., 1994; Bodnar et al., 1998). Yee and co-workers also demonstrated c-Myc and Klf4 expression in keratinocytes (Yee, 2010). The expression of c-Myc and Klf4 is associated with but not restricted to ES cells. Proliferation and malignant transformation of somatic cells is well known to be regulated by c-Myc and Klf4. The function of c-Myc and Klf4 is highly dose and cell context dependent. Expression of c-Myc is present during pancreatic development as well as in pancreatic ductal adenocarcinoma (Skoudy et al., 2011). Therefore, c-Myc is classified as an oncogene. For example, breast cancer is related to increased c-Myc expression (Liao and Dickson, 2000) and lymphomas can derive from hematopoietic stem cells when c-Myc-triggered B cell formation is not restricted by apoptosis (Strasser et al., 1996). Klf4 is also classified as an oncogene. For example, laryngeal squamous cell carcinoma and ductal carcinoma of the breast with poor prognosis are associated with Klf4 expression (Foster et al., 2000). Accordingly, clinical application of human iPS cells is problematic when oncogenes such as c-Myc and Klf4 are applied (Huangfu et al., 2008b). During human embryogenesis, c-Myc binds to a large number of loci to guide proliferation. In adult tissues c-Myc promotes differentiation of human epidermal stem cells (Gandarillas and Watt, 1997).

Klf4 is highly expressed in gut and skin epithelia where it acts as an anti-proliferative factor (Shields et al., 1996; Ghaleb et al., 2007). Importantly, Klf4 is involved in self-renewal of ES cells (Li et al., 2005; Jiang et al., 2008). Together, c-Myc and Klf4 expression in L87, BJ-5ta, and other somatic donor cells facilitates reprogramming.

The present study demonstrated that Thomson factors Sox2, Nanog and Lin28 were absent in BJ-5ta cells and L87 cells (**FIG. 9 B**). Notably, Oct4, Nanog and Sox2 belong to the core pluripotency network (Boyer et al., 2005; Loh et al., 2006; Wang et al., 2006). Importantly, Lin28 up regulates Oct4 expression in human ES cells (Qiu et al., 2010). Studies in Lin28 knockout mice revealed that Lin28 regulates developmental timing and growth because knockout mice were smaller and died early (Zhu et al., 2010). However, Lin28, as well as c-Myc and Klf4, is expressed in cancer (Reya et al., 2001; Clarke et al., 2006; Visvader and Lindeman, 2008). Interestingly, the human genome encodes two paralogs Lin28 (also termed as Lin28A) and Lin28B (Guo et al., 2006). In the present study, primers specifically detected Lin28 mRNA because Lin28 (and not Lin28B) is capable to reprogram somatic cells. For example, Lin28B is involved in timing of puberty and determination of human height (Zhu et al., 2010). However, both Lin28 and Lin28B are associated with cancer. Lin28 and Lin28B occur in several tumors with approximately equally frequency (Piskounova et al., 2011). Importantly, Lin28 and Lin28B are not expressed together, which is suitable to distinguish different classes of breast cancers (Piskounova et al., 2011). Therefore, different regulatory mechanisms most probably regulate Lin28 or Lin28B expression. Accordingly, the analysis of Lin28B expression is not important for the characterization of pluripotency.

In the present study, keratinocytes expressed Oct4B, Nanog, Sox2, and Lin28 (**FIG. 9 C**), which indicates the presence of keratinocyte stem cells in primary cultures. Another study by Sasahara and co-authors verified expression of Oct4B, Nanog, and Lin28 in human keratinocyte stem cells (Sasahara et al., 2009). The expression of these crucial reprogramming factors in primary keratinocyte cultures correlates with more efficient reprogramming compared to fibroblasts (Aasen et al., 2008; Ohmine et al., 2012). Correspondingly, reprogramming factors instead of Oct4, especially Oct4A, might be dispensable for reprogramming of keratinocytes. According to that hypothesis, Sox2-expressing mouse neural stem cells were recently reprogrammed without Sox2 delivery (Kim et al., 2008). The different expression of pluripotency marker genes in L87 cells, BJ-5ta cells, and keratinocytes is the rationale for the idea that the choice of the somatic donor influences the efficiency and the quality of reprogramming.

4.2.2. Pluripotency-Associated Markers

In the present study, there was a set of 6 pluripotency markers (Rex1, Podxl, Gdf3, Dppa2/4, Oct4A), which were not expressed in L87 MSCs, BJ-5ta fibroblasts, and keratinocytes (**FIG. 9 B/C**). Rex1 is present in trophoblast tissues and in the ICM of the blastocyst (Rogers et al., 1991). Therefore, Rex1 is a common pluripotency marker in human ES cells (Brivanlou et al., 2003). Rex1 knockout mouse ES cells fail to differentiate visceral endoderm and cell cycle progression is delayed (Scotland et al., 2009). Bhandari and co-authors reported that Rex1 expression is required to preserve the osteogenic differentiation potential in human umbilical cord blood-derived MSCs (Bhandari et al., 2010). In contrast to that observation, human bone marrow-derived L87 MSCs did not express Rex1. This contributes to the idea that reprogramming of umbilical cord blood-derived MSCs and adipose tissue-derived MSCs is more efficient compared to bone marrow-derived MSCs. Comparison of MSCs

originated from different tissues verified that c-Myc expression is high and Rex1 expression is low in bone marrow-derived MSCs (Adegani et al., 2013). Interestingly, Adegani and co-workers demonstrated that adipose tissue-derived MSCs express high levels of Sox2, Klf4 and Lin28. Further, umbilical cord blood-derived MSCs express high levels of Oct4 and Rex1. However, these data illustrate the differences between MSCs derived from different tissues. Podocalyxin-like (Podxl) is expressed in human ES cells and early progenitors of bone marrow-derived MSCs (Lee et al., 2009). Podxl was absent in L87 MSCs. Further, Podxl is a common marker for aggressive carcinomas including those of breast, colon, and pancreas (Cheung et al., 2011; Dallas et al., 2012) and function of Podxl remains to be clarified in human ES cells and carcinomas. Gdf3 is expressed in human ES cells and in the early embryo (Clark et al., 2004). Gdf3 knockout mice develop developmental abnormalities demonstrating the importance of Gdf3 expression (Caricasole et al., 1998). However, Gdf3 is classified as an oncogene because it is expressed in several cancers such as breast carcinomas (Ezeh et al., 2005). According to that observation, Nanog activates Gdf3 expression in embryonic carcinoma cells (Park et al., 2012). Interestingly, Gdf3 inhibits growth of breast cancer (Li et al., 2012). Therefore, Gdf3 expression might be a marker, which identifies iPS cells with low tumorigenic potential. Developmental pluripotency associated 2 (Dppa2) and Dppa4 were both absent in L87 MSCs, BJ-5ta fibroblasts, and keratinocytes. These factors regulate chromatin structures in mouse and human ES cells. Dppa2 and Dppa4 are restricted to pluripotent stem cells suggesting that these factors are involved in self-renewal and maintenance of pluripotency (Watabe, 2012). Double knockout of Dppa2 and Dppa4 generated viable mice until birth but almost all mutant mice died around birth with respiratory defect (Nakamura et al., 2011). Loss of Dppa4 expression induces differentiation and loss of pluripotency of mouse ES cells (Masaki et al., 2007). According to that observation, Monk and co-workers could demonstrate that the human homolog of Dppa2 is co-expressed with Oct4 in human ES cells, in the blastocyst, and in primordial germ cells (Monk et al., 2008). Importantly, Dppa2 is involved in normal lung development and pathogenesis of non-small cell lung cancers (Monk and Holding, 2001). Therefore, Dppa2 and Dppa4 play an important role in ES cells, normal development and tumorigenesis. Altogether, the pluripotency markers Rex1, Podxl, Gdf3, Dppa2, and Dppa4 are the most important markers to analyze the induction of pluripotency in L87, BJ-5ta, and most probably in other somatic cells. Analysis of associated signaling pathways will help to understand process of reprogramming, especially of MSCs, fibroblasts and keratinocytes.

The majority of the analyzed pluripotency marker genes was expressed in L87 MSCs, BJ-5ta fibroblasts, and keratinocytes (**FIG. 9**). These genes are involved in maintenance of pluripotency but their expression is additionally crucial during development. For example, Nodal induces TGF β signaling for differentiation of mouse and human ES cells into endoderm (Schroeder et al., 2006; D'Amour et al., 2006). Inhibition of TGF β signaling inhibitors are suitable to replace c-Myc and Sox2 during retroviral reprogramming (Maherali and Hochedlinger, 2009). However, in the human system Nanog was reported to be positively regulated being a direct target of activin A/TGF β signaling (Xu et al., 2008). Further, pluripotency of human ES cells was maintained by activin A/TGF β signaling in a feeder free system (Beattie et al., 2005) and repression of TGF β was demonstrated to induce mesenchymal progenitors (Mahmood et al., 2010). According to these observations Nodal expression appears to be differentially regulated during early embryogenesis involved in maintenance of pluripotency as well as during cell fate decisions.

As described earlier, Oct4 transcript variants and isoforms do have very different functions during induction, maintenance, and loss of pluripotency. Currently, there are no different Sox2, Nanog, Lin28, c-Myc and Klf4 transcript variants annotated on NCBI Reference Sequence database. In the present study, primers specifically detected the annotated transcript variant as indicated. Importantly, little is known about the influence of alternative splicing of core network pluripotency factors such as Sox2, Nanog, Lin28, c-Myc, and Klf4. The impact of alternative splicing on reprogramming is currently not well understood. Alternative splicing occurs in about 74% of the human genes (Johnson et al., 2003). Not all exon changes result in a new protein isoform. Approximately 30% of alternative exons introduce frame shifts and stop codons (Cheong and Lufkin, 2011). However, there is evidence that alternative splicing and/or translation of different isoforms also occurs in Sox2, Nanog, Lin28, c-Myc and Klf4. Interestingly, the Sox2 gene lays within a long non-coding RNA annotated as Sox2ot (Amaral et al., 2009). In W9.5 mouse ES cells, Amaral and co-authors showed that alternative splicing of Sox2ot generates different transcripts termed as Sox2 overlapping transcripts A (Sox2otA) and Sox2otB. However, Sox2 and Sox2otA/B were differently expressed during EB differentiation of mouse ES cells suggesting independent regulation. Another study by Das and co-workers reported that J1 mouse ES cells do express different Nanog transcript variants termed as NanogA, NanogB, and NanogC (Das et al., 2011). Importantly, Das and co-workers demonstrated that NanogB less efficient preserves pluripotency. Alternative splicing of Klf4 was reported in human and mouse pancreatic cancer cells, which expressed different transcript variants termed as Klf4wt, Klf4 α , Klf4 β , Klf4 γ , and Klf4 δ (Wei et al., 2010). However, Wei and colleagues showed that alternative splicing was linked to the occurrence of DNA Polymorphisms within splice-regulatory protein-binding site of the Klf4 gene. Unfortunately, analysis of alternative splicing during reprogramming was not aim of the present study. However, further analysis should include the analysis of alternative splicing because it is an important regulatory mechanism during reprogramming.

In the present study, BJ-5ta and L87 cells revealed a very different expression of pluripotency markers in comparison to human ES and iPS cells. Importantly reprogramming factors Oct4, Sox2, Nanog, and Lin28 were absent. In contrast, keratinocytes expressed reprogramming factors instead of Oct4A. This observation suggests a different importance of Oct4 transcript variants. Because retroviral reprogramming of keratinocytes is more efficient, even non-viral reprogramming is most probably more efficient when keratinocytes are used.

4.3. Non-Viral Reprogramming of L87 MSCs and BJ-5ta Fibroblasts

Currently, the use of MSCs and fibroblasts as suggested in the present study by the use of L87 and BJ-5ta cells is reasonable. MSCs are the most commonly used cell source in regenerative medicine. Obtained from various tissues including bone marrow, adipose tissue and peripheral blood, they can be propagated *in vitro* and show a certain differentiation potential due to their multipotency. These characteristics also make them ideal candidates for reprogramming strategies. Fibroblasts are the most commonly used cell source for studies in reprogramming because they are easy to obtain from several origins such as human adult skin fibroblasts, human neonatal foreskin fibroblasts, mouse tail tip fibroblasts, and MEFs. However, successful iPS cell generation was reported from a variety of different cell types and most probably every somatic cell type is suitable for the generation of patient- and disease-specific iPS cells. Human iPS cells have been derived from several cell types including dermal fibroblasts, keratinocytes, and MSCs (TAB. 3).

TABLE 3: Different sources for the generation of iPS cells.

Donor	Method	Reference
primary human dermal fibroblasts from T1D patients	retroviral; Oct4, Sox2, Klf4	(Maehr et al., 2009)
primary human neonatal dermal fibroblasts	retroviral; Oct4, Sox2, Klf4, c-Myc	(Lowry et al., 2008)
primary mouse pancreatic beta cells	retroviral; Oct4, Sox2, Klf4, c-Myc	(Stadtfeld et al., 2008)
primary human fetal neural stem cells	retroviral; Oct4 or Oct4 and Klf4	(Kim et al., 2009c)
primary mouse immature and mature B cells	retroviral; Oct4, Sox2, Klf4, c-Myc	(Hanna et al., 2008)
primary mouse hepatocytes and gastric epithelial cells	retroviral; Oct4, Sox2, Klf4, c-Myc	(Aoi et al., 2008)
primary human keratinocytes from plucked hair	retroviral; Oct4, Sox2, Klf4, c-Myc	(Aasen and Izpisua Belmonte, 2010)
primary human cord blood CD34-positive progenitors	retroviral; Oct4, Sox2, Klf4, c-Myc	(Takenaka et al., 2010)
primary mouse MSCs, tail tip fibroblasts, osteoblast progenitors	retroviral; Oct4, Sox2, Klf4, c-Myc	(Niibe et al., 2011)
primary human hair follicle MSCs	retroviral; Oct4, Sox2, Klf4, c-Myc	(Wang et al., 2012b)

Interestingly, iPS cells are known to retain a somatic memory but the impact on their developmental potential needs to be clarified. Differentiation of iPS cells into neural and blood lineage was described to be less efficient compared to human ES cells (Feng et al., 2010; Hu et al., 2010). Recent studies explained transcriptional differences between human ES cells and iPS cells by different DNA methylation and not by histone modification. According to that more recently iPS cells were demonstrated to retain their promoter DNA methylation status of somatic genes (Chin et al., 2009; Deng et al., 2009; Polo et al., 2010; Bock et al., 2011; Lister et al., 2011). Importantly, mouse iPS cells showed an increased potential to differentiate into the donor cell type (Polo et al., 2010). Most probably, a pool of validated cell types is necessary for reprogramming due to the desired cell type after differentiation. However, hepatocyte-derived iPS cells were not more efficient than fibroblast-derived iPS cells to differentiate towards endoderm (Ohi et al., 2011). Interestingly, somatic memory genes were also associated with cancer (Chapman et al., 2008; Jung et al., 2008). Reprogramming requires the induction of different pluripotency-associated properties depending on starting cell type, which affects efficiency and kinetics of molecular reprogramming (Aoi et al., 2008; Kim et al., 2008). Many different laboratories generated iPS cells but methods for calculating the efficiency of reprogramming drastically varies between different techniques (Maherali and Hochedlinger, 2008). It is difficult to draw an exact conclusion, which cell type is the most useful for generation of iPS cells. Currently, efficiency and quality of reprogrammed cells is different for many cell types and can be explained by different expression of pluripotency-associated genes affecting a variety of reprogramming pathways.

Reprogramming changes several signaling pathways, prevents apoptosis, and modifies several epigenetic modifications of DNA and histones. The delivery of ectopically expressed transcription

factors modifies gene expression in somatic cells. Ectopic expression is achieved by viral vectors, transposons, and episomal vectors (Gonzalez et al., 2011). However, reprogramming factors are dispensable or exchangeable when treatment with small molecules, delivery of miRs, and/or hypoxia are applied (Page et al., 2009; Li and Ding, 2010; Foja et al., 2013). Accordingly, application of non-viral methods was analyzed in L87 and BJ-5ta cells.

4.3.1. Non-Viral Reprogramming Induced by Episomal Vectors

Non-viral episomal vectors such as plasmids or minicircles carrying pluripotency genes are able to reprogram distinct types of human somatic cells. However, episomal vectors show low efficient reprogramming compared to viral vectors. Episomal vector-derived reprogramming depends on undisturbed uptake, access to nucleus, intracellular vector stability, and finally transcription and translation efficiencies. Undisturbed uptake and access to the nucleus is ruled by the transfection technique whereat vector stability and expression efficiencies depend on the vector design.

4.3.1.1. Comparison of Different Transfection Procedures

In the present study, Gene Pulser® II was applied using several approaches with different settings of pulse duration and electric field strength for delivery of episomal vectors into L87 cells with adverse effects on cell viability (**APP. 1**). Another study by Helledie and co-authors also reported low cell viability after electroporation of MSCs (Helledie et al., 2008). In the present study, adverse effects on cell viability were most probably caused by not suitable protocols rather than by electroporation in general. Pulse duration and electric field strength are key parameters and optimal settings are required for preservation of cell viability and efficient transfection (Jordan et al., 2008). Nevertheless, the choice of buffers, wave form of the given pulse, and the density of cells additionally alters electroporation (Jordan et al., 2008). Additionally, application of other commercial electroporation-based transfection techniques might be suitable. For example, nucleofection is suitable for transfection of human MSCs yielding about 50% transfected cells (Aslan et al., 2006). There are several techniques for transfection such as chemical transfection, electroporation, nucleofection, and viral transduction with different efficiencies (Yates and Daley, 2006). However, electroporation, and nucleofection are very often used for the delivery of nucleic acids into mammalian cells. Techniques based on physical mechanism of electroporation are commercially available such as Gene Pulser® (Bio-Rad, München, Germany), Amaxa Nucleofactor (Lonza, Köln, Germany), and Neon Transfection System (Life Technologies, Darmstadt, Germany). The transfection efficiency depends on the cell type as well as on the technique (Jordan et al., 2008). For example, human HL60 promyelocytic leukemia cells were transfected by different techniques yielding up to 3% transfected cells by Amaxa Nucleofactor and up to 23% transfected cells by Neon Transfection System (Chen et al., 2010). In contrast, both techniques are very efficient in human adipose-derived stem cells yielding more than 90% transfected cells (Bezaire et al., 2009). In a reprogramming strategy, the amount of affordable primary cells is restricted and avoidance of cell death is very important. It is important to highlight that chemical transfection is suitable to reduce cell toxicity. Accordingly, there is a need to improve or replace electroporation methods for gentle and efficient delivery of STEMcircles™ into L87, BJ-5ta, and other somatic donor cells.

4.3.1.2. Comparison of Lipofection Techniques

In this work, liposome-based chemical transfection by INTERFERin™ was demonstrated to be suitable and applicable for transfection of STEMcircles™ into L87 MSCs (**FIG. 10**). Cell viability was preserved and efficient lipofection of up to 28.5% was demonstrated in L87 MSCs. INTERFERin™ is a liposomal cationic amphiphile transfection reagent for delivery of nucleic acids, especially small RNAs, into mammalian cells in culture (Caffrey et al., 2011). Therefore, lipofection is suitable for delivery of minicircles and miRs for reprogramming. Lipofectamine™ 2000 and Lipofetamine™ LTX transfection reagents were less suitable in optimization assays for L87 MSCs. However, MSCs derived from other donors were successfully transfected with Lipofectamine™ transfection reagents. Cell viability above 85% and efficiency between 2-35% pVAX-GFP-positive cells were reported by application of Lipofectamine™ 2000 in primary bone marrow-derived MSCs (Madeira et al., 2010). Other studies reported application of Lipofectamine™ 2000 with efficiencies of 5-20% transfected MSCs (Gheisari et al., 2008; Yang et al., 2009). According to these studies, transfection of L87 MSCs by Lipofectamine™ reagents might be successful by currently unknown parameters of plasmid DNA, cell amount, and volume of transfection reagent. However, different MSCs differ dramatically between their properties (Hass et al., 2011), which is due to variable behavior in response to different transfection reagents. Currently, different transfection reagents are commercially available. For example, the FuGENE™ transfection reagent revealed up to 24% pmaxGFP-expressing murine MSCs (Krause et al., 2011). Accordingly, another chemical transfection method possibly improves the delivery of STEMcircles™.

Importantly, transfection reagents affect the differentiation of MSCs (Madeira et al., 2010), which suggests that also reprogramming is altered by transfection procedures. Further studies are needed to elucidate the impact of transfection reagents on cell's ability for reprogramming. In general, MSCs are more sensitive to lipofection procedures than many other cell types (Krause et al., 2011). Therefore, the established lipofection protocol for STEMcircles™ delivery into L87 MSCs is most probably suitable for the preservation of L87 MSCs, BJ-5ta fibroblasts, and primary keratinocytes as well.

Episomal vector stability and expression efficiency depends on the vector design. Conventional plasmids have lower transfection efficiencies and ectopic gene expression is lowered because of exogenous silencing mechanisms (Chen et al., 2005). Minicircles are supercoiled DNA plasmids that have no bacterial origin of replication and no antibiotic resistance genes. According to that, these DNA molecules predominantly bear eukaryotic DNA. Silencing of episomal-derived gene expression is mainly enhanced by bacterial DNA sequences (Chen et al., 2004). STEMcircles™ are minicircles derived from P2PhiC31-LGNSO plasmids, which contain a single expression cassette for ONSL and GFP each separated by self-cleaving 2A peptides (Jia et al., 2010). Further, the bacterial plasmid backbone of STEMcircles™ is included in attachment sites and removal is achieved by phage phiC31 integrase to obtain backbone-free minicircles. STEMcircles™ are used to produce iPS cells from human adipose stem cells (Jia et al., 2010). However, the protocol is suited to human adipose stem cells and efficiency is substantially lower (up to 0.004%) compared with viral techniques (Narsinh et al., 2011). Narsinh and Jia mentioned limitations of the protocol and suggested further improvement with small molecules to achieve more efficient reprogramming of other cell types.

In the present study, STEMcircles™-derived GFP expression was increased until day 3 yielding up to 28.5% GFP-expressing L87 cells (**FIG. 10 A**). The number of GFP-positive cells was much lower in

BJ-5ta cells (**FIG. 10 B**). GFP expression in L87 and BJ-5ta cells was decreased at day 7. Accordingly, Jia and Narsinh mentioned sorting of GFP-positive cells because of moderate efficiencies (Jia et al., 2010; Narsinh et al., 2011). In accordance with the present study, Jia and co-authors observed a maximum of GFP-positive human adipose stem cells at day 3.

Loss of GFP expression indicates loss of STEMcirclesTM-derived gene expression in transfected cultures. This observation shows that the host cells did not replicate STEMcirclesTM to preserve constant gene expression. Separation and loss of vectors occurred during cell division because no selective culture conditions were applied. Additionally, DNA methylation silenced minicircles-derived gene expression. However, loss of ectopic gene expression is needed for the differentiation of a permanent iPS cell and therefore is crucial for iPS cell generation. For example, retroviral vectors are almost silenced by the host (Takahashi et al., 2007; Takahashi and Yamanaka, 2006). The application of excisable lentiviral vectors improves the differentiation potential of iPS cells (Sommer et al., 2010).

4.3.1.3. Impermanent Induction of ONSL, Klf4, and c-Myc by Episomal Vectors

In the present study, qRT PCR analysis demonstrated that STEMcirclesTM only temporary induced Oct4A and Sox2 mRNA expression in L87 cells and BJ-5ta cells (**FIG. 11**). Expression was almost lost at day 5. Importantly, Oct4 and Sox2 expression rely on each other. For example, silencing of Oct4 or Sox2 by RNA interference leads to reduction of both genes (Chew et al., 2005). Moreover, Oct4 and Sox2 show similar expression pattern through pre-implantation development of mice (Avilion et al., 2003) and Oct4-Sox2 heterodimers regulate expression of several pluripotency-associated genes such as Oct4, Sox2, and fibroblast growth factor 4 (Fgf4) (Yuan et al., 1995; Tomioka et al., 2002; Boyer et al., 2005). Taken together, preservation of STEMcirclesTM-derived Oct4 or Sox2 expression requires stable preservation of both Oct4 and Sox2. According to that, Oct4A and Sox2 mRNA levels analyzed in the present study were probably affected by absent Sox2 because Sox2 mRNA was induced much lower compared to Oct4 mRNA. Interestingly, Oct4A and Sox2 mRNA induction was delayed in BJ-5ta fibroblasts. Vector uptake and access to the nucleus required more time because fibroblasts do have a lower division rate compared to MSCs. In accordance with that observation, lipofection of DNA is less efficient when cells do not divide (Zou et al., 2010). Interestingly, Zou and co-workers could show that only DNA but not RNA delivery is affected by proliferation suggesting that access to the nucleus is hindered in non-dividing cells. Importantly, qRT PCR analysis demonstrated that STEMcirclesTM-derived Oct4B, Nanog, and Lin28 mRNA expression was preserved until day 5 in BJ-5ta cells. Nevertheless, Oct4A and Sox2 expression are required for induction of pluripotency in L87, BJ-5ta, and other somatic cells.

Klf4 and c-Myc were already expressed in L87 MSCs and BJ-5ta fibroblasts suggesting that induction of Klf4 and c-Myc is not required for reprogramming of these cells (**FIG. 9 B, 11 A/C**). According to that idea, delivery of reprogramming factors (instead of Oct4) is not necessary when endogenous expression already exists (Kim et al., 2009c). In the present work, Klf4 and c-Myc mRNA levels were temporary elevated after STEMcirclesTM delivery but expression returned to levels of non-transfected cells. Notably, different levels of Klf4 and c-Myc differently influence embryonic development and malignancy of human cancers as well (Lin et al., 2012a; Hu et al., 2012; Strauss et al., 2012). Currently, it is not clear whether different levels of endogenous Klf4 and c-Myc expression differently support reprogramming.

According to the data from qRT PCR analysis of L87 MSCs, IF analysis revealed that Oct4A, Sox2, and Nanog were expressed at the protein level (**FIG. 11 B/D**). Further, transcription factors were localized to the nucleus suggesting that host's gene expression was changed by ONSL. In the present study, the Oct4 antibody detected amino acids 1-134 of the N-terminus of the Oct4A protein. In accordance with our procedures, Atlasi and co-authors used the same Oct4A-specific antibody for the analysis of Oct4A expression (Atlasi et al., 2008). Further, comparison with antibodies detecting the C-terminus of Oct4 revealed that Oct4A and Oct4B are bond as well (Atlasi et al., 2008). Importantly, Oct4B is mainly localized to the cytoplasm (Cauffman et al., 2006; Lee et al., 2006). However, protein expression was rarely detected due to moderate transfection efficiencies measured in the present study (up to 28.5% in L87 cells) and low reprogramming efficiencies (up to 0.004%) reported by Jia and Narsinh (Jia et al., 2010; Narsinh et al., 2011).

Oct4A protein was detected in a few L87 cells at day 3 but in small colonies at day 7 suggesting that Oct4A was permanently induced by STEMcircles™ in a subset of proliferating L87 cells (**FIG 11 B**). In contrast, Sox2 and Nanog protein was detected in loose cells suggesting that protein expression was not localized to proliferating colonies. Importantly, induction of proliferation is required for the generation of iPS cells. Viral reprogramming by OSKM is more efficient when proliferation of somatic donor cells is increased by accelerated cell cycle progression (Ruiz et al., 2011). Additionally, cell cycle arrest inhibits successful iPS cell generation (Ruiz et al., 2011). However, Ruiz and co-authors mentioned that the characteristic cell cycle signature of human ES cells is required for reprogramming. Therefore, proliferation needs to be modified in context to properties of the somatic donor cell. According to that, hyperproliferation is not valuable for efficient reprogramming (Xu et al., 2013). Xu and co-authors reported that induction of proliferation by c-Myc decreased OSKM-mediated viral reprogramming of MEFs because of hyperproliferation. Xu and co-workers could show that ablation of c-Myc revealed lower proliferations rates and more efficient reprogramming. In the present study, Oct4-stained colonies of proliferating L87 MSCs were not analyzed whether hyperproliferation has occurred. It is important to analyze whether hyperproliferation affected efficient reprogramming of L87 MSCs. In contrast, delivery of STEMcircles™ into BJ-5ta fibroblasts did not show Oct4A-expressing small colonies at day 7 suggesting low proliferation capacities of transfected cells. This observation is due to delayed induction of Oct4A mRNA. Enhancement of proliferation appeared to be necessary for reprogramming of BJ-5ta cells.

BJ-5ta cells failed to express Sox2 and Nanog proteins after STEMcircles™ delivery (**FIG. 11 D**). Most probably, Sox2 and Nanog mRNA levels were low leading to low protein expression. On the other hand, inefficient translation of ONSL might have reduced ONSL protein levels. Recently, *in silico* estimation of translation efficiency in human cell lines revealed that the majority of genes is expressed in up to 5 cell types with comparable efficiencies (Stevens and Brown, 2013). Interestingly, a subset of genes showed cell type-associated deviations possibly caused by different mechanisms for protein degradation and/or translational control (Stevens and Brown, 2013). Further studies might clarify, whether cell type-dependent translation efficiencies (of ONSL, Klf4, and c-Myc) affect reprogramming of distinct cell types such as L87 MSCs and BJ-5ta fibroblasts.

Successful induction of endogenous ONSL expression clearly showed induction of pluripotency characteristics in L87 MSCs and BJ-5ta fibroblasts. These data are consistent with studies, which also used STEMcircles™ for reprogramming (Jia et al., 2010; Narsinh et al., 2011). Broad changes in the

transcriptome of L87 cells and BJ-5ta cells most likely occurred induced by the endogenous ONSL expression as an initial shift towards pluripotency.

Endogenous expression was analyzed to verify the transfected cells started their own gene expression of ONSL (**FIG. 12**), which is one of the most crucial steps during reprogramming. ONSL transcription factors directly bind to their own gene and to the 3 other factors to regulate gene expression (Loh et al., 2006; Wang et al., 2006). According to that, ectopically expressed ONSL induce endogenous ONSL expression in somatic cells. Identification of endogenous Oct4 expression did not differ between Oct4 transcript variants because Oct4 mRNA was absent in L87 cells and BJ-5ta cells. RT-PCR analysis verified induction of Oct4A and Oct4B as well suggesting endogenous induction of Oct4A and Oct4B. Other studies, which also used STEMcircles™, did not differ between endogenous Oct4A and endogenous Oct4B expression as well (Jia et al., 2010; Narsinh et al., 2011). It would be very interesting to determine the ratio of endogenous Oct4 transcript variants.

Lipofection of STEMcircles™ successfully generated ONSL-expressing ES cell-like cells. However, permanent reprogrammed cells were not generated. Apparently, prolongation or enhancement of ectopic ONSL expression was required. Following that idea, enhancement aimed by treatment with human ES cell-specific miRs, hypoxia, human ES cell specific culture conditions, small molecule media supplements, and repeated lipofection of STEMcircles™.

4.3.2. Non-Viral Reprogramming Induced by miR-302a-d & 372

Reprogramming factors do have many target genes for shifting the transcriptome of somatic cells towards pluripotency. However, human ES cell-specific miR-302a-d & 372 also regulate the expression of many genes, which is sufficient to shift the transcriptome of somatic cells as well. Currently, there are different kinds of synthetic mature-like miRs commercially available differing between their chemical modifications. In the present study, mature-like synthetic miR-302a-d & 372 were purchased from Ambion. Ambion's Pre-miR™ miRNA Precursor Molecules are small, chemically modified double stranded RNA molecules designed to mimic endogenous mature miRs expression. One strand is identical to the mature miR-302a-d & 372 whereas the other strand is modified to optimize uptake and processing of the double-stranded RNA molecule. Importantly, Pre-miR™ miRNA Precursor Molecules are not hairpin constructs and should not be confused with pre-miRs. More importantly, these mature-like miRs should not be confused with miR mimics. In contrast to mature-like miRs, the miR mimic technology is an innovative and effective tool for gene silencing. Mimics act in a gene-specific fashion. The 5' end of miR mimics is designed to bind to a unique motif in the 3' UTR of one selected target gene (Wang, 2011). Importantly, reprogramming requires application of mature-like miR-302a-d & 372 to broadly change mRNA levels in somatic cells.

4.3.2.1. Comparison with other Lipofection Techniques

Manufacturer's instructions often suggest miR concentrations between 1-100 nM. In the present study, cells were transfected with up to 50 nM miRs (**FIG. 13**). Accordingly, protocols established by other groups usually do not use more than 50 nM miRs (Suzuki et al., 2009; Tili et al., 2011) because higher amounts often lead to more adverse effects. However, the use of 100 nM miRs was demonstrated to be suitable for the differentiation of mouse ES cells (Tay et al., 2008). In the present study, miR-1 and its target gene Ptk9 were analyzed as positive controls to verify transfection procedures for miR delivery (**FIG. 13**). Ptk9 encodes twinfilin-1, which is an abundantly expressed

cytoskeleton regulatory protein and miR-1 is thought to induce cleavage of the Ptk9 mRNA (Lim et al., 2005). However, miR-1 is not involved in reprogramming, it is an important regulator of cardiac differentiation (Glass and Singla, 2011). In accordance with many other studies, Ptk9 mRNA was down regulated in a dose-dependent manner. It is important to highlight that dose-dependent repression of target mRNAs is one general characteristic of miRs. However, dose-dependent differential target gene selection was reported (Shu et al., 2012). In the present study, Ptk9 mRNA was repressed 48 h (about -90%) after transfection. Accordingly, Ptk9 mRNA repression (about -70%) was reported 48 h after lipofection of A5 mouse cutaneous spindle cells (Fleming et al., 2013). Importantly, Fleming and co-workers demonstrated that significant repression of other miR-1-related target genes occurred 72 h after miR-1 delivery. Transfection of miR-1 (and Cy3TM-labeled Anti-miRTM or miR-302a-d & 372) with INTERFERinTM was applied in the present work and did not affect morphology of L87 MSCs and BJ-5ta fibroblasts. Accordingly, other studies demonstrated treatment with INTERFERinTM without adverse effects in MSCs and fibroblasts (Renaud et al., 2007; Wang et al., 2012a).

Transfection of Cy3TM-labeled Anti-miRsTM allowed quantification of transfected cells by flow cytometry yielding up to 97.4% dye-positive L87 MSCs (**FIG. 14**). These data are consistent with data from Iyer and co-workers, who also applied flow cytometry yielding more than 90% dye-positive cells after transfection of FAMTM-labeled Anti-miRsTM (Iyer et al., 2012). In accordance with results obtained from STEMcirclesTM delivery, dye-labeled Anti-miRsTM were less efficiently introduced into BJ-5ta cells. Fluorescence was predominantly localized across the cytoplasm in L87 and BJ-5ta fibroblasts suggesting efficient uptake and correct destination of miR delivery. Importantly, there is no evidence that the use of Anti-miRsTM instead of miRs alters transfection efficiency. Therefore, data obtained by transfection of dye-labeled Anti-miRsTM are transferrable to the delivery of miR-302a-d & 372.

4.3.2.2. Pluripotency Requires Human ES Cell-Specific miRs

The present study aimed at the induction of reprogramming using human ES cell-specific miR-302a-d & 372. There are many human ES cell-associated miRs and many miRs are involved in the regulation of induction, maintenance, and loss of pluripotency. Recently, a study by Suh and co-workers revealed that about 14 miRs are expressed in a human ES cell-specific manner including miR-302a-d & 372 (Suh et al., 2004). Suh and colleagues isolated 36 prevalent miRs from SNU-hES3 human ES cells, which were cultured on murine feeder layers. There were 20 miRs, which were not observed in mammalian adult tissues and cell lines. Suh and co-authors showed that 3 miRs were common between mouse and human ES cells namely, miR-296, miR-301, and miR-302a (miR-302 in mice). Northern blot analysis of miRs in SNU-hES3 and MIZ-hES1 revealed 7 miRs, which were specific to human ES cells namely miR-200c, miR-368, miR-154*, and miRs from the miR-371-373 cluster. Additionally, 7 miRs from the miR-302a-367 cluster were also strongly expressed in human ES cells, but also present in EC cells. Together, 14 miRs are expressed in a human ES cell-specific manner (termed as ES cell-specific) and 11 of these 14 miRs are processed from 2 primary transcripts of the miR-371-373 and miR-302-367 cluster, respectively.

The expression of other ES cell-associated miRs such as miR-21, miR-301, miR-374 and miR-29b is low in human ES cells but is abundant in feeder cells (Suh et al., 2004). Further, their expression increases upon differentiation of human ES cells (Suh et al., 2004) suggesting a role in early differentiation and development comparable to the let-7 cluster in *C. elegans* (Reinhart et al., 2000).

Other miRs such as miR-16 were highly expressed in human ES cells and in several human cell lines, which contributes to the idea that a set of miRs is dedicated to regulate general aspects of cell biology also in human ES cells.

ES cell-specific miRs (i) preserve self-renewal, (ii) maintain the differentiation capacity, (iii) prevent differentiation, and (iv) manipulate early cell fate decisions. In ES cells, self-renewal is restricted by the progression of the cell cycle, which is composed of four consecutive phases: G1, S, G2, and M. Mouse ES cells have cell cycle lengths of about ~12 h in contrast to murine somatic cells, which have an average cell cycle length of about ~24 h. The short cell cycle of mouse and human ES cells is achieved by a very short G1 phase and subsequent unrestricted G1 to S phase transition. In mouse ES cells, the cell cycle is delayed in the absence of *Dicer1*, which is a master regulator of the miR machinery (Liu et al., 2004). Defective *Dgcr8* expression in mouse ES cells also lowered cell cycle progression and arrested cells in the G1 phase (Wang et al., 2007). The RNA-binding protein *Dgcr8* interacts with *Drosha* to enable processing of pri-miRs. Importantly, there is a set of miRs including members of the miR-290-295 cluster (mouse homologue to miR-371-373 cluster) and the miR-302a-367 cluster, which were able to compensate proliferation defects in *Dicer1* and *Dgcr8* mutant mouse ES cells (Sinkkonen et al., 2008; Wang et al., 2008; Kim and Choi, 2012). In human ES cells, miR-372 targets *Cdkn1a*, which encodes p21 and negatively regulates G1 to S transition (Qi et al., 2009). Another study by Dolezalova and co-workers demonstrated that DNA damage response-enhanced cell cycle progression increased expression of the miR-371-373 and miR-302a-367 cluster and depleted p21 expression (Dolezalova et al., 2012). Cell cycle progression is also preserved by miR-372-mediated downregulation of *Ccna1* (Tian et al., 2011). Other miRs such as miR-92a (Sengupta et al., 2009), microRNA-195 (Qi et al., 2009) also promote cell cycle progression in human ES cells but further studies are required to appreciate their impact on pluripotency in general. Together, human ES cell-specific miR-302a-367 cluster and miR-371-373 cluster are key regulators of the cell cycle implicating a major role during reprogramming.

The differentiation capacity of ES cells also relies on ES cell-specific miRs. *Dicer1*-deficient mouse ES cells fail to express crucial early differentiation markers for lineage induction and specification (Kanellopoulou et al., 2005). In the absence of *Dicer1*, several mesoderm and endoderm markers were not induced (Bernstein et al., 2003). Wild type ES cells are capable to form EBs, which consist of a heterogeneous mix of differentiating cells of all the three germ layers. *Dicer1* knockout cells formed EBs, which failed to grow after a few days (Bernstein et al., 2003). Prevention of differentiation is another characteristic of ES cell-specific miRs. The miR-302a-367 cluster prevents DNA methylation, which indirectly prevents differentiation (Lin et al., 2011). For example, the miR-302a-d & 372 do repress neuronal ectoderm formation via downregulation of *Nr2f2* (Rosa and Brivanlou, 2011). Interestingly, the miR-302a-367 cluster targets BMP inhibitors in human ES cells to inhibit neural cell fate determination (Lipchina et al., 2011). However, BMP signaling predominantly promotes differentiation of ES cells suggesting that there are further mechanisms to prevent BMP signaling. It is important to highlight that target genes directly involved in differentiation need to be identified. Interestingly, early cell fate decisions in general depend on the presence of the miR machinery. Maturation of miRs (and siRNAs) requires the *Dicer1* enzyme and absence of *Dicer1* leads to embryonic lethality in mice (Bernstein et al., 2003). *Ago2*, which is responsible for cleavage of miRs (and other RNAs), was shown to be crucial for mouse development (Liu et al., 2004). Accordingly, ES

cells are viable without miRs, but they fail to preserve self-renewal and lose their differentiation capacity *in vitro* (Calabrese et al., 2007). The present study aimed at the identification of miR-302a-d & 372 target genes.

4.3.2.3. Reprogramming Requires miR-302a-d & 372

In accordance with the given literature, 5 human ES cell-specific miRs derived from the miR-302a-367 and miR-371-373 cluster were applied in non-viral reprogramming because they are potent regulators of pluripotency, namely miR-302a-d & miR-372 (**FIG. 15**). Importantly, human ES cell-specific miRs are regulated by reprogramming factors. Oct4, Nanog, and Sox2 predominantly bind to promoters of ES cell-associated miRs including the miR-302a-367 and miR-371-373 cluster (Barroso-delJesus et al., 2008; Card et al., 2008; Marson et al., 2008). Therefore, several approaches aim at the combination of miRs with other reprogramming techniques to improve efficiency and quality of reprogramming. Viral reprogramming of MEFs by retroviruses was more efficient when synthetic miRs from the miR-290-295 cluster were transfected (Judson et al., 2009). Further, viral mediated expression of the miR-302a-367 cluster and depletion of Hdac2 was sufficient to generate iPS cells from MEFs and human dermal fibroblasts (Anokye-Danso et al., 2011). Besides the miR-302a-367 cluster, expression of miR-25 was useful for more efficient reprogramming when retroviral vectors were applied in mouse fibroblasts (Lu et al., 2012). MicroRNA-25 targets ubiquitin ligases, which are proposed to be regulators of Oct4 and c-Myc. Another approach reported that Nanog expression was indirectly up regulated by miR-214 in ovarian cancer cell lines (Xu et al., 2012a). Xu and co-authors suggested that Nanog induction was achieved by miR-214-mediated repression of the p53 signaling pathway. Reprogramming is still challenging, because the underlying mechanisms have yet to be fully elucidated (Sridharan and Plath, 2008; Okita and Yamanaka, 2011). It is important to highlight that efficient miR delivery and preservation of functional miRs (as mentioned before) as well as repression of unwanted targets is required for miR-mediated reprogramming (Guan et al., 2013). It is highly debated as to which step in the reprogramming process is the most crucial. However, ES cell-enriched miRs are immediately elevated during reprogramming and miRs therefore appear to be a powerful tool for non-viral reprogramming.

ES cell-associated miRs were reported to be sufficient for reprogramming on their own. Human and mouse adipose stromal cells were transfected with synthetic mature-like miR-200c, miR-302a-d, miR-369, and miR-369* to generate iPS cells (Miyoshi et al., 2011). However, the efficiency was very low (>0.01%). Interestingly, the transfection of miRs into human dermal fibroblasts only generated partially reprogrammed cells because these cells failed to induce teratomas. The expression of miR-200c is abundant in ES cells and thought to be ES cell-specific (Suh et al., 2004). By contrast, miR-369 expression is low in human ES cells (Suh et al., 2004). More recently, the miR-200 family, including the miR-200c-141 cluster, was shown to be involved in EMT and MET as well (Korpala et al., 2008). Further analysis are required to verify whether miR-200c and miR-369 promote reprogramming in general. Most probably, reprogramming of adipose stromal cells was ruled by miR-302a-d.

4.3.2.4. Target Genes of miR-302a-d & 372

The present study also aimed at the prediction and verification of unknown miR-302a-d & 372 target genes. Identifying of miR target genes is challenging because analysis rely on base pair complementary between mature miRs and 3'UTRs of mRNAs. Conservation of genes between

different species and/or secondary structures of mRNAs are included to narrow prediction results. Different algorithms of prediction tools allow some mismatches and the penalty of mismatches is different. Currently, there are several miR target prediction tools available online or provided for download. There are at least 4 very popular methods for miR target gene prediction (Le and Bar-Joseph, 2013), which are available online namely miRanda (John et al., 2004), Target Scan (Lewis et al., 2005), PicTar (Krek et al., 2005), and MicroCosm (Griffiths-Jones et al., 2006). In the present study, Target Scan, PicTar, and MicroCosm (not miRanda) were applied, which is consistent with other reports such as target prediction of human ES-cell-specific miR-200c (Rebustini et al., 2012). Interestingly, there are target prediction tools such as miRWalk (Dweep et al., 2011), which compare prediction results from own and third party target prediction tools. It is important to highlight that miR-302a target gene prediction by miRWalk and 9 third party prediction tools (not linked to MicroCosm) provides only 2 common genes namely derlin 2 (Derl2) and B cell translocation gene 1 (Btg1). Derl2 is involved in the homeostasis of the ER suggesting involvement in general aspects of biology. Interestingly, Btg1 counteracts proliferation (Lundin et al., 2012) and repression by miR-302a might be important for reprogramming. Analysis of miR-372 by miRWalk revealed no common target genes but 2 genes were predicted by 9 out of 10 prediction tools namely profilin 2 (Pfn2) and E2F transcription factor 5 (E2F5). Pfn2 is involved in actin polymerization suggesting involvement in general aspects of biology. Interestingly, E2F5 is involved in cell cycle regulation in a variety of human tissues and targeting by miR-372 appears to be suitable for reprogramming. Nevertheless, further analysis will elucidate whether Btg1 and/or E2F5 are involved in the regulation of pluripotency. However, target prediction leads to many false positive and some false negative results (Betel et al., 2010). False positive results depend on the short length of miRs. False negative probably result from conservation analysis, which might be conflicting because not well-conserved real targets genes might be excluded. According to that, analysis in plants identified not well-conserved real miR-targets (Barakat et al., 2007) suggesting the presence of evolutionary young (not conserved) miR target genes in animals as well. Together, circumstantial verification of miR-302a-d & 372 targets was required.

Target gene prediction by Target Scan, PicTar, MicroCosm, and EIMMo (**FIG. 15**) provided hundreds of possible target genes but most probably, a subset of these predicted genes is really regulated by miR-302a-d & 372. EIMMo target prediction was applied because the EIMMo algorithm includes analysis of pathways, in particular those of the KEGG pathway database (Gaidatzis et al., 2007). However, the EIMMo did not provide certain target genes, which are obviously involved in reprogramming. Importantly, different prediction tools provided conflicting results. Prediction by MicroCosm included Dnmt1, Ccna1, and Wdr61 (not Klf13). In contrast to that observation, Target Scan, PicTar, and EIMMo included prediction of Klf13 without Dnmt1, Ccna1, and Wdr61. Because target prediction tools use different algorithms and updates are released frequently, miR-302a-d & 372 target gene prediction generates different possible target genes depending on the current status of available target prediction tools. For example, Ccna1 is confirmed by miRanda and miRWalk target gene prediction. Several studies aggregate results from different databases to broaden the number of predicted targets for example for array analysis. In contrast to that, the present study needed to narrow the number of possible miR-302a-d & 372 targets and aggregation of results was unneeded. Importantly, datasets, which were obtained from Target Scan, PicTar, MicroCosm, and EIMMo, were filtered for target genes, which are involved signaling pathways responsible for induction, maintenance

and loss of pluripotency. Accordingly, Klf13, Dnmt1, Ccna1, and Wdr61 were selected for validation (**FIG. 15**). Klf13 is a member of the KLF-family of zinc finger transcription factors and binds GC-rich DNA in a sequence specific manner (McConnell and Yang, 2010). Dnmt1 is responsible for CpG methylation of the DNA during mitosis in adult cells (Qin et al., 2011). Dnmt1 preserves the methylation status of the DNA, which contributes to the regulation of gene expression. Ccna1 is crucial for G1-S transition and for entering the M-phase of the cell cycle in vertebrates, especially in the germ line (Wolgemuth, 2011). Wdr61 is a regulator of transcriptional processes and are involved in events downstream of RNA synthesis, such as RNA surveillance (Zhu et al., 2005).

The present study verified currently unknown but predicted miR-302a-d & 372 target genes namely Klf13, Dnmt1, Ccna1, and Wdr61 (**FIG. 16**). Transfection of miR-302a, miR-372, and a cocktail of miR-302a-d & 372 was applied. Both, miR-302a and miR-372, strongly repressed target mRNAs at day 3 but target gene expression returned at day 5. This study revealed that the miR cocktail elongated strong target gene repression until day 13. Different cocktail concentrations repressed targets in a dose-dependent manner. Therefore, functional miR-302a-d & 372 was proven according to data obtained from miR-1 delivery. It is important to highlight that strong mRNA repression (more than -50%) only occurs in a minor subset of about 150 genes (Baek et al., 2008). The majority of miR target genes (several hundreds) is regulated more modestly yielding about -30% downregulation (Baek et al., 2008). Moderate repression for example is suitable to target mRNA levels to ensure optimal protein expression in switch and tuning interactions (Bartel, 2009). However, strong repression of target genes by miR-302a-d & 372 suggests robust downregulation of Ccna1, Klf13, Dnmt1, and Wdr61 mRNA and alteration of pluripotency signaling pathways.

It is important to highlight that this study does not provide characterization of all members of the miR-302a-367 and the miR-371-373 cluster. The pri-miR-302a-367 (302b*-302b-302c*-302c-302a*-302a-367) is transcribed from chromosome 4 (Suh et al., 2004). Target recognition of miR-302a is most probably very similar to that of miR-302b-d because they are highly homologous (Suh et al., 2004). Function of miR-367 appears to be different because the seed sequence 5'-AUUGCAC-3' (2-8 nt) differs from miR-302a-d suggesting different target genes. The pri-miR-371-373 (371-372-373*-373) is encoded on chromosome 19 (Suh et al., 2004). Mature miR-302a-d & 372 share the same seed sequence 5'-AAGUGCU-3' (2-8 nt). Interestingly, miR-373 but not miR-367 and not miR-371 (5'-CUCAAAC-3'; 2-8 nt) also contains the same seed sequence and miR-373 expression is restricted to human ES cells (Suh et al., 2004). However, expression of miR-373 was reported to be very low (Suh et al., 2004) suggesting insignificant impact on the transcriptome of human ES cells. Accordingly, miR-373 was not included into the miR-302a-d & 372 cocktail used in this study. In contrast, there is evidence that even low expressed miRs might have biological significant functions suggesting the analysis of miR-373.

In the present study, repression of Ccna1 by miR-372 was demonstrated (**FIG. 16 B**). This is in accordance with previous studies in HeLa cells (Tian et al., 2011). However, miR-302a less efficiently repressed Ccna1 mRNA (**FIG. 16 A**). Inefficient repression of Ccna1 by miR-302a was recently demonstrated in human ES cells by Card and co-workers, which reported that miR-302a is not capable to repress Ccna1 protein within 3 days (Card et al., 2008). Differences probably result from low homology of miR-302a and miR-372. Importantly, atypical sites within the mature miR sequence might have improved interaction of miR-372 and Ccna1 mRNA. The presence of supplementary

and/or compensatory (atypical) sites is thought to be present in a minor subset of miRs (about 4%) (Bartel, 2009). In the present study, target gene prediction by MicroCosm revealed the presence of atypical 3' compensatory sites in mature miR-302a-d & 372. Therefore, there is a need to investigate mechanisms behind these atypical sites. Interestingly, data from the present study suggest that efficacy differs between miR-302a-d. Efficacy probably depends on atypical sites. Mature miR-302a repressed Ccna1 at day 3 but expression returned at day 5. The miR cocktail including miR-302b-d counteracted Ccna1 repression at day 3 leading to delayed but more stable repression at day 5 until day 13. One can conclude that miR-302b, miR-302c, and/or miR-302d differently (more and less efficiently) regulate Ccna1 mRNA repression as well as the repression of other target genes. Thus, atypical sites within miR-302b-d might be responsible for delayed and more efficient Ccna1 repression.

4.3.2.5. Induction of Endogenous miR-302a-d & 372 by Autoregulation

In the present study, mature miR-302a-d & 372 were highly enriched at day 1 in L87 and BJ-5ta cells (**FIG. 17 E**). It was reasonable that a subset of detected miRs at day 1 represent transfected synthetic mature-like miR-302a-d & 372. The majority of studies prove the presence of synthetic miRs from day 1 until day 3 after miR delivery without extended time course analysis. Importantly, the present study demonstrated that mature miR-302a-d & 372 were detectable for up to 13 days suggesting endogenous expression of mature miR-302a-d & 372. Accordingly, the present study verified induction of the miR-302a-367 cluster. Expression of pri-mir-302a-367 and pre-miR-302a-d and 372 was immediately induced at day 1 after miR delivery (**FIG. 17 D/F**). Thereafter, endogenous expression continuously decreased. In the present study, human ES cell-specific culture conditions were applied to preserve endogenous miR-302a-d & 372 levels. MEF culture was applied at day 6 after miR-302a-d & 372 delivery. Importantly, MEF culture was suitable to elevate precursor miR-302a & c-d & 372 expression at day 8. Subsequently, mature miR-302a-d & 372 were present at day 8. However, induction was not permanent because mature and precursor miRs were strongly reduced at day 13. These results indicate that MEF culture is suitable to enhance induction of miR-302a-d & 372 but MEFs do not preserve expression of these miRs. One can suggest that MEFs indirectly promote expression of miR-302a-d & 372. MEFs up regulate certain pluripotency-associated transcription factors, which are responsible for miR-302a-367 and miR-371-373 in human ES cells (Barroso-delJesus et al., 2008; Card et al., 2008; Marson et al., 2008). Currently, there is no evidence that MEFs directly mediate induction or elevation of miR-302a-d & 372. Thus, mature and precursor miR induction needs to be combined with other reprogramming methods even including MEF cultures.

Importantly, endogenous expression of mature miR-302a-d & 372 was induced at different levels (**FIG. 17 E**). These data contribute to the expression pattern of miR-302a-d & 372 in SNU-hES3 human ES cells, which do express miR-302a-d & 372 at different levels (Suh et al., 2004). One can conclude that L87 and BJ-5ta cells directed a desired expression level regarding natural miR levels of human ES cells. This conclusion is supported by that fact that certain miRs from the miR-302a-367 cluster are differently regulated by ultraviolet radiation or chemotherapeutic agents (Zheng et al., 2011; Dolezalova et al., 2012; Zhang et al., 2013a). Dolezalova and co-workers could show that ultraviolet radiation of human ES cells particularly increased miR-302c and miR-302d. Another two studies reported that chemotherapeutic agents Epirubicin and Clioquinol differently induce miR-302b and miR-302c.

In the present study, synthetic mature-like miR-302a-d & 372 induced the expression of the miR-302a-367 and miR-371-373 cluster. This observation contributes to the idea that miR genes can be permanently activated by autoregulation. The expression of miR genes is thought to be regulated by their own promoter region and gene expression is expected to mimic molecular mechanisms found in protein-coding genes. Interestingly, several studies showed that autoregulation of intragenic miR genes is regulated by their host genes. Intragenic miR genes (particularly intronic miRs) reside within known mRNA transcripts and experimental and computational results demonstrated that these miRs are co-transcribed with their host gene (Bosia et al., 2012). For example, intronic miR-388 supports own gene expression and expression of apoptosis-associated tyrosine kinase (AatK) by silencing genes that are functionally antagonistic to the AatK mRNA (Barik, 2008). However, the miR-302a-367 and the miR-371-373 cluster are thought to be intergenic miR genes, which are transcribed independently from surrounding genes. Further, common mechanisms for autoregulation of intergenic miRs are not likely suggesting a certain mechanism for autoregulation of miR-302a-d & 372. Such mechanism is currently unknown but common target genes might be involved. Importantly, lessons from intragenic miR genes help to elucidate autoregulation of the miR-302a-367 and miR-371-373 cluster.

Interestingly, the present study revealed that miR-302a-d up regulates miR-372 expression (**FIG. 17 B**). Further, detailed analysis revealed that miR-302a does not induce miR-372 (**FIG. 17 C**) suggesting that miR-302b-d are involved in upregulation of miR-372. The underlying mechanisms remained to be clarified. However, upregulation of mature miR-372 might have resulted from upregulation of pri-miR-371-373. The transcription of pri-miRs is similar to that of mRNA. Importantly, like protein-coding genes, promoters of miR genes contain CpG islands, TATA box sequences, initiation elements, and histone modifications (Ozsolak et al., 2008). Therefore, these data suggest analysis whether miR-302b-d regulates pri-miR-372 expression.

4.3.2.6. Indirect Regulation of Oct4, Nanog, and Thy1

This study demonstrated that induction of endogenous miR-302a-d & miR-372 expression is associated with induction of Oct4 and Nanog expression (**FIG. 18 A/B**). Oct4 was identified as an early marker for induction of reprogramming and Nanog was subsequently induced. In accordance with these results, Rosa and co-workers demonstrated upregulation of Oct4 after transfection of miR-302a-d into HEK-393T cells (Rosa and Brivanlou, 2011). Subsequent Nanog induction occurs to be plausible because Nanog gene expression requires binding of Oct4-Sox2 heterodimers to the Nanog promoter (Loh et al., 2006). Accordingly, Nanog activation also implicates induction of Sox2 expression, but further studies are needed to verify this presumption.

In the present study, the fibroblast marker gene Thy1 was down regulated by miR-302a-d & 372 delivery (**FIG. 18 C**). Thy1 (also classified as CD90) is a glycosphosphatidylinositol-anchored glycoprotein expressed on the surface of fibroblasts and other somatic cell types (Ramirez et al., 2011). Importantly, Ramirez and co-authors demonstrated that the lack of Thy1 correlates with high proliferation, migratory capacity, and upregulation of TGF β signaling in lung fibroblasts of patients suffering from idiopathic pulmonary fibrosis. Accordingly, downregulation of Thy1 is a potent marker for dedifferentiation during reprogramming of somatic cells. Thy1 is not predicted to be a target gene of miR-302a-d & 372. Further, Thy1 and miR-302a-d & 372 obviously do not share signaling pathways, which contributes to the idea that Thy1 is a general marker for the differentiation status of every Thy1-positive somatic cells. Taken together, non-viral delivery of human ES cell-specific

miR-302a-d & 372 was capable to convert somatic cells into ES cell-like cells because exclusive properties of human ES cells were induced in both L87 MSCs and BJ-5ta fibroblasts.

4.3.3. Dnmt1 Repression by miR-302a-d & 372 Regulates Oct4 Induction

In the present study, Oct4 induction was achieved by upregulation of miR-302a-d & 372. The questions remained how miRs were able to induce Oct4 expression. Detailed pathway analysis of miR-302a-d & 372 target genes raised evidence that miR-mediated regulation of Dnmt1 expression subsequently regulates Oct4. Dnmt1 is responsible for maintaining methylation during replication and predominantly methylates hemimethylated DNA. The enzyme is capable of transferring a methyl group to a 5' cytosine of one CpG dinucleotide. S-adenosyl methionine (SAM) is required as the methyl donor. In humans and in other mammals, 70-80% of CpGs are methylated (Takai and Jones, 2002). Interestingly, the amount of CpGs in the human genome is much lower as expected by chance. Methylated cytosines are mutational hotspots, which has led to CpG depletion during evolution (Takai and Jones, 2002). Importantly, CpGs occur within clusters and are located near the transcription start site of genes. DNA with more than 200 bp, a CG content higher than 50%, and an observed CpG/expected CpG ratio above 0.6 is defined as CpG island (Takai and Jones, 2002). CpG islands occur within 300-3000 bp long DNA fragments in or near to approximately 40% of promoters of the mammalian genome and about 70% of human promoters have a high CpG content (Saxonov et al., 2006). Methylated CpG islands are potent repressors of gene expression being a wide spread mechanism for gene regulation. Notably, the Oct4 promoter region contains a CpG island, which is methylated during differentiation to repress Oct4 transcription (Park et al., 2013). Thus, the present study searched for a Dnmt1-dependent mechanism regulating Oct4 expression.

4.3.3.1. Dnmt1 Regulation by miR-302a-d & 372

The present study demonstrated that Dnmt1 protein levels were strongly repressed by miR-302a-d & 372 in human somatic cells (**FIG. 19 B**). This repression suggests even low Dnmt1 enzymatic activity. It is important to highlight that low Dnmt1 activity does not only affect the Oct4 promoter, it does affect the whole genome with maybe unpredictable side effects. However, Dnmt1 is weakly expressed in human ES cells (Okano et al., 1999; Sayin et al., 2010; Sayin et al., 2010) suggesting that repression of Dnmt1 is suitable to mimic the epigenetic status of pluripotent stem cells. Interestingly, miR-302a-d & 372 did not repress Dnmt1 mRNA levels suggesting that Dnmt1 mRNA was not degraded. Repression of Dnmt1 protein is due to inhibition of Dnmt1 translation. In contrast to the miR cocktail, high concentrations of only miR-302a down regulated Dnmt1 mRNA levels. The miR cocktail (each 10 nM) and miR-302a (50 nM) were applied at the same concentration suggesting that this observation is associated with high miR-302a molarity. Accordingly, many studies reported that a change in miR molarity can lead to different targeting of mRNAs. For example, let-7 significantly down regulated Dicer1 only at low concentrations whereat c-Myc was only repressed by high let-7 concentration (Shu et al., 2012). The results of the present study raise evidence that each miR of the miR-302a-d & 372 cluster has a different potential to repress Dnmt1 and other shared target genes.

Interestingly, the present study did not verify Dnmt1 protein repression in 3T3-L1 mouse fibroblasts suggesting that regulation by miR-302a-d & 372 relies on species-specific mechanism (**FIG. 19 C**). Accordingly, the human ES cell-specific miR-371-373 cluster is not expressed in mouse ES cells because it is the human homologue to the mouse ES cell-specific miR-290-295 cluster. Studies by

Brautigam and co-workers demonstrated in mouse ES cells and P19 embryonic carcinoma cells that expression of the miR-371-373 cluster is differently regulated in mouse and the human pluripotent cells (Brautigam et al., 2013). Therefore, function of miR-372 most probably differs between both species. The function of miR-302a-367 cluster most probably also differs between both species. The miR-290-295 cluster and the miR-302a-367 are suggested to act almost redundantly in the mouse system (Wang et al., 2008). Accordingly, mouse ES cells do only express moderate levels of the miR-302a-367 cluster (Brautigam et al., 2013). In the mouse embryo, the expression of the miR-302a-367 cluster is more restricted and excluded from preimplantation stages (Brautigam et al., 2013). A variety of studies intensively described species-specific gene regulation in mouse and human ES and iPS cells. However, there is a need to clarify different functions of miR-302a-d & 372 in mouse and human pluripotent cells.

Data obtained from the present study revealed short-term repression of Dnmt1 (**FIG. 19 B**). This observation is due to short-term induction of endogenous pre-miR-302a-d & 372 suggesting that retained Dnmt1 expression is most probably not a result of a miR-independent endogenous regulation. Importantly, Oct4 is regulated by a self-sustaining circuitry consisting of positive autoregulatory mechanisms and feed-forward loops (Jaenisch and Young, 2008). Accordingly, short-term repression of Dnmt1 and subsequent short-term Oct4 expression should be suitable for permanent Oct4 induction. However, the recovery of the Dnmt1 expression associated with the Oct4 downregulation suggests that not only Oct4, but also other pluripotency factors are involved in maintaining the repression of Dnmt1 in pluripotent stem cells. Detailed analysis on Dnmt1 promoter binding sites will help to predict involved pluripotency factors.

Importantly, the present study demonstrated for the first time that Dnmt1 is a direct target gene of miR-302a-d & 372. Luciferase 3'UTR assays proofed interaction with miR-302a-d & 372 to the Dnmt1 mRNA (**FIG. 20**). Interestingly, another study reported Dnmt1 protein repression after plasmid-mediated expression of the miR-302a-367 cluster in human hair follicle cells (Lin et al., 2011). In contrast to the present study, Lin and co-authors suggested that Dnmt1 protein repression was subsequently regulated after miR-mediated repression of Kdm1a (also known as Aof2). Importantly, Lin and co-workers applied Target Scan and PicTar databases for Kdm1a target gene prediction, which (in accordance with own results) do not predict Dnmt1 as target of miR-302a-d. Accordingly, the study of Lin and co-workers did not include 3'UTR analysis of Dnmt1. Therefore, combined with data from the present study, miR-302a-d most probably targets Kdm1a to accelerate Dnmt1 downregulation. This model suggests that miR-302a-d affects expression of different targets within the Dnmt1 signaling pathway. According to this model, Dnmt1 protein was not affected by miR-302a or miR-372 alone suggesting the presence of unknown Dnmt1-associated target genes. One can conclude that miR-302a-d & 372 might similarly act on other ES cell-associated signaling pathways.

The present study verified Dnmt1 as a target gene using luciferase 3'UTR assays (**FIG. 20**). The cocktail of miR-302a-d & 372, miR-302a, and miR-372 very efficiently repressed luciferase transcription of the reporter plasmid. The cocktail more efficiently repressed luciferase transcription than single use of miR-302a or miR-372, which mirrors results from Dnmt1 protein analysis. Interestingly, luciferase repression using pmiR-302a carrying a miR-302a complementary strand was as efficient as repression using pmiR-Dnmt1 containing a mature sequence from the Dnmt1 3'UTR. This observation validates that binding of the seed region and interaction of the compensatory sites of

miR-302a-d & 372 is sufficient to obtain maximal Dnmt1 repression. It is important to highlight that miR-302a-d & 372 almost silenced luciferase activity, which is in accordance with other reports (Zeng and Cullen, 2003). The present study included the analysis of luciferase repression in the presence of doubled miR-302a-d & 372 binding sites leading also to almost silenced luciferase activity (data not shown). Nevertheless, this approach became unnecessary but was designed because repression of mRNAs and their translation also depends on the number of miR binding sites. For example, the 3'UTR of TGF beta receptor 2 (Tgfb2) contains 2 miR-302a-d & 372 binding sites predicted by Target Scan. It is important to highlight that *in vivo* behavior of miRs is usually more ineffective leading to low or moderate repression of gene expression (Bartel, 2009). Presumably, efficient downregulation of Dnmt1 presented in this work might not mirror the *in vivo* behavior of miR-302a-d & 372. Downregulation of Dnmt1 during early embryogenesis is most probably regulated by additional signaling pathways besides repression by miR-302a-d & 372.

The pmiR-GLO vector, which was used in the present study, encodes both Firefly luciferase for 3' UTR analysis and *Renilla* luciferase for normalization. Luciferase 3'UTR assays are described by several approaches including vectors such pGL2 (Sun et al., 2010), pGL3 (Sengupta et al., 2009), pGL4 (Yoo et al., 2012), pLightSwitch (Xu et al., 2012b), psiCHECK-1/2 (Yang et al., 2013), pMIR-REPORT (Papagregoriou et al., 2012), and pmiR-GLO (Guo et al., 2013; Zhang et al., 2013b). In contrast to Sun and co-workers, application of pGL2 was challenging and generation of reporter vectors was not successful within the present study (data not shown). In the present study, luciferase 3'UTR assays were performed in L87 MSCs and BJ-5ta fibroblasts to underline suitability of observed regulatory mechanisms. Interestingly, similar studies are usually performed in easy to transfect HEK293T human embryonic kidney cells (Ouyang et al., 2012; Zhang et al., 2013b), but other cell types have been described such as mouse keratinocytes (Fleming et al., 2013) and human ES cells (Sengupta et al., 2009). However, there is no evidence that the cell type or even the type of the reporter vector influences the way of function within 3'UTR analysis. However, improved reporter vectors carrying both firefly luciferase and *Renilla* luciferase produce more reliable data.

The present study applied the pmiR-GLO vectors carrying a short sequence of the Dnmt1 3'UTR (**FIG. 20 A**). This short sequence contained the SCR and the opposite region of the miR-302a-d & 372, which is in accordance with other studies. Importantly, the opposite region included atypical 3' compensatory sites of miR-302a-d & 372. In accordance with the present work, other researchers successfully applied luciferase-based 3' UTR analysis. For example, Lin and co-workers performed 3'UTR assays most similar to the present approach. Porcine granulosa cells were transfected with the pmiR-GLO vector carrying the predicted miR-26b binding site (44 nt) of ataxia telangiectasia mutated (Atm) (Lin et al., 2012b). However, other approaches included large parts or even the whole 3'UTR of the target mRNA of interest. Sengupta and co-workers performed 3'UTR assays in H1 human ES cells transfected with the pGL3 vector carrying about one quarter of the tumor protein 57 (p57) 3'UTR (206 nt) within the 3'UTR of the firefly luciferase (Sengupta et al., 2009). Normalization was performed by delivery of a second pRL-TK vector encoding TK-driven *Renilla* luciferase. Another approach performed 3'UTR assays in C5N mouse keratinocytes and A5 mouse squamous carcinoma cells using the pGL3 vector carrying about one third of the p54 (also known as Est1) 3'UTR (1278 nt) within the 3'UTR of the firefly luciferase (Fleming et al., 2013). Fleming and co-workers performed delivery of the pRL-TK vector for normalization. Interestingly, a study by Ouyang and co-authors in HEK293T cells

applied pRL-TK carrying the whole 3'UTR (2373 nt) of B cell CCL/lymphoma 2 (Bcl2) without normalization (Ouyang et al., 2012). Application of longer 3'UTR sequences is more reliable for mimicking the *in vivo* behavior of a certain miRs because they allow interaction of secondary mRNA structures and RBP. The secondary structures of mRNAs influence gene expression, mRNA stability, and mRNA decay (Wu and Brewer, 2012). Therefore, it is reasonable that miR binding is altered by secondary mRNA structures. Moreover, binding of miRs to the target mRNAs is known to be regulated by specific binding proteins. For example, ELAV-like RBP 1 (Elavl1, also known as HuR) is one common RBP, which binds to AU-enriched sequences in mRNAs and Elavl1 is thought to protect mRNAs from degradation (Gorospe et al., 2011; Meisner and Filipowicz, 2010). Further, Elavl1 specifically interacts with the 3'UTR of the c-Myc mRNA to allow repression by let-7b/c (Kim et al., 2009a). Interestingly, c-Myc repression is also regulated by another RBP. RBP L11 binds to the c-Myc mRNA and recruits a miR-24-loaded RISC (Challagundla et al., 2011). Subsequently, the c-Myc translation is inhibited by miR-24. Together, it remains to be clarified whether strong miR-302a-d & 372-mediated Dnmt1 repression observed in the present study is regulated by secondary mRNA structures and/or certain RBPs.

4.3.3.2. Oct4 Promoter Methylation is Regulated by Dnmt1

Oct4 promoter analysis, performed in the present study, focused on the analysis of the 5' regulatory domains of the Oct4 promoter (**FIG. 21**). Oct4 expression is orchestrated by CpG methylation targeting different sites within the Oct4 promoter. Eukaryotic promoters are composed of a core promoter and different 5' regulatory domains and at least 10 different eukaryotic promoter are classified (Gagniuc and Ionescu-Tirgoviste, 2012). The core promoter is composed of promoter elements such as TATA box or initiator element (INR) (Gagniuc and Ionescu-Tirgoviste, 2012). Interestingly, like about 90% of the human genes, Oct4 has a TATA-less core promoter with several regulatory elements located within the first 250 bp (Nordhoff et al., 2001; Carninci et al., 2006). However, 5' regulatory domains play a central role in driving cell-type-specific gene expression. Importantly, 5' regulatory domains contain several transcription factor binding sites classified as enhancers, silencers, and insulators. The human genome encodes about 20 000- 25 000 genes and about 400 000 putative human enhancer-associated modifications of histones and DNA are annotated by the ENCODE project (Calo and Wysocka, 2013). For example, RNA polymerase II-associated factor complex (PAF1C) binds to the Oct4 enhancer stabilizing the open chromatin structure in ES cells to up regulate Oct4 gene expression (Ding et al., 2009). The paf1c is at least composed of 5 known binding proteins. Knockdown of Paf1c components performed by Ding and colleagues affects Oct4 expression. The diversity of different epigenetic mechanisms demonstrates that Oct4 promoter DNA methylation is a key regulator of Oct4 gene expression.

The present study focused on the analysis of CpG methylation within the conserved region 4 (CR4) of the Oct4 distal enhancer. It is important to highlight that CpG methylation of CR4 has been poorly described in the literature. Therefore, the analyzed Oct4 promoter sequence (-2623/-2273 nt of Genbank sequence AJ297525) identical to human chromosome 6 (alternate assembly HuRefrefAC_000138.1) included CR4 (-2557/-2426 nt). The analyzed sequence contained 5 CpGs (**FIG. 21 A**). Enhancers typically reside in distance of several 100 nt to the promoter, which remains true for the Oct4 enhancer elements. The Oct4 promoter contains 2 enhancer elements, the distal (1A site) and the proximal (2A site) enhancer (Nordhoff et al., 2001). Distal and proximal enhancer are

capable to drive Oct4 expression in ES and EC cells (Nordhoff et al., 2001). Importantly, it is well described that the distal and the proximal enhancer becomes methylated during embryonic development (Pan et al., 2002). Oct4 enhancer activity is temporal and spatial regulated during embryonic development. Moreover, the distal enhancer drives Oct4 expression in the morula, the ICM, and in primordial germ cells whereas the proximal enhancer guides Oct4 expression in the epiblast (Nordhoff et al., 2001). Comparison of human, mouse, and bovine Oct4 promoters revealed 4 conserved regions (CR1-4) (Nordhoff et al., 2001). The proximal enhancer contains CR1 and CR2 and the distal enhancer includes CR3 and CR4. Interestingly, there is an E-box in CR4 (and in CR2 and CR3). The E-box binds transcription factors of the basic helix-loop-helix family such as c-Myc (Levine and Tjian, 2003) contributing to the idea of a pluripotency network. Taranger and co-workers reported CpG methylation within the Oct4 promoter sequence (-1748/-1510) containing CR2 and CR3 in response to RA (Taranger et al., 2005). Accordingly, another study by Smith and co-authors reported RA-induced methylation of certain CpGs in the Oct4 distal (-2317, -1399) and proximal (-759, -231) enhancer but not in CR4 (Smith et al., 2010). Together, studies by others suggest that CpG methylation in the Oct4 distal enhancer and particularly in CR4 is regulated independently from RA-induced differentiation and is even more important for ES cells than for epiblast stem cells.

The present study recommends that the distal enhancer significantly regulates the Oct4 promoter (**FIG. 21 C**). Currently, insulator and silencer elements have not been described within the Oct4 promoter. 5' regulatory domains such as insulators are capable to block function of enhancers. For example, in HCT116 human colon colorectal carcinoma cells repression of Dnmt1 lowers CpG methylation of a certain insulator located within the telomerase reverse transcriptase (Tert) promoter, which enables binding of a certain Tert repressor (Georgia et al., 2013). Silencers are bound by repressors to restrict gene expression and can be found several 100 nt upstream of the gene, within introns and exons, or within the 3'UTR. The majority of repressors are constitutively expressed, only allowing activation of a certain gene by either inhibiting the enhancer or by activating an silencer (Ogbourne and Antalis, 1998). For example, the neuronal-restrictive silencer factor (NRSF), which is encoded by the RE1-silencing transcription factor (Rest) gene, is constitutively expressed in ES cells to permanently repress neuronal genes that are essential for localization of neuronal tissues (Ogbourne and Antalis, 1998). Interestingly, the Oct4 promoter contains a transcription factor AP-2Yc (Tcfap2c) binding site and luciferase assay revealed that Tcfap2c binds the Oct4 promoter for repression. However, detailed analysis in mouse zygotes and ES cells could not verify that Tcfap2c is responsible for Oct4 silencing (Choi et al., 2013). Notably, there is evidence that other genes such as caudal type homeobox 2 (Cdx2) (Choi et al., 2013) target the Oct4 promoter at an unknown binding site. Possibly, detailed epigenetic studies may elucidate unknown insulators and silencer.

The present study quantified loss of Oct4 promoter methylation in a time course after treatment with miR-302a-d & 372 (**FIG. 21 C**). In L87 MSCs, the Oct4 promoter was methylated about 85% and Oct4 expression was absent. Another study in rat MSCs by Duan and co-workers reported CpG methylation of the Oct4 promoter (-85, -293) with comparable amounts yielding about 79% of CpG methylation (Duan et al., 2012). Treatment of miR-302a-d & 372 lowered Oct4 promoter methylation down to about 30% sufficient to induce Oct4 gene expression. This is due to data from Dnmt1 protein analysis within the present study demonstrating that Dnmt1 protein expression was strongly repressed, but not silenced by miR-302a-d & 372 (**FIG. 19 B**). Importantly, quantification of CpG

methylation did not differ between CpGs within the analyzed promoter sequence. On the one hand, one can conclude that almost all cells did not fully lose CpG methylation. On the other hand, only a subset of cells might have completely lost CpG methylation. Accordingly, the remaining 30% CpG methylation could also be explained by the presence of not transfected cells bearing fully methylated Oct4 promoters. Modern sequencing methods are required to answer these questions accordingly. Importantly, even H9 human ES cells showed about 30% promoter methylation, which can be explained by the presence of MEFs, which do have methylated Oct4 promoters. Further studies should include separation of MEFs.

In accordance with the present study, several studies by others reported Oct4 promoter DNA demethylation during reprogramming (Aasen et al., 2008; Aoi et al., 2008; Huangfu et al., 2008a; Kim et al., 2009c). Interestingly, bisulphate sequencing is most often applied for the analysis of DNA methylation. Bisulphite treatment of DNA or a desired PCR fragment converts cytosine within CpGs to uracil by deamination of 5-methylcytosine (5-mC). Subsequently, the DNA can be analyzed for the presence of uracil conversion using a variety of techniques such as direct sequencing, high-throughput screening by pyrosequencing, or methylation specific primers. Importantly, quantification of CpG methylation is challenging when direct sequencing is applied because of the low number of replications. Further, bisulphate conversion is generally limited by uracil conversion of non-CpG 5-hydroxymethylcytosine (5-hmC), incomplete conversion caused by incomplete DNA denaturation (Fraga and Esteller, 2002), and up to 90% DNA degradation (Grunau et al., 2001). The presence of 5-hmC is thought to prevent maintenance methylation by Dnmt1 (Huang et al., 2010). Further, 5-hmC in CpGs differs dramatically between different cell types yielding about 5% in ES cells or about 20% in cerebellar Purkinje cells (Huang et al., 2010). Bisulphite-independent methods provide one opportunity to obtain more reliable data for quantification of CpG methylation. The present study applied bisulphite-independent DNA digestion by MSREs and subsequent real-time-based quantification of CpG methylation using the OneStep qMethyl™ Kit (**FIG. 21**). Similar approaches with other genes of interest were recently applied by others (Sanders et al., 2012; van et al., 2012; Rao et al., 2012). However, even if MSRE-based CpG analysis leads to more reliable data, MSREs only target a subset of possible CpG motifs narrowing their field of application.

4.3.3.3. Dnmt3a and Dnmt3b are Not Essential for Oct4 Promoter Methylation

The human genome encodes Dnmt1, Dnmt2, Dnmt3a, Dnmt3b, and Dnmt3l (Sayin et al., 2010). Loss of Dnmt1, Dnmt3a and Dnmt3b leads to variety of developmental defects (Okano et al., 1999). Dnmt3a knockout mice die after birth and Dnmt3b knockout mice are viable but suffer from several developmental defects (Okano et al., 1999). In the present study, miR-302a-d & 372 did not affect Dnmt3a and Dnmt3b mRNA levels (**FIG. 22**). This observation suggests that Oct4 promoter DNA demethylation did not depend on failed *de novo* methylation. Dnmt3a and Dnmt3b are responsible for *de novo* DNA methylation of the Oct4 promoter and subsequent downregulation of Oct4 expression during differentiation (Butler et al., 2012). However, *de novo* methylation of Oct4 is regulated by Dnmt3a and Dnmt3b during reprogramming (Pawlak and Jaenisch, 2011). Interestingly, Dnmt3b protein was increased after transfection of miR-302a-d & 372 in the present study (**FIG. 22 B**), but more detailed analysis are required to verify the induction of Dnmt3b by miR-302a-d & 372. Dnmt3b is suggested to be a target of Oct4 (Tan et al., 2013), which might contribute to Oct4 induction by miR-302a-d & 372 (**FIG. 18 B**). Additionally, Dnmt3b is one pluripotency-associated marker gene

(Takahashi et al., 2007). Several studies well described that Dnmt1 is predominantly dedicated to maintenance methylation. Further on, Dnmt1 maintenance methylation sufficiently represses Oct4 expression in somatic cells starting during early embryonic differentiation (Hattori et al., 2004). Accordingly, there is no evidence that either Dnmt3a or Dnmt3b are particularly involved in the Oct4 promoter demethylation after induction of reprogramming by miR-302a-d & 372.

The present study did not include the analysis of Dnmt2 expression levels because it is not essential for DNA methylation. Dnmt2 has strong sequence similarities with Dnmt1, Dnmt3a, Dnmt3b, and Dnmt3l, but maintenance and *de novo* methylation are not affected in Dnmt2 knockout mouse ES cells (Okano et al., 1998). Interestingly, Dnmt2 is present in many human tissues, but at very low levels (Sayin et al., 2010). Dnmt2 lacks the regulator amino terminal, but the enzyme is capable of methylating DNA suggesting that Dnmt2 might be involved in DNA repair of a few special target sites (Sayin et al., 2010). However, a common target of Dnmt2 is the 5' cytosine of aspartic acid in transfer RNAs (tRNAs) (Sayin et al., 2010). Accordingly, Dnmt2 is officially termed as tRNA aspartic acid methyltransferase 1 (Trdmt1). The present study did also not include the analysis of Dnmt3l because it is not catalytically active and acts as cofactor for the *de novo* methyltransferases Dnmt3a and Dnmt3b (Arand et al., 2012). Dnmt2 and Dnmt3l are somehow involved in epigenetic patterning, but their impact on maintenance and *de novo* methylation remains to be clarified. In accordance with the literature, there is no evidence that Dnmt2 or Dnmt3l are directly involved in the methylation of the Oct4 promoter.

The present study did not differ between different isoforms of Dnmt1, Dnmt3a, and Dnmt3b. The expression of different isoforms is one mechanism to restrict epigenetic modification to distinct chromatin structures. Dnmt1 is expressed by at least 3 different isoforms. Dnmt1s is constantly expressed in embryonic and adult somatic cells but Dnmt1o2 and Dnmt1o2 are restricted to oocyte and embryo (Giraldo et al., 2013). There is the possibility that even alteration of distinct Dnmt3a and Dnmt3b isoforms is involved in Oct4 promoter methylation. Dnmt3a is expressed by at least 2 different isoforms in mice and humans and Dnmt3a2 is the major isoform in J1 mouse ES cells (Chen et al., 2002). Contradictory, Dnmt3a was detected at low mRNA levels and approaches to detect Dnmt3a proteins in L87 and BJ-5ta cells failed because of low Dnmt3a protein content (data not shown). It remains to be clarified whether delivery of miR-302a-d & 372 affects even low Dnmt3a protein expression. Dnmt3b is expressed by over 30 different isoforms, which are generated by alternative splicing and/or alternative promoter usage (Gordon et al., 2013). These variety of isoforms includes active and inactive molecules, which interact with several cofactors for epigenetic modification of certain DNA patterns and histones (Gordon et al., 2013). Detailed analysis of Dnmt3b isoforms might lead to the identification of ES and iPS cell-associated Dnmt3b isoforms. Importantly, it remains to be elucidated, which isoforms of Dnmt1, Dnmt3a, and Dnmt3b are involved in ES cell-specific epigenetic patterning including Oct4 regulation. Importantly, there are other demethyltransferases such as methyl-CpG binding domain protein 2 (Mbd2) and lysine (K)-specific demethylase 3a (Kdm3a; also known as Jmjd1a) (Li and Zhao, 2008). According to the literature, it is unlikely that only Dnmt1 predominantly regulates Oct4 promoter methylation. Moreover, DNA methylation does not only depend on the activity of DNA methyltransferases. Interestingly, methylated DNA recruits methyl-CpG binding proteins (MBDs) to improve gene repression (Li and Zhao, 2008). Research on

demethyltransferases and MBDs might reveal a new approach for more directed Oct4 activation during reprogramming.

The present study did not include analysis of Oct4-related histone modifications. Importantly, because Oct4 expression was induced by miR-302a-d & 372, histone modifications of the Oct4-related chromatin were most probably indirectly and/or subsequently adjusted after miR-302a-d & 372 delivery. For example, histone demethylation by Jumonji domain 1a (Jmjd1a) and Jmjd2c is necessary for Oct4 upregulation (Loh et al., 2007). Histone demethylation removes repressive H3K9me in the chromatin downstream of the promoters of Oct4, Nanog, and other pluripotency-associated marker genes (Butler et al., 2012). In contrast, H3K9me of the Oct4-related chromatin is mediated by the histone methyltransferase G9a (Feldman et al., 2006). It is important to highlight, that histone modifications such as methylation, acetylation, ubiquitination, SUMOylation, crotonylation, butyrylation, propionylation, citrullination, ADP-ribosylation, phosphorylation, and glycosylation have been shown to be potent regulators of gene expression (Musselman et al., 2012). Histone modifications allow activation as well as repression of gene expression. Histone methylation and acetylation are most frequently and Oct4 expression predominantly depends on histone methylation and acetylation (Herrmann et al., 2013). Mono-, di-, or tri-methylation is responsible for activation and repression as well. Activation is achieved by methylation of H3(K4,K36,K79), H3(R17,R23), and H4(R3). Repression is caused by methylation of H3(K9,K27), H4(K20). Interestingly, acetylation generally activates gene expression by acetylation of H3(K9,K14,K18,K56), H4(K5,K8,K13,K16). However, it would be interesting to analyze even rare histone modifications during reprogramming. There is a need to analyze how miR-302a-d & 372 changed the chromatin status of Oct4 and to identify these miR-regulated histone marks.

4.3.4. Hypoxia Facilitates Non-Viral Reprogramming

The oxygen supply is different within the human body and depends on the co-localization of oxygen-providing blood vessels. Fibroblasts are typically localized to the connective tissue, which abundantly contains capillaries responsible for proper oxygen supply in healthy human beings. In contrast, bone marrow derived MSCs typically reside within a hematopoietic stem cell niche providing a microenvironment with a limited oxygen supply. Even MSCs derived from mesenchymal stem cell niche (such as adipose tissue-derived MSCs) reside within hypoxic conditions (Mohyeldin et al., 2010). Accordingly, low oxygen supply also improves preservation of explanted umbilical cord blood-derived MSCs (Shima et al., 2009). The present study applied 5% oxygen to mimic hypoxic culture conditions of the mesenchymal stem cell niche. The *in vivo* microenvironment of human bone marrow-derived MSCs provides 1-9% oxygen to constitute a physiologic normal oxygen level (Simon and Keith, 2008; Chow et al., 2001; Mohyeldin et al., 2010). Despite these findings, very little attention has been paid to the metabolic milieu of fibroblasts and the MSC niche when cells are used as a somatic donor for reprogramming. The present study examined whether hypoxic culture conditions not only would improve culture of MSCs, but whether it would also promote reprogramming of BJ-5ta fibroblasts and L87 MSCs. Analysis of hypoxic culture conditions extensively applied within the present study, aimed at the facilitation of a strong initial reprogramming impulse given by STEMcircles™ and/or miR-302a-d & 372. Combination of hypoxia with miR delivery, episomal vectors, or other non-viral reprogramming techniques was demonstrated and offers a promising opportunity to trigger efficiency and quality of non-viral reprogramming.

4.3.4.1. Hypoxia-Induced Oct4A and Nanog expression

Importantly, in the present study, hypoxia induced Oct4A and Nanog expression in L87 MSCs independently from other non-viral reprogramming techniques (**FIG. 23, 25 C**). Studies in primary human bone marrow derived MSCs also demonstrated induction of Oct4 and Nanog by hypoxic conditions (Foja et al., 2013). Interestingly, Oct4A but not Nanog expression was induced in BJ-5ta cells (**FIG. 23**) suggesting that immaturity of MSCs might contribute to hypoxia-mediated induction of Nanog and reprogramming factors in general. In accordance with the present study, hypoxic culture of primary human dermal and muscle-derived fibroblasts induced Oct4 (Page et al., 2009). In conflict with own results, Page and co-authors reported the induction of Nanog, which could be explained by the use of primary fibroblasts and/or the use of fibroblasts of a different origin. In contrast to the present study, Page and co-authors described application of glass surfaces, which were frequently applied within the present study without any effect (data not shown). The present study revealed that Sox2 was not induced by hypoxia in BJ-5ta fibroblasts and L87 MSCs (**FIG. 23, 25 B**). Importantly, the study by page and co-workers verified that Sox2 is not induced in dermal and muscle-derived fibroblast. These observations do not contribute to studies in other cell culture models. It has been shown that human ES cells cultured under hypoxic conditions for 3 d expressed higher levels of the pluripotency factors Oct4, Nanog and Sox2 (Forristal et al., 2010). This induction was mediated by hypoxia-inducible factor 2a (Hif2a). Likewise, Mathieu and co-workers revealed Hif1a and Hif2a mediated induction of Oct4 and Nanog in the human lung adenocarcinoma cell line A549 cultured at 2% O₂, while Sox2 was induced by HIF1a (Mathieu et al., 2011). Naturally, human ES cells and carcinoma cells harbor more pluripotency-associated properties than the multipotent MSCs explaining the deviating results. Importantly, stabilization of hypoxia-inducible factors (HIFs) is necessary for the expression of Oct4, Nanog and Sox2 (Mohyeldin et al., 2010), which clearly shows that hypoxia regulates pluripotency in human ES cells and the generation of iPS cells.

4.3.4.2. Hypoxia Improves Induction of Oct4A and Nanog by miR-302a-a & 372

In the present study, miR-302a was induced in L87 MSCs only by hypoxia and human ES cell-specific conditions (**FIG. 24 C**). According to this observation, another study demonstrated miR-302a-d & 372 induction in primary human bone marrow derived MSCs by similar conditions (Foja et al., 2013). The miR-302 cluster positively regulates Oct4 expression by suppressing Nr2f2, a member of the nuclear orphan receptor family of transcriptional repressors (Kuo et al., 2012). Therefore, the induction of Oct4 in MSCs and fibroblasts may be also explained by the hypoxia-mediated induction of the ES-specific miR-302-367 cluster.

Importantly, hypoxia combined with delivery of 5x 10 nM miR-302a-d & 372 revealed prominent Nanog expression demonstrated at day 7 in BJ-5ta fibroblasts (**FIG. 23 B**). Analysis of L87 MSCs demonstrated miR-mediated induction at lower levels later than day 7 (**FIG. 18 B**). One can conclude that application of miR-302a-d & 372 and hypoxic conditions led to additive effects on the induction of Oct4A and Nanog. Recently, another study in 11 cancer cell lines reported that hypoxia, through HIFs, can induce a human ES cell-like transcriptional program, including the miR-302-367 cluster and the reprogramming factors Oct4, Nanog, Sox2, Klf4, and c-Myc (Mathieu et al., 2011). Further Mathieu and co-authors demonstrated more efficient iPS cell generation from A549 somatic donors when retroviral expression of HIF1a and HIF2a and lentiviral expression of ONSL was combined. Data from

the present study contribute to the hypothesis that HIFs and ES cell associated miRs target similar signaling pathways.

4.3.4.3. ES cell-Specific Conditions Improve Oct4A Induction by miR-302a-a & 372

Transfection of miR-302a-d & 372 was applied under normoxic conditions to verify that induction of Oct4 depends on hypoxic conditions. Of course, ES cell-specific conditions are necessary for the preservation of ES and iPS cells. Interestingly, the present study revealed that even ES cell-specific but normoxic conditions enabled Oct4A induction by miR-302a-d & 372 in fibroblasts (**FIG. 23 A**). In contrast to hypoxia, Nanog and other reprogramming factors were not induced. Interestingly, another study demonstrated that ES cell-specific conditions were also required for induction of Oct4 in human dermal fibroblasts by transfection of miR-302a-d combined with miR-200c, miR-369, and miR-369* (Miyoshi et al., 2011). Miyoshi and co-workers also reported induction of Nanog and other reprogramming factors, which may depend on the different somatic donor, different provider of synthetic miRs, and a different transfection protocol. However, Oct4A induction by miR-302a-d & 372 under ES cell-specific conditions raised evidence that induction of reprogramming is even improved by ES cell-specific conditions.

4.3.4.4. Hypoxia Improves Induction of ONSL by STEMcircles™

L87 and BJ-5ta cells were transfected with STEMcircles™ and the impact of hypoxia on ONSL induction was analyzed within the present study (**FIG. 25**). Data obtained from L87 MSCs demonstrated that hypoxia up regulates STEMcircles™-induced endogenous Nanog and Lin28 levels (**FIG. 25 B**). Further, endogenous Nanog levels were preserved by hypoxia. This contributes to induction of Nanog in L87 MSCs only by hypoxia demonstrating that episomal reprogramming and hypoxia led to additive effects on the induction of Nanog. It is reasonable that elevated Lin28 levels result from high Nanog transcription levels rather than from hypoxia. There is no evidence that Lin28 is regulated by HIFs or other hypoxia-related pathways (Mohyeldin et al., 2010). Further, the Lin28 promoter is occupied by Nanog and other reprogramming factors (Marson et al., 2008). There is the possibility that hypoxia even have induced other pluripotency-associated genes also enhancing Lin28 expression. Treatment with STEMcircles™ under hypoxia did not elevate endogenous Oct4 and Sox2 expression levels in L87 MSCs. It is important to highlight that Oct4 expression was not up regulated but preserved (**FIG. 25 B/C**). It is possible that hypoxia even preserves Sox2 expression because it is also regulated by HIFs (Mohyeldin et al., 2010), which needs to be analyzed. It is not clear whether significant levels of Sox2 and Oct4 transcription factors have been expressed. Maintenance of pluripotency is not a binary on-off system. It has been described by others that moderate levels of Oct4 keep ES cells pluripotent but higher or lower levels are associated with differentiation (Niwa et al., 2000; Karwacki-Neisius et al., 2013). Accordingly, Oct4 induction might have reached levels sufficient for induction of pluripotency. There is a need to clarify whether significant levels of Sox2 and Oct4 have been expressed even in a low number of cells. However, preservation of Oct4 expression contributes to induction of Oct4 in L87 MSCs only by hypoxia demonstrating that episomal reprogramming and hypoxia led to additive effects on the induction of Oct4. In conclusion, hypoxia enhanced (Nanog, Lin28) and preserved (Nanog, Oct4) the induction of reprogramming factors by STEMcircles™ suggesting a general effect on episomal vector-based reprogramming strategies

making this approach also available for those cell source that previously have not been amenable for episomal reprogramming.

In contrast to L87 MSCs, BJ-5ta fibroblasts failed induction of Lin28 when STEMcircles™ were transfected under hypoxic conditions (**FIG. 25 A**). Importantly, Page and co-workers even mentioned that Lin28 induction depends on the origin of fibroblasts. Hypoxia induced Lin28 in dermal fibroblasts but not in muscle-derived fibroblasts (Page et al., 2009). BJ-5ta lung fibroblasts are suggested to be more similar to muscle-derived fibroblasts. Failed induction of Lin28 might contribute to the observation by Pandit and co-workers, which reported that the Lin28 antagonist let7 hinders differentiation of myofibroblasts (Pandit et al., 2010). Let7 is known to be a counterpart of Lin28 and interplay of both ensures appropriate stem cell functions such as prevention of stem cell growth (Thornton and Gregory, 2012). As mentioned before, there is no evidence that Lin28 is regulated by HIFs (Mohyeldin et al., 2010). Accordingly, further studies are required to characterize the impact of hypoxia on fibroblasts especially during early reprogramming.

4.3.4.5. Hypoxia is Capable to Enhance Proliferation

To assess enhanced proliferation by hypoxia, primary bone marrow derived MSCs were applied in the present study because they rapidly lose their capacity to expand and to differentiate into desired cells types within less than 15 passages (Digirolamo et al., 1999; Vacanti et al., 2005). The primordial status of MSCs usually is preserved until passage 5 and deregulated during the following passages leading to actin accumulation, reduced adherence and reduced telomerase activity (D'Ippolito et al., 2004; Vacanti et al., 2005). Culture of primary MSCs as well as of MSC lines routinely is performed under normoxic conditions (Rastegar et al., 2010). However, these culture conditions are associated with adverse effects such as the gradual loss of their growth and phenotypic characteristics (Bruder et al., 1997; Tsai et al., 2011). Hypoxia increases the population doubling rate of primary bone marrow-derived MSCs of diseased individuals (Foja et al., 2013). This is in agreement with findings by Grayson and co-authors, who showed a clear link between 2% oxygen and the enhancement of proliferation of MSCs from healthy individuals (Grayson et al., 2007). Tsai and colleagues demonstrated inhibition of senescence and maintenance of MSC properties in the presence of 1% oxygen (Tsai et al., 2011). In the present study, the MSC-specific morphology of primary MSCs was preserved (data not shown). Enhancement of proliferation in the present study was verified by the expression of Poli and Mcm5, two factors crucial for DNA replication (**FIG. 26 B**). Studies by others also reported induction of Poli and Mcm5 during reprogramming of mouse fibroblasts and B lymphocytes using retroviral vectors demonstrating that both are essential markers to detect enhanced proliferation during iPS cell generation (Mikkelsen et al., 2008; Ruiz et al., 2011). Together, these data from the present study reveal that even less stringent, easily achievable hypoxic conditions result in an improvement of the MSC culture.

Another approach of the present study verified hypoxia-mediated enhanced proliferation in L87 MSCs by Ki67 staining (**FIG. 26 A**). The name Ki67 is derived from the prototype monoclonal antibody-producing clone 67 developed in Kiel, Germany. Antibodies against the Ki67 (also known as MKI67) protein detect proliferating cells (Hua et al., 2013). Another study by Ghule and co-workers reported that increased Ki67 staining is associated with reprogramming of fibroblasts (Ghule et al., 2011) and absent Ki67 staining in MSCs is associated with senescence (Shibata et al., 2007).

Therefore, hypoxia-induced Ki67 might demonstrate that hypoxia even contributes to reprogramming of L87 cells and BJ-5ta cells.

Enhanced proliferation might have been subsequently occurred after hypoxia-mediated induction of a few signaling pathways including HIFs, miR-302a-d & 372, and Oct4 and Nanog. HIFs are broadly involved in cell cycle regulation in order to allow wound healing and many other physiological processes (Semenza, 2011). The miR-371-373 and miR-302a-367 clusters are involved in the enhancement of cell cycle progression as already mentioned (Tian et al., 2011; Dolezalova et al., 2012). Cell cycle regulation by reprogramming factors was previously demonstrated by Zhang and co-authors, which reported that Nanog is directly involved in G1 to S transition in human ES cells by binding to cyclin-dependent kinase 6 (Cdk6) and cell division cycle 25a (Cdc25a) (Zhang et al., 2009).

Together, these data from the present study emphasize that it is possible to support reprogramming of somatic cells very efficiently by modifying the *in vitro* culture conditions. Hypoxia enhanced proliferation and enhanced or preserved a subset of reprogramming factors induced by miR-302a-d & 372 or STEMcircles™. However, the present study revealed that Sox2 was not induced or elevated neither by hypoxia nor by hypoxia combined with STEMcircles™ and miR-302a-d & 372 in BJ-5ta fibroblasts and L87 MSCs. On the other hand, cells used in the present study either exhibited abundant expression of c-Myc and Klf4 that are routinely used for reprogramming strategies or these 2 factors were easily induced by hypoxia alone. Recently, Nemajerova and co-authors suggested that there is a partial functional redundancy between Sox2 and Klf4 (Nemajerova et al., 2012). Therefore, Sox2 expression may not be a prerequisite for induction of successful reprogramming and delayed induction of Sox2 might be successful using additional non-viral reprogramming techniques.

4.3.5. Small Molecules Facilitate Non-Viral Reprogramming

The present study demonstrated that sets of epigenetic modulators, signal transduction inhibitors, and kinase inhibitors were suitable to preserve AP-positive pre-iPS colonies after delivery of miR-302a-d & 372 or STEMcircles™. Clonal growth and proper proliferation are prerequisites for reprogramming representing fundamental properties of pluripotent stem cells. However, fully reprogrammed iPS cells were not generated because proliferation stopped within the first 10 passages. Colonies of pre-iPS cells are therefore categorized as partially reprogrammed bearing only a subset of pluripotency-associated properties.

The present study revealed that L87 and BJ-5ta cells were much more sensitive to epigenetic modulators after transfection procedures (**FIG. 27 B**). This observation highlights again the massive impact even of optimized delivery protocols. There is no evidence that hypoxia affected treatment with epigenetic modulators. Moreover, hypoxia possibly contributed to cell viability. Interestingly, senescent cells with flat cell morphology were rarely detected but cell debris was observed. This observation can be explained by another study using a p53 deficient cell culture model, which demonstrated that hypoxia suppresses conversion from cell cycle arrest to cellular senescence (Leontieva et al., 2012).

Small molecules are organic compounds regulating a variety of physiological processes with high specificity. These are termed as small molecules because of their low molecular weight. The absolute molecular weight of small molecules is differently described ranging from 500 to 900 Da (Leeson and Springthorpe, 2007; Skaper et al., 2009). However, these molecules rapidly diffuse across the cell membrane due to their small size. Recently published studies used a several cell types and a number of small molecule concentrations depending on the used protocol (Lyssiotis et al., 2011; Nie et al.,

2012; Walia et al., 2012). Analysis of small molecules was extensively applied within the present study to promote a strong initial reprogramming impulse given by STEMcircles™ or miR-302a-d & 372. The application of epigenetic modulators (RG108, VPA, SBT, BIX), signal transduction inhibitors (PFT, BayK, BIO), and kinase inhibitors (THIA, SB, PD) was investigated (**TAB. 1**). The use of different molecule sets aimed at the alteration of different signaling pathways, which regulate epigenetic patterning of DNA and their histones, control apoptosis, and induce or prevent differentiation. However, combining of small molecules is challenging because of undesired events leading to cell toxicity.

4.3.5.1. Epigenetic Modulators Enhance Colony Formation

Epigenetic modulators predominantly regulate epigenetic patterning in order to enable or improve reprogramming (Huangfu et al., 2008a). Further, VPA, RG, BIX, and SBT have been applied by others instead of certain reprogramming factors during viral reprogramming but with lowered efficiencies (Huangfu et al., 2008b; Shi et al., 2008).

Morphology changed and accumulation of treated cells within cell aggregates was observed demonstrating a strong impact of single treatment with VPA, RG, BIX, and SBT (**APP. 9**). It remains unclear whether this atypical morphology of L87 and BJ-5ta cells contributes or affects induction of reprogramming. Analyzing effects and side effects of small molecules is challenging because these molecules are most often identified by chemical screens and their function is only subsequently described (Federation et al., 2013). VPA and SBT are currently used as drugs and RG and BIX are analyzed by clinical trials for example for the treatment of psychiatric disorders (Abel and Zukin, 2008).

VPA treatment using a broad range of different concentrations (2 μ M-2 mM) was shown in the present study to be suitable for treatment of L87 MSCs and BJ-5ta fibroblasts (**APP. 9**). This observation is due to several studies using a variety of different concentration ranging from 0.5-1 mM (Huangfu et al., 2008a; Huangfu et al., 2008b), 0.5-10 mM (Cipro et al., 2012), 0.2-4 mM (Teng et al., 2010), or using 1 mM VPA (Tang et al., 2004). Further, VPA enables viral reprogramming using only Oct4 and Sox2 (Huangfu et al., 2008b). Detailed studies by others in P19 mouse embryonic carcinoma cells recently described that VPA up regulates Oct4 expression to enhance reprogramming (Teng et al., 2010). Accordingly, VPA was shown to sustain self-renewal of MEFs under hypoxic conditions (Lee and Kim, 2012). Importantly, VPA also induces differentiation and apoptosis in cancer cells (Tang et al., 2004). Therefore, VPA treatment under hypoxic conditions was analyzed by others answering the question whether VPA-induced apoptosis of cancer cells was counteracted by hypoxic conditions in solid tumors (Cipro et al., 2012). Cipro and co-authors reported that hypoxia elevated apoptosis during VPA treatment. They explained their observation by the fact that hypoxia via HIF1a is capable to stabilize p53 (An et al., 1998), which is a key regulator inducing apoptosis. In contrast, hypoxia counteracts apoptosis and drives proliferation in stem cells and cancer cells as described earlier. However, more detailed analysis of VPA is required to understand its bivalent behavior in different cell culture models.

RG was applied within the present study using concentration between 2.0-20.0 μ M without adverse effects (**APP. 9**). Studies by others applied 0.04 μ M (Shi et al., 2008), 3 μ M (Szablowska-Gadomska et al., 2012), 10 μ M (Brueckner et al., 2005), 100 μ M (Stresemann et al., 2006), and up to 500 μ M RG (Pasha et al., 2011). Further, RG and BIX together enable viral iPS cell generation only by Oct4 and Klf4 (Shi et al., 2008). Interestingly, high RG using 500 μ M was sufficient to convert skeletal muscle

cell into iPS cells without viral delivery of transgenes (Pasha et al., 2011). Pasha and co-workers demonstrate that cell type specific optimization can result in successful reprogramming.

BIX treatment in the present study was analyzed using a broad range of concentrations (0.5-2.0 μ M) without affecting cell viability (APP. 9). Other studies reported the use of 1 μ M BIX (Shi et al., 2008; Medvedev et al., 2011), 1.25 μ M (Culmes et al., 2013), and 5 μ M BIX (Yang et al., 2012). Further, enhanced reprogramming by BIX was previously reported by others (Shi et al., 2008; Medvedev et al., 2011). Treatment of bone marrow-derived MSCs with BIX induced cardiac properties suggesting that BIX somehow reprogrammed MSCs (Mezentseva et al., 2013). BIX is a G9a HMT inhibitor. G9a is responsible for H3K9me1/2 required for euchromatin (Chang et al., 2009). Repression of G9a might prevent gene expression of differentiation-associated genes. However, BIX-mediated G9a repression also induces contrary effects. Adipose-derived MSCs more efficiently differentiate into endothelial cells in the presence of BIX (Culmes et al., 2013). Inhibition of G9a using BIX blocks proliferation of ovine smooth muscle cells (Yang et al., 2012). Detailed analysis on molecular mechanisms behind G9a inhibition by BIX would help to understand contrary observations.

SBT was applied using 0.3-1.0 mM without negative effects on treated cells in the present study (APP. 9). This observation contributes to reports suggesting the use of 0.1-10.0 mM (Biermann et al., 2011), 2.0-5.0 mM (Kato et al., 2011), and 2.5-5.0 mM SBT (Winbanks et al., 2013). Sendai virus-mediated reprogramming is improved by SBT (Trokovic et al., 2012). This observation can be explained by SBT-mediated repression of apoptosis. SBT preserves acetylation of H3K9. Accordingly, it is reasonable that up regulated genes are somehow involved in the regulation of proliferation and apoptosis. SBT does delay spontaneous cell death of primary rat retinal ganglion cells (Biermann et al., 2011). This neuroprotective effect was confirmed by others demonstrating enhanced proliferation through upregulation of brain-derived neurotrophic factors (Bdnf) in rats (Kim et al., 2009b). SBT can regulate a variety of physiological processes such as proliferation of muscle cells and apoptosis of immune cells (Berni et al., 2012). Interestingly, another study by Kato and co-workers demonstrated in endometrial cancer cells that SBT is also suitable to suppress proliferation (Kato et al., 2011). One can conclude that the effect of SBT varies between different cell types.

Combined treatment with 2 or more small molecules (e. g. RG and VPA) was challenging (**FIG. 27, APP. 9**). Interestingly, the use of small molecule sets is poorly described. Combined treatment provokes unknown side effects. However, application of a set molecules is reasonable. The use of low amounts of both 1.0 mM BIX and 0.04 μ M RG together was recently described in MEFs (Shi et al., 2008). Accordingly, sets applied in the present study contained low amounts of small molecules and adverse effects were avoided using less than 0.5 mM VPA, 0.5 μ M RG, 1.0 μ M BIX, and 0.3 mM SBT. However, it remains to be clarified whether every small molecule has a significant biological impact because fully reprogrammed iPS cells were not established.

Epigenetic modulators were combined with miR-302a-d & 372 delivery. Importantly, colonies with moderate AP-staining were obtained from L87 cells (**FIG. 27**). Cells underwent cell death within the first 10 passages suggesting that these cells were not fully reprogrammed. It is important to highlight that treatment by different sets of epigenetic modulators was intensively studied. Variation of treatment strategies did not improve the induction of ES cell-like colonies. This observation is most probably due to the less specific mode of action as described earlier. Targeting DNA or histone modifying enzymes regulates several epigenetic patterns. Not all epigenetic modification promote reprogramming. VPA is

mood-stabilizing and pain-relieving drug with teratogenic and neuropsychiatric side effects upon in utero exposure (Jacob et al., 2014). Teratogenic side effects in vivo might contribute to VPA's ability to enhance of reprogramming. Jacob and co-authors used a zebrafish model to show that VPA is responsible for indirect silencing of Achaete-scute family basic helix-loop-helix transcription factor 1 (Ascl1), a gene regulating neuronal differentiation (Jacob et al., 2014). However, VPA even prevents proliferation of pericytes involved in wound healing (Karen et al., 2011), inhibits angiogenesis suitable for anticancer therapy (Michaelis et al., 2004), and affects stellate cell activation in liver fibrosis (Mannaerts et al., 2010). Accordingly, VPA-mediated alteration of epigenetic patterning regulates several off target signaling pathways when reprogramming is desired. The same most probably is true for RG, BIX, and SBT because these molecules also change epigenetic patterning of the whole genome. Accordingly, one can conclude that combined treatment with VPA, RG, BIX, and SBT led to accumulation of side effects counteracting reprogramming. The enhancing effect on reprogramming of epigenetic modulators is predominantly described using single treatment approaches.

4.3.5.2. Signal Transduction Inhibitors Enhance Colony Formation

In contrast to epigenetic modulators, combined use of PFT, BayK, and BIO did not affect cell viability (**FIG 28 A**) suggesting that these small molecules bear a lower potential of toxicity. Modifying of signaling pathways indeed is less toxic because DNA and histones are not affected. The small molecules PFT, BayK, and BIO were shown to regulate pluripotency-related signaling pathways but whether they support non-viral reprogramming had to be clarified.

Application of PFT in L87 MSCs is supported by another study in bone marrow derived MSCs, which demonstrates preserved proliferation and reduced apoptosis after PFT treatment (Yan et al., 2011). Recent studies also revealed that the p53 signaling pathway counteracts pluripotency (Lin et al., 2005) and reprogramming (Zhao et al., 2008; Kawamura et al., 2009; Utikal et al., 2009) as well. Lin and co-workers reported that Nanog is repressed by p53 (Lin et al., 2005). Kawamura and co-authors enhanced viral reprogramming in the absence of c-Myc by treatment with p53 siRNA. Treatment of L87 and BJ-5ta cells with 10.0 μ M PFT is comparable to other studies using 10.0-20.0 μ M (Abdelalim and Tooyama, 2012), 20.0 μ M (Yan et al., 2011), and 20.0 μ M PFT (Deng et al., 2012). Importantly, PFT was recently applied in buffalo fetal fibroblasts to increase efficiency of iPS cell generation (Deng et al., 2012). Nonetheless, in the present study human pre-iPS colonies underwent cell death within the first 10 passages. One can implicate that PFT is not suitable for human iPS cell generation. Accordingly, PFT was demonstrated to reduce the proliferation capacity of human ES cells (Abdelalim and Tooyama, 2012) implicating a bivalent impact even on reprogramming. It is important to remark that cell death is mediated by a variety of also p53-independent signaling pathways. However, there is a need to proof whether PFT is a suitable tool for p53 repression.

BayK is a rampant tool to analyze second messenger signaling by calcium in neural cells (Rushton et al., 2013). Calcium ions directly for example via protein kinase C or indirectly through calmodulin regulate gene expression, cell division, and cell signaling. Studies in mice using P19 embryonic carcinoma cells and adult MSCs demonstrated that especially L-type calcium channels are involved in neurogenesis (Resende et al., 2010). Resende and co-workers further showed that the L-type agonist BayK increases neuronal differentiation. Another approach by Wamhoff and co-workers revealed that L-type calcium channels also stimulate differentiation smooth muscle cells (Wamhoff et al., 2004). One

complete different approach used BayK and BIX to enable reprogramming only by Oct4 and Sox2 (Shi et al., 2008). According to Shi and co-authors, 2.0 μM BayK were applied in the present study, which is comparable to differentiation studies using 1.0 μM (Rushton et al., 2013), 5.0 μM (Wamhoff et al., 2004) and 10.0 μM (Resende et al., 2010). Currently, there is no model to describe how BayK promotes reprogramming. Analysis of BayK target genes is required to optimize treatment procedures.

BIO has not been described to promote viral reprogramming strategies, but GSK3 inhibition is essential for maintenance of pluripotency as described earlier. However, BIO promotes reprogramming mediated by cell fusion (Lluis et al., 2008). Proliferation is also stimulated by BIO demonstrated in immortalized pancreatic MSCs (Cao et al., 2012). The concentrations used by others such as 0.1-1.0 μM (Holowacz et al., 2013), 0.5-2.0 μM (Lian et al., 2012), and 3.0-10.0 μM (Kirby et al., 2012) support the use of 2.0 μM BIO in the present study. Interestingly, mouse adult neural stem cells even require GSK3 inhibition but GSK3 downregulation is different between different sources of neural stem cells (Holowacz et al., 2013). This observation suggests that it is important how GSK3 inhibition is achieved to sustain a certain reprogrammed stem cell. Further, GSK3 inhibition by BIO in human ES cell stem cultures stimulates induction of cardiac differentiation (Lian et al., 2012) suggesting that BIO treatment does not only interact with signaling pathways contributing to stem cell preservation. Interestingly, a competitive study in mouse ES cells demonstrated different behavior of 3 different GSK3 inhibitors BIO, CHIR99021, and SB216763 (Kirby et al., 2012). Kirby and co-workers reported that not BIO but SB216763 could replace LIF supplementation. Accordingly, the use of other signal transduction inhibitors including GSK3 needs to be considered.

It is important to underscore that treatment with miR-302a-d & 372 combined with PFT, BayK, and BIO was capable to induce AP-positive colonies within 30 days (**FIG. 28 C-E**). Interestingly, in contrast to the majority of the present data, AP-positive colonies were obtained from BJ-5ta fibroblasts and not from L87 MSCs (**FIG. 28 E**). This observation contributes to other studies, which reported reprogramming of BJ-5ta fibroblasts (Warren et al., 2010). However, picked colonies did not preserve clonal growth hindering passaging of these partially reprogrammed cells. According to the given literature, one can debate about the set of signal transduction inhibitors. Nonetheless, a strong impact on the generation of AP-positive colonies was demonstrated making treatment with signal transduction inhibitors a powerful tool within a non-viral reprogramming strategy.

4.3.5.3. Kinase Inhibitors Enhance Colony Formation

The present study showed that STEMcirclesTM-induced AP-positive colonies can be maintained after treatment with THIA, SB and PD kinase inhibitors but cells underwent cell death within the first 10 passages (**FIG. 29**). Therefore, these pre-iPS colonies were not fully reprogrammed. In contrast to that, another study by Lin and co-workers reported successful reprogramming of human fibroblasts using retroviruses and treatment with THIA, SB, and PD (Lin et al., 2009). However, successful reprogramming operated by Lin and co-workers most probably dependent on the use of viral vectors. Nagy and co-authors reported non-viral Piggy Bac-induced reprogramming of equine fibroblasts via treatment with 5 small molecules including THIA, SB, and PD (Nagy et al., 2011). Importantly, Nagy and co-workers combined treatment with 2 signaling transduction inhibitors namely, GSK3 inhibitor CHIR99021 and TGF β inhibitor A83-01. One can conclude that treatment with additional small molecules enabled successful iPS cell generation by Nagy and colleagues.

The present study applied 2 μM THIA, which is commonly used to improve survival of human ES and iPS cells after passaging by targeting the ROCK (Sebastiano et al., 2011). Interestingly, there is evidence that THIA is less important for induction of reprogramming. Merkl and colleagues reported that rat iPS cells can be obtained using a non-viral plasmid carrying OSKM, but THIA did not enhance the efficiency (Merkl et al., 2013). Accordingly, another study used SB, PD, and SBT instead of THIA promote reprogramming of human fibroblasts by a viral expression vector (Zhang et al., 2011). Reprogramming studies by others applied comparable amounts of 0.5-2.0 μM THIA (Lin et al., 2009; Zhang et al., 2011; Merkl et al., 2013).

PD treatment in the present study was carried out using 0.5 μM PD according to concentrations used by others. Fussner and colleagues applied 0.5 μM PD in mouse partial reprogrammed cells (Fussner et al., 2011). Another protocol was published using 1 μM PD for viral ONSL induction (Si-Tayeb et al., 2010).

Treatment with 2.0 μM SB in the present study was applied according to studies by Nagy and Lin as described earlier. Importantly, Ichida and co-workers applied 25 μM SB to replace Sox2 but they also described that lower concentrations do promote reprogramming (Ichida et al., 2009). Interestingly, SB is also a potent tool to enhance neural induction in human ES cells when culture conditions contribute to neural lineages (Denham et al., 2012), which might contribute to the idea of combined treatment with a set of kinase inhibitors or other small molecules.

Together, improved reprogramming by kinase inhibitors is described in the present study and by others using different reprogramming procedures. Furthermore, a strong impact on the generation of AP-positive colonies mediated by small molecules was described making them a powerful tool within a non-viral reprogramming strategy.

4.3.5.4. *STEMcirclesTM and Small Molecules Preserve Colonies*

In order to establish a non-viral reprogramming strategy, reprogramming tools described within the present study were combined. Preservation of ONSL reprogramming factors was induced and preserved only by episomal vectors and small molecules (**FIG. 32 B**). However, even combining of reprogramming techniques did not reveal a non-viral reprogramming strategy for the generation of permanent iPS cell lines. Nevertheless, based on the present study, a general strategy for the use of non-viral methods to reprogram human somatic cells was established (**FIG. 43**). The endogenous expression of ONSL or OSKM is a prerequisite for reprogramming as describe earlier. Prominent endogenous induction is required and most often achieved by delivery of vectors, which ectopically express the reprogramming factors. *STEMcirclesTM* induced endogenous ONSL in L87 MSCs and BJ-5ta fibroblasts intensively described within this study. Accordingly, the present study recommends the use of episomal vectors to induce a strong initial impulse towards reprogramming.

In the present study, the repeated treatment with *STEMcirclesTM* did not lead to additive effects (**FIG. 31**). Contrary, repeated transfection of *STEMcirclesTM* for successful reprogramming using different somatic donors was recently described by other studies (Jia et al., 2010; Narsinh et al., 2011). Even sorting of *STEMcirclesTM*-positive cells for subsequent treatment was not successful (**FIG. 31 C-E**). These data suggest that the impact of episomal vectors on reprogramming is not sufficient to fully reprogram L87 and BJ-5ta cells. Currently, there is no report providing successful *STEMcirclesTM*-based reprogramming of donors similar to those used in the present study. This contributes to the hypothesis that subsequent treatment with different non-viral methods is required.

The co-transfection of STEMcirclesTM and miR-302a-d & 372 did not lead to additive effects on the induction of ONSL (**FIG. 30 C**). Moreover, the transfection efficiency of STEMcirclesTM was affected (**FIG. 30 A/B**). These results provide the hypothesis that subsequent application of reprogramming methods is more reasonable. According to this hypothesis, another study successfully applied expression of the miR-302 cluster after transposon-based OSKM induction (Grabundzija et al., 2013). Nevertheless, the induction of endogenous miR-302a-d & 372 is a prerequisite for reprogramming. Zhang and co-workers demonstrated that reprogramming is hindered by knockdown of the miR-302-367 cluster expression using transcription activator-like effectors (TALE) or TALE nucleases (Zhang et al., 2013c). Accordingly, the present study verified that endogenous miR-302a-d & 372 provides a strong initial impulse towards reprogramming (**FIG. 43**). The transfection of miR-302a-d & 372 induced promising ES cell-like properties in L87 MSCs and BJ-5ta fibroblasts, but treatment less efficiently induced reprogramming factors described in the present study. A lower impact on reprogramming factors can be explained by miR's indirect mode of action. Together, human ES cell-specific miRs are a potent tool for the generation of non-viral iPS cells, but more suitable combining with other non-viral methods needs to be established.

Enhancement sustains clonal growth of pre-iPS cells, which express pluripotency-associated factors including reprogramming factors. In the present study, treatment with kinase inhibitors and signaling transduction inhibitors enabled growth of pre-iPS, but treatment without small molecules did neither preserve Sox2 nor Oct4A expression (**FIG. 32 B**). Accordingly, another study applied MEK and GSK3 inhibition in mouse blastocysts to elevate the amount of Oct4-expressing cells (Van der Jeught et al., 2013). Therefore, application of small molecules is recommended to enhance clonal growth and gene expression of pluripotency factors (**FIG. 43**).

It is important to note that maintenance of pre-iPS cells is challenging because pre-iPS cultures contain partially and fully reprogrammed clones. For maintenance of fully reprogrammed cells, human ES cell-specific culture conditions are suitable to sustain the proliferation capacity, the expression of pluripotency factors, and the enzymatic activity of AP (**FIG. 43**). The present study successfully applied MEF-conditioned medium and matrices in order to prevent MEF-dependent culture conditions (**FIG. 32, APP. 15**). Recently, another study even applied similar culture conditions for the generations

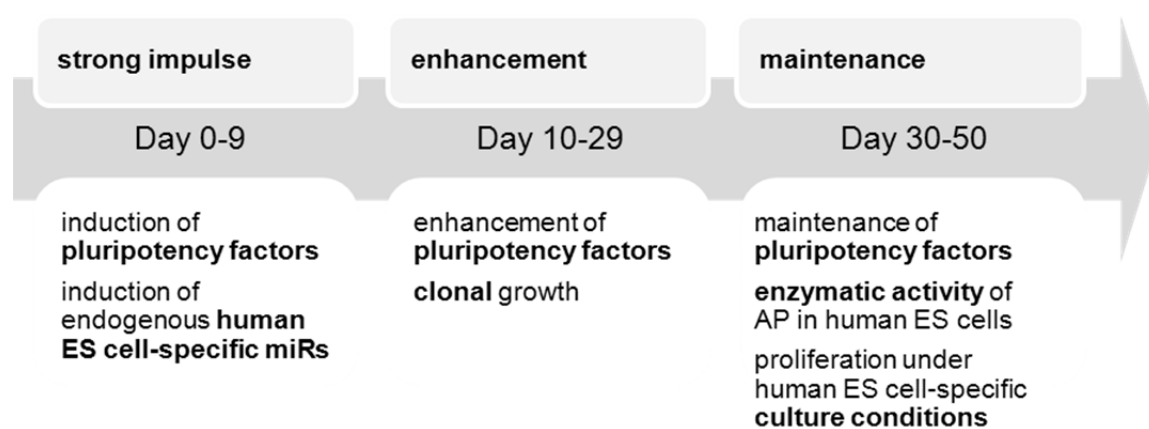


FIGURE 43: Strategy for the use of non-viral methods to reprogram human somatic cells. Reprogramming of somatic cells is suggested to require three steps to obtain fully reprogrammed cells. Once given in a first step of reprogramming, a strong initial impulse needs to be enhanced in a second step. At least maintenance of pre-iPS clones is required in a third step. The most important features of cells during reprogramming are highlighted below the time line.

of iPS cells (Grabundzija et al., 2013). It is important to note that the establishment of feeder-free chemically defined culture conditions suitable to preserve pluripotency. The present study used IMR90 iPS cells cultured on MatrigelTM and mTeSR1TM. The use of other chemically defined media such as Essential 8TM and other matrices such as vitronectin was recently described (Chen et al., 2011). However, long-term culture of human ES and iPS cells is frequently done using irradiated or mitotically inactivated MEFs even in this study.

In the present study, hypoxia was combined with a few non-viral methods without beneficial effects on reprogramming. There are different explanations for this observation. On the one hand hypoxia might have elevated stress-related failed behavior. One can suggest that application of hypoxia might be more suitable during enhancement or maintenance of reprogramming. On the other hand, daily change of media was not applied under hypoxic conditions limiting the effect of hypoxia.

Together, the production of a permanent iPS cell line was hindered by two crucial road blocks. After isolation of pre-iPS cell clones, (i) proliferation was lowered and (ii) cells underwent cell death within 10 passages.

4.3.5.5. Affords to overcome partial reprogramming

This study presented a reprogramming strategy for the use of non-viral methods but only partial reprogramming was achieved. Non-viral reprogramming methods generate a lower and more time restricted impact on somatic cells than viral vectors for the expression of ONSL or OSKM. Signaling transduction and kinase inhibitors appear to be very potent reprogramming tools because conversion of partial reprogrammed cells into fully reprogrammed cells was described by MEK and GSK3 inhibition in mice (Fussner et al., 2011). It is important to note that current approaches aim at the improvement of recently described non-viral or viral but not integrative approaches even by small molecule treatment. The use of Sendai virus was combined with kinase inhibitors virus (Kahler et al., 2013). Therefore, the order of reprogramming methods or the way of treatment rather than the choice methods most probably is responsible for failed full reprogramming.

In accordance with the literature, further optimization of small molecule concentrations might reveal cell type-tailored treatment procedures more suitable for non-viral reprogramming. It is important to highlight that there are several small molecules suitable and not suitable for iPS cell generation (Federation et al., 2013). For example, Azacytidine is a DNMT inhibitor suitable to increase viral iPS cell generation by OSKM (Mikkelsen et al., 2008). However, Azacytidine incorporates into the DNA because it is a chemical analogue of the cytidine base. Low levels induce hypomethylation of the DNA because methylation of the Azacytidine is not possible. Importantly high levels prevent DNA synthesis. According to the described molecular mechanism, treatment using Azacytidine was not mentioned in the present study. Application of iPS cells for disease modeling requires unaffected patient DNA.

There are supplements, which might be suitable for reprogramming of L87 and BJ-5ta cells. For example, treatment with vitamin C might be suitable for prevention of apoptosis during reprogramming (Esteban et al., 2010; Blaschke et al., 2013). Treatment using mitogenic supplements such as N2 and B27 supplements were suitable for non-viral reprogramming of rat MSCs (Merkl et al., 2013). Another study combined GSK3 inhibition with a TGF β inhibitor A83-01 was (Nagy et al., 2011). Accordingly, application of modified small molecule sets should be analyzed in further studies.

It is important to note that there is no clear approach to overcome partial reprogramming. Nevertheless, further affords might include the modulation of minor signaling pathways not directly

linked to reprogramming. It was reported that low pH can trigger the non-viral induction of iPS cells obtained from a distinct mouse lymphoblast population expressing protein tyrosine phosphatase, receptor type C (Ptpcr; also known as CD45) (Obokata et al., 2014). Another example, the tricarboxylic acid cycle-associated genes are down regulated during reprogramming suggesting a crucial role of mitochondria and oxidative stress (Ohmine et al., 2012). Besides p53-mediated signaling, other pathways regulating senescence and apoptosis such as retinoblastoma protein regulating cyclin-dependent kinases (Ohmine et al., 2012) might be a suitable target for non-viral reprogramming. Another afford relays on the fact that old murine somatic donors are much harder to reprogramming compared to young donors (Li et al., 2009). Elucidating of molecular mechanisms might help to remove road blocks of reprogramming. Notably, media used for different studies vary between their contents making them more or less suitable for a certain cell type. However, the cause of compatibility is often poorly understood.

Partial reprogramming is not sufficient when a pluripotent stem cell model is required as it was aimed in the present study. However, there is the possibility to immediately apply partial iPS cells for differentiation studies without a stable state of pluripotency. This hypothesis is verified by Zou and co-workers reporting direct conversion of fibroblasts into neuronal progenitors using reprogramming factors and neuronal lineage factors as well (Zou et al., 2014). Another approach demonstrated direct conversion of fibroblasts into hepatic-like cells by the forced expression of liver-associated transcription factors (Ji et al., 2013). Accordingly, even partial non-viral reprogrammed iPS cells bear a promising potential.

4.4. Pancreatic Differentiation of iPS Cells

The iPS cell technology generates disease-specific stem cells suitable for disease-specific differentiation. Most importantly, the iPS cell technology is the only approach capable to generate pluripotent stem cells from adult and therefore fully characterized patients. However, the growing number of studies using iPS cells is due to a growing number of differences between iPS and ES cells. Accordingly, ES cells represent a gold standard of pluripotency implicating that ES cells are a more reliable tool for differentiation studies mimicking the *in vivo* development. It is important to notice that more than 60 disease-specific ES cell lines have been established for genetic disorders such as Duchenne and Becker muscular dystrophy, fragile-X syndrome, Huntington disease, and T1DM (Verlinsky et al., 2005; Aran et al., 2012; Jang et al., 2012). Preimplantation genetic diagnosis was used for screening of genetic disorders and subsequent selection of diseased embryos for the generation of disease-specific ES cell lines. In Germany, the generation of ES cell lines after preimplantation genetic diagnosis is prohibited by law because of numerous unsolved ethical and legal issues. These embryos are protected by the Embryo Protection Act (ESchG) and the Preimplantation Diagnostic Act (PräimpG). Notably, the number of registered ES cell lines in the EU (www.hescereg.eu) and the number of ES cell lines worldwide is continuously growing (Aran et al., 2012). ES cell lines from T2DM patients have not been described but one can predict that currently unknown or poorly described T2DM-associated DNA variations will be found in recently established ES cell lines. However, mouse ES cells are frequently used instead of human ES cells to study general aspects of the mammalian development. Moreover, mouse ES cells represent a potent tool to verify general applicability of the present culture models. Caution must be exercised in extrapolation of data obtained from mouse ES cells because there are differences between mouse and human ES cells and

organogenesis of the pancreas (Ginis et al., 2004; Bonal and Herrera, 2008). However, general aspects of DE progenitor formation and pancreatic induction are most similar in between the mouse and the human system (Bonal and Herrera, 2008). Together, the combined use of iPS cells and ES cells remains to be the most reliable approach to study pancreatic differentiation in the context of diabetes. Nevertheless, pancreatic differentiation of iPS and ES cells needs to be improved by more suitable 3D culture conditions. Therefore, it is reasonable that the present study applied IMR90 iPS and H9 ES cells to study organotypic pancreatic differentiation.

4.4.1. Pancreatic Differentiation on 3D Matrices

The raw material for the production of 3D biological matrices had to be (i) easy accessible, (ii) easy to produce, and (iii) suitable for pancreatic differentiation. Notably, porcine jejunum is easy accessible. The evaluation of processing and suitability of matrices is however more challenging. The present study verified that 3D biological matrices can be easily obtained from porcine jejunum (**FIG. 33**). Porcine jejunum was already applied for the generation of decellularized matrices within a biological vascularised scaffold (Schanz et al., 2010). This biological scaffold developed by Schanz and co-workers is suitable for human organotypic models of liver, intestine, trachea, and skin. Importantly, the applicability of porcine jejunum-derived matrices for pancreatic differentiation was first analyzed in the present study.

4.4.1.1. Advantages of 3D Biological Matrices

To understand the importance of the ECM provided by biological matrices, it is necessary to highlight how ECM molecules are involved in embryogenesis. ECM matrix proteins include glycosaminoglycans and proteoglycans, glycoproteins, and collagens. These molecules are important physiological regulators guiding proliferation and differentiation of stem cells during embryogenesis and growth. Laminin appears early at the 2-cell stage in mice (Goh et al., 2013b). Fibronectin and collagen IV occurs during formation of the ICM in murine blastocysts (Goh et al., 2013b). Fibronectin and collagen IV knock outs are embryonic lethal (Rozario and DeSimone, 2010). ECM molecules are adhesive substrates, which track migratory cells such as pancreatic progenitors. Structures provided by the ECM are needed to build tissue boundaries, to preserve plasticity of the developing and adult organ, to allow degradation of cells. These essential functions are required in the pancreas and in every other organ of the human body. The ECM controls tissue-specific interactions of growth factors and receptors. Pancreatic islets are embedded in a vascular niche providing ECM proteins secreted by ECs. Laminin binds to alpha6beta1-integrin on beta cells and collagen IV binds to alpha1beta1-integrin, both necessary for pancreatic development (Nikolova et al., 2007). Alpha1- and beta1-integrin knock outs are embryonic lethal (Rozario and DeSimone, 2010). The ECM is capable to regulate growth factor release and organizes morphogen gradients. Together, these functions described above are necessary for the pancreatic development *in vivo* and *in vitro*.

It is important to note that SEM visualized the structure of decellularized porcine jejunum revealing a tight framework of ECM compounds (**FIG. 34 A**). Such a framework allows spontaneous immigration and accumulation of pancreatic progenitors to form 3D cell agglomerates. Similar to the present study, high resolution microscopic techniques were also applied by others to study the structure of other biological matrices. For example, decellularized lung matrices produced by Jensen and co-workers showed a tight framework of ECM compounds almost similar to the present data (Jensen et al., 2012).

The present study verified immigration of mouse ES cells into 3D matrices and agglomeration of cells in creases and grooves (**FIG. 34 E/F**). Immigrating cells are a prerequisite for 3D organotypic differentiation. There is evidence that 3D matrices are suitable to guide self-organizing assembly of organotypic equivalents (Woodford and Zandstra, 2012). Accordingly, 3D matrices should principally allow immigration and agglomeration of seeded cells to mimic a 3D culture environment.

The present work described culture of mouse ES cells in 3D matrices without induction of differentiation (**FIG. 34 B**). This observation is verified by another study applied decellularized matrices instead of MEFs for the stable propagation of human ES cells (Abraham et al., 2010). The present study also demonstrated that 3D matrices can be applied for the differentiation into all 3 germ layers (**FIG. 34 C/D**). Interestingly, biological decellularized matrices obtained from murine lung (Jensen et al., 2012) and kidney (Ross et al., 2009) have been shown to support proliferation and differentiation of mouse ES cells as well. The protocol of Jensen and co-authors for lung decellularization was slightly different using sodium deoxycholate but in addition to Triton X-100, sodium chloride, and DNA removal by DNase within a 24 h protocol. Ross and colleagues applied a protocol almost similar to Ross and colleagues. One can conclude that the treatment with detergents somehow modifies the ECM proteins. However, there is no evidence that a certain decelluraization protocol is more or less suitable for culture or differentiation of a certain cell type.

The differentiation of pancreatic progenitors in 3D porcine matrices raises questions whether these matrices can be applied as xenotransplants. Importantly, the clinical application of porcine matrices is challenging because of concerns about the immunogenicity. Currently, several studies focus on the preparation of immunogen-reduced matrices such as from porcine liver (Park et al., 2013). General applicability for transplantation is needed to be analyzed in animal models. One can predict that progenitors will be capable to mature inside the animal because the *in vivo* maturation of human pancreatic progenitors has been described in mice (Kroon et al., 2008; Rezanian et al., 2012).

One alternative to the use of decellularized matrices is the use of 3D biomaterials, which have demonstrated promising effects on the culture and the differentiation of pluripotent stem cells. The application of polyethylene glycol hydrogels, synthetic polymers, and natural polymers has been described in the context of culture or differentiation of pancreatic derivatives. Interestingly, 3D culture conditions allow 3D differentiation of stem cells and the preservation of primary pancreatic cells. For example, Hydrogels were applied to preserve pancreatic progenitors obtained from E15 rat embryos (Mason et al., 2009). The presence of collagen I in hydrogels promotes the differentiation of pancreatic precursor cells into glucose-responsive beta-like cells (Mason et al., 2009). Natural polymer scaffolds made of dextran and gelatin were applied for the differentiation of adipose tissue-derived stem MSCs into islet-like cells (Aloysious and Nair, 2013). Polymer microbeads modified with pancreas-specific ECM compounds were successfully applied to enhance stability and insulin production of rat beta cells (Li et al., 2013). Together, several promising 3D biomaterials have been described but mimicking the complex architecture of natural 3D structures and the sophisticated composition of organ-associated ECM is challenging. Further studies might investigate the application of 3D biomaterials and their ability to replace biological decellularized scaffolds.

4.4.1.2. 3D Matrices Allow Pancreatic Differentiation

2D and 3D mouse pancreatic differentiation described in the present study relied on characterization of DE pancreatic progenitors. Bra mRNA expression was detected in the present

study (**FIG. 34 D, 35 B/C**) representing a prerequisite for the development of mesoderm and endoderm (Kubo et al., 2004; Baetge, 2008). DE progenitors were identified by Sox17, Foxa2, and Cxcr4 mRNA expression (**FIG. 34 C/D, 35 B/C, 36 A/B**), which contributes to the human *in vivo* development (Yasunaga et al., 2005). Successful DE differentiation was verified by IF analysis of CGR8-S17 cells, but Sox17 expression was dedicated to a minor subset of spontaneously differentiated cells (**FIG. 34 C**). Activin A strongly elevated the induction of DE progenitors monitored by Sox17-DSred expression (data not shown). According to this observation flow cytometry of CGR8-S17 revealed about 20% DE differentiated cells (Schroeder et al., 2012). Importantly, gene expression of Foxa2 and Cxcr4 was not detected during spontaneous differentiation (**FIG. 34 D**). Sox17 and Foxa2 most often characterize DE (Borowiak et al., 2009; Filby et al., 2011). Notably, Sox17, Foxa2, and Cxcr4 are also each expressed in other embryonic tissues. For example, Sox17 is also expressed in extraembryonic tissues (Takayama et al., 2011). Therefore, extraembryonic formation was analyzed in the present study using the extraembryonic markers Sox7 and Sdf1 (**FIG. 34 D, 35 B/C, 36 A**), which contributes to other studies (Seguin et al., 2008; Schroeder et al., 2012). Cxcr4 is a DE marker gene and its expression is present in proliferating pancreatic duct cells and other developmental lineages of blood derivatives, ECs, and smooth muscle cells (Katsumoto and Kume, 2013). The expression of Foxa2 is closely related to endoderm-derived organs (Friedman and Kaestner, 2006). There is no exclusive DE marker gene. Accordingly, DE can be analyzed by additional DE-associated marker genes such as Foxa1, goosoid (Gsc), gata binding protein 4 (Gata4), and hepatocyte nuclear factor 4a (Hnf4a) to harden the received expression data (Borowiak et al., 2009; Wang et al., 2012).

The present work verified that directed 2D pancreatic differentiation of mouse ES cells generated Pdx1-expressing pancreatic progenitors via EB formation (**FIG. 35 B**). In contrast, spontaneous differentiation generated progenitors of all 3 germ layers, but Pdx1-expressing cells were not detected. Directed pancreatic differentiation generated cells expressing, Pdx1, Pax6, but not Ngn3 and Amy2 on the mRNA level (**FIG. 35 B**). Pdx1 is a key transcription factor during pancreatic differentiation as mentioned earlier implicating the presence of pancreatic progenitors. Especially, Pdx1 is expressed in beta cells to support the expression of Ins and solute carrier family 2 member 2 (Slc2a2; also known as Glut2) (Serup et al., 1995). For the development of pancreatic alpha cells Pax6 is required (Ashery-Padan et al., 2004). The development of beta, delta, PP, and epsilon cells depends on the expression of Pax4 and Pax6 (Collombat et al., 2003). One can suggest that in the present work absent Ngn3 was induced at earlier stages of the protocol because Pdx1 and Pax6 were already expressed. Ngn3 is a key regulator of pancreatic endocrine cells (Apelqvist et al., 1999). Ngn3 knockout mice fail to develop the endocrine pancreas (Gradwohl et al., 2000). However, it has been described that upregulation of Ngn3 in Pdx1 expressing cells increases the neural marker Tubb3 (Kubo et al., 2011). It is important to highlight that neuroectodermal and pancreatic differentiation are regulated by the same transcription factors such as Ngn3 and Pax6 (Gradwohl et al., 2000; Habener et al., 2005). Therefore, the presence of Pax6 in pancreatic differentiated cells (**FIG. 35 B**) possibly contributes to the presence of neural derivatives because Pax6 is associated with ectodermal and neuroectodermal cell fates (Koch et al., 2009). Interestingly, interpretation of the data became more interesting since studies in zebrafish revealed that Ngn3 is not a unique regulator (Flasse et al., 2013). Achaete-scute complex-like 1b (Ascl1b) and neuronal differentiation 1 (Neurod1) ensure development of the

zebrafish endocrine pancreas when Ngn3 is absent. Flasse and co-authors suggest that production of insulin-producing from mouse and human ES cells might be possible without Ngn3 but with another ASCL/ARP factor such as *Ascl1* and/or *Neurod1*. The ASCL/ARP factors include the Achaete scute-like (ASCL) family and the *atonal*-related protein (ARP) family, which is subdivided into *atonal*, *neurogenin* and *neurod* subfamilies (Flasse et al., 2013). It would be very interesting to analyze whether both genes are up regulated presence of Ngn3 using protocols presented in the present work. The absence of *Amy2* exocrine marker contributes to the pancreatic endocrine development (FIG. 35 B). For example, conversion of rat exocrine-like cells into a beta-like state is associated with downregulation of *Amy2* (Akinci et al., 2013). Together, the present data implicate that mouse pancreatic endocrine progenitors have been generated using a 2D differentiation protocol. However, there was a need to improve mouse pancreatic differentiation. Accordingly application of 3D matrices within the established mouse pancreatic differentiation appeared to be a reasonable approach.

The formation of EBs is a well-established method to generate germ layer derivatives and seeding of EBs was applied after formation of DE progenitors. Cells of the EB provide a certain kind of 3D matrix. Interestingly, synthesis and organization of ECM proteins changes dramatically during differentiation of murine EBs (Shukla et al., 2010; Nair et al., 2012). Fibronectin and laminin are increased contributing to its use in several differentiation protocols including the differentiation of MSCs into insulin-producing cells (Lin et al., 2010). In the present study, laminin treatment was applied in 2D cultures and fibronectin was avoided because it is also applied for the formation of ectodermal derivatives such as neural stem cells (Koch et al., 2009). Interestingly, another study used ECM aggregates from EBs to promote proliferation and differentiation of D3 murine ES cells (Nair et al., 2008). 3D biomaterials such as porous alginate scaffolds were recently applied to improve EB formation from human ES cells towards vascularization (Gerecht-Nir et al., 2004).

The efficient generation of DE endoderm was thought to be a critical step during pancreatic differentiation. Accordingly, the application of 3D matrices aimed at the preservation or induction of DE and multipotent pancreatic progenitors. Therefore, the present study applied 3D matrices aiming at the improved differentiation of DE pancreatic progenitors, but a clear preference for the endodermal differentiation was not observed by the mRNA expression of DE markers (FIG. 35 C). Further, IF analysis verified absent *Cxcr4* protein (FIG. 35 D). 3D matrices did also not lead to the preservation of pluripotent cells or the induction of neuronal progenitors demonstrated by absent *SSEA1* and *Tubb3* protein. Together, 3D matrices did neither enhance nor affect the generation of DE progenitors, but it remains to be clarified whether insulin-producing cells can be obtained on 3D matrices by terminal pancreatic differentiation, which was not analyzed in the present study.

Human pancreatic beta cells create their own ECM, but they depend on neighboring cells such as ECs, which provide a microenvironment that is termed as the vascular niche (Nikolova et al., 2007). 3D biological matrices are a promising tool because of their ECM compounds, which are composed in a natural manner depending on the origin. Notably, the use of decellularized pancreas might be more suitable and has been described previously from rat (De et al., 2010), pig (Mirmalek-Sani et al., 2013), and mouse (Goh et al., 2013a). However, the generation of matrices from pancreas is much more challenging compared to matrices from the jejunum. Additionally, the raw material is hardly accessible. The head of the pancreas is surrounded by the duodenum followed by the jejunum suggesting that matrices from the jejunum are also suitable for the culture of pancreatic cells. Further, endocrine cells

such as proglucagon-expressing cells can be found in the pancreas (alpha cells) and in the jejunum (L cells) but processing is different generating glucagon or glucagon-like peptides (Theodorakis et al., 2006). According to the literature, the application of jejunum-derived matrices is reasonable.

Together, the present study generated mouse Pdx1-expressing progenitors under 2D culture conditions. Results from 2D cultures underline the importance of directed differentiation protocols even on 3D scaffolds. These data suggest that 3D pancreatic differentiation allowed, but not induced the differentiation of DE and multipotent progenitors.

4.4.1.3. 3D Matrices Promote DE Differentiation

In order to improve DE formation, the present study contains a competitive analysis of DE induction by activin A, IDE1, IDE2, and nodal (**FIG. 36 A/B**). DE was generated without EB formation on 3D biological matrices. The presented work highlighted that activin A is the most potent inducer of DE verified by Sox17 mRNA expression in CGR8-S17 cells. Activin A is suitable to replace nodal either alone (D'Amour et al., 2006; Schroeder et al., 2006; McLean et al., 2007; Agarwal et al., 2008) or in combination with wnt3a (D'Amour et al., 2006; Hay et al., 2008; Sumi et al., 2008; Fu et al., 2011) to direct DE differentiation of mouse and human ES cells. For example, Schroder and colleagues reported up to 20% Sox17 expressing cells obtained from CGR8-S17 mouse ES cells. Treatment of mouse ES cells with activin A and wnt3a generates up to 40% Sox17-expressing cells (Fu et al., 2011). Interestingly, activin A treatment of HUES4 and HUES8 human ES cells yields up to 64% Sox17-expressing cells (Borowiak et al., 2009). Hay and co-authors generated about 70-90% endodermal albumin-positive cells from H1 and H9 human ES cells using activin A and wnt3a. Wnt3 signaling is required during gastrulation to support endoderm formation (Liu et al., 1999), which explains why Wnt3a supports and accelerates endoderm differentiation (D'Amour et al., 2006; Hay et al., 2008). Wnt3a treatment was not applied in the present study, but especially its acceleration potential needs to be considered in further studies.

The present work demonstrated that IDE1/2 and activin A induced Sox17 mRNA expression, but at lower levels compared to activin A alone (**FIG. 36 A/B**). IDE1/2 are small molecules, which have been initially described in mouse and human ES cells (Borowiak et al., 2009). Borowiak and co-authors reported that IDE1/2 induce and improve DE differentiation. Treatment of mouse ES cells with IDE1 or IDE2 yielded more than 40% Sox17-expressing cells (Borowiak et al., 2009). It is important to mention that molecular mechanisms behind IDE1/2 treatment are poorly described. Currently, there is no clear explanation why IDE1/2 less efficiently induced DE in the present work. Target genes of IDE1/2 are unknown and their investigation most probably will help to understand the function of these small molecules. However, there is evidence that DE induction can be triggered by other media supplements. For example, Bone and co-workers combined activin A and a Gsk3 inhibitor to improve DE differentiation of human ES cells yielding more than 60% Cxcr4-expressing cells (Bone et al., 2011). To date, other small molecules have been described as DE differentiating agents such as wortmanin, SBT, BIO, and inhibitors of glucose-6-phosphat (Jiang et al., 2007; Zhang et al., 2009a; Kunisada et al., 2012; Manganelli et al., 2012). Interestingly, not all DE progenitors are suitable for pancreatic differentiation. Another approach reported that treatment with rapamycin is suitable to improve DE induction by activin A (Tahamtani et al., 2013). Tahamtani and colleagues efficiently generated DE progenitors, which fail to differentiate into pancreatic endocrine cells demonstrating that there are different qualities of DE progenitors. According to that report, differences between nodal and

activin A-induced pancreatic differentiation affecting Pdx1-expressing cells have been described (Chen et al., 2013). Findings by Chen and co-workers suggest that DE generation influences the terminal maturation of Pdx1-expressing cells. In order to avoid activin A treatment, DE differentiation of human iPS cells by Wnt3a and IDE1/2 has been described in 2D cultures (Borowiak et al., 2009) and 3D polymer scaffolds (Hoveizi et al., 2013). Together, studies analyzing DE formation of human pluripotent stem cells agree about the use of activin A for the induction of DE in mouse and human pluripotent stem cells. However, the use of small molecules remains to be considered for more efficient DE differentiation. Activin A-independent DE development may provide new insights into the pancreatic differentiation.

Interestingly, the present work demonstrated spontaneous induction of Pdx1 transcripts at day 10 without activin A only by the presence of 3D biological matrices (**FIG. 36 C**). One can conclude that matrices guide endodermal induction without growth factors and small molecules. Matrices provide an origin-specific ECM mimicking a certain cellular environment, which has been described earlier. Importantly, induction of Pdx1-expressing cells has been described to rely on the differentiation of DE progenitors (Borowiak et al., 2009; D'Amour et al., 2006; Kroon et al., 2008; Van et al., 2009). Therefore, analysis of DE differentiation without EB formation and activin A treatment offers one alternative approach for the 3D differentiation of pancreatic progenitors. However, there is a need to characterize these Pdx1-expressing cells.

Mouse pancreatic 3D differentiation served as a model to study and to verify general aspects of mammalian 3D pancreatic differentiation. Obtained data highly recommend application of 3D matrices in a strategy including co-cultures with ECs to generate insulin-producing cells (**FIG. 44**). However, the mouse model had to be transferred and adapted to human pluripotent stem cells.

4.4.2. Pancreatic Differentiation of Human iPS Cells

At first, it is important to highlight that human and mouse pancreatic differentiation mimic the same sequential arrangement of developmental stages. DE induction by activin A is a prerequisite for mouse and human pancreatic differentiation of ES and iPS cells as described earlier. DE differentiation using EBs and monolayer cultures has been described in mouse and human ES cells (D'Amour et al., 2006; Schroeder et al., 2006; Xu et al., 2006; Wang et al., 2012). Interestingly, mouse DE is most efficiently generated during EB formation, but human DE is most efficiently differentiated in monolayer cultures.

4.4.2.1. Differentiation of Pancreatic Endocrine Progenitors

Notably, the induction of DE endoderm by activin A relies on the pluripotency of ES cells. Therefore, developmental unrestricted and fully reprogrammed iPS cells are required for efficient activin A-induced differentiation. Accordingly, not fully reprogrammed pre-iPS cells generated within the present study are not suitable when protocols for pluripotent stem cells are required. In the present study, commercially available and viral generated IMR90 iPS cells were applied. This cell lines was established in 2007 (Yu et al., 2007) and clone derivatives still can be purchased from the Wisconsin International Stem Cell Bank demonstrating that these cells are fully and permanently reprogrammed. The expression of pluripotency marker genes in IMR90 iPS cells was verified in the present study (**FIG. 39**). The IMR90 iPS cell line is intensively analyzed and characterized by other studies and known to be very similar to human ES cells (Yu et al., 2007). Studies using both IMR90 iPS and H9 cells demonstrated almost similar behavior during neural differentiation (Zhou et al., 2010) or vascular

and hematopoietic differentiation (Hu et al., 2010). Moreover, IMR90 iPS cells yield quantities of DE and pancreatic progenitors similar to H1 and H9 human ES cells (Xu et al., 2011). Importantly, neural stem cells obtained from IMR90 iPS cells showed insulin concentration-dependent behavior similar to H9-derived cells (Rhee et al., 2013). According to several opportunities, one can suggest that the IMR90 iPS cell line is gold standard for other iPS lines. Therefore, IMR90 iPS cells represent a well-established tool for differentiation studies.

Activin A-induced DE progenitors have been derived from iPS cells in the present work. DE differentiation was demonstrated by epithelial morphology and protein expression of Sox17, Foxa2, and Cxcr4 (**FIG. 40**). There are a few studies, which quantified induction of DE using protocols similar to the present study. Differentiation into DE yields about 62% Sox17-expressing cells, 33% Cxcr4-positive cells, 20% Foxa2-expressing cells around day 4 (Borowiak et al., 2009; Filby et al., 2011; Kuijk et al., 2011). Interestingly, efficiencies vary between different studies because different pluripotent stem cell lines exhibit different developmental potentials (Kuijk et al., 2011). Significant DE progenitor formation has been verified in the present work representing a potent population of cells suitable to generate pancreatic endocrine progenitors.

The present study demonstrated the generation of human Pdx1-expressing endocrine progenitors via stepwise pancreatic differentiation (**FIG. 40, 41**). Pdx1 protein expression was associated with the mRNA expression of Ngn3, Nkx6.1, and Gcg. Pdx1-positive cells did express neither Nkx2.2 nor Ins. Ins was not expressed but absent Ins contributes to the differentiation potential and the immature developmental stage of pancreatic progenitors. Induction of Ins-expressing cells would require prolongation of the differentiation protocol to generate hormone-expressing endocrine cells (D'Amour et al., 2006). According to the given data, endocrine progenitors are recommended for the generation of insulin-producing cells. The differentiation protocol aimed at the subsequent differentiation into multipotent progenitors, pancreatic progenitors, and endocrine progenitors, which contributes to the *in vivo* development of pancreatic endocrine cells. Stepwise differentiation mimicked developmental stages namely, primitive gut tube, posterior foregut, and pancreatic endoderm (Bonal and Herrera, 2008; Borowiak, 2010; Van et al., 2009).

Multipotent progenitor formation mimicking the primitive gut tube formation was analyzed at day 6 (**FIG. 41 B**). Pdx1, Nkx6.1, and Gcg transcription verified multipotent progenitor differentiation. Nkx6.1 expression marks the development of multipotent progenitors at moderate levels and its expression is maintained until differentiation of insulin-producing cells (Schaffer et al., 2013). Nkx6.1 is essential for the differentiation of functional insulin-producing cells (Taylor et al., 2013). Therefore, induction of Nkx6.1 contributes to the differentiation of insulin-producing cells. Gcg mRNA was induced during pancreatic differentiation suggesting the presence of immature endocrine progenitors. *In vivo* development of pancreatic endocrine cells is characterized by 2 transitions, which generate hormone-producing cells (Bonal and Herrera, 2008). The first transition generates endocrine cells within the primitive gut tube, which produce glucagon, insulin, PP, and ghrelin. Interestingly, blocking of glucagon but not of glucagon-like peptide 1, an alternate gene product of preproglucagon mRNA, prevents the development of insulin-producing cells during the second transition (Prasadan et al., 2002). Accordingly, induction of Gcg might be beneficial for the generation of insulin-producing cells.

The generation of endocrine progenitors mimicking the pancreatic endoderm was analyzed at day 12 (**FIG. 41 B**). Pdx1, Nkx6.1, Gcg, and Ngn3 transcripts verified endocrine progenitor

differentiation. These pancreatic markers are associated with the differentiation of pancreatic endocrine progenitors. Multipotent progenitors residing within the primitive gut tube give rise to endocrine progenitors, which can be characterized by Pdx1, Nkx6.1, Nkx2.2, and Ngn3 (D'Amour et al., 2006; Van et al., 2009). It is important to mention that Nkx2.2 mRNA was induced during DE formation, but expression disappeared and remained to be absent during pancreatic differentiation. Nkx2.2 is thought to be induced as early as Nkx6.1, but expression is necessary for alpha and beta cell development (Van et al., 2009). In pancreatic beta cells, Nkx2.2 is part of a repressor complex for the inhibition of areistaless related homeobox (Arx), which is essential for alpha cell specification. Accordingly, loss of Nkx2.2 is associated with beta to alpha cell transdifferentiation. One can suggest that absent Nkx2.2 probably would affect the terminal differentiation of endocrine progenitors into insulin-expressing cells.

Notably, even the directed differentiation of pancreatic endocrine progenitors contains a major subset of non-endocrine cell derivatives demonstrated by morphological, mRNA, and IF analysis (**FIG. 40/41**). The induction of exocrine pancreas marker Mist1 mRNA contributes to the generation of pancreatic progenitors. The induction of Pax6 transcription is due to pancreatic endocrine development and ectodermal and neuroectodermal cell fates as described earlier. It is important to mention again that Tubb3 expression was hardly detectable in contrast to spontaneously-induced pancreatic differentiation. Interestingly, Gfap and Map2 are expressed in multipotent precursors from adult mouse pancreas (Seaberg et al., 2004). However, the expression of Gfap and Map2 in the present work implicates the differentiation of neural derivatives as introduced earlier. This observation is accordance with studies by others (D'Amour et al., 2006; Schroeder et al., 2009; Zhang et al., 2009b) also demonstrating that non-endodermal cells are differentiated even by application of protocols for the directed pancreatic differentiation.

4.4.2.2. Heterogeneity of the Pancreatic Endocrine Progenitors

The differentiation protocol applied within the present work was initially described D'Amour and co-authors in 2006. The protocol was verified by other investigators with minor modifications, but terminal differentiation was predominantly investigated by semi-quantitative expression analysis (Kroon et al., 2008; Zhang et al., 2009b). Supplementation of LY-374973 (also known as DAPT), exendin 4, and glucagon-like protein 1 has been described during differentiation of endocrine precursors, but treatment yields marginal effects (D'Amour et al., 2006). Accordingly, treatment with LY-374973 did not improve pancreatic differentiation in the present study (data not shown). It is important to mention that other differentiating agents has been described to improve generation of pancreatic progenitors such as dorsomorphin, EGF, FGF2, and Noggin (Mfopou et al., 2010). For example, dorsomorphin suppresses BMP signaling to promote the pancreatic lineage (Chung et al., 2010). It is also important to mention that B27 supplement contains a mixture of differentiating agents. B27 is currently applied in several protocols to mediate differentiation of endocrine progenitors and hormone-expressing cells (D'Amour et al., 2006; Zhang et al., 2009a; Ohmine et al., 2012; Schroeder et al., 2012). This mixture is neither adapted to the pancreatic lineage nor restricted to a certain developmental stage during pancreatic differentiation. Together, there is a need to consider a more sophisticated treatment strategy combining differentiating agents in a physiological manner.

Differences between IMR90 iPS and H9 ES cells were observed during differentiation of endocrine progenitors (**FIG. 40, 41 B/C**). H9 ES cells differentiated into DE within 4 d, but IMR90 iPS cells

generated DE within 3 d. Interestingly, for differentiation of DE 3 to 5 day have been described using different human iPS and ES cell lines and different culture media during activin A treatment (Borowiak et al., 2009; Kroon et al., 2008; Ohmine et al., 2012). Accordingly, it is very important to adjust pancreatic differentiation protocols to the peak of most abundant generation of DE progenitors. However, the analysis of H9 cells during pancreatic differentiation revealed that Pdx1 and Ngn3 expression was detected earlier during multipotent progenitor formation at day 7 (**41 B/C**). There are two different explanations. One the one hand, one can suggest that different mRNA expression levels or expression durations depend on the reprogrammed status of iPS cells and/or the general heterogeneity of pluripotent ES and iPS cell lines as described earlier. On the other hand, one can suggest that differences depend on the general variability of the differentiation protocol. It is important to notice that even protocols for the directed differentiation bear a strong spontaneous differentiation potential making the more terminal differentiation stages more and more variable. In this context, it is important to mention that IMR90 iPS cells were analyzed for their ability to spontaneously derive DE by treatment with FCS. Endodermal, mesodermal, ectodermal, and extraembryonic lineage marker genes were spontaneously induced on the mRNA level (**FIG. 40 D/F**) suggesting that IMR90 iPS cells are amenable for the differentiation of all 3 germ layers. It is not possible to draw a clear conclusion according to different efficiencies and the qualities of IMR90- and H9-derived endocrine progenitors. However, there is evidence that differences between IMR90 and iPS cells contribute to the variability of differentiation protocols rather than to the reprogrammed status of IMR90 iPS cells.

Different pluripotent stem cell lines were known to have different preferences for lineage specification in dependence on their somatic background (Kim et al., 2010). However, it is highly debated whether different differentiation potentials may depend on the heterogeneity of reprogrammed cells rather than the origin of the donor cell type (Nasu et al., 2013). This argumentation is underscored by the fact that human ES cells also show different differentiation potentials demonstrating their heterogeneity as well. Interestingly, HUES cell lines such as HUES3 and HUES4 have been described yielding more efficient endodermal differentiation (Borowiak et al., 2009; Johannesson et al., 2009) compared to H9 cells (Zhang et al., 2009a; Xu et al., 2011) or Cyt203 and Cyt49 cells (D'Amour et al., 2006; Kroon et al., 2008). Competitive studies including these human ES cell lines are needed to analyze whether distinct cell lines more efficiently generate pancreatic endocrine cells. However, according to the literature, there is no evidence that IMR90 iPS cells are more or less suitable for the differentiation of pancreatic endocrine cells.

Currently, it is unknown, which kind of human iPS cell lines are the best suited for therapeutic purposes and what type would be unsuitable. Human iPS cells cannot be analyzed by germ line transmission. One very stringent property is the capability to generate well-differentiated teratomas following injection into immunodeficient mice (Brivanlou et al., 2003). For instance, iPS cell lines, which have a strong tendency to form teratocarcinomas are not suitable for animal studies and cell replacement therapies (Brivanlou et al., 2003). Efforts to minimize teratocarcinoma-forming cells have been described such as the isolation of SSEA5-positive stem cells to remove cell with a high teratocarcinoma-forming potential (Tang et al., 2011). However, defining pluripotency in iPS cells is even more difficult in comparison to the mouse system.

The present work demonstrated successful generation of Pdx1-expressing endocrine progenitors from IMR90 iPS cells suitable for terminal differentiation of insulin-producing cells. However, IF

analysis indicated moderate efficiencies underscoring the need of improved culture conditions. Nevertheless, successful differentiation of pancreatic endocrine progenitors recommends their use in co-culture and organotypic differentiation studies.

4.4.3. Co-Culture with ECs during Pancreatic Differentiation

The *in vivo* development of pancreatic progenitors depends on the presence of ECs as introduced earlier. In order to mimic this relationship *in vitro*, the co-culture with primary ECs was studied during pancreatic differentiation within the present study.

4.4.3.1. Primary ECs for Co-Cultures

The present study required mature and functional ECs capable to regulate pancreatic differentiation. Notably, the application of primary ECs appeared to be the most reasonable approach. Permanent EC lines do not preserve all natural characteristics of primary ECs. EC lines such as human microvascular endothelial cell line 1 (HMEC-1) were analyzed by several studies in comparison to primary ECs. Interestingly, lymphatic marker genes are expressed in HMEC-1 indicating increased plasticity of immortalized ECs (Keuschnigg et al., 2013). One should consider that immortality of ECs is a non-physiologic property. Accordingly, EC lines stably preserve properties of ECs, but it is often discussed that EC lines are not capable to model all properties of fully differentiated and matured ECs. HMEC-1 barely express endothelial surface proteins vascular cell molecule (Vcam) and selectin E (Sele) (Lidington et al., 1999). Other human EC lines have been described to fail other crucial EC markers such as vWF (Nisato et al., 2004). According to that, application of permanent EC lines such as HMEC-1 provides a standardized model especially when quantitative analysis are required. However, in the present study fully matured cells were required.

Primary MVECs, HUVECs, and HDMECs are known to preserve natural characteristics. HUVECS have an average life span of 10 serial passages and can be kept in culture up to 5 months (Moll et al., 2013). Thereafter, these ECs became senescent and stop proliferation. In the present study, ECs were applied at passage 3 because later on their proliferation capacity and their capability to express ES markers is lowered. The present study demonstrated rapid loss of EC markers was induced by HPDM (**FIG. 38**). Interestingly, semi-quantitative PCR analysis of EC markers did not reveal any differences highlighting the importance of protein expression analysis. These results implicated the establishment of a co-culture medium providing adapted culture conditions. These conditions basically included a 1:1 mixture of ECGM and HPDM basal media supplemented with the full amount of growth factors (pancreatic and endothelial). Of course, these growth factors possibly promote and counteract each other as well. The present study demonstrated that HUVECs induced or lost mRNA expression of certain differentiation markers in the presence of the co-culture medium during pancreatic differentiation (**FIG. 41**). This observation suggests that ECs respond to pancreatic differentiating agents. Accordingly, one can suggest that ECs differently effected pancreatic differentiation. However, the described co-culture medium presented the most suitable approach to preserve natural characteristics of primary ECs during co-culture differentiation studies.

Primary ECs were characterized at passage 3 by the mRNA and protein expression of crucial EC marker genes without noticeable differences in isolates from different sources (**FIG. 37**). The vWF is an essential EC marker because loss of vWF causes the von Willebrand disease, which is an autosomally inherited bleeding disorder (Lillicrap, 2013). Tie1 and Tie2, have been described as

EC-specific RTKs. Loss of Tie1 and Tie2 in null mice leads to embryonic death (Ruan and Kazlauskas, 2013). Tie2 is not essential for EC differentiation but it is required for maintenance and proliferation of ECs. Ephb2 and Ephb4 are RTKs, which play a key role during angiogenesis (Mosch et al., 2010). Ephb2 is expressed on arteries and Ephb4 is expressed on veins and known to regulate smooth muscle formation around blood vessels (Mosch et al., 2010). To ensure the presence of blood-vascular ECs, it would be interesting to check whether lymphatic EC markers Sox family transcription factor 18 (Sox18) and pro-sepero homeobox 1 (Prox1) are expressed (Simons and Eichmann, 2013). Eng is a receptor of the TGF β family predominantly expressed in proliferating vascular ECs (Banerjee et al., 2012). Eng-deficient mice die during embryogenesis because of angiogenesis and cardiovascular defects (Banerjee et al., 2012). VEcad is an endothelial-specific membrane protein ensuring cell to cell contacts (Lampugnani et al., 1992). Pecam1 is expressed by multiple isoforms in the endothelium acting as an adhesive structure and modulates integrin-mediated cellular processes (Thompson et al., 2001). Vascular endothelial growth factor receptor 2 (Vegfr2; officially termed as Kdr) is expressed on ECs responsible for interaction with integrins of neighboring cells (Nikolova et al., 2007). The phenotype and the functionality of ECs can be analyzed by more sophisticated techniques. The presence of Weibel-Palade-bodies inside of ECs storing vWF and the expression of other EC markers such as intercellular adhesion molecule 1 (Icam1), Vcam, and selectin E are crucial characteristics of the EC phenotype (Lidington et al., 1999). The secretion of vWF, the uptake of acetylated low density lipoprotein, and active Angiotensin-converting enzymes are stringent characteristics of functional ECs. Together, the present study sufficiently characterized and verified natural characteristics of ECs, but functional studies may elucidate functional properties of applied ECs. Characterization demonstrated the presence of artery- and vein-derived proliferating and mature endothelial cells suitable for co-culture differentiation studies with pancreatic cells.

Primary ECs were successfully isolated and characterized from different sources generating MVECs from skin biopsies and HUVECs from umbilical cord. Contamination with other cell types such as fibroblasts was negligible. Interestingly, the morphology slightly differed between sources but not between isolates (**FIG. 37**) implicating different specification according to the skin or umbilical cord. The morphology and the behavior of ECs obtained from different origins is known to be different. Interestingly, the microvasculature inside the pancreas is differently specialized as well. ECs inside the islet of Langerhans, ECs show about 10 times more fenestrations compared to the exocrine pancreas (Zanone et al., 2008). Further, islet-related mouse ECs can be characterized by the expression of alpha-1 antitrypsin (A1AT; officially termed as Serpina1) (Lou et al., 1999). However, there is no source for the isolation of human islet-derived ECs. Accordingly, the use of another applicable source for the isolation of mature and functional ECs for sure isolates endothelial subtypes not specialized for the pancreatic islet. Primary ECs from different origins have been applied in competitive studies generating different results (Yue et al., 2011; Patel et al., 2013) suggesting that the origin of primary ECs would also have unknown different effects on pancreatic cells. Accordingly, one can discuss suitability of MVECs, HUVECs and HDEMCs as well.

4.4.3.2. Differentiation of Pancreatic Progenitors is Affected by Co-Culture with ECs

The present study could demonstrate that ECs proliferate and form big clusters neighboring islet-like clusters (**FIG. 41 A**). Transcript analysis of 2D co-cultures revealed no strong impact of ECs on the induction of pancreatic endocrine marker genes such as Pdx1 and Ngn3 (**FIG. 41 B/C**). These

results are in conflict with studies by others. Notably, other reports demonstrated successful improvement of pancreatic differentiation by 2D co-cultures with ECs. These reports applied approaches different to the present study as described below.

The present approach seeded a cell suspension containing both DE progenitors and ECs. This approach might have disturbed the formation of pancreatic and/or endothelial colonies. Another approach in the mouse system described seeding of spontaneously differentiated EBs at day 5 and subsequent seeding (24 h later) of primary aortic ECs (Talavera-Adame et al., 2011). Direct interaction was demonstrated to promote the expression of pancreatic progenitor and beta cell markers *in vitro* (Talavera-Adame et al., 2011). This approach by Talavera-Adame increased the expression of pancreatic lineage markers such as Pdx1, Ngn3, and Nkx6.1 implicating enhanced differentiation of pancreatic progenitors. Plated EBs at day 5 usually contain cells similar to germ layer progenitors. Differences might rather depend on the differentiation status of EBs than on the separate culture of pancreatic cells and ECs. There is a need to verify Talavera-Adame's protocol in human system.

In the present study DE progenitors were applied for co-culture studies because DE progenitors generate Pdx1-expressing early pancreatic progenitors. However, ECs might have induced maturation instead of proliferation of Pdx1-expressing progenitors. Another approach applied rat heart microvascular ECs to guide only the final stage of mouse pancreatic differentiation (Banerjee et al., 2011; Jaramillo and Banerjee, 2012). R1 ES cells were differentiated hormone-expressing beta-like cells according to D'Amour's protocol adapted to the mouse system. Both studies yield maturation of hormone-expressing endocrine cells yielding up to 60% Ins1-expressing cells. Accordingly, co-cultures with ECs might be more easily applicable for improved maturation of pancreatic progenitors.

Pancreatic beta cells *in vivo* and *in vitro* require the presence of ECs providing a pancreatic extra cellular environment as described earlier. Therefore, co-culture with ECs provides a reasonable approach to improve culture of pancreatic cells in a strategy to generate insulin-producing cells (FIG. 44). Several studies by others included co-cultures with ECs to promote culture and differentiation of other functional cell types. For example, EC were applied in osteogenic tissue-engineered constructs (Pedersen et al., 2013). However, ECs are predominantly applied for terminal differentiation of maturation of cells highlighting that in general more sophisticated culture techniques are required to enable co-culture differentiation studies. Most importantly, this implicates that 2D co-cultures are less suitable to improve pancreatic differentiation raising evidence that 3D organotypic approaches are more suitable.

4.4.4. Organotypic Pancreatic Differentiation of Human iPS Cells

For the first time, iPS cells were applied in 3D biological matrices in co-culture with ECs to organotypic pancreatic differentiation model. 3D matrices and co-culture with ECs aim at the improved generation and maturation of pancreatic progenitors.

4.4.4.1. Organotypic Differentiation in 3D Biological Matrices with ECs

The 3D differentiation model described in the present study relied on application of 3D biological matrices. Importantly, staining of viable and dying cells revealed that 3D matrices are optimal to preserve viability of pancreatic differentiating cells alone and in co-culture with ECs (FIG. 42). Moreover, islet-like clusters as described in 2D cultures were increased recognized in co-cultures. Pancreatic endocrine cells optimally function when clustered in islet-like clusters (Kroon et al., 2008;

Van et al., 2009). These data strongly recommend the general applicability of 3D matrices derived from porcine jejunum. Accordingly, 3D biological matrices should be a part of a strategy including co-culture conditions to generate insulin-producing cells (**FIG. 44**).

Organotypic culture models have been described for the generation of other organs such as liver (LeCluyse et al., 2012), skin (Bechetoille et al., 2011), and retina (Kador and Goldberg, 2012). Organotypic liver culture models are very interesting because hepatocytes originate from endodermal precursors likewise pancreatic endocrine cells. The liver contains specific sinusoidal ECs, which are essential for development, maintenance and function of hepatic cells (LeCluyse et al., 2012). Accordingly, mixed cultures of hepatic cells and ECs were successfully applied for organotypic culture models including 3D culture and co-culture (LeCluyse et al., 2012). Bechetoille and co-workers pre-seeded fibroblasts for the culture of dermal macrophages. Another disease model for Barret's esophagus also applied fibroblasts for 3D co-culture with keratinocytes (Kosoff et al., 2012). In accordance with these models, another study highlighted the importance of stromal cells within an organotypic pancreatic cancer model (Froeling et al., 2009). These approaches are interesting because connective tissue present in every organ. Accordingly, it would be interesting to study co-culture with fibroblasts, ECs, and pancreatic progenitors.

Another approach demonstrated that transplantation of organotypic scaffolds carrying retinal progenitors into degenerated retinal explants (Kador and Goldberg, 2012). Retinal progenitors immigrate into explants and differentiate. However, Kador and co-authors mentioned that translation into a therapeutic approaches (such as toxicity tests, disease model, or transplantation) would require application of differentiated implants. Even though, Kroon and co-workers also demonstrated *in vivo* differentiation of pancreatic progenitors, therapeutic approaches of pancreatic implants would also require application of differentiated cells. According to this, organotypic terminal differentiation appears to be a major challenge.

4.4.4.2. Pancreatic Differentiation is Affected by ECs in 3D Biological Matrices

As described earlier, propagation of primary ECs is affected in the presence of HPDM. Therefore, it was very important to analyze whether even EC-preserving growth factors somehow influence pancreatic differentiation. To analyze the effects of ECGM, pancreatic differentiation of CGR8-S17 on 3D biological matrices was analyzed focusing on the induction of mesodermal and ectodermal markers (**FIG. 35 C**). ECGM stabilized endoderm marker Cxcr4, but induced mesoderm marker Foxf1

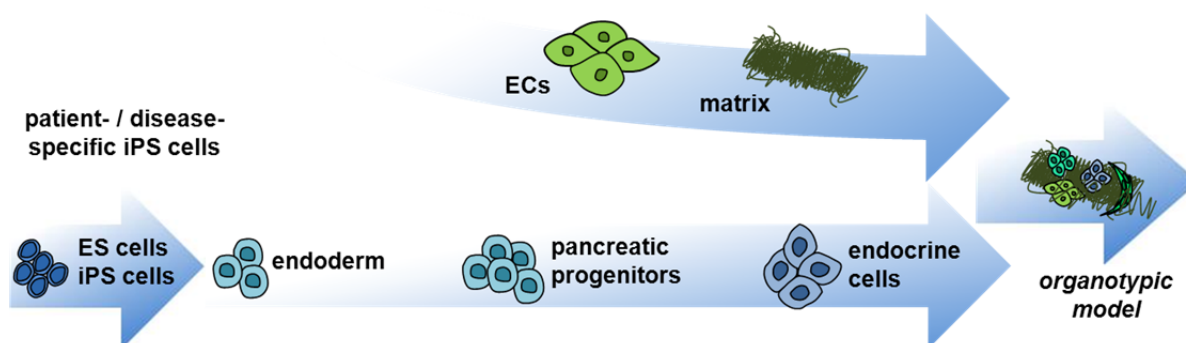


FIGURE 44: Strategy for the use of 3D biological matrices and co-culture conditions to generate insulin-producing cells. Patient-/disease-specific and human ES cells need to be differentiated into endocrine pancreatic progenitors. Co-culture with ECs within a 3D biological matrix provide an organotypic model aiming at the generation of mature insulin-producing cells

and ectoderm marker Shh. Endoderm formation was not affected, but the induction non-pancreatic lineage markers suggests less efficient pancreatic progenitor differentiation. This observation contributes to the induction of germ layer marker genes in 2D co-cultures during differentiation of IMR90 iPS. Studies by others showed that induction of early differentiation marker genes such as Sox17 is associated with enhanced self-renewal and acquirement of fetal properties (Chhabra and Mikkola, 2011). Further, ECs have been shown to support proliferation and regeneration by providing a kind of stem cell niche (Li et al., 2010; Zhu et al., 2011), which might contribute to the induction early differentiation marker genes.

The present work demonstrated application of DE progenitors on matrices with ECs within a unique culture model. However, seeding of DE progenitors appears to be less suitable because pancreatic progenitor formation was affected in the present organotypic 3D culture model (**FIG. 42**). This observation contributes to data obtained from 2D co-cultures. Another study reported the endodermal differentiation of mouse ES cells into cells with lung phenotypes using decellurized lung matrices (Jensen et al., 2012). In contrast to the present approach, Jensen and co-authors did not apply DE progenitors. They applied predifferentiated cells with properties of alveolar epithelial cells for their 3D biological differentiation model. Lung matrices were coated with Matrigel™, but in the present study coating with additional ECM proteins was not applied. It would be necessary to proof whether coating of 3D biological matrices from porcine jejunum would substantially improve the present organotypic culture model. Besides Matrigel™, further studies should include coating with pancreas-associated integrins and collagens as described earlier.

Transcript analysis of crucial pancreatic lineage markers revealed DE progenitors co-cultured with ECs on 3D matrices induced a subset of endodermal and pancreatic lineage markers (**FIG. 42**). However, terminal pancreatic differentiation of iPS cells was abolished with or without ECs on 3D matrices at day 12. These data on the one hand demonstrated that both co-culture with ECs and culture on 3D matrices hindered generation of endocrine progenitors. However, on the other hand, the presence of ECs might have preserved pancreatic progenitors for a short-time period. Together, one can suggest that both ECs and 3D matrices counteract proliferation and differentiation of pancreatic progenitors. According to this conclusion, a recent report demonstrated that ECs are involved in repression of Wnt and Notch signaling for hepatic specification (Han et al., 2011) highlighting an essential role in maturation rather than in proliferation during liver development.

Together, pancreatic differentiation analyzed by several approaches in the present study leads to one clear conclusion. Porcine 3D matrices do not enhance or improve the differentiation of pancreatic progenitors neither by differentiation of mouse ES cells nor by differentiation of human ES cells. The data highly recommend that pancreatic progenitor formation is affected by the presence of primary ECs rather than by co-culture media or the presence of 3D biological matrices. This conclusion strongly suggests co-culture with ECs during terminal differentiation stages as recommended in a strategy for the use of 3D biological matrices and co-culture conditions to generate insulin-producing cells (**FIG. 44**). Finally, this implicates that there is still a need to improve 2D cultures for the differentiation of DE progenitor into pancreatic progenitors.

5. SUMMARY

This work investigates a common question in these days. How is it possible to study genetic predispositions and their underlying molecular mechanisms? In the present study, the question was addressed to DNA variations associated to type 2 diabetes mellitus (T2DM). There is evidence that distinct DNA variations are associated with onset, progression, and treatment of T2DM. To answer the question, the workflow comprised of 3 consecutive steps. At first, primary cells had to be isolated from donors. Next, cells had to be reprogrammed. Finally, cells had to be differentiated into the pancreatic lineage.

The first step required the isolation of primary cells from patients. Therefore, primary keratinocytes were obtained from plucked hairs of healthy donors. Keratinocytes expressed several pluripotency-associated markers making them a reasonable source for the generation of induced pluripotent stem (iPS) cells.

At second, it was necessary to generate iPS cells. To preserve the integrity of the genome, it was mandatory to avoid viral reprogramming methods, which are already described in the literature. To establish a non-viral reprogramming strategy, mesenchymal stem cells (MSCs) and fibroblasts were applied. The present study analyzed non-viral methods namely, transfection of episomal vectors, transfection of ES cell-specific miRs, low oxygen supply (hypoxia), and treatment with small molecules.

Transfection with episomal vectors aimed at the ectopic expression of Oct4, Nanog, Sox2, and Lin28 (ONSL). Optimized conditions yielded transfection efficiencies of about 30% in MSCs and 1.5% in fibroblasts. The mRNA and protein expression of ONSL was verified. Moreover, the endogenous expression of ONSL was induced.

Another approach aimed at the induction of pluripotency by the transfection of miR-302a-d & 372, which are almost only expressed in ES cell. Optimization of the transfection procedure revealed transfection efficiencies of about 97% in MSCs and about 44% in fibroblasts. It was very important to verify pluripotency-regulating target genes of these miRs, because they are poorly described in the literature. Using a cell culture model, *Ccna1*, *Klf13*, *Dnmt1*, and *Wfr61* were shown to be repressed on the mRNA level by miR-302a-d & 372. Further, transfection induced the endogenous expression of miR-302a-d & 372 examined by the induction of pre-miRs and pri-miRs. Moreover, the induction of Oct4 and Nanog mRNA expression was observed. Question remained how Oct4 induction was achieved by miR-302a-d & 372. To clarify this question, Oct4 induction was intensively studied. Strong *Dnmt1* protein repression by miR-302a-d & 372 suggested that DNA methylation of the Oct4 promoter has been occurred. Using a luciferase-reporter-construct, binding of miR-302a-d & 372 to the 3' untranslated region of the *Dnmt1* mRNA was demonstrated. Real-time PCR-based quantification of CpG methylation revealed that miR-302a-d & 372 lowered methylation within the conserved region 4 of the Oct4 promoter.

To improve the reprogramming process, hypoxia was applied. Hypoxia was sufficient to induce the expression of Oct4 and miR-302a. Further, hypoxia increased or preserved Oct4, Nanog, and Lin28 mRNA levels after delivery of episomal vectors. The amount of Ki67-positive cells was elevated by hypoxia.

Treatment with small molecules promoted the formation of colonies after transfection with episomal vectors or miR-302a-d & 372. These colonies acquired alkaline phosphatase activity. Epigenetic

modulators, signal transduction inhibitors, and kinase inhibitors were applied. The combination of episomal vectors, signal transduction inhibitors, and kinase inhibitors was the only setup, which successfully retained ONSL expression in picked clones.

The third step included the analysis of the pancreatic differentiation and the establishment of three-dimensional (3D) co-cultures. Therefore, 3D matrices were established from porcine matrices. It was analyzed whether matrices are applicable and suitable for the pancreatic differentiation. 3D matrices allowed the culture of mouse embryonic stem (ES) cells carrying a Sox17-DSred reporter. Paraffin sections demonstrated that cells immigrated into the 3D scaffold. Further, the induction of multipotent pancreatic progenitors was supported.

The pancreatic differentiation of mouse ES cells was verified using an embryoidbody-based approach for the generation of pancreatic progenitors. This model was transferred to 3D matrices. The differentiation into endodermal precursors was not affected by 3D matrices. Treatment with a co-culture medium also not affected the differentiation into endodermal precursors.

Co-cultures required the generation primary endothelial cell cultures from skin biopsies and human umbilical cords. Primary cultures were validated by the protein expression of crucial markers genes such as the von Willbrand factor, but pancreatic differentiation medium down regulated these markers. Therefore, natural characteristics of endothelial cells had to be preserved by a co-culture medium.

Data obtained from the mouse system were transferred to the pancreatic differentiation of human IMR90 iPS and H9 ES cells. The protein expression of pluripotency markers was verified in IMR90 iPS cells. Next, directed iPS cell differentiation towards the pancreatic lineage was verified without 3D co-cultures. These data were compared to the spontaneous differentiation of iPS cells. The directed differentiation generated Pdx1-positive multipotent pancreatic progenitors. The differentiation protocol was transferred to co-culture conditions using IMR90 iPS and H9 ES cells. Transcript analysis revealed that markers crucial for the generation of pancreatic endocrine cells were not elevated or down regulated. The differentiation protocol was also transferred to 3D co-culture conditions. Staining of life and dead cells revealed that cells remained viable. However, transcript analysis revealed that markers crucial for the generation of pancreatic endocrine cells were down regulated. One can conclude that co-cultures at a later stage of the pancreatic differentiation might be more suitable.

Altogether, this study does not give a clear answer according to question raised at the beginning of the study, but obtained data highlight that the given approaches are promising. Modification of the established treatment protocols might reveal a more efficient non-viral reprogramming strategy. Further, modification of the co-culture conditions might reveal an organotypic differentiation model suitable to promote terminal pancreatic differentiation.

6. ZUSAMMENFASSUNG

In dieser Arbeit wurde eine heutzutage allgegenwärtige Fragestellung bearbeitet. Wie kann man genetische Prädispositionen untersuchen und deren Wirkmechanismus aufklären? Die Fragestellung in dieser Arbeit basierte auf der Kenntnis, dass es genetische Variationen mit der Entstehung, dem Krankheitsverlauf und der Behandlung von Diabetes Mellitus Typ 2 (T2DM) assoziiert sind. Diese Arbeit beschreibt wie man Risikogene für die Erkrankung an T2DM genauer untersuchen kann. Grundlegend waren 3 aufeinander folgende Arbeitsschritte. Primäre Zellen mussten von Spendern gewonnen, diese reprogrammiert und in die pankreatische Linie differenziert werden.

In einem ersten Schritt wurden primäre Zellen aus gesunden Probanden isoliert. Primäre Keratinozyten wurden aus gezupften Haaren gewonnen. Keratinozyten exprimierten zahlreiche Pluripotenz-assoziierte Gene, was sie für die Herstellung induziert-pluripotenter Stammzellen (iPS-Zellen) prädestiniert.

In einem zweiten Schritt war es notwendig iPS-Zellen herzustellen. Um jedoch die Unversehrtheit des Genoms zu gewährleisten, war notwendig von in der Literatur bereits beschriebenen Methoden zur viralen Reprogrammierung ab zu weichen. Als Ausgangsmaterial für die Etablierung eines nicht-viralen Protokolls wurden mesenchymale Stammzellen (MSCs) und Fibroblasten gewählt. Nicht-virale Methoden waren die Transfektion spezieller Plasmide, die Transfektion ES-Zell-spezifischer microRNAs (miRs), einer sehr niedriger Sauerstoffgehalt (Hypoxie) und die Behandlung mit Molekülen zur Veränderung von Signalwegen.

Die Transfektion episomaler Vektoren zielte auf die ektopische Expression der Reprogrammierungsfaktoren Oct4, Nanog, Sox2 und Lin28 (ONSL) ab. Unter optimierten Bedingungen wurden etwa 30 % der MSCs und etwa 1,5 % der Fibroblasten transfiziert. Die mRNA- und Proteinexpression von ONSL wurde nachgewiesen. ONSL wurden endogen induziert.

Weiterhin wurde die Transfektion von miR-302a-d & 372, welche fast ausschließlich in ES-Zellen exprimiert werden, untersucht. Etwa 97 % der MSCs und etwa 44 % der Fibroblasten wurden erfolgreich transfiziert. Wichtig war die Voraussage gegenwärtig kaum beschriebener Pluripotenz-relevanter Zielgene. Diese Studie konnte im Zellkulturmodell betätigen, dass die Transkription von Ccna1, Klf13, Dnmt1 und Wdr61 durch die Gabe von miR-302a-d & 372 herunter reguliert wird. Weiterhin führte die Gabe dieser miRs zur endogenen Expression von Pre-miRs und Pri-miRs. Nach Transfektion von miR-302a-d & 372 wurde auch die Genexpression von Oct4 und Nanog induziert. In weiteren Analysen wurde genauer untersucht wie die Induktion von Oct4 zu erklären war. Die starke Repression der Dnmt1 Proteinexpression legte nahe, dass die DNA-Methylierung des Oct4 Promoters dafür ursächlich gewesen sein könnte. Eine genaue Analyse verwendete einen Luciferase-Reporter-Konstrukt um die Bindung von miR-302a-d & 372 an die 3' untranskribierte Region der Dnmt1 mRNA zu beweisen. Ein Real-Time-PCR-basiertes Verfahren konnte zeigen, dass CpGs in der konservierten Region 4 des Oct4 Promoters nach Transfektion der miR-302a-d & 372 weniger methyliert sind.

Zur Unterstützung der Reprogrammierung wurden hypoxische Kulturbedingungen angewendet. Hypoxie induzierte die Expression von Oct4 und miR-302a. Nach Transfektion des episomalen Vektors konnte die Transkription von Oct4, Nanog, und Lin28 stärker oder länger andauernd angeschaltet werden. Der Anteil Ki67-positiver proliferierender Zellen wurde durch Hypoxie erhöht.

Die Behandlung mit niedermolekularen Wirkstoffen begünstigte die Entstehung teilweise reprogrammierter Kolonien nach der Transfektion von episomalen Vektoren oder miR-302a-d & 372. Die Kolonien zeigten die Aktivität alkalischer Phosphatasen. Epigenetische Modulatoren, Inhibitoren bestimmter Signalmoleküle und Inhibitoren bestimmter Kinasen wurden eingesetzt. Nur die Behandlung mit episomalen Vektoren in Verbindung mit der Inhibition bestimmter Signalmoleküle und Kinasen unter normoxischen Bedingungen führte zur Erhaltung der ONSL Expression in gepickten Kolonien.

In einem dritten Schritt war die Analyse der pankreatischen Differenzierung und die Etablierung eines dreidimensionalen (3D) Co-Kultursystems notwendig. Hierzu wurden 3D Matrizen aus dem Schweinedarm präpariert. Es wurde analysiert, in wie fern dieses 3D Gerüst die pankreatische Differenzierung ermöglicht. Die Kultur muriner transgener Sox17-DSred-exprimierende embryonaler Stammzellen (ES-Zellen) und deren Differenzierung in entodermale Vorläuferzellen des Pankreas wurde gezeigt. Paraffin-Schnitte belegten, dass Zellen in das 3D Gerüst hinein wandern. Die Entwicklung multipotenter pankreatischer Vorläuferzellen wurde durch die Matrizen begünstigt.

Die pankreatische Differenzierung muriner ES Zellen wurde anhand eines Embyoidbody-basierten Differenzierungsmodells ohne Matrizen validiert. Die Anwendung von 3D Matrizen wurde in einem nächsten Schritt in das Protokoll aufgenommen. Die Differenzierung entodermaler Vorläufer wurde auch auf 3D Matrizen bestätigt. Der Einsatz eines Co-Kulturmediums behinderte die Differenzierung entodermaler Vorläufer nicht.

Zur Co-Kultivierung wurden primäre Endothelzellen aus Hautbiopsien und aus der Nabelschnur gewonnen. Die Proteinexpression wichtiger Endothelzellmarker wie von-Willebrand-Faktor wurde durch das pankreatische Differenzierungsmedium herunterreguliert. Um dies zu verhindern wurde ein spezielles Co-Kulturmedium etabliert.

Die Erkenntnisse aus dem murinen System wurden auf die Differenzierung von IMR90 iPS- und H9 ES-Zellen übertragen. Die Proteinexpression von ONSL und weitere Pluripotenzmarker in IMR90 iPS-Zellen wurde validiert. Danach wurde die pankreatische Differenzierung ohne 3D Co-Kultur validiert. Dabei wurde eine gerichtete Induktion entodermaler Vorläuferzellen einer spontanen Differenzierung gegenüber gestellt. Die gerichtete Differenzierung führte zur Bildung Pdx1-positiver multipotenter pankreatischer Vorläuferzellen. Nachfolgend wurde die pankreatische Differenzierung von entodermalen Vorläuferzellen in der Gegenwart von Endothelzellen analysiert. Die Transkriptanalyse zeigte, dass Marker für die Differenzierung endokriner Vorläuferzellen in der Co-Kultur mit Endothelzellen gleichbleibend exprimiert oder herunter reguliert werden. Weiterhin wurden Co-Kulturen auf die Matrizen aufgebracht und analysiert. Die Analyse mit Lebend- und Tot-Farbstoffen zeigte, dass differenzierende Zellen als auch Endothelzellen vital co-kultiviert wurden. Eine Transkriptanalyse belegte jedoch, dass Marker für die Differenzierung endokrine Vorläuferzellen in der 3D Co-Kultur mit Endothelzellen herunter reguliert werden. Eine Co-Kultur zu einem späteren Differenzierungszeitpunkt lässt sich daraus ableiten.

Eine endgültige Antwort auf die Frage wie sich genetische Prädispositionen analysieren lassen kann diese Arbeit nur im Ansatz beantworten. Basierend auf den gewonnen Erkenntnissen erscheint es jedoch möglich, dass durch weitere Modifikation der nicht-viralen Reprogrammierungs-Methoden die Herstellung nicht-viraler iPS-Zellen ermöglicht werden kann. Die Modifikation des Co-Kulturmodells stellt eine organotypische terminale Differenzierung in Aussicht.

7. REFERENCES

- Aasen, T. and Izpisua Belmonte, J.C. (2010). Isolation and cultivation of human keratinocytes from skin or plucked hair for the generation of induced pluripotent stem cells. *Nat. Protoc.* 5, 371-382.
- Aasen, T.; Raya, A.; Barrero, M.J.; Garreta, E. et al. (2008). Efficient and rapid generation of induced pluripotent stem cells from human keratinocytes. *Nat. Biotechnol.* 26, 1276-1284.
- Abdelalim, E.M. and Tooyama, I. (2012). The p53 inhibitor, pifithrin- α , suppresses self-renewal of embryonic stem cells. *Biochem. Biophys. Res. Commun.* 420, 605-610.
- Abel, T. and Zukin, R.S. (2008). Epigenetic targets of HDAC inhibition in neurodegenerative and psychiatric disorders. *Curr. Opin. Pharmacol.* 8, 57-64.
- Abraham, S.; Sheridan, S.D.; Miller, B.; Rao, R.R. (2010). Stable propagation of human embryonic and induced pluripotent stem cells on decellularized human substrates. *Biotechnol. Prog.* 26, 1126-1134.
- Abu-Remaileh, M.; Gerson, A.; Farago, M.; Nathan, G. et al. (2010). Oct-3/4 regulates stem cell identity and cell fate decisions by modulating Wnt/ β -catenin signalling. *EMBO J.* 29, 3236-3248.
- Adegani, F.J.; Langroudi, L.; Arefian, E.; Shafiee, A. et al. (2013). A comparison of pluripotency and differentiation status of four mesenchymal adult stem cells. *Mol. Biol. Rep.* 40, 3693-3703.
- Agarwal, S.; Holton, K.L.; Lanza, R. (2008). Efficient differentiation of functional hepatocytes from human embryonic stem cells. *Stem Cells* 26, 1117-1127.
- Akinci, E.; Banga, A.; Tungatt, K.; Segal, J. et al. (2013). Reprogramming of various cell types to a beta-like state by Pdx1, Ngn3 and MafA. *PLoS. One.* 8, e82424.
- Aloysius, N. and Nair, P.D. (2013). Enhanced survival and function of islet like clusters differentiated from adipose stem cells on a three dimensional natural polymeric scaffold: An in vitro study. *Tissue Eng Part A.*
- Altun, G.; Loring, J.F.; Laurent, L.C. (2010). DNA methylation in embryonic stem cells. *J. Cell Biochem.* 109, 1-6.
- Amani, D.; Farjadian, S.; Ghaderi, A. (2008). The frequency of transforming growth factor- β 1 gene polymorphisms in a normal southern Iranian population. *Int. J. Immunogenet.* 35, 145-151.
- Amaral, P.P.; Neyt, C.; Wilkins, S.J.; Askarian-Amiri, M.E. et al. (2009). Complex architecture and regulated expression of the Sox2ot locus during vertebrate development. *RNA.* 15, 2013-2027.
- An, W.G.; Kanekal, M.; Simon, M.C.; Maltepe, E. et al. (1998). Stabilization of wild-type p53 by hypoxia-inducible factor 1 α . *Nature* 392, 405-408.
- Anokye-Danso, F.; Trivedi, C.M.; Jühr, D.; Gupta, M. et al. (2011). Highly efficient miRNA-mediated reprogramming of mouse and human somatic cells to pluripotency. *Cell Stem Cell* 8, 376-388.
- Aoi, T.; Yae, K.; Nakagawa, M.; Ichisaka, T. et al. (2008). Generation of pluripotent stem cells from adult mouse liver and stomach cells. *Science* 321, 699-702.
- Apelqvist, A.; Li, H.; Sommer, L.; Beatus, P. et al. (1999). Notch signalling controls pancreatic cell differentiation. *Nature* 400, 877-881.
- Aran, B.; Sole, M.; Rodriguez-Piza, I.; Parriego, M. et al. (2012). Vitrified blastocysts from Preimplantation Genetic Diagnosis (PGD) as a source for human Embryonic Stem Cell (hESC) derivation. *J. Assist. Reprod. Genet.* 29, 1013-1020.
- Arand, J.; Spieler, D.; Karius, T.; Branco, M.R. et al. (2012). In vivo control of CpG and non-CpG DNA methylation by DNA methyltransferases. *PLoS. Genet.* 8, e1002750.
- Ashery-Padan, R.; Zhou, X.; Marquardt, T.; Herrera, P. et al. (2004). Conditional inactivation of Pax6 in the pancreas causes early onset of diabetes. *Dev. Biol.* 269, 479-488.
- Aslan, H.; Zilberman, Y.; Arbeli, V.; Sheyn, D. et al. (2006). Nucleofection-based ex vivo nonviral gene delivery to human stem cells as a platform for tissue regeneration. *Tissue Eng* 12, 877-889.
- Assady, S.; Maor, G.; Amit, M.; Itskovitz-Eldor, J. et al. (2001). Insulin production by human embryonic stem cells. *Diabetes* 50, 1691-1697.
- Atlasi, Y.; Mowla, S.J.; Ziaee, S.A.; Gokhale, P.J. et al. (2008). OCT4 spliced variants are differentially expressed in human pluripotent and nonpluripotent cells. *Stem Cells* 26, 3068-3074.
- Avilion, A.A.; Nicolis, S.K.; Pevny, L.H.; Perez, L. et al. (2003). Multipotent cell lineages in early mouse development depend on SOX2 function. *Genes Dev.* 17, 126-140.
- Baek, D.; Villen, J.; Shin, C.; Camargo, F.D. et al. (2008). The impact of microRNAs on protein output. *Nature* 455, 64-71.
- Baetge, E.E. (2008). Production of beta-cells from human embryonic stem cells. *Diabetes Obes. Metab* 10 Suppl 4, 186-194.
- Baiu, D.; Meriam, F.; Odorico, J. (2011). Potential pathways to restore beta-cell mass: pluripotent stem cells, reprogramming, and endogenous regeneration. *Curr. Diab. Rep.* 11, 392-401.
- Banerjee, I.; Sharma, N.; Yamush, M. (2011). Impact of co-culture on pancreatic differentiation of embryonic stem cells. *J. Tissue Eng Regen. Med.* 5, 313-323.
- Banerjee, S.; Dhara, S.K.; Bacanamwo, M. (2012). Endoglin is a novel endothelial cell specification gene. *Stem Cell Res.* 8, 85-96.
- Bar-Nur, O.; Russ, H.A.; Efrat, S.; Benvenisty, N. (2011). Epigenetic memory and preferential lineage-specific differentiation in induced pluripotent stem cells derived from human pancreatic islet beta cells. *Cell Stem Cell* 9, 17-23.
- Barakat, A.; Wall, P.K.; DiIoreto, S.; Depamphilis, C.W. et al. (2007). Conservation and divergence of microRNAs in *Populus*. *BMC. Genomics* 8, 481.
- Barik, S. (2008). An intronic microRNA silences genes that are functionally antagonistic to its host gene. *Nucleic Acids Res.* 36, 5232-5241.
- Barrandon, Y. and Green, H. (1987). Three clonal types of keratinocyte with different capacities for multiplication. *Proc. Natl. Acad. Sci. U. S. A* 84, 2302-2306.
- Barroso-delJesus, A.; Romero-Lopez, C.; Lucena-Aguilar, G.; Melen, G.J. et al. (2008). Embryonic stem cell-specific miR302-367 cluster: human gene structure and functional characterization of its core promoter. *Mol. Cell Biol.* 28, 6609-6619.
- Bartel, D.P. (2009). MicroRNAs: target recognition and regulatory functions. *Cell* 136, 215-233.
- Beattie, G.M.; Lopez, A.D.; Bucay, N.; Hinton, A. et al. (2005). Activin A maintains pluripotency of human embryonic stem cells in the absence of feeder layers. *Stem Cells* 23, 489-495.
- Bechetolle, N.; Vachon, H.; Gaydon, A.; Boher, A. et al. (2011). A new organotypic model containing dermal-type macrophages. *Exp. Dermatol.* 20, 1035-1037.
- Bentwich, I.; Avniel, A.; Karov, Y.; Aharonov, R. et al. (2005). Identification of hundreds of conserved and nonconserved human microRNAs. *Nat. Genet.* 37, 766-770.

- Berardi, E.; Poes, M.; Thorrez, L.; Sampaolesi, M. (2012). miRNAs in ESC differentiation. *Am. J. Physiol Heart Circ. Physiol* 303, H931-H939.
- Berni, C.R.; Di, C.M.; Leone, L. (2012). The epigenetic effects of butyrate: potential therapeutic implications for clinical practice. *Clin. Epigenetics* 4, 4.
- Bernstein, B.E.; Meissner, A.; Lander, E.S. (2007). The mammalian epigenome. *Cell* 128, 669-681.
- Bernstein, E.; Kim, S.Y.; Carmell, M.A.; Murchison, E.P. et al. (2003). Dicer is essential for mouse development. *Nat. Genet.* 35, 215-217.
- Betel, D.; Koppal, A.; Agius, P.; Sander, C. et al. (2010). Comprehensive modeling of microRNA targets predicts functional non-conserved and non-canonical sites. *Genome Biol.* 11, R90.
- Bezair, V.; Mairal, A.; Ribet, C.; Lefort, C. et al. (2009). Contribution of adipose triglyceride lipase and hormone-sensitive lipase to lipolysis in hMADS adipocytes. *J. Biol. Chem.* 284, 18282-18291.
- Bhandari, D.R.; Seo, K.W.; Roh, K.H.; Jung, J.W. et al. (2010). REX-1 expression and p38 MAPK activation status can determine proliferation/differentiation fates in human mesenchymal stem cells. *PLoS. One.* 5, e10493.
- Biermann, J.; Boyle, J.; Pielen, A.; Lagreze, W.A. (2011). Histone deacetylase inhibitors sodium butyrate and valproic acid delay spontaneous cell death in purified rat retinal ganglion cells. *Mol. Vis.* 17, 395-403.
- Bird, A. (2002). DNA methylation patterns and epigenetic memory. *Genes Dev.* 16, 6-21.
- Blanpain, C. and Fuchs, E. (2009). Epidermal homeostasis: a balancing act of stem cells in the skin. *Nat. Rev. Mol. Cell Biol.* 10, 207-217.
- Blaschke, K.; Ebata, K.T.; Karimi, M.M.; Zepeda-Martinez, J.A. et al. (2013). Vitamin C induces Tet-dependent DNA demethylation and a blastocyst-like state in ES cells. *Nature* 500, 222-226.
- Blyszczuk, P.; Asbrand, C.; Rozzo, A.; Kania, G. et al. (2004). Embryonic stem cells differentiate into insulin-producing cells without selection of nestin-expressing cells. *Int. J. Dev. Biol.* 48, 1095-1104.
- Blyszczuk, P.; Czyz, J.; Kania, G.; Wagner, M. et al. (2003). Expression of Pax4 in embryonic stem cells promotes differentiation of nestin-positive progenitor and insulin-producing cells. *Proc. Natl. Acad. Sci. U. S. A* 100, 998-1003.
- Bock, C.; Kiskinis, E.; Verstappen, G.; Gu, H. et al. (2011). Reference Maps of human ES and iPS cell variation enable high-throughput characterization of pluripotent cell lines. *Cell* 144, 439-452.
- Bodnar, A.G.; Ouellette, M.; Frolkis, M.; Holt, S.E. et al. (1998). Extension of life-span by introduction of telomerase into normal human cells. *Science* 279, 349-352.
- Bonal, C. and Herrera, P.L. (2008). Genes controlling pancreas ontogeny. *Int. J. Dev. Biol.* 52, 823-835.
- Bone, H.K.; Nelson, A.S.; Goldring, C.E.; Tosh, D. et al. (2011). A novel chemically directed route for the generation of definitive endoderm from human embryonic stem cells based on inhibition of GSK-3. *J. Cell Sci.* 124, 1992-2000.
- Borowiak, M. (2010). The new generation of beta-cells: replication, stem cell differentiation, and the role of small molecules. *Rev. Diabet. Stud.* 7, 93-104.
- Borowiak, M.; Maehr, R.; Chen, S.; Chen, A.E. et al. (2009). Small molecules efficiently direct endodermal differentiation of mouse and human embryonic stem cells. *Cell Stem Cell* 4, 348-358.
- Bosia, C.; Osella, M.; Baroudi, M.E.; Cora, D. et al. (2012). Gene autoregulation via intronic microRNAs and its functions. *BMC. Syst. Biol.* 6, 131.
- Boyd, A.S.; Wu, D.C.; Higashi, Y.; Wood, K.J. (2008). A comparison of protocols used to generate insulin-producing cell clusters from mouse embryonic stem cells. *Stem Cells* 26, 1128-1137.
- Boyer, L.A.; Lee, T.I.; Cole, M.F.; Johnstone, S.E. et al. (2005). Core transcriptional regulatory circuitry in human embryonic stem cells. *Cell* 122, 947-956.
- Brautigam, C.; Raggioli, A.; Winter, J. (2013). The Wnt/beta-catenin pathway regulates the expression of the miR-302 cluster in mouse ESCs and P19 cells. *PLoS. One.* 8, e75315.
- Brissova, M.; Fowler, M.J.; Nicholson, W.E.; Chu, A. et al. (2005). Assessment of human pancreatic islet architecture and composition by laser scanning confocal microscopy. *J. Histochem. Cytochem.* 53, 1087-1097.
- Brivanlou, A.H.; Gage, F.H.; Jaenisch, R.; Jessell, T. et al. (2003). Stem cells. Setting standards for human embryonic stem cells. *Science* 300, 913-916.
- Bruder, S.P.; Jaiswal, N.; Haynesworth, S.E. (1997). Growth kinetics, self-renewal, and the osteogenic potential of purified human mesenchymal stem cells during extensive subcultivation and following cryopreservation. *J. Cell Biochem.* 64, 278-294.
- Brueckner, B.; Garcia, B.R.; Siedlecki, P.; Musch, T. et al. (2005). Epigenetic reactivation of tumor suppressor genes by a novel small-molecule inhibitor of human DNA methyltransferases. *Cancer Res.* 65, 6305-6311.
- Burdon, T.; Stracey, C.; Chambers, I.; Nichols, J. et al. (1999). Suppression of SHP-2 and ERK signalling promotes self-renewal of mouse embryonic stem cells. *Dev. Biol.* 210, 30-43.
- Butler, A.E.; Janson, J.; Bonner-Weir, S.; Ritzel, R. et al. (2003). Beta-cell deficit and increased beta-cell apoptosis in humans with type 2 diabetes. *Diabetes* 52, 102-110.
- Butler, J.S.; Koutelou, E.; Schibler, A.C.; Dent, S.Y. (2012). Histone-modifying enzymes: regulators of developmental decisions and drivers of human disease. *Epigenomics* 4, 163-177.
- Caffrey, D.R.; Zhao, J.; Song, Z.; Schaffer, M.E. et al. (2011). siRNA off-target effects can be reduced at concentrations that match their individual potency. *PLoS. One.* 6, e21503.
- Calabrese, J.M.; Seila, A.C.; Yeo, G.W.; Sharp, P.A. (2007). RNA sequence analysis defines Dicer's role in mouse embryonic stem cells. *Proc. Natl. Acad. Sci. U. S. A* 104, 18097-18102.
- Calo, E. and Wysocka, J. (2013). Modification of enhancer chromatin: what, how, and why? *Mol. Cell* 49, 825-837.
- Campbell, P.A.; Perez-Iratxeta, C.; Andrade-Navarro, M.A.; Rudnicki, M.A. (2007). Oct4 targets regulatory nodes to modulate stem cell function. *PLoS. One.* 2, e553.
- Cantz, T.; Key, G.; Bleidissel, M.; Gentile, L. et al. (2008). Absence of OCT4 expression in somatic tumor cell lines. *Stem Cells* 26, 692-697.
- Cao, F.; Wagner, R.A.; Wilson, K.D.; Xie, X. et al. (2008). Transcriptional and functional profiling of human embryonic stem cell-derived cardiomyocytes. *PLoS. One.* 3, e3474.
- Cao, H.; Chu, Y.; Lv, X.; Qiu, P. et al. (2012). GSK3 inhibitor-BIO regulates proliferation of immortalized pancreatic mesenchymal stem cells (iPMSCs). *PLoS. One.* 7, e31502.
- Card, D.A.; Hebbar, P.B.; Li, L.; Trotter, K.W. et al. (2008). Oct4/Sox2-regulated miR-302 targets cyclin D1 in human embryonic stem cells. *Mol. Cell Biol.* 28, 6426-6438.
- Caricasole, A.A.; van Schaik, R.H.; Zeinstra, L.M.; Wierix, C.D. et al. (1998). Human growth-differentiation factor 3 (hGDF3): developmental regulation in human teratocarcinoma cell lines and expression in primary testicular germ cell tumours. *Oncogene* 16, 95-103.

- Caminci, P.; Sandelin, A.; Lenhard, B.; Katayama, S. et al. (2006). Genome-wide analysis of mammalian promoter architecture and evolution. *Nat. Genet.* 38, 626-635.
- Cauffman, G.; Liebaers, I.; Van, S.A.; Van, d., V (2006). POU5F1 isoforms show different expression patterns in human embryonic stem cells and preimplantation embryos. *Stem Cells* 24, 2685-2691.
- Challagundla, K.B.; Sun, X.X.; Zhang, X.; DeVine, T. et al. (2011a). Ribosomal protein L11 recruits miR-24/miRISC to repress c-Myc expression in response to ribosomal stress. *Mol. Cell Biol.* 31, 4007-4021.
- Challagundla, K.B.; Sun, X.X.; Zhang, X.; DeVine, T. et al. (2011b). Ribosomal protein L11 recruits miR-24/miRISC to repress c-Myc expression in response to ribosomal stress. *Mol. Cell Biol.* 31, 4007-4021.
- Chambers, S.M.; Fasano, C.A.; Papapetrou, E.P.; Tomishima, M. et al. (2009). Highly efficient neural conversion of human ES and iPS cells by dual inhibition of SMAD signaling. *Nat. Biotechnol.* 27, 275-280.
- Chang, Y.; Zhang, X.; Horton, J.R.; Upadhyay, A.K. et al. (2009). Structural basis for G9a-like protein lysine methyltransferase inhibition by BIX-01294. *Nat. Struct. Mol. Biol.* 16, 312-317.
- Chapman, E.J.; Kelly, G.; Knowles, M.A. (2008). Genes involved in differentiation, stem cell renewal, and tumorigenesis are modulated in telomerase-immortalized human urothelial cells. *Mol. Cancer Res.* 6, 1154-1168.
- Chen, A.E.; Borowiak, M.; Sherwood, R.I.; Kweudjeu, A. et al. (2013). Functional evaluation of ES cell-derived endodermal populations reveals differences between Nodal and Activin A-guided differentiation. *Development* 140, 675-686.
- Chen, G.; Gulbranson, D.R.; Hou, Z.; Bolin, J.M. et al. (2011). Chemically defined conditions for human iPSC derivation and culture. *Nat. Methods* 8, 424-429.
- Chen, T.; Ueda, Y.; Xie, S.; Li, E. (2002). A novel Dnmt3a isoform produced from an alternative promoter localizes to euchromatin and its expression correlates with active de novo methylation. *J. Biol. Chem.* 277, 38746-38754.
- Chen, Y.; Yao, Y.; Sumi, Y.; Li, A. et al. (2010). Purinergic signaling: a fundamental mechanism in neutrophil activation. *Sci. Signal.* 3, ra45.
- Chen, Z.Y.; He, C.Y.; Kay, M.A. (2005). Improved production and purification of minicircle DNA vector free of plasmid bacterial sequences and capable of persistent transgene expression in vivo. *Hum. Gene Ther.* 16, 126-131.
- Chen, Z.Y.; He, C.Y.; Meuse, L.; Kay, M.A. (2004). Silencing of episomal transgene expression by plasmid bacterial DNA elements in vivo. *Gene Ther.* 11, 856-864.
- Cheong, C.Y. and Lufkin, T. (2011). Alternative splicing in self-renewal of embryonic stem cells. *Stem Cells Int.* 2011, 560261.
- Cheung, H.H.; Davis, A.J.; Lee, T.L.; Pang, A.L. et al. (2011). Methylation of an intronic region regulates miR-199a in testicular tumor malignancy. *Oncogene* 30, 3404-3415.
- Chew, J.L.; Loh, Y.H.; Zhang, W.; Chen, X. et al. (2005). Reciprocal transcriptional regulation of Pou5f1 and Sox2 via the Oct4/Sox2 complex in embryonic stem cells. *Mol. Cell Biol.* 25, 6031-6046.
- Chhabra, A. and Mikkola, H.K. (2011). Return to youth with Sox17. *Genes Dev.* 25, 1557-1562.
- Chien, E.K.; Saunders, T.; Phillippe, M. (1996). The mechanisms underlying Bay K 8644-stimulated phasic myometrial contractions. *J. Soc. Gynecol. Investig.* 3, 106-112.
- Chin, M.H.; Mason, M.J.; Xie, W.; Volinia, S. et al. (2009). Induced pluripotent stem cells and embryonic stem cells are distinguished by gene expression signatures. *Cell Stem Cell* 5, 111-123.
- Choi, I.; Carey, T.S.; Wilson, C.A.; Knott, J.G. (2013). Evidence that transcription factor AP-2gamma is not required for Oct4 repression in mouse blastocysts. *PLoS. One.* 8, e65771.
- Choi, S.H.; Heo, K.; Byun, H.M.; An, W. et al. (2011). Identification of preferential target sites for human DNA methyltransferases. *Nucleic Acids Res.* 39, 104-118.
- Chow, D.C.; Wenning, L.A.; Miller, W.M.; Papoutsakis, E.T. (2001). Modeling pO(2) distributions in the bone marrow hematopoietic compartment. II. Modified Kroghian models. *Biophys. J.* 81, 685-696.
- Chung, W.S.; Andersson, O.; Row, R.; Kimelman, D. et al. (2010). Suppression of Alk8-mediated Bmp signaling cell-autonomously induces pancreatic beta-cells in zebrafish. *Proc. Natl. Acad. Sci. U. S. A* 107, 1142-1147.
- Cipro, S.; Hrebackova, J.; Hrabeta, J.; Poljakova, J. et al. (2012). Valproic acid overcomes hypoxia-induced resistance to apoptosis. *Oncol. Rep.* 27, 1219-1226.
- Clark, A.T.; Rodriguez, R.T.; Bodnar, M.S.; Abeyta, M.J. et al. (2004). Human STELLAR, NANOG, and GDF3 genes are expressed in pluripotent cells and map to chromosome 12p13, a hotspot for teratocarcinoma. *Stem Cells* 22, 169-179.
- Clarke, M.F.; Dick, J.E.; Dirks, P.B.; Eaves, C.J. et al. (2006). Cancer stem cells—perspectives on current status and future directions: AACR Workshop on cancer stem cells. *Cancer Res.* 66, 9339-9344.
- Cleaver, O. and Dor, Y. (2012). Vascular instruction of pancreas development. *Development* 139, 2833-2843.
- Coccheri, S. (2007). Approaches to prevention of cardiovascular complications and events in diabetes mellitus. *Drugs* 67, 997-1026.
- Coleman, M.L. and Olson, M.F. (2002). Rho GTPase signalling pathways in the morphological changes associated with apoptosis. *Cell Death. Differ.* 9, 493-504.
- Collombat, P.; Mansouri, A.; Hecksher-Sorensen, J.; Serup, P. et al. (2003). Opposing actions of Arx and Pax4 in endocrine pancreas development. *Genes Dev.* 17, 2591-2603.
- Culmes, M.; Eckstein, H.H.; Burgkart, R.; Nussler, A.K. et al. (2013). Endothelial differentiation of adipose-derived mesenchymal stem cells is improved by epigenetic modifying drug BIX-01294. *Eur. J. Cell Biol.* 92, 70-79.
- D'Amour, K.A.; Bang, A.G.; Eliazar, S.; Kelly, O.G. et al. (2006). Production of pancreatic endocrine cells from human embryonic stem cells. *Nat. Biotechnol.* 24, 1392-1401.
- D'Ippolito, G.; Diabira, S.; Howard, G.A.; Menei, P. et al. (2004). Marrow-isolated adult multilineage inducible (MIAMI) cells, a unique population of postnatal young and old human cells with extensive expansion and differentiation potential. *J. Cell Sci.* 117, 2971-2981.
- Dallas, M.R.; Chen, S.H.; Streppel, M.M.; Sharma, S. et al. (2012). Sialofucosylated podocalyxin is a functional E- and L-selectin ligand expressed by metastatic pancreatic cancer cells. *Am. J. Physiol Cell Physiol* 303, C616-C624.
- Daneman, D. (2006). Type 1 diabetes. *Lancet* 367, 847-858.
- Das, S.; Jena, S.; Levasseur, D.N. (2011). Alternative splicing produces Nanog protein variants with different capacities for self-renewal and pluripotency in embryonic stem cells. *J. Biol. Chem.* 286, 42690-42703.
- De, C.E.; Baiguera, S.; Conconi, M.T.; Vigolo, S. et al. (2010). Pancreatic acellular matrix supports islet survival and function in a synthetic tubular device: in vitro and in vivo studies. *Int. J. Mol. Med.* 25, 195-202.

- De, C.P.; Bartsch, G., Jr.; Siddiqui, M.M.; Xu, T. et al. (2007). Isolation of amniotic stem cell lines with potential for therapy. *Nat. Biotechnol.* 25, 100-106.
- Deng, J.; Shoemaker, R.; Xie, B.; Gore, A. et al. (2009). Targeted bisulfite sequencing reveals changes in DNA methylation associated with nuclear reprogramming. *Nat. Biotechnol.* 27, 353-360.
- Deng, Y.; Liu, Q.; Luo, C.; Chen, S. et al. (2012). Generation of induced pluripotent stem cells from buffalo (*Bubalus bubalis*) fetal fibroblasts with buffalo defined factors. *Stem Cells Dev.* 21, 2485-2494.
- Denham, M.; Bye, C.; Leung, J.; Conley, B.J. et al. (2012). Glycogen synthase kinase 3beta and activin/nodal inhibition in human embryonic stem cells induces a pre-neuroepithelial state that is required for specification to a floor plate cell lineage. *Stem Cells* 30, 2400-2411.
- Denoon, A. (2011). *Brustle v. Greenpeace: implications for stem cell research.* *Regen. Med.* 6, 85-87.
- Digirolamo, C.M.; Stokes, D.; Colter, D.; Phinney, D.G. et al. (1999). Propagation and senescence of human marrow stromal cells in culture: a simple colony-forming assay identifies samples with the greatest potential to propagate and differentiate. *Br. J. Haematol.* 107, 275-281.
- Ding, L.; Paszkowski-Rogacz, M.; Nitzsche, A.; Slabicki, M.M. et al. (2009). A genome-scale RNAi screen for Oct4 modulators defines a role of the Paf1 complex for embryonic stem cell identity. *Cell Stem Cell* 4, 403-415.
- Direnzo, D.; Hess, D.A.; Damsz, B.; Hallett, J.E. et al. (2012). Induced *Mist1* expression promotes remodeling of mouse pancreatic acinar cells. *Gastroenterology* 143, 469-480.
- Dolezalova, D.; Mraz, M.; Barta, T.; Plevova, K. et al. (2012). MicroRNAs regulate p21(*Waf1/Cip1*) protein expression and the DNA damage response in human embryonic stem cells. *Stem Cells* 30, 1362-1372.
- Dor, Y.; Brown, J.; Martinez, O.I.; Melton, D.A. (2004). Adult pancreatic beta-cells are formed by self-duplication rather than stem-cell differentiation. *Nature* 429, 41-46.
- Duan, P.; Zhang, Y.; Han, X.; Liu, J. et al. (2012). Effect of neuronal induction on NSE, Tau, and Oct4 promoter methylation in bone marrow mesenchymal stem cells. *In Vitro Cell Dev. Biol. Anim* 48, 251-258.
- Dvorak, P.; Dvorakova, D.; Koskova, S.; Vodinska, M. et al. (2005). Expression and potential role of fibroblast growth factor 2 and its receptors in human embryonic stem cells. *Stem Cells* 23, 1200-1211.
- Dweep, H.; Sticht, C.; Pandey, P.; Gretz, N. (2011). miRWalk—database: prediction of possible miRNA binding sites by "walking" the genes of three genomes. *J. Biomed. Inform.* 44, 839-847.
- Edghill, E.L.; Flanagan, S.E.; Patch, A.M.; Boustred, C. et al. (2008). Insulin mutation screening in 1,044 patients with diabetes: mutations in the *INS* gene are a common cause of neonatal diabetes but a rare cause of diabetes diagnosed in childhood or adulthood. *Diabetes* 57, 1034-1042.
- Elstner, A.; Damaschun, A.; Kurtz, A.; Stacey, G. et al. (2009). The changing landscape of European and international regulation on embryonic stem cell research. *Stem Cell Res.* 2, 101-107.
- Esteban, M.A.; Wang, T.; Qin, B.; Yang, J. et al. (2010). Vitamin C enhances the generation of mouse and human induced pluripotent stem cells. *Cell Stem Cell* 6, 71-79.
- Evans, M.J. and Kaufman, M.H. (1981). Establishment in culture of pluripotential cells from mouse embryos. *Nature* 292, 154-156.
- Evans, W.E. and McLeod, H.L. (2003). Pharmacogenomics—drug disposition, drug targets, and side effects. *N. Engl. J. Med.* 348, 538-549.
- Ezashi, T.; Das, P.; Roberts, R.M. (2005). Low O₂ tensions and the prevention of differentiation of hES cells. *Proc. Natl. Acad. Sci. U. S. A* 102, 4783-4788.
- Ezeh, U.I.; Turek, P.J.; Reijo, R.A.; Clark, A.T. (2005). Human embryonic stem cell genes OCT4, NANOG, STELLAR, and GDF3 are expressed in both seminoma and breast carcinoma. *Cancer* 104, 2255-2265.
- Fabian, M.R.; Sonenberg, N.; Filipowicz, W. (2010). Regulation of mRNA translation and stability by microRNAs. *Annu. Rev. Biochem.* 79, 351-379.
- Federation, A.J.; Bradner, J.E.; Meissner, A. (2013). The use of small molecules in somatic-cell reprogramming. *Trends Cell Biol.*
- Feldman, N.; Gerson, A.; Fang, J.; Li, E. et al. (2006). G9a-mediated irreversible epigenetic inactivation of Oct-3/4 during early embryogenesis. *Nat. Cell Biol.* 8, 188-194.
- Feng, Q.; Lu, S.J.; Klimanskaya, I.; Gomes, I. et al. (2010). Hemangioblastic derivatives from human induced pluripotent stem cells exhibit limited expansion and early senescence. *Stem Cells* 28, 704-712.
- Filby, C.E.; Williamson, R.; van, K.P.; Pebay, A. et al. (2011). Stimulation of Activin A/Nodal signaling is insufficient to induce definitive endoderm formation of cord blood-derived unrestricted somatic stem cells. *Stem Cell Res. Ther.* 2, 16.
- Flasse, L.C.; Pirson, J.L.; Stem, D.G.; Von, B., V et al. (2013). *Ascl1b* and *Neurod1*, instead of *Neurog3*, control pancreatic endocrine cell fate in zebrafish. *BMC. Biol.* 11, 78.
- Fleming, J.L.; Gable, D.L.; Samadzadeh-Tarighat, S.; Cheng, L. et al. (2013). Differential expression of miR-1, a putative tumor suppressing microRNA, in cancer resistant and cancer susceptible mice. *PeerJ.* 1, e68.
- Foja, S.; Jung, M.; Harwardt, B.; Riemann, D. et al. (2013). Hypoxia supports reprogramming of mesenchymal stromal cells via induction of embryonic stem cell-specific microRNA-302 cluster and pluripotency-associated genes. *Cell Reprogram.* 15, 68-79.
- Forstall, C.E.; Wright, K.L.; Hanley, N.A.; Oreffo, R.O. et al. (2010). Hypoxia inducible factors regulate pluripotency and proliferation in human embryonic stem cells cultured at reduced oxygen tensions. *Reproduction.* 139, 85-97.
- Foster, K.W.; Frost, A.R.; McKie-Bell, P.; Lin, C.Y. et al. (2000). Increase of GSKF messenger RNA and protein expression during progression of breast cancer. *Cancer Res.* 60, 6488-6495.
- Fraga, M.F. and Esteller, M. (2002). DNA methylation: a profile of methods and applications. *Biotechniques* 33, 632, 634, 636-632, 634, 649.
- Friedman, J.R. and Kaestner, K.H. (2006). The *Foxa* family of transcription factors in development and metabolism. *Cell Mol. Life Sci.* 63, 2317-2328.
- Friedman, R.C.; Farh, K.K.; Burge, C.B.; Bartel, D.P. (2009). Most mammalian mRNAs are conserved targets of microRNAs. *Genome Res.* 19, 92-105.
- Froeling, F.E.; Mirza, T.A.; Feakins, R.M.; Seedhar, A. et al. (2009). Organotypic culture model of pancreatic cancer demonstrates that stromal cells modulate E-cadherin, beta-catenin, and Ezrin expression in tumor cells. *Am. J. Pathol.* 175, 636-648.
- Fu, S.; Fei, Q.; Jiang, H.; Chuai, S. et al. (2011). Involvement of histone acetylation of *Sox17* and *Foxa2* promoters during mouse definitive endoderm differentiation revealed by microRNA profiling. *PLoS. One.* 6, e27965.
- Fussner, E.; Djuric, U.; Strauss, M.; Hotta, A. et al. (2011). Constitutive heterochromatin reorganization during somatic cell reprogramming. *EMBO J.* 30, 1778-1789.
- Gagnic, P. and Ionescu-Tirgoviste, C. (2012). Eukaryotic genomes may exhibit up to 10 generic classes of gene promoters. *BMC. Genomics* 13, 512.
- Gaidatzis, D.; van, N.E.; Hausser, J.; Zavolan, M. (2007). Inference of miRNA targets using evolutionary conservation and pathway analysis. *BMC. Bioinformatics.* 8, 69.

- Gandarillas, A. and Watt, F.M. (1997). c-Myc promotes differentiation of human epidermal stem cells. *Genes Dev.* 11, 2869-2882.
- Georgia, S.; Kanji, M.; Bhushan, A. (2013). DNMT1 represses p53 to maintain progenitor cell survival during pancreatic organogenesis. *Genes Dev.* 27, 372-377.
- Gerecht-Nir, S.; Cohen, S.; Ziskind, A.; Itskovitz-Eldor, J. (2004). Three-dimensional porous alginate scaffolds provide a conducive environment for generation of well-vascularized embryoid bodies from human embryonic stem cells. *Biotechnol. Bioeng.* 88, 313-320.
- Ghaleb, A.M.; McConnell, B.B.; Nandan, M.O.; Katz, J.P. et al. (2007). Haploinsufficiency of Kruppel-like factor 4 promotes adenomatous polyposis coli dependent intestinal tumorigenesis. *Cancer Res.* 67, 7147-7154.
- Gheisari, Y.; Soleimani, M.; Azadmanesh, K.; Zeinali, S. (2008). Multipotent mesenchymal stromal cells: optimization and comparison of five cationic polymer-based gene delivery methods. *Cytotherapy.* 10, 815-823.
- Ghule, P.N.; Medina, R.; Lengner, C.J.; Mandeville, M. et al. (2011). Reprogramming the pluripotent cell cycle: restoration of an abbreviated G1 phase in human induced pluripotent stem (iPS) cells. *J. Cell Physiol* 226, 1149-1156.
- Gill, J.G.; Langer, E.M.; Lindsley, R.C.; Cai, M. et al. (2011). Snail and the microRNA-200 family act in opposition to regulate epithelial-to-mesenchymal transition and germ layer fate restriction in differentiating ESCs. *Stem Cells* 29, 764-776.
- Ginis, I.; Luo, Y.; Miura, T.; Thies, S. et al. (2004). Differences between human and mouse embryonic stem cells. *Dev. Biol.* 269, 360-380.
- Giraldo, A.M.; DeCourcy, K.; Ball, S.F.; Hylan, D. et al. (2013). Gene expression of Dnmt1 isoforms in porcine oocytes, embryos, and somatic cells. *Cell Reprogram.* 15, 309-321.
- Glamodlija, U. and Jevric-Causevic, A. (2010). Genetic polymorphisms in diabetes: influence on therapy with oral antidiabetics. *Acta Pharm.* 60, 387-406.
- Glass, C. and Singla, D.K. (2011). MicroRNA-1 transfected embryonic stem cells enhance cardiac myocyte differentiation and inhibit apoptosis by modulating the PTEN/Akt pathway in the infarcted heart. *Am. J. Physiol Heart Circ. Physiol* 301, H2038-H2049.
- Goh, S.K.; Bertera, S.; Olsen, P.; Candiello, J.E. et al. (2013a). Perfusion-decellularized pancreas as a natural 3D scaffold for pancreatic tissue and whole organ engineering. *Biomaterials* 34, 6760-6772.
- Goh, S.K.; Olsen, P.; Banerjee, I. (2013b). Extracellular matrix aggregates from differentiating embryoid bodies as a scaffold to support ESC proliferation and differentiation. *PLoS. One.* 8, e61856.
- Gonzalez, F.; Boue, S.; Izpisua Belmonte, J.C. (2011). Methods for making induced pluripotent stem cells: reprogramming a la carte. *Nat. Rev. Genet.* 12, 231-242.
- Gordon, C.A.; Hartono, S.R.; Chedin, F. (2013). Inactive DNMT3B splice variants modulate de novo DNA methylation. *PLoS. One.* 8, e69486.
- Gorospe, M.; Tominaga, K.; Wu, X.; Fahling, M. et al. (2011). Post-Transcriptional Control of the Hypoxic Response by RNA-Binding Proteins and MicroRNAs. *Front Mol. Neurosci.* 4, 7.
- Grabel, L. (2012). Prospects for pluripotent stem cell therapies: into the clinic and back to the bench. *J. Cell Biochem.* 113, 381-387.
- Grabundzija, I.; Wang, J.; Sebe, A.; Erdei, Z. et al. (2013). Sleeping Beauty transposon-based system for cellular reprogramming and targeted gene insertion in induced pluripotent stem cells. *Nucleic Acids Res.* 41, 1829-1847.
- Gradwohl, G.; Dierich, A.; LeMeur, M.; Guillemot, F. (2000). neurogenin3 is required for the development of the four endocrine cell lineages of the pancreas. *Proc. Natl. Acad. Sci. U. S. A* 97, 1607-1611.
- Grandjean, V.; Gounon, P.; Wagner, N.; Martin, L. et al. (2009). The miR-124-Sox9 paramutation: RNA-mediated epigenetic control of embryonic and adult growth. *Development* 136, 3647-3655.
- Grayson, W.L.; Zhao, F.; Bunnell, B.; Ma, T. (2007). Hypoxia enhances proliferation and tissue formation of human mesenchymal stem cells. *Biochem. Biophys. Res. Commun.* 358, 948-953.
- Greber, B.; Lehrach, H.; Adjaye, J. (2007a). Fibroblast growth factor 2 modulates transforming growth factor beta signaling in mouse embryonic fibroblasts and human ESCs (hESCs) to support hESC self-renewal. *Stem Cells* 25, 455-464.
- Greber, B.; Lehrach, H.; Adjaye, J. (2007b). Silencing of core transcription factors in human EC cells highlights the importance of autocrine FGF signaling for self-renewal. *BMC. Dev. Biol.* 7, 46.
- Griffiths-Jones, S.; Grocock, R.J.; van, D.S.; Bateman, A. et al. (2006). miRBase: microRNA sequences, targets and gene nomenclature. *Nucleic Acids Res.* 34, D140-D144.
- Gropp, M.; Shilo, V.; Vainer, G.; Gov, M. et al. (2012). Standardization of the teratoma assay for analysis of pluripotency of human ES cells and biosafety of their differentiated progeny. *PLoS. One.* 7, e45532.
- Gross, B.; Sgoddar, M.; Rasche, M.; Schambach, A. et al. (2013). Improved generation of patient-specific induced pluripotent stem cells using a chemically-defined and matrigel-based approach. *Curr. Mol. Med.* 13, 765-776.
- Grunau, C.; Clark, S.J.; Rosenthal, A. (2001). Bisulfite genomic sequencing: systematic investigation of critical experimental parameters. *Nucleic Acids Res.* 29, E65.
- Guan, D.; Zhang, W.; Zhang, W.; Liu, G.H. et al. (2013). Switching cell fate, ncRNAs coming to play. *Cell Death. Dis.* 4, e464.
- Gunaseeli, I.; Doss, M.X.; Antzelevitch, C.; Hescheler, J. et al. (2010). Induced pluripotent stem cells as a model for accelerated patient- and disease-specific drug discovery. *Curr. Med. Chem.* 17, 759-766.
- Guo, R.; Abdelmohsen, K.; Morin, P.J.; Gorospe, M. (2013). Novel MicroRNA Reporter Uncovers Repression of Let-7 by GSK-3beta. *PLoS. One.* 8, e66330.
- Guo, Y.; Chen, Y.; Ito, H.; Watanabe, A. et al. (2006). Identification and characterization of lin-28 homolog B (LIN28B) in human hepatocellular carcinoma. *Gene* 384, 51-61.
- Habener, J.F.; Kemp, D.M.; Thomas, M.K. (2005). Minireview: transcriptional regulation in pancreatic development. *Endocrinology* 146, 1025-1034.
- Haldorsen, I.S.; Vesterhus, M.; Raeder, H.; Jensen, D.K. et al. (2008). Lack of pancreatic body and tail in HNF1B mutation carriers. *Diabet Med.* 25, 782-787.
- Han, S.; Dziedzic, N.; Gadue, P.; Keller, G.M. et al. (2011). An endothelial cell niche induces hepatic specification through dual repression of Wnt and Notch signaling. *Stem Cells* 29, 217-228.
- Hankowski, K.E.; Hamazaki, T.; Umezawa, A.; Terada, N. (2011). Induced pluripotent stem cells as a next-generation biomedical interface. *Lab Invest* 91, 972-977.
- Hanna, J.; Markoulaki, S.; Schorderet, P.; Carey, B.W. et al. (2008). Direct reprogramming of terminally differentiated mature B lymphocytes to pluripotency. *Cell* 133, 250-264.
- Hansson, M.; Tonning, A.; Frandsen, U.; Petri, A. et al. (2004). Artfactual insulin release from differentiated embryonic stem cells. *Diabetes* 53, 2603-2609.

- Hass, R.; Kasper, C.; Bohm, S.; Jacobs, R. (2011). Different populations and sources of human mesenchymal stem cells (MSC): A comparison of adult and neonatal tissue-derived MSC. *Cell Commun. Signal.* 9, 12.
- Hattori, N.; Nishino, K.; Ko, Y.G.; Hattori, N. et al. (2004). Epigenetic control of mouse Oct-4 gene expression in embryonic stem cells and trophoblast stem cells. *J. Biol. Chem.* 279, 17063-17069.
- Hay, D.C.; Fletcher, J.; Payne, C.; Terrace, J.D. et al. (2008). Highly efficient differentiation of hESCs to functional hepatic endoderm requires ActivinA and Wnt3a signaling. *Proc. Natl. Acad. Sci. U. S. A* 105, 12301-12306.
- Helledie, T.; Nurcombe, V.; Cool, S.M. (2008). A simple and reliable electroporation method for human bone marrow mesenchymal stem cells. *Stem Cells Dev.* 17, 837-848.
- Herder, C. and Roden, M. (2011). Genetics of type 2 diabetes: pathophysiologic and clinical relevance. *Eur. J. Clin. Invest* 41, 679-692.
- Herrera, P.L. (2000). Adult insulin- and glucagon-producing cells differentiate from two independent cell lineages. *Development* 127, 2317-2322.
- Herrera, P.L.; Nepote, V.; Delacour, A. (2002). Pancreatic cell lineage analyses in mice. *Endocrine.* 19, 267-278.
- Herrmann, D.; Dahl, J.A.; Lucas-Hahn, A.; Collas, P. et al. (2013). Histone modifications and mRNA expression in the inner cell mass and trophoctoderm of bovine blastocysts. *Epigenetics.* 8, 281-289.
- Hezroni, H.; Tzchori, I.; Davidi, A.; Mattout, A. et al. (2011). H3K9 histone acetylation predicts pluripotency and reprogramming capacity of ES cells. *Nucleus.* 2, 300-309.
- Hock, J. and Meister, G. (2008). The Argonaute protein family. *Genome Biol.* 9, 210.
- Hoffman, L.M. and Carpenter, M.K. (2005). Characterization and culture of human embryonic stem cells. *Nat. Biotechnol.* 23, 699-708.
- Holm, F.; Nikitin, H.; Kjartansdottir, K.R.; Gaudenzi, G. et al. (2013). Passaging techniques and ROCK inhibitor exert reversible effects on morphology and pluripotency marker gene expression of human embryonic stem cell lines. *Stem Cells Dev.* 22, 1883-1892.
- Holowacz, T.; Alexson, T.O.; Coles, B.L.; Doble, B.W. et al. (2013). The responses of neural stem cells to the level of GSK-3 depend on the tissue of origin. *Biol. Open.* 2, 812-821.
- Hong, H.; Takahashi, K.; Ichisaka, T.; Aoi, T. et al. (2009). Suppression of induced pluripotent stem cell generation by the p53-p21 pathway. *Nature* 460, 1132-1135.
- Hori, Y.; Rulifson, I.C.; Tsai, B.C.; Heit, J.J. et al. (2002). Growth inhibitors promote differentiation of insulin-producing tissue from embryonic stem cells. *Proc. Natl. Acad. Sci. U. S. A* 99, 16105-16110.
- Hou, P.; Li, Y.; Zhang, X.; Liu, C. et al. (2013). Pluripotent stem cells induced from mouse somatic cells by small-molecule compounds. *Science* 341, 651-654.
- Hoveizi, E.; Nabiuni, M.; Parivar, K.; Ai, J. et al. (2013). Definitive endoderm differentiation of human-induced pluripotent stem cells using signaling molecules and IDE1 in three-dimensional polymer scaffold. *J. Biomed. Mater. Res. A.*
- Hu, B.Y.; Weick, J.P.; Yu, J.; Ma, L.X. et al. (2010a). Neural differentiation of human induced pluripotent stem cells follows developmental principles but with variable potency. *Proc. Natl. Acad. Sci. U. S. A* 107, 4335-4340.
- Hu, B.Y.; Weick, J.P.; Yu, J.; Ma, L.X. et al. (2010b). Neural differentiation of human induced pluripotent stem cells follows developmental principles but with variable potency. *Proc. Natl. Acad. Sci. U. S. A* 107, 4335-4340.
- Hu, D.; Zhou, Z.; Davidson, N.E.; Huang, Y. et al. (2012). Novel insight into KLF4 proteolytic regulation in estrogen receptor signaling and breast carcinogenesis. *J. Biol. Chem.* 287, 13584-13597.
- Hua, H.; Shang, L.; Martinez, H.; Freeby, M. et al. (2013). iPSC-derived beta cells model diabetes due to glucokinase deficiency. *J. Clin. Invest* 123, 3146-3153.
- Huang, Y.; Pastor, W.A.; Shen, Y.; Tahiliani, M. et al. (2010). The behaviour of 5-hydroxymethylcytosine in bisulfite sequencing. *PLoS. One.* 5, e8888.
- Huangfu, D.; Maehr, R.; Guo, W.; Eijkelenboom, A. et al. (2008a). Induction of pluripotent stem cells by defined factors is greatly improved by small-molecule compounds. *Nat. Biotechnol.* 26, 795-797.
- Huangfu, D.; Osafune, K.; Maehr, R.; Guo, W. et al. (2008b). Induction of pluripotent stem cells from primary human fibroblasts with only Oct4 and Sox2. *Nat. Biotechnol.* 26, 1269-1275.
- Ichida, J.K.; Blanchard, J.; Lam, K.; Son, E.Y. et al. (2009). A small-molecule inhibitor of TGF-beta signaling replaces Sox2 in reprogramming by inducing Nanog. *Cell Stem Cell* 5, 491-503.
- Inada, A.; Nienaber, C.; Katsuta, H.; Fujitani, Y. et al. (2008). Carbonic anhydrase II-positive pancreatic cells are progenitors for both endocrine and exocrine pancreas after birth. *Proc. Natl. Acad. Sci. U. S. A* 105, 19915-19919.
- Inman, G.J.; Nicolas, F.J.; Callahan, J.F.; Harling, J.D. et al. (2002). SB-431542 is a potent and specific inhibitor of transforming growth factor-beta superfamily type I activin receptor-like kinase (ALK) receptors ALK4, ALK5, and ALK7. *Mol. Pharmacol.* 62, 65-74.
- Islam, M.S. and Zhou, H. (2007). Isolation and characterization of putative epidermal stem cells derived from Cashmere goat fetus. *Eur. J. Dermatol.* 17, 302-308.
- Jacob, J.; Ribes, V.; Moore, S.; Constable, S.C. et al. (2014). Valproic acid silencing of *asc1b/Ascl1* results in the failure of serotonergic differentiation in a zebrafish model of fetal valproate syndrome. *Dis. Model. Mech.* 7, 107-117.
- Jaenisch, R. and Young, R. (2008). Stem cells, the molecular circuitry of pluripotency and nuclear reprogramming. *Cell* 132, 567-582.
- James, D.; Levine, A.J.; Besser, D.; Hemmati-Brivanlou, A. (2005). TGFbeta/activin/nodal signaling is necessary for the maintenance of pluripotency in human embryonic stem cells. *Development* 132, 1273-1282.
- Jang, J.; Yoo, J.E.; Lee, J.A.; Lee, D.R. et al. (2012). Disease-specific induced pluripotent stem cells: a platform for human disease modeling and drug discovery. *Exp. Mol. Med.* 44, 202-213.
- Jaramillo, M. and Banerjee, I. (2012). Endothelial cell co-culture mediates maturation of human embryonic stem cell to pancreatic insulin producing cells in a directed differentiation approach. *J. Vis. Exp.*
- Jensen, P.L.; Beck, H.C.; Petersen, J.; Hreinsson, J. et al. (2013). Proteomic analysis of human blastocoel fluid and blastocyst cells. *Stem Cells Dev.* 22, 1126-1135.
- Jensen, T.; Roszell, B.; Zang, F.; Girard, E. et al. (2012). A rapid lung de-cellularization protocol supports embryonic stem cell differentiation in vitro and following implantation. *Tissue Eng Part C. Methods* 18, 632-646.
- Ji, S.; Zhang, L.; Hui, L. (2013). Cell fate conversion: direct induction of hepatocyte-like cells from fibroblasts. *J. Cell Biochem.* 114, 256-265.
- Jia, F.; Wilson, K.D.; Sun, N.; Gupta, D.M. et al. (2010). A nonviral minicircle vector for deriving human iPS cells. *Nat. Methods* 7, 197-199.
- Jiang, J.; Au, M.; Lu, K.; Eshpeter, A. et al. (2007). Generation of insulin-producing islet-like clusters from human embryonic stem cells. *Stem Cells* 25, 1940-1953.
- Jiang, J.; Chan, Y.S.; Loh, Y.H.; Cai, J. et al. (2008). A core Klf circuitry regulates self-renewal of embryonic stem cells. *Nat. Cell Biol.* 10, 353-360.

- Joglekar, M.V.; Parekh, V.S.; Hardikar, A.A. (2011). Islet-specific microRNAs in pancreas development, regeneration and diabetes. *Indian J. Exp. Biol.* 49, 401-408.
- Johannesson, M.; Stahlberg, A.; Ameri, J.; Sand, F.W. et al. (2009). FGF4 and retinoic acid direct differentiation of hESCs into PDX1-expressing foregut endoderm in a time- and concentration-dependent manner. *PLoS. One.* 4, e4794.
- Johansson, B.M. and Wiles, M.V. (1995). Evidence for involvement of activin A and bone morphogenetic protein 4 in mammalian mesoderm and hematopoietic development. *Mol. Cell Biol.* 15, 141-151.
- Johansson, M.; Mattsson, G.; Andersson, A.; Jansson, L. et al. (2006). Islet endothelial cells and pancreatic beta-cell proliferation: studies in vitro and during pregnancy in adult rats. *Endocrinology* 147, 2315-2324.
- John, B.; Enright, A.J.; Aravin, A.; Tuschl, T. et al. (2004). Human MicroRNA targets. *PLoS. Biol.* 2, e363.
- Johnson, J.M.; Castle, J.; Garrett-Engele, P.; Kan, Z. et al. (2003). Genome-wide survey of human alternative pre-mRNA splicing with exon junction microarrays. *Science* 302, 2141-2144.
- Jonsson, J.; Carlsson, L.; Edlund, T.; Edlund, H. (1994). Insulin-promoter-factor 1 is required for pancreas development in mice. *Nature* 371, 606-609.
- Jordan, E.T.; Collins, M.; Terefe, J.; Ugozzoli, L. et al. (2008). Optimizing electroporation conditions in primary and other difficult-to-transfect cells. *J. Biomol. Tech.* 19, 328-334.
- Judson, R.L.; Babiarz, J.E.; Venere, M.; Belloch, R. (2009). Embryonic stem cell-specific microRNAs promote induced pluripotency. *Nat. Biotechnol.* 27, 459-461.
- Jung, D.Y.; Park, J.B.; Joo, S.Y.; Joh, J.W. et al. (2009). Effect of nicotinamide on early graft failure following intraportal islet transplantation. *Exp. Mol. Med.* 41, 782-792.
- Jung, Y.; Park, J.; Bang, Y.J.; Kim, T.Y. (2008). Gene silencing of TSPYL5 mediated by aberrant promoter methylation in gastric cancers. *Lab Invest* 88, 153-160.
- Jung, M.; Schroeder, I.S. (2013) Pluripotency and Early Cell Fate Decisions are Orchestrated by microRNAs. Sahu, S.C. (editor): *mircoRNAs in Toxicology and Medicine*. West Sussex, United Kingdom: John Wiley & Sons Ltd.
- Kador, K.E. and Goldberg, J.L. (2012). Scaffolds and stem cells: delivery of cell transplants for retinal degenerations. *Expert. Rev. Ophthalmol.* 7, 459-470.
- Kahan, B.W.; Jacobson, L.M.; Hullett, D.A.; Ochoada, J.M. et al. (2003). Pancreatic precursors and differentiated islet cell types from murine embryonic stem cells: an in vitro model to study islet differentiation. *Diabetes* 52, 2016-2024.
- Kahler, D.J.; Ahmad, F.S.; Ritz, A.; Hua, H. et al. (2013). Improved methods for reprogramming human dermal fibroblasts using fluorescence activated cell sorting. *PLoS. One.* 8, e59867.
- Kaido, T.; Yebra, M.; Cirulli, V.; Montgomery, A.M. (2004). Regulation of human beta-cell adhesion, motility, and insulin secretion by collagen IV and its receptor alpha1beta1. *J. Biol. Chem.* 279, 53762-53769.
- Kanai-Azuma, M.; Kanai, Y.; Gad, J.M.; Tajima, Y. et al. (2002). Depletion of definitive gut endoderm in Sox17-null mutant mice. *Development* 129, 2367-2379.
- Kane, N.M.; Nowrouzi, A.; Mukherjee, S.; Blundell, M.P. et al. (2010). Lentivirus-mediated reprogramming of somatic cells in the absence of transgenic transcription factors. *Mol. Ther.* 18, 2139-2145.
- Kanellopoulou, C.; Muljo, S.A.; Kung, A.L.; Ganesan, S. et al. (2005). Dicer-deficient mouse embryonic stem cells are defective in differentiation and centromeric silencing. *Genes Dev.* 19, 489-501.
- Karen, J.; Rodriguez, A.; Friman, T.; Dencker, L. et al. (2011). Effects of the histone deacetylase inhibitor valproic acid on human pericytes in vitro. *PLoS. One.* 6, e24954.
- Karwacki-Neisius, V.; Goke, J.; Osomo, R.; Halbritter, F. et al. (2013). Reduced Oct4 expression directs a robust pluripotent state with distinct signaling activity and increased enhancer occupancy by Oct4 and Nanog. *Cell Stem Cell* 12, 531-545.
- Katahira, J. and Yoneda, Y. (2011). Nucleocytoplasmic transport of microRNAs and related small RNAs. *Traffic.* 12, 1468-1474.
- Kato, K.; Kuhara, A.; Yoneda, T.; Inoue, T. et al. (2011). Sodium butyrate inhibits the self-renewal capacity of endometrial tumor side-population cells by inducing a DNA damage response. *Mol. Cancer Ther.* 10, 1430-1439.
- Katsumoto, K. and Kume, S. (2011). Endoderm and mesoderm reciprocal signaling mediated by CXCL12 and CXCR4 regulates the migration of angioblasts and establishes the pancreatic fate. *Development* 138, 1947-1955.
- Katsumoto, K. and Kume, S. (2013). The role of CXCL12-CXCR4 signaling pathway in pancreatic development. *Theranostics.* 3, 11-17.
- Kawamura, T.; Suzuki, J.; Wang, Y.V.; Menendez, S. et al. (2009). Linking the p53 tumour suppressor pathway to somatic cell reprogramming. *Nature* 460, 1140-1144.
- Kayam, G.; Kohl, A.; Magen, Z.; Peretz, Y. et al. (2013). A novel role for Pax6 in the segmental organization of the hindbrain. *Development* 140, 2190-2202.
- Keuschnigg, J.; Karinen, S.; Auvinen, K.; Irljala, H. et al. (2013). Plasticity of blood- and lymphatic endothelial cells and marker identification. *PLoS. One.* 8, e74293.
- Kim, B.M. and Choi, M.Y. (2012). Non-canonical microRNAs miR-320 and miR-702 promote proliferation in Dgcr8-deficient embryonic stem cells. *Biochem. Biophys. Res. Commun.* 426, 183-189.
- Kim, D.; Kim, C.H.; Moon, J.I.; Chung, Y.G. et al. (2009a). Generation of human induced pluripotent stem cells by direct delivery of reprogramming proteins. *Cell Stem Cell* 4, 472-476.
- Kim, H.H.; Kuwano, Y.; Srikantan, S.; Lee, E.K. et al. (2009b). HuR recruits let-7/RISC to repress c-Myc expression. *Genes Dev.* 23, 1743-1748.
- Kim, H.J.; Leeds, P.; Chuang, D.M. (2009c). The HDAC inhibitor, sodium butyrate, stimulates neurogenesis in the ischemic brain. *J. Neurochem.* 110, 1226-1240.
- Kim, J.B.; Greber, B.; Arauzo-Bravo, M.J.; Meyer, J. et al. (2009d). Direct reprogramming of human neural stem cells by OCT4. *Nature* 461, 649-3.
- Kim, J.B.; Zaehres, H.; Wu, G.; Gentile, L. et al. (2008). Pluripotent stem cells induced from adult neural stem cells by reprogramming with two factors. *Nature* 454, 646-650.
- Kim, K.; Doi, A.; Wen, B.; Ng, K. et al. (2010). Epigenetic memory in induced pluripotent stem cells. *Nature* 467, 285-290.
- Kim, S.H.; Ma, X.; Weremowicz, S.; Ercolino, T. et al. (2004). Identification of a locus for maturity-onset diabetes of the young on chromosome 8p23. *Diabetes* 53, 1375-1384.
- Kirby, L.A.; Schott, J.T.; Noble, B.L.; Mendez, D.C. et al. (2012). Glycogen synthase kinase 3 (GSK3) inhibitor, SB-216763, promotes pluripotency in mouse embryonic stem cells. *PLoS. One.* 7, e39329.

- Koch, P.; Opitz, T.; Steinbeck, J.A.; Ladewig, J. et al. (2009). A rosette-type, self-renewing human ES cell-derived neural stem cell with potential for in vitro instruction and synaptic integration. *Proc. Natl. Acad. Sci. U. S. A* 106, 3225-3230.
- Korpal, M.; Lee, E.S.; Hu, G.; Kang, Y. (2008). The miR-200 family inhibits epithelial-mesenchymal transition and cancer cell migration by direct targeting of E-cadherin transcriptional repressors ZEB1 and ZEB2. *J. Biol. Chem.* 283, 14910-14914.
- Koscianska, E.; Starega-Roslan, J.; Krzyzosiak, W.J. (2011). The role of Dicer protein partners in the processing of microRNA precursors. *PLoS. One.* 6, e28548.
- Kosoff, R.E.; Gardiner, K.L.; Merlo, L.M.; Pavlov, K. et al. (2012). Development and characterization of an organotypic model of Barrett's esophagus. *J. Cell Physiol* 227, 2654-2659.
- Kouzarides, T. (2007). SnapShot: Histone-modifying enzymes. *Cell* 131, 822.
- Krause, C.D.; Izotova, L.S.; Ren, G.; Yuan, Z.R. et al. (2011). Efficient co-expression of bicistronic proteins in mesenchymal stem cells by development and optimization of a multifunctional plasmid. *Stem Cell Res. Ther.* 2, 15.
- Krek, A.; Grun, D.; Poy, M.N.; Wolf, R. et al. (2005). Combinatorial microRNA target predictions. *Nat. Genet.* 37, 495-500.
- Kress, H. (2008). [Yes to research, no to utilization? Medical, pharmacological and toxicological utilization of human embryonic stem cells from an ethical point of view]. *Bundesgesundheitsblatt. Gesundheitsforschung. Gesundheitsschutz.* 51, 965-972.
- Kretsovali, A.; Hadjimichael, C.; Champilas, N. (2012). Histone deacetylase inhibitors in cell pluripotency, differentiation, and reprogramming. *Stem Cells Int.* 2012, 184154.
- Krichevsky, A.M.; Sonntag, K.C.; Isacson, O.; Kosik, K.S. (2006). Specific microRNAs modulate embryonic stem cell-derived neurogenesis. *Stem Cells* 24, 857-864.
- Kroon, E.; Martinson, L.A.; Kadoya, K.; Bang, A.G. et al. (2008). Pancreatic endoderm derived from human embryonic stem cells generates glucose-responsive insulin-secreting cells in vivo. *Nat. Biotechnol.* 26, 443-452.
- Kubicek, S.; O'Sullivan, R.J.; August, E.M.; Hickey, E.R. et al. (2007). Reversal of H3K9me2 by a small-molecule inhibitor for the G9a histone methyltransferase. *Mol. Cell* 25, 473-481.
- Kubo, A.; Shinozaki, K.; Shannon, J.M.; Kouskoff, V. et al. (2004). Development of definitive endoderm from embryonic stem cells in culture. *Development* 131, 1651-1662.
- Kubo, A.; Stull, R.; Takeuchi, M.; Bonham, K. et al. (2011). Pdx1 and Ngn3 overexpression enhances pancreatic differentiation of mouse ES cell-derived endoderm population. *PLoS. One.* 6, e24058.
- Kuijk, E.W.; Chuva de Sousa Lopes SM; Geijsen, N.; Macklon, N. et al. (2011). The different shades of mammalian pluripotent stem cells. *Hum. Reprod. Update.* 17, 254-271.
- Kunisada, Y.; Tsubooka-Yamazoe, N.; Shoji, M.; Hosoya, M. (2012). Small molecules induce efficient differentiation into insulin-producing cells from human induced pluripotent stem cells. *Stem Cell Res.* 8, 274-284.
- Kuo, C.H.; Deng, J.H.; Deng, Q.; Ying, S.Y. (2012). A novel role of miR-302/367 in reprogramming. *Biochem. Biophys. Res. Commun.* 417, 11-16.
- Lammert, E.; Gu, G.; McLaughlin, M.; Brown, D. et al. (2003). Role of VEGF-A in vascularization of pancreatic islets. *Curr. Biol.* 13, 1070-1074.
- Lampugnani, M.G.; Resnati, M.; Raiteri, M.; Pigott, R. et al. (1992). A novel endothelial-specific membrane protein is a marker of cell-cell contacts. *J. Cell Biol.* 118, 1511-1522.
- Landsman, L.; Nijagal, A.; Whitchurch, T.J.; Vanderlaan, R.L. et al. (2011). Pancreatic mesenchyme regulates epithelial organogenesis throughout development. *PLoS. Biol.* 9, e1001143.
- Le, H.S. and Bar-Joseph, Z. (2013). Integrating sequence, expression and interaction data to determine condition-specific miRNA regulation. *Bioinformatics.* 29, i89-i97.
- LeCluyse, E.L.; Witek, R.P.; Andersen, M.E.; Powers, M.J. (2012). Organotypic liver culture models: meeting current challenges in toxicity testing. *Crit Rev. Toxicol.* 42, 501-548.
- Lee, H.J. and Kim, K.W. (2012). Suppression of HIF-1alpha by Valproic Acid Sustains Self-Renewal of Mouse Embryonic Stem Cells under Hypoxia. *In Vitro. Biomol. Ther. (Seoul.)* 20, 280-285.
- Lee, J.; Kim, H.K.; Rho, J.Y.; Han, Y.M. et al. (2006). The human OCT-4 isoforms differ in their ability to confer self-renewal. *J. Biol. Chem.* 281, 33554-33565.
- Lee, J.S.; Ward, W.O.; Knapp, G.; Ren, H. et al. (2012). Transcriptional ontogeny of the developing liver. *BMC. Genomics* 13, 33.
- Lee, R.H.; Seo, M.J.; Pulin, A.A.; Gregory, C.A. et al. (2009). The CD34-like protein PODXL and alpha6-integrin (CD49f) identify early progenitor MSCs with increased clonogenicity and migration to infarcted heart in mice. *Blood* 113, 816-826.
- Lee, Y.; Kim, M.; Han, J.; Yeom, K.H. et al. (2004). MicroRNA genes are transcribed by RNA polymerase II. *EMBO J.* 23, 4051-4060.
- Lee, Y.S. and Dutta, A. (2009). MicroRNAs in cancer. *Annu. Rev. Pathol.* 4, 199-227.
- Leeson, P.D. and Springthorpe, B. (2007). The influence of drug-like concepts on decision-making in medicinal chemistry. *Nat. Rev. Drug Discov.* 6, 881-890.
- Leontieva, O.V.; Natarajan, V.; Demidenko, Z.N.; Burdelya, L.G. et al. (2012). Hypoxia suppresses conversion from proliferative arrest to cellular senescence. *Proc. Natl. Acad. Sci. U. S. A* 109, 13314-13318.
- Levine, A.J. and Brivanlou, A.H. (2006). GDF3, a BMP inhibitor, regulates cell fate in stem cells and early embryos. *Development* 133, 209-216.
- Levine, M. and Tjian, R. (2003). Transcription regulation and animal diversity. *Nature* 424, 147-151.
- Lewis, B.P.; Burge, C.B.; Bartel, D.P. (2005). Conserved seed pairing, often flanked by adenosines, indicates that thousands of human genes are microRNA targets. *Cell* 120, 15-20.
- Li, B.; Bailey, A.S.; Jiang, S.; Liu, B. et al. (2010). Endothelial cells mediate the regeneration of hematopoietic stem cells. *Stem Cell Res.* 4, 17-24.
- Li, H.; Collado, M.; Villasante, A.; Strati, K. et al. (2009a). The Ink4/Arf locus is a barrier for iPS cell reprogramming. *Nature* 460, 1136-1139.
- Li, J.; Wang, G.; Wang, C.; Zhao, Y. et al. (2007a). MEK/ERK signaling contributes to the maintenance of human embryonic stem cell self-renewal. *Differentiation* 75, 299-307.
- Li, J.; Wang, G.; Wang, C.; Zhao, Y. et al. (2007b). MEK/ERK signaling contributes to the maintenance of human embryonic stem cell self-renewal. *Differentiation* 75, 299-307.
- Li, Q.; Ling, Y.; Yu, L. (2012). GDF3 inhibits the growth of breast cancer cells and promotes the apoptosis induced by Taxol. *J. Cancer Res. Clin. Oncol.* 138, 1073-1079.
- Li, W. and Ding, S. (2010). Small molecules that modulate embryonic stem cell fate and somatic cell reprogramming. *Trends Pharmacol. Sci.* 31, 36-45.
- Li, W.; Lee, S.; Ma, M.; Kim, S.M. et al. (2013a). Microbead-based biomimetic synthetic neighbors enhance survival and function of rat pancreatic beta-cells. *Sci. Rep.* 3, 2863.

- Li, W.; Zhou, H.; Abujarour, R.; Zhu, S. et al. (2009b). Generation of human-induced pluripotent stem cells in the absence of exogenous Sox2. *Stem Cells* 27, 2992-3000.
- Li, X. and Zhao, X. (2008). Epigenetic regulation of mammalian stem cells. *Stem Cells Dev.* 17, 1043-1052.
- Li, Y.; Feng, H.; Gu, H.; Lewis, D.W. et al. (2013b). The p53-PUMA axis suppresses iPSC generation. *Nat. Commun.* 4, 2174.
- Li, Y.; McClintock, J.; Zhong, L.; Edenberg, H.J. et al. (2005). Murine embryonic stem cell differentiation is promoted by SOCS-3 and inhibited by the zinc finger transcription factor Klf4. *Blood* 105, 635-637.
- Lian, X.; Hsiao, C.; Wilson, G.; Zhu, K. et al. (2012). Robust cardiomyocyte differentiation from human pluripotent stem cells via temporal modulation of canonical Wnt signaling. *Proc. Natl. Acad. Sci. U. S. A* 109, E1848-E1857.
- Liao, D.J. and Dickson, R.B. (2000). c-Myc in breast cancer. *Endocr. Relat Cancer* 7, 143-164.
- Lidington, E.A.; Moyes, D.L.; McCormack, A.M.; Rose, M.L. (1999). A comparison of primary endothelial cells and endothelial cell lines for studies of immune interactions. *Transpl. Immunol.* 7, 239-246.
- Liedtke, S.; Enczmann, J.; Wadlawczyk, S.; Wernet, P. et al. (2007). Oct4 and its pseudogenes confuse stem cell research. *Cell Stem Cell* 1, 364-366.
- Lillicrap, D. (2013). von Willebrand disease: advances in pathogenetic understanding, diagnosis, and therapy. *Blood* 122, 3735-3740.
- Lim, L.P.; Lau, N.C.; Garrett-Engle, P.; Grimson, A. et al. (2005). Microarray analysis shows that some microRNAs downregulate large numbers of target mRNAs. *Nature* 433, 769-773.
- Lima, M.J.; Docherty, H.M.; Chen, Y.; Vallier, L. et al. (2012). Pancreatic transcription factors containing protein transduction domains drive mouse embryonic stem cells towards endocrine pancreas. *PLoS. One.* 7, e36481.
- Lin, C.Y.; Loven, J.; Rahl, P.B.; Paranal, R.M. et al. (2012a). Transcriptional amplification in tumor cells with elevated c-Myc. *Cell* 151, 56-67.
- Lin, F.; Li, R.; Pan, Z.X.; Zhou, B. et al. (2012b). miR-26b promotes granulosa cell apoptosis by targeting ATM during follicular atresia in porcine ovary. *PLoS. One.* 7, e38640.
- Lin, H.Y.; Tsai, C.C.; Chen, L.L.; Chiou, S.H. et al. (2010). Fibronectin and laminin promote differentiation of human mesenchymal stem cells into insulin producing cells through activating Akt and ERK. *J. Biomed. Sci.* 17, 56.
- Lin, S.L.; Chang, D.C.; Lin, C.H.; Ying, S.Y. et al. (2011). Regulation of somatic cell reprogramming through inducible mir-302 expression. *Nucleic Acids Res.* 39, 1054-1065.
- Lin, T.; Ambasudhan, R.; Yuan, X.; Li, W. et al. (2009). A chemical platform for improved induction of human iPSCs. *Nat. Methods* 6, 805-808.
- Lin, T.; Chao, C.; Saito, S.; Mazur, S.J. et al. (2005). p53 induces differentiation of mouse embryonic stem cells by suppressing Nanog expression. *Nat. Cell Biol.* 7, 165-171.
- Ling, H.Y.; Wen, G.B.; Feng, S.D.; Tuo, Q.H. et al. (2011). MicroRNA-375 promotes 3T3-L1 adipocyte differentiation through modulation of extracellular signal-regulated kinase signalling. *Clin. Exp. Pharmacol. Physiol* 38, 239-246.
- Ling, T.Y.; Kuo, M.D.; Li, C.L.; Yu, A.L. et al. (2006). Identification of pulmonary Oct-4+ stem/progenitor cells and demonstration of their susceptibility to SARS coronavirus (SARS-CoV) infection in vitro. *Proc. Natl. Acad. Sci. U. S. A* 103, 9530-9535.
- Lipchina, I.; Elkabetz, Y.; Hafner, M.; Sheridan, R. et al. (2011). Genome-wide identification of microRNA targets in human ES cells reveals a role for miR-302 in modulating BMP response. *Genes Dev.* 25, 2173-2186.
- Lister, R.; Pelizzola, M.; Kida, Y.S.; Hawkins, R.D. et al. (2011). Hotspots of aberrant epigenomic reprogramming in human induced pluripotent stem cells. *Nature* 471, 68-73.
- Liu, J.; Carmell, M.A.; Rivas, F.V.; Marsden, C.G. et al. (2004). Argonaute2 is the catalytic engine of mammalian RNAi. *Science* 305, 1437-1441.
- Liu, P.; Wakamiya, M.; Shea, M.J.; Albrecht, U. et al. (1999). Requirement for Wnt3 in vertebrate axis formation. *Nat. Genet.* 22, 361-365.
- Liu, Y.; Zhang, Z.C.; Qian, S.W.; Zhang, Y.Y. et al. (2013). MicroRNA-140 promotes adipocyte lineage commitment of C3H10T1/2 pluripotent stem cell via targeting Osteopetrosis-associated transmembrane protein 1. *J. Biol. Chem.*
- Lluis, F.; Pedone, E.; Pepe, S.; Cosma, M.P. (2008). Periodic activation of Wnt/beta-catenin signaling enhances somatic cell reprogramming mediated by cell fusion. *Cell Stem Cell* 3, 493-507.
- Lo, B. and Parham, L. (2009). Ethical issues in stem cell research. *Endocr. Rev.* 30, 204-213.
- Loh, Y.H.; Wu, Q.; Chew, J.L.; Vega, V.B. et al. (2006). The Oct4 and Nanog transcription network regulates pluripotency in mouse embryonic stem cells. *Nat. Genet.* 38, 431-440.
- Loh, Y.H.; Zhang, W.; Chen, X.; George, J. et al. (2007). Jmjd1a and Jmjd2c histone H3 Lys 9 demethylases regulate self-renewal in embryonic stem cells. *Genes Dev.* 21, 2545-2557.
- Lou, J.; Triponez, F.; Oberholzer, J.; Wang, H. et al. (1999). Expression of alpha-1 proteinase inhibitor in human islet microvascular endothelial cells. *Diabetes* 48, 1773-1778.
- Lowry, W.E.; Richter, L.; Yachechko, R.; Pyle, A.D. et al. (2008). Generation of human induced pluripotent stem cells from dermal fibroblasts. *Proc. Natl. Acad. Sci. U. S. A* 105, 2883-2888.
- Lu, D.; Davis, M.P.; Abreu-Goodger, C.; Wang, W. et al. (2012). MiR-25 regulates Wwp2 and Fbxw7 and promotes reprogramming of mouse fibroblast cells to iPSCs. *PLoS. One.* 7, e40938.
- Lumelsky, N.; Blondel, O.; Laeng, P.; Velasco, I. et al. (2001). Differentiation of embryonic stem cells to insulin-secreting structures similar to pancreatic islets. *Science* 292, 1389-1394.
- Lundin, C.; Hjorth, L.; Behrendtz, M.; Nordgren, A. et al. (2012). High frequency of BTG1 deletions in acute lymphoblastic leukemia in children with down syndrome. *Genes Chromosomes. Cancer* 51, 196-206.
- Lyssiotis, C.A.; Lairson, L.L.; Boitano, A.E.; Wurdak, H. et al. (2011). Chemical control of stem cell fate and developmental potential. *Angew. Chem. Int. Ed Engl.* 50, 200-242.
- Madeira, C.; Mendes, R.D.; Ribeiro, S.C.; Boura, J.S. et al. (2010). Nonviral gene delivery to mesenchymal stem cells using cationic liposomes for gene and cell therapy. *J. Biomed. Biotechnol.* 2010, 735349.
- Maehr, R.; Chen, S.; Snitow, M.; Ludwig, T. et al. (2009). Generation of pluripotent stem cells from patients with type 1 diabetes. *Proc. Natl. Acad. Sci. U. S. A* 106, 15768-15773.
- Magenheim, J.; Ilovich, O.; Lazarus, A.; Klochendler, A. et al. (2011). Blood vessels restrain pancreas branching, differentiation and growth. *Development* 138, 4743-4752.
- Maherali, N. and Hochedlinger, K. (2008). Guidelines and techniques for the generation of induced pluripotent stem cells. *Cell Stem Cell* 3, 595-605.
- Maherali, N. and Hochedlinger, K. (2009). Tgfbeta signal inhibition cooperates in the induction of iPSCs and replaces Sox2 and cMyc. *Curr. Biol.* 19, 1718-1723.

- Mahmood, A.; Harkness, L.; Schroder, H.D.; Abdallah, B.M. et al. (2010). Enhanced differentiation of human embryonic stem cells to mesenchymal progenitors by inhibition of TGF-beta/activin/nodal signaling using SB-431542. *J. Bone Miner. Res.* 25, 1216-1233.
- Manganelli, G.; Fico, A.; Masullo, U.; Pizzolongo, F. et al. (2012). Modulation of the pentose phosphate pathway induces endodermal differentiation in embryonic stem cells. *PLoS. One.* 7, e29321.
- Mannaerts, I.; Nuytten, N.R.; Rogiers, V.; Vanderkerken, K. et al. (2010). Chronic administration of valproic acid inhibits activation of mouse hepatic stellate cells in vitro and in vivo. *Hepatology* 51, 603-614.
- Marson, A.; Foreman, R.; Chevalier, B.; Bilodeau, S. et al. (2008a). Wnt signaling promotes reprogramming of somatic cells to pluripotency. *Cell Stem Cell* 3, 132-135.
- Marson, A.; Levine, S.S.; Cole, M.F.; Frampton, G.M. et al. (2008b). Connecting microRNA genes to the core transcriptional regulatory circuitry of embryonic stem cells. *Cell* 134, 521-533.
- Martinez, C.; Comejo, V.H.; Lois, P.; Ellis, T. et al. (2013). Proliferation of murine midbrain neural stem cells depends upon an endogenous sonic hedgehog (Shh) source. *PLoS. One.* 8, e65818.
- Masaki, H.; Nishida, T.; Kitajima, S.; Asahina, K. et al. (2007). Developmental pluripotency-associated 4 (DPPA4) localized in active chromatin inhibits mouse embryonic stem cell differentiation into a primitive ectoderm lineage. *J. Biol. Chem.* 282, 33034-33042.
- Mason, M.N.; Arnold, C.A.; Mahoney, M.J. (2009). Entrapped collagen type 1 promotes differentiation of embryonic pancreatic precursor cells into glucose-responsive beta-cells when cultured in three-dimensional PEG hydrogels. *Tissue Eng Part A* 15, 3799-3808.
- Mathieu, J.; Zhang, Z.; Zhou, W.; Wang, A.J. et al. (2011). HIF induces human embryonic stem cell markers in cancer cells. *Cancer Res.* 71, 4640-4652.
- Matin, M.M.; Walsh, J.R.; Gokhale, P.J.; Draper, J.S. et al. (2004). Specific knockdown of Oct4 and beta2-microglobulin expression by RNA interference in human embryonic stem cells and embryonic carcinoma cells. *Stem Cells* 22, 659-668.
- Matveyenko, A.V.; Georgia, S.; Bhushan, A.; Butler, P.C. (2010). Inconsistent formation and nonfunction of insulin-positive cells from pancreatic endoderm derived from human embryonic stem cells in athymic nude rats. *Am. J. Physiol Endocrinol. Metab* 299, E713-E720.
- Mayr, F.; Schutz, A.; Doge, N.; Heinemann, U. (2012). The Lin28 cold-shock domain remodels pre-let-7 microRNA. *Nucleic Acids Res.* 40, 7492-7506.
- McCarthy, M.I. (2010). Genomics, type 2 diabetes, and obesity. *N. Engl. J. Med.* 363, 2339-2350.
- McConnell, B.B. and Yang, V.W. (2010). Mammalian Kruppel-like factors in health and diseases. *Physiol Rev.* 90, 1337-1381.
- McKnight, K.D.; Wang, P.; Kim, S.K. (2010). Deconstructing pancreas development to reconstruct human islets from pluripotent stem cells. *Cell Stem Cell* 6, 300-308.
- McLean, A.B.; D'Amour, K.A.; Jones, K.L.; Krishnamoorthy, M. et al. (2007). Activin efficiently specifies definitive endoderm from human embryonic stem cells only when phosphatidylinositol 3-kinase signaling is suppressed. *Stem Cells* 25, 29-38.
- Medvedev, S.P.; Grigoreva, E.V.; Shevchenko, A.I.; Malakhova, A.A. et al. (2011). Human induced pluripotent stem cells derived from fetal neural stem cells successfully undergo directed differentiation into cartilage. *Stem Cells Dev.* 20, 1099-1112.
- Meisner, N.C. and Filipowicz, W. (2010). Properties of the regulatory RNA-binding protein HuR and its role in controlling miRNA repression. *Adv. Exp. Med. Biol.* 700, 106-123.
- Merkel, C.; Saalfrank, A.; Riesen, N.; Kuhn, R. et al. (2013). Efficient generation of rat induced pluripotent stem cells using a non-viral inducible vector. *PLoS. One.* 8, e55170.
- Mezentseva, N.V.; Yang, J.; Kaur, K.; Iaffaldano, G. et al. (2013). The histone methyltransferase inhibitor BIX01294 enhances the cardiac potential of bone marrow cells. *Stem Cells Dev.* 22, 654-667.
- Mfopou, J.K.; Chen, B.; Matezel, I.; Sermon, K. et al. (2010a). Noggin, retinoids, and fibroblast growth factor regulate hepatic or pancreatic fate of human embryonic stem cells. *Gastroenterology* 138, 2233-45, 2245.
- Mfopou, J.K.; Chen, B.; Sui, L.; Sermon, K. et al. (2010b). Recent advances and prospects in the differentiation of pancreatic cells from human embryonic stem cells. *Diabetes* 59, 2094-2101.
- Michaelis, M.; Michaelis, U.R.; Fleming, I.; Suhan, T. et al. (2004). Valproic acid inhibits angiogenesis in vitro and in vivo. *Mol. Pharmacol.* 65, 520-527.
- Mikkelsen, T.S.; Hanna, J.; Zhang, X.; Ku, M. et al. (2008). Dissecting direct reprogramming through integrative genomic analysis. *Nature* 454, 49-55.
- Mirmalek-Sani, S.H.; Orlando, G.; McQuilling, J.P.; Pareta, R. et al. (2013). Porcine pancreas extracellular matrix as a platform for endocrine pancreas bioengineering. *Biomaterials* 34, 5488-5495.
- Mitchell, J.A. and Yochim, J.M. (1968). Intrauterine oxygen tension during the estrous cycle in the rat: its relation to uterine respiration and vascular activity. *Endocrinology* 83, 701-705.
- Miyoshi, N.; Ishii, H.; Nagano, H.; Haraguchi, N. et al. (2011). Reprogramming of mouse and human cells to pluripotency using mature microRNAs. *Cell Stem Cell* 8, 633-638.
- Mohyeldin, A.; Garzon-Muvdi, T.; Quinones-Hinojosa, A. (2010). Oxygen in stem cell biology: a critical component of the stem cell niche. *Cell Stem Cell* 7, 150-161.
- Moll, C.; Reboredo, J.; Schwarz, T.; Appelt, A. et al. (2013). Tissue engineering of a human 3D in vitro tumor test system. *J. Vis. Exp.*
- Monk, M.; Hitchins, M.; Hawes, S. (2008). Differential expression of the embryo/cancer gene ECSA(DPPA2), the cancer/testis gene BORIS and the pluripotency structural gene OCT4, in human preimplantation development. *Mol. Hum. Reprod.* 14, 347-355.
- Monk, M. and Holding, C. (2001). Human embryonic genes re-expressed in cancer cells. *Oncogene* 20, 8085-8091.
- Mosch, B.; Reissenweber, B.; Neuber, C.; Pietzsch, J. (2010). Eph receptors and ephrin ligands: important players in angiogenesis and tumor angiogenesis. *J. Oncol.* 2010, 135285.
- Mostoslavsky, G. (2012). Concise review: The magic act of generating induced pluripotent stem cells: many rabbits in the hat. *Stem Cells* 30, 28-32.
- Mountford, P.; Zevnik, B.; Duwel, A.; Nichols, J. et al. (1994). Dicotronic targeting constructs: reporters and modifiers of mammalian gene expression. *Proc. Natl. Acad. Sci. U. S. A* 91, 4303-4307.
- Movassat, J.; Beattie, G.M.; Lopez, A.D.; Hayek, A. (2002). Exendin 4 up-regulates expression of PDX 1 and hastens differentiation and maturation of human fetal pancreatic cells. *J. Clin. Endocrinol. Metab* 87, 4775-4781.
- Mueller, T.; Luetzkendorf, J.; Nerger, K.; Schmoll, H.J. et al. (2009). Analysis of OCT4 expression in an extended panel of human tumor cell lines from multiple entities and in human mesenchymal stem cells. *Cell Mol. Life Sci.* 66, 495-503.
- Muller, G. (2010). Personalized prognosis and diagnosis of type 2 diabetes—vision or fiction? *Pharmacology* 85, 168-187.
- Murtaugh, L.C.; Stanger, B.Z.; Kwan, K.M.; Melton, D.A. (2003). Notch signaling controls multiple steps of pancreatic differentiation. *Proc. Natl. Acad. Sci. U. S. A* 100, 14920-14925.

- Musselman, C.A.; Lalonde, M.E.; Cote, J.; Kutateladze, T.G. (2012). Perceiving the epigenetic landscape through histone readers. *Nat. Struct. Mol. Biol.* 19, 1218-1227.
- Nagy, A.; Rossant, J.; Nagy, R.; Abramow-Newerly, W. et al. (1993). Derivation of completely cell culture-derived mice from early-passage embryonic stem cells. *Proc. Natl. Acad. Sci. U. S. A* 90, 8424-8428.
- Nagy, K.; Sung, H.K.; Zhang, P.; Laflamme, S. et al. (2011). Induced pluripotent stem cell lines derived from equine fibroblasts. *Stem Cell Rev.* 7, 693-702.
- Nair, R.; Ngangan, A.V.; Kemp, M.L.; McDevitt, T.C. (2012). Gene expression signatures of extracellular matrix and growth factors during embryonic stem cell differentiation. *PLoS. One.* 7, e42580.
- Nair, R.; Shukla, S.; McDevitt, T.C. (2008). Acellular matrices derived from differentiating embryonic stem cells. *J. Biomed. Mater. Res. A* 87, 1075-1085.
- Nakamura, T.; Nakagawa, M.; Ichisaka, T.; Shiota, A. et al. (2011). Essential roles of ECAT15-2/Dppa2 in functional lung development. *Mol. Cell Biol.* 31, 4366-4378.
- Nakanishi, M. and Otsu, M. (2012). Development of Sendai virus vectors and their potential applications in gene therapy and regenerative medicine. *Curr. Gene Ther.* 12, 410-416.
- Narsinh, K.H.; Jia, F.; Robbins, R.C.; Kay, M.A. et al. (2011). Generation of adult human induced pluripotent stem cells using nonviral minicircle DNA vectors. *Nat. Protoc.* 6, 78-88.
- Nasu, A.; Ikeya, M.; Yamamoto, T.; Watanabe, A. et al. (2013). Genetically matched human iPS cells reveal that propensity for cartilage and bone differentiation differs with clones, not cell type of origin. *PLoS. One.* 8, e53771.
- Nemajerova, A.; Kim, S.Y.; Petrenko, O.; Moll, U.M. (2012). Two-factor reprogramming of somatic cells to pluripotent stem cells reveals partial functional redundancy of Sox2 and Klf4. *Cell Death. Differ.* 19, 1268-1276.
- Nguemo, F.; Fleischmann, B.K.; Gupta, M.K.; Saric, T. et al. (2013). The L-type Ca²⁺ channels blocker nifedipine represses mesodermal fate determination in murine embryonic stem cells. *PLoS. One.* 8, e53407.
- Nie, B.; Wang, H.; Laurent, T.; Ding, S. (2012). Cellular reprogramming: a small molecule perspective. *Curr. Opin. Cell Biol.* 24, 784-792.
- Niibe, K.; Kawamura, Y.; Araki, D.; Morikawa, S. et al. (2011). Purified mesenchymal stem cells are an efficient source for iPS cell induction. *PLoS. One.* 6, e17610.
- Nikolova, G.; Jabs, N.; Konstantinova, I.; Domogatskaya, A. et al. (2006). The vascular basement membrane: a niche for insulin gene expression and Beta cell proliferation. *Dev. Cell* 10, 397-405.
- Nikolova, G.; Strlic, B.; Lammer, E. (2007). The vascular niche and its basement membrane. *Trends Cell Biol.* 17, 19-25.
- Nir, T.; Melton, D.A.; Dor, Y. (2007). Recovery from diabetes in mice by beta cell regeneration. *J. Clin. Invest* 117, 2553-2561.
- Nisato, R.E.; Harrison, J.A.; Buser, R.; Orci, L. et al. (2004). Generation and characterization of telomerase-transfected human lymphatic endothelial cells with an extended life span. *Am. J. Pathol.* 165, 11-24.
- Niwa, H.; Miyazaki, J.; Smith, A.G. (2000). Quantitative expression of Oct-3/4 defines differentiation, dedifferentiation or self-renewal of ES cells. *Nat. Genet.* 24, 372-376.
- Niwa, H.; Ogawa, K.; Shimosato, D.; Adachi, K. (2009). A parallel circuit of LIF signalling pathways maintains pluripotency of mouse ES cells. *Nature* 460, 118-122.
- Nordhoff, V.; Hubner, K.; Bauer, A.; Orlova, I. et al. (2001). Comparative analysis of human, bovine, and murine Oct-4 upstream promoter sequences. *Mamm. Genome* 12, 309-317.
- Norton, G.R.; Brooksbank, R.; Woodiwiss, A.J. (2010). Gene variants of the renin-angiotensin system and hypertension: from a trough of disillusionment to a welcome phase of enlightenment? *Clin. Sci. (Lond)* 118, 487-506.
- Nowak, J.A.; Polak, L.; Pasolli, H.A.; Fuchs, E. (2008). Hair follicle stem cells are specified and function in early skin morphogenesis. *Cell Stem Cell* 3, 33-43.
- Nyunt, O.; Wu, J.Y.; McGown, I.N.; Harris, M. et al. (2009). Investigating maturity onset diabetes of the young. *Clin. Biochem. Rev.* 30, 67-74.
- Obokata, H.; Wakayama, T.; Sasai, Y.; Kojima, K. et al. (2014). Stimulus-triggered fate conversion of somatic cells into pluripotency. *Nature* 505, 641-647.
- Offield, M.F.; Jetton, T.L.; Labosky, P.A.; Ray, M. et al. (1996). PDX-1 is required for pancreatic outgrowth and differentiation of the rostral duodenum. *Development* 122, 983-995.
- Ogbourne, S. and Antalis, T.M. (1998). Transcriptional control and the role of silencers in transcriptional regulation in eukaryotes. *Biochem. J.* 331 (Pt 1), 1-14.
- Ohi, Y.; Qin, H.; Hong, C.; Blouin, L. et al. (2011). Incomplete DNA methylation underlies a transcriptional memory of somatic cells in human iPS cells. *Nat. Cell Biol.* 13, 541-549.
- Ohmine, S.; Squillace, K.A.; Hartjes, K.A.; Deeds, M.C. et al. (2012). Reprogrammed keratinocytes from elderly type 2 diabetes patients suppress senescence genes to acquire induced pluripotency. *Aging (Albany, NY)* 4, 60-73.
- Ohnishi, Y.; Totoki, Y.; Toyoda, A.; Watanabe, T. et al. (2010). Small RNA class transition from siRNA/piRNA to miRNA during pre-implantation mouse development. *Nucleic Acids Res.* 38, 5141-5151.
- Okano, M.; Bell, D.W.; Haber, D.A.; Li, E. (1999). DNA methyltransferases Dnmt3a and Dnmt3b are essential for de novo methylation and mammalian development. *Cell* 99, 247-257.
- Okano, M.; Xie, S.; Li, E. (1998). Dnmt2 is not required for de novo and maintenance methylation of viral DNA in embryonic stem cells. *Nucleic Acids Res.* 26, 2536-2540.
- Okita, K. and Yamanaka, S. (2011). Induced pluripotent stem cells: opportunities and challenges. *Philos. Trans. R. Soc. Lond B Biol. Sci.* 366, 2198-2207.
- Oliver-Krasinski, J.M. and Stoffers, D.A. (2008). On the origin of the beta cell. *Genes Dev.* 22, 1998-2021.
- Oren, M. (2003). Decision making by p53: life, death and cancer. *Cell Death. Differ.* 10, 431-442.
- Ou, D.B.; Zeng, D.; Jin, Y.; Liu, X.T. et al. (2013). The long-term differentiation of embryonic stem cells into cardiomyocytes: an indirect co-culture model. *PLoS. One.* 8, e55233.
- Ouyang, Y.B.; Lu, Y.; Yue, S.; Giffard, R.G. (2012). miR-181 targets multiple Bcl-2 family members and influences apoptosis and mitochondrial function in astrocytes. *Mitochondrion.* 12, 213-219.
- Ozsolak, F.; Poling, L.L.; Wang, Z.; Liu, H. et al. (2008). Chromatin structure analyses identify miRNA promoters. *Genes Dev.* 22, 3172-3183.
- Page, R.L.; Ambady, S.; Holmes, W.F.; Vilner, L. et al. (2009). Induction of stem cell gene expression in adult human fibroblasts without transgenes. *Cloning Stem Cells* 11, 417-426.

- Pain, D.; Chim, G.W.; Strassel, C.; Kemp, D.M. (2005). Multiple retroseudogenes from pluripotent cell-specific gene expression indicates a potential signature for novel gene identification. *J. Biol. Chem.* 280, 6265-6268.
- Pan, G.J.; Chang, Z.Y.; Scholer, H.R.; Pei, D. (2002). Stem cell pluripotency and transcription factor Oct4. *Cell Res.* 12, 321-329.
- Pan, X.; Xue, W.; Li, Y.; Feng, X. et al. (2011). Islet graft survival and function: concomitant culture and transplantation with vascular endothelial cells in diabetic rats. *Transplantation* 92, 1208-1214.
- Pandit, K.V.; Corcoran, D.; Yousef, H.; Yarlagadda, M. et al. (2010). Inhibition and role of let-7d in idiopathic pulmonary fibrosis. *Am. J. Respir. Crit Care Med.* 182, 220-229.
- Papagregoriou, G.; Erguler, K.; Dweep, H.; Voskarides, K. et al. (2012). A miR-1207-5p binding site polymorphism abolishes regulation of HBEGF and is associated with disease severity in CFHR5 nephropathy. *PLoS. One.* 7, e31021.
- Park, I.H.; Arora, N.; Huo, H.; Maherali, N. et al. (2008). Disease-specific induced pluripotent stem cells. *Cell* 134, 877-886.
- Park, K.M.; Park, S.M.; Yang, S.R.; Hong, S.H. et al. (2013a). Preparation of immunogen-reduced and biocompatible extracellular matrices from porcine liver. *J. Biosci. Bioeng.* 115, 207-215.
- Park, S.W.; Lim, H.Y.; Do, H.J.; Sung, B. et al. (2012). Regulation of human growth and differentiation factor 3 gene expression by NANOG in human embryonic carcinoma NCCIT cells. *FEBS Lett.* 586, 3529-3535.
- Park, Y.; Lee, J.M.; Hwang, M.Y.; Son, G.H. et al. (2013b). NonO binds to the CpG island of oct4 promoter and functions as a transcriptional activator of oct4 gene expression. *Mol. Cells* 35, 61-69.
- Pasha, Z.; Haider, H.K.; Ashraf, M. (2011). Efficient non-viral reprogramming of myoblasts to stemness with a single small molecule to generate cardiac progenitor cells. *PLoS. One.* 6, e23667.
- Patel, H.; Chen, J.; Das, K.C.; Kavdia, M. (2013). Hyperglycemia induces differential change in oxidative stress at gene expression and functional levels in HUVEC and HMVEC. *Cardiovasc. Diabetol.* 12, 142.
- Pawlak, M. and Jaenisch, R. (2011). De novo DNA methylation by Dnmt3a and Dnmt3b is dispensable for nuclear reprogramming of somatic cells to a pluripotent state. *Genes Dev.* 25, 1035-1040.
- Pedersen, T.O.; Blois, A.L.; Xing, Z.; Xue, Y. et al. (2013). Endothelial microvascular networks affect gene-expression profiles and osteogenic potential of tissue-engineered constructs. *Stem Cell Res. Ther.* 4, 52.
- Pera, M.F. and Tam, P.P. (2010). Extrinsic regulation of pluripotent stem cells. *Nature* 465, 713-720.
- Perez, R.J.; Benoit, Y.D.; Gudas, L.J. (2013). Deletion of retinoic acid receptor beta (RARbeta) impairs pancreatic endocrine differentiation. *Exp. Cell Res.* 319, 2196-2204.
- Piskounova, E.; Polyarchou, C.; Thornton, J.E.; LaPierre, R.J. et al. (2011). Lin28A and Lin28B inhibit let-7 microRNA biogenesis by distinct mechanisms. *Cell* 147, 1066-1079.
- Polo, J.M. and Hochedlinger, K. (2010). When fibroblasts MET iPSCs. *Cell Stem Cell* 7, 5-6.
- Polo, J.M.; Liu, S.; Figueroa, M.E.; Kulalert, W. et al. (2010). Cell type of origin influences the molecular and functional properties of mouse induced pluripotent stem cells. *Nat. Biotechnol.* 28, 848-855.
- Polouliakh, N. (2013). Reprogramming resistant genes: in-depth comparison of gene expressions among iPS, ES, and somatic cells. *Front Physiol* 4, 7.
- Prasad, K.; Daume, E.; Preuett, B.; Spilde, T. et al. (2002). Glucagon is required for early insulin-positive differentiation in the developing mouse pancreas. *Diabetes* 51, 3229-3236.
- Puri, S. and Hebrok, M. (2010). Cellular plasticity within the pancreas—lessons learned from development. *Dev. Cell* 18, 342-356.
- Qi, J.; Yu, J.Y.; Shcherbata, H.R.; Mathieu, J. et al. (2009). microRNAs regulate human embryonic stem cell division. *Cell Cycle* 8, 3729-3741.
- Qin, W.; Leonhardt, H.; Pichler, G. (2011). Regulation of DNA methyltransferase 1 by interactions and modifications. *Nucleus.* 2, 392-402.
- Qiu, C.; Ma, Y.; Wang, J.; Peng, S. et al. (2010). Lin28-mediated post-transcriptional regulation of Oct4 expression in human embryonic stem cells. *Nucleic Acids Res.* 38, 1240-1248.
- Rajendran, G.; Shanmuganandam, K.; Bendre, A.; Muzumdar, D. et al. (2011). Epigenetic regulation of DNA methyltransferases: DNMT1 and DNMT3B in gliomas. *J Neurooncol.* 104, 483-494.
- Ramirez, G.; Hagood, J.S.; Sanders, Y.; Ramirez, R. et al. (2011). Absence of Thy-1 results in TGF-beta induced MMP-9 expression and confers a profibrotic phenotype to human lung fibroblasts. *Lab Invest* 91, 1206-1218.
- Ramsahoye, B.H.; Biniszkiwicz, D.; Lyko, F.; Clark, V. et al. (2000). Non-CpG methylation is prevalent in embryonic stem cells and may be mediated by DNA methyltransferase 3a. *Proc. Natl. Acad. Sci. U. S. A* 97, 5237-5242.
- Rao, J.S.; Keleshian, V.L.; Klein, S.; Rapoport, S.I. (2012). Epigenetic modifications in frontal cortex from Alzheimer's disease and bipolar disorder patients. *Transl. Psychiatry* 2, e132.
- Rastegar, F.; Shenaq, D.; Huang, J.; Zhang, W. et al. (2010). Mesenchymal stem cells: Molecular characteristics and clinical applications. *World J. Stem Cells* 2, 67-80.
- Rebustini, I.T.; Hayashi, T.; Reynolds, A.D.; Dillard, M.L. et al. (2012). miR-200c regulates FGFR-dependent epithelial proliferation via Vldlr during submandibular gland branching morphogenesis. *Development* 139, 191-202.
- Reichelt, J. and Haase, I. (2010). Establishment of spontaneously immortalized keratinocyte lines from wild-type and mutant mice. *Methods Mol. Biol.* 585, 59-69.
- Reinhart, B.J.; Slack, F.J.; Basson, M.; Pasquinelli, A.E. et al. (2000). The 21-nucleotide let-7 RNA regulates developmental timing in *Caenorhabditis elegans*. *Nature* 403, 901-906.
- Renaud, S.; Pugacheva, E.M.; Delgado, M.D.; Braunschweig, R. et al. (2007). Expression of the CTCF-paralogous cancer-testis gene, brother of the regulator of imprinted sites (BORIS), is regulated by three alternative promoters modulated by CpG methylation and by CTCF and p53 transcription factors. *Nucleic Acids Res.* 35, 7372-7388.
- Resende, R.R.; da Costa, J.L.; Kihara, A.H.; Adhikari, A. et al. (2010). Intracellular Ca²⁺ regulation during neuronal differentiation of murine embryonal carcinoma and mesenchymal stem cells. *Stem Cells Dev.* 19, 379-394.
- Reya, T.; Morrison, S.J.; Clarke, M.F.; Weissman, I.L. (2001). Stem cells, cancer, and cancer stem cells. *Nature* 414, 105-111.
- Rezania, A.; Bruin, J.E.; Riedel, M.J.; Mojibian, M. et al. (2012). Maturation of human embryonic stem cell-derived pancreatic progenitors into functional islets capable of treating pre-existing diabetes in mice. *Diabetes* 61, 2016-2029.
- Rhee, Y.H.; Choi, M.; Lee, H.S.; Park, C.H. et al. (2013). Insulin concentration is critical in culturing human neural stem cells and neurons. *Cell Death. Dis.* 4, e766.
- Rheinwald, J.G. and Green, H. (1975). Serial cultivation of strains of human epidermal keratinocytes: the formation of keratinizing colonies from single cells. *Cell* 6, 331-343.

- Robinton, D.A. and Daley, G.Q. (2012). The promise of induced pluripotent stem cells in research and therapy. *Nature* 481, 295-305.
- Rochat, A.; Claudinot, S.; Nicolas, M.; Barrandon, Y. (2007). Stem cells and skin engineering. *Swiss. Med. Wkly.* 137 Suppl 155, 49S-54S.
- Rogers, M.B.; Hosler, B.A.; Gudas, L.J. (1991). Specific expression of a retinoic acid-regulated, zinc-finger gene, Rex-1, in preimplantation embryos, trophoblast and spermatocytes. *Development* 113, 815-824.
- Ronen, D. and Benvenisty, N. (2012). Genomic stability in reprogramming. *Curr. Opin. Genet. Dev.* 22, 444-449.
- Rosa, A. and Brivanlou, A.H. (2011). A regulatory circuitry comprised of miR-302 and the transcription factors OCT4 and NR2F2 regulates human embryonic stem cell differentiation. *EMBO J.* 30, 237-248.
- Rosner, M.H.; De Santo, R.J.; Amheiter, H.; Staudt, L.M. (1991). Oct-3 is a maternal factor required for the first mouse embryonic division. *Cell* 64, 1103-1110.
- Ross, E.A.; Williams, M.J.; Hamazaki, T.; Terada, N. et al. (2009). Embryonic stem cells proliferate and differentiate when seeded into kidney scaffolds. *J. Am. Soc. Nephrol.* 20, 2338-2347.
- Roth, J.; Qureshi, S.; Whitford, I.; Vranic, M. et al. (2012). Insulin's discovery: new insights on its ninetieth birthday. *Diabetes Metab Res. Rev.* 28, 293-304.
- Rozario, T. and DeSimone, D.W. (2010). The extracellular matrix in development and morphogenesis: a dynamic view. *Dev. Biol.* 341, 126-140.
- Ruan, G.X. and Kazlauskas, A. (2013). Lactate engages receptor tyrosine kinases Axl, Tie2, and vascular endothelial growth factor receptor 2 to activate phosphoinositide 3-kinase/Akt and promote angiogenesis. *J. Biol. Chem.* 288, 21161-21172.
- Ruiz, S.; Panopoulos, A.D.; Herrerias, A.; Bissig, K.D. et al. (2011). A high proliferation rate is required for cell reprogramming and maintenance of human embryonic stem cell identity. *Curr. Biol.* 21, 45-52.
- Rushton, D.J.; Mattis, V.B.; Svendsen, C.N.; Allen, N.D. et al. (2013). Stimulation of GABA-induced Ca²⁺ influx enhances maturation of human induced pluripotent stem cell-derived neurons. *PLoS. One.* 8, e81031.
- Saito, H.; Takeuchi, M.; Chida, K.; Miyajima, A. (2011). Generation of glucose-responsive functional islets with a three-dimensional structure from mouse fetal pancreatic cells and iPS cells in vitro. *PLoS. One.* 6, e28209.
- Sanders, Y.Y.; Ambalavanan, N.; Halloran, B.; Zhang, X. et al. (2012). Altered DNA methylation profile in idiopathic pulmonary fibrosis. *Am. J. Respir. Crit Care Med.* 186, 525-535.
- Sasahara, Y.; Yoshikawa, Y.; Morinaga, T.; Nakano, Y. et al. (2009). Human keratinocytes derived from the bulge region of hair follicles are refractory to differentiation. *Int. J. Oncol.* 34, 1191-1199.
- Sato, N.; Meijer, L.; Skaltsounis, L.; Greengard, P. et al. (2004). Maintenance of pluripotency in human and mouse embryonic stem cells through activation of Wnt signaling by a pharmacological GSK-3-specific inhibitor. *Nat. Med.* 10, 55-63.
- Savkovic, V.; Dieckmann, C.; Milkova, L.; Simon, J.C. (2012). Improved method of differentiation, selection and amplification of human melanocytes from the hair follicle cell pool. *Exp. Dermatol.* 21, 948-950.
- Saxonov, S.; Berg, P.; Brutlag, D.L. (2006). A genome-wide analysis of CpG dinucleotides in the human genome distinguishes two distinct classes of promoters. *Proc. Natl. Acad. Sci. U. S. A.* 103, 1412-1417.
- Sayin, D.B.; Kurekci, E.; Karabulut, H.G.; Ezer, U. et al. (2010). DNA methyltransferase expression differs with proliferation in childhood acute lymphoblastic leukemia. *Mol. Biol. Rep.* 37, 2471-2476.
- Schaffer, A.E.; Taylor, B.L.; Benthuyens, J.R.; Liu, J. et al. (2013). Nkx6.1 controls a gene regulatory network required for establishing and maintaining pancreatic Beta cell identity. *PLoS. Genet.* 9, e1003274.
- Schanz, J.; Pusch, J.; Hansmann, J.; Walles, H. (2010). Vascularised human tissue models: a new approach for the refinement of biomedical research. *J. Biotechnol.* 148, 56-63.
- Scholer, H.R.; Ruppert, S.; Suzuki, N.; Chowdhury, K. et al. (1990). New type of POU domain in germ line-specific protein Oct-4. *Nature* 344, 435-439.
- Schroeder, I.S.; Rolletschek, A.; Blyszczuk, P.; Kania, G. et al. (2006). Differentiation of mouse embryonic stem cells to insulin-producing cells. *Nat. Protoc.* 1, 495-507.
- Schroeder, I.S.; Sulzbacher, S.; Nolden, T.; Fuchs, J. et al. (2012). Induction and selection of Sox17-expressing endoderm cells generated from murine embryonic stem cells. *Cells Tissues. Organs* 195, 507-523.
- Schroeder, I.S.; Wiese, C.; Truong, T.T.; Rolletschek, A. et al. (2009). Differentiation analysis of pluripotent mouse embryonic stem (ES) cells in vitro. *Methods Mol. Biol.* 530, 219-250.
- Schwartz, S.D.; Hubschman, J.P.; Heilwell, G.; Franco-Cardenas, V. et al. (2012). Embryonic stem cell trials for macular degeneration: a preliminary report. *Lancet* 379, 713-720.
- Schwitzgebel, V.M.; Scheel, D.W.; Conners, J.R.; Kalamaras, J. et al. (2000). Expression of neurogenin3 reveals an islet cell precursor population in the pancreas. *Development* 127, 3533-3542.
- Scotland, K.B.; Chen, S.; Sylvester, R.; Gudas, L.J. (2009). Analysis of Rex1 (zfp42) function in embryonic stem cell differentiation. *Dev. Dyn.* 238, 1863-1877.
- Seaberg, R.M.; Smukler, S.R.; Kieffer, T.J.; Enikolopov, G. et al. (2004). Clonal identification of multipotent precursors from adult mouse pancreas that generate neural and pancreatic lineages. *Nat. Biotechnol.* 22, 1115-1124.
- Sebastiano, V.; Maeder, M.L.; Angstman, J.F.; Haddad, B. et al. (2011). In situ genetic correction of the sickle cell anemia mutation in human induced pluripotent stem cells using engineered zinc finger nucleases. *Stem Cells* 29, 1717-1726.
- Seguin, C.A.; Draper, J.S.; Nagy, A.; Rossant, J. (2008). Establishment of endoderm progenitors by SOX transcription factor expression in human embryonic stem cells. *Cell Stem Cell* 3, 182-195.
- Semenza, G.L. (2011). Hypoxia. Cross talk between oxygen sensing and the cell cycle machinery. *Am. J. Physiol Cell Physiol* 301, C550-C552.
- Sengupta, S.; Nie, J.; Wagner, R.J.; Yang, C. et al. (2009). MicroRNA 92b controls the G1/S checkpoint gene p57 in human embryonic stem cells. *Stem Cells* 27, 1524-1528.
- Serup, P.; Petersen, H.V.; Pedersen, E.E.; Edlund, H. et al. (1995). The homeodomain protein IPF-1/STF-1 is expressed in a subset of islet cells and promotes rat insulin 1 gene expression dependent on an intact E1 helix-loop-helix factor binding site. *Biochem. J.* 310 (Pt 3), 997-1003.
- Shah, S.R.; Esni, F.; Jakub, A.; Paredes, J. et al. (2011). Embryonic mouse blood flow and oxygen correlate with early pancreatic differentiation. *Dev. Biol.* 349, 342-349.
- Shapiro, A.M.; Lakey, J.R.; Ryan, E.A.; Korbitt, G.S. et al. (2000). Islet transplantation in seven patients with type 1 diabetes mellitus using a glucocorticoid-free immunosuppressive regimen. *N. Engl. J. Med.* 343, 230-238.
- Shi, Y.; Desponts, C.; Do, J.T.; Hahm, H.S. et al. (2008). Induction of pluripotent stem cells from mouse embryonic fibroblasts by Oct4 and Klf4 with small-molecule compounds. *Cell Stem Cell* 3, 568-574.

- Shibata, K.R.; Aoyama, T.; Shima, Y.; Fukiage, K. et al. (2007). Expression of the p16INK4A gene is associated closely with senescence of human mesenchymal stem cells and is potentially silenced by DNA methylation during in vitro expansion. *Stem Cells* 25, 2371-2382.
- Shields, J.M.; Christy, R.J.; Yang, V.W. (1996). Identification and characterization of a gene encoding a gut-enriched Kruppel-like factor expressed during growth arrest. *J. Biol. Chem.* 271, 20009-20017.
- Shima, H.; Takubo, K.; Iwasaki, H.; Yoshihara, H. et al. (2009). Reconstitution activity of hypoxic cultured human cord blood CD34-positive cells in NOG mice. *Biochem. Biophys. Res. Commun.* 378, 467-472.
- Shu, J.; Xia, Z.; Li, L.; Liang, E.T. et al. (2012). Dose-dependent differential mRNA target selection and regulation by let-7a-7f and miR-17-92 cluster microRNAs. *RNA. Biol.* 9, 1275-1287.
- Shukla, S.; Nair, R.; Rolle, M.W.; Braun, K.R. et al. (2010). Synthesis and organization of hyaluronan and versican by embryonic stem cells undergoing embryoid body differentiation. *J. Histochem. Cytochem.* 58, 345-358.
- Si-Tayeb, K.; Noto, F.K.; Sepac, A.; Sedlic, F. et al. (2010). Generation of human induced pluripotent stem cells by simple transient transfection of plasmid DNA encoding reprogramming factors. *BMC. Dev. Biol.* 10, 81.
- Simon, M.C. and Keith, B. (2008). The role of oxygen availability in embryonic development and stem cell function. *Nat. Rev. Mol. Cell Biol.* 9, 285-296.
- Simons, M. and Eichmann, A. (2013). Physiology. Lymphatics are in my veins. *Science* 341, 622-624.
- Sinkkonen, L.; Hugenschmidt, T.; Beminger, P.; Gaidatzis, D. et al. (2008). MicroRNAs control de novo DNA methylation through regulation of transcriptional repressors in mouse embryonic stem cells. *Nat. Struct. Mol. Biol.* 15, 259-267.
- Skaper, S.D.; Debetto, P.; Giusti, P. (2009). P2X(7) Receptors in Neurological and Cardiovascular Disorders. *Cardiovasc. Psychiatry Neurol.* 2009, 861324.
- Skoudy, A.; Hernandez-Munoz, I.; Navarro, P. (2011). Pancreatic ductal adenocarcinoma and transcription factors: role of c-Myc. *J. Gastrointest. Cancer* 42, 76-84.
- Smirnova, L.; Grafe, A.; Seiler, A.; Schumacher, S. et al. (2005). Regulation of miRNA expression during neural cell specification. *Eur. J. Neurosci.* 21, 1469-1477.
- Smith, J.A.; Ndoye, A.M.; Geary, K.; Lisanti, M.P. et al. (2010). A role for the Werner syndrome protein in epigenetic inactivation of the pluripotency factor Oct4. *Aging Cell* 9, 580-591.
- Solar, M.; Cardalda, C.; Houbracken, I.; Martin, M. et al. (2009). Pancreatic exocrine duct cells give rise to insulin-producing beta cells during embryogenesis but not after birth. *Dev. Cell* 17, 849-860.
- Somers, A.; Jean, J.C.; Sommer, C.A.; Omari, A. et al. (2010). Generation of transgene-free lung disease-specific human induced pluripotent stem cells using a single excisable lentiviral stem cell cassette. *Stem Cells* 28, 1728-1740.
- Sommer, C.A.; Sommer, A.G.; Longmire, T.A.; Christodoulou, C. et al. (2010). Excision of reprogramming transgenes improves the differentiation potential of iPS cells generated with a single excisable vector. *Stem Cells* 28, 64-74.
- Soria, B.; Roche, E.; Bema, G.; Leon-Quinto, T. et al. (2000). Insulin-secreting cells derived from embryonic stem cells normalize glycemia in streptozotocin-induced diabetic mice. *Diabetes* 49, 157-162.
- Sotomayor, P.; Godoy, A.; Smith, G.J.; Huss, W.J. (2009). Oct4A is expressed by a subpopulation of prostate neuroendocrine cells. *Prostate* 69, 401-410.
- Sridharan, R. and Plath, K. (2008). Illuminating the black box of reprogramming. *Cell Stem Cell* 2, 295-297.
- Stadtfeld, M.; Brennand, K.; Hochedlinger, K. (2008). Reprogramming of pancreatic beta cells into induced pluripotent stem cells. *Curr. Biol.* 18, 890-894.
- Stanger, B.Z.; Tanaka, A.J.; Melton, D.A. (2007). Organ size is limited by the number of embryonic progenitor cells in the pancreas but not the liver. *Nature* 445, 886-891.
- Stevens, S.G. and Brown, C.M. (2013). In silico estimation of translation efficiency in human cell lines: potential evidence for widespread translational control. *PLoS. One.* 8, e57625.
- Stoffers, D.A.; Ferrer, J.; Clarke, W.L.; Habener, J.F. (1997). Early-onset type-II diabetes mellitus (MODY4) linked to IPF1. *Nat. Genet.* 17, 138-139.
- Strasser, A.; Elefanti, A.G.; Harris, A.W.; Cory, S. (1996). Progenitor tumours from Emu-bcl-2-myc transgenic mice have lymphomyeloid differentiation potential and reveal developmental differences in cell survival. *EMBO J.* 15, 3823-3834.
- Strauss, R.; Hamerlik, P.; Lieber, A.; Bartek, J. (2012). Regulation of stem cell plasticity: mechanisms and relevance to tissue biology and cancer. *Mol. Ther.* 20, 887-897.
- Stresemann, C.; Brueckner, B.; Musch, T.; Stopper, H. et al. (2006). Functional diversity of DNA methyltransferase inhibitors in human cancer cell lines. *Cancer Res.* 66, 2794-2800.
- Stumvoll, M.; Goldstein, B.J.; van Haefen, T.W. (2005). Type 2 diabetes: principles of pathogenesis and therapy. *Lancet* 365, 1333-1346.
- Suh, M.R.; Lee, Y.; Kim, J.Y.; Kim, S.K. et al. (2004). Human embryonic stem cells express a unique set of microRNAs. *Dev. Biol.* 270, 488-498.
- Sumi, T.; Tsuneyoshi, N.; Nakatsuji, N.; Suemori, H. (2008). Defining early lineage specification of human embryonic stem cells by the orchestrated balance of canonical Wnt/beta-catenin, Activin/Nodal and BMP signaling. *Development* 135, 2969-2979.
- Sun, Y.; Ge, Y.; Dmievich, J.; Zhao, Y. et al. (2010). Mammalian target of rapamycin regulates miRNA-1 and follistatin in skeletal myogenesis. *J. Cell Biol.* 189, 1157-1169.
- Suo, G.; Han, J.; Wang, X.; Zhang, J. et al. (2005). Oct4 pseudogenes are transcribed in cancers. *Biochem. Biophys. Res. Commun.* 337, 1047-1051.
- Suzuki, A.; Raya, A.; Kawakami, Y.; Morita, M. et al. (2006). Nanog binds to Smad1 and blocks bone morphogenetic protein-induced differentiation of embryonic stem cells. *Proc. Natl. Acad. Sci. U. S. A.* 103, 10294-10299.
- Suzuki, H.I.; Yamagata, K.; Sugimoto, K.; Iwamoto, T. et al. (2009). Modulation of microRNA processing by p53. *Nature* 460, 529-533.
- Szablowska-Gadomska, I.; Sypecka, J.; Zayat, V.; Podobinska, M. et al. (2012). Treatment with small molecules is an important milestone towards the induction of pluripotency in neural stem cells derived from human cord blood. *Acta Neurobiol. Exp. (Wars.)* 72, 337-350.
- Tachibana, M.; Amato, P.; Sparman, M.; Gutierrez, N.M. et al. (2013). Human embryonic stem cells derived by somatic cell nuclear transfer. *Cell* 153, 1228-1238.
- Tahamtani, Y.; Azamia, M.; Farokhi, A.; Sharifi-Zarchi, A. et al. (2013). Treatment of human embryonic stem cells with different combinations of priming and inducing factors toward definitive endoderm. *Stem Cells Dev.* 22, 1419-1432.
- Tai, M.H.; Chang, C.C.; Kiupel, M.; Webster, J.D. et al. (2005). Oct4 expression in adult human stem cells: evidence in support of the stem cell theory of carcinogenesis. *Carcinogenesis* 26, 495-502.

- Takahashi, K.; Tanabe, K.; Ohnuki, M.; Narita, M. et al. (2007). Induction of pluripotent stem cells from adult human fibroblasts by defined factors. *Cell* 131, 861-872.
- Takahashi, K. and Yamanaka, S. (2006). Induction of pluripotent stem cells from mouse embryonic and adult fibroblast cultures by defined factors. *Cell* 126, 663-676.
- Takai, D. and Jones, P.A. (2002). Comprehensive analysis of CpG islands in human chromosomes 21 and 22. *Proc. Natl. Acad. Sci. U. S. A* 99, 3740-3745.
- Takayama, K.; Inamura, M.; Kawabata, K.; Tashiro, K. et al. (2011). Efficient and directive generation of two distinct endoderm lineages from human ESCs and iPSCs by differentiation stage-specific SOX17 transduction. *PLoS. One* 6, e21780.
- Takeda, J.; Seino, S.; Bell, G.I. (1992). Human Oct3 gene family: cDNA sequences, alternative splicing, gene organization, chromosomal location, and expression at low levels in adult tissues. *Nucleic Acids Res.* 20, 4613-4620.
- Takenaga, M.; Fukumoto, M.; Hori, Y. (2007). Regulated Nodal signaling promotes differentiation of the definitive endoderm and mesoderm from ES cells. *J. Cell Sci.* 120, 2078-2090.
- Takenaka, C.; Nishishita, N.; Takada, N.; Jakt, L.M. et al. (2010). Effective generation of iPSCs from CD34+ cord blood cells by inhibition of p53. *Exp. Hematol.* 38, 154-162.
- Talavera-Adame, D.; Wu, G.; He, Y.; Ng, T.T. et al. (2011). Endothelial cells in co-culture enhance embryonic stem cell differentiation to pancreatic progenitors and insulin-producing cells through BMP signaling. *Stem Cell Rev.* 7, 532-543.
- Tam, P.P. and Loebel, D.A. (2007). Gene function in mouse embryogenesis: get set for gastrulation. *Nat. Rev. Genet.* 8, 368-381.
- Tan, M.H.; Au, K.F.; Leong, D.E.; Foygel, K. et al. (2013). An Oct4-Sall4-Nanog network controls developmental progression in the pre-implantation mouse embryo. *Mol. Syst. Biol.* 9, 632.
- Tang, C.; Lee, A.S.; Volkmer, J.P.; Sahoo, D. et al. (2011). An antibody against SSEA-5 glycan on human pluripotent stem cells enables removal of teratoma-forming cells. *Nat. Biotechnol.* 29, 829-834.
- Tang, R.; Faussat, A.M.; Majdak, P.; Perrot, J.Y. et al. (2004). Valproic acid inhibits proliferation and induces apoptosis in acute myeloid leukemia cells expressing P-gp and MRP1. *Leukemia* 18, 1246-1251.
- Taranger, C.K.; Noer, A.; Sorensen, A.L.; Hakelien, A.M. et al. (2005). Induction of dedifferentiation, genomewide transcriptional programming, and epigenetic reprogramming by extracts of carcinoma and embryonic stem cells. *Mol. Biol. Cell* 16, 5719-5735.
- Tay, Y.; Zhang, J.; Thomson, A.M.; Lim, B. et al. (2008). MicroRNAs to Nanog, Oct4 and Sox2 coding regions modulate embryonic stem cell differentiation. *Nature* 455, 1124-1128.
- Taylor, B.L.; Liu, F.F.; Sander, M. (2013). Nkx6.1 is essential for maintaining the functional state of pancreatic beta cells. *Cell Rep.* 4, 1262-1275.
- Tenchini, M.L.; Ranzati, C.; Malcoovati, M. (1992). Culture techniques for human keratinocytes. *Burns* 18 Suppl 1, S11-S16.
- Teng, H.F.; Kuo, Y.L.; Loo, M.R.; Li, C.L. et al. (2010). Valproic acid enhances Oct4 promoter activity in myogenic cells. *J. Cell Biochem.* 110, 995-1004.
- Terabayashi, T.; Itoh, T.J.; Yamaguchi, H.; Yoshimura, Y. et al. (2007). Polarity-regulating kinase partitioning-defective 1/microtubule affinity-regulating kinase 2 negatively regulates development of dendrites on hippocampal neurons. *J. Neurosci.* 27, 13098-13107.
- Thalmeier, K.; Meissner, P.; Reisbach, G.; Falk, M. et al. (1994). Establishment of two permanent human bone marrow stromal cell lines with long-term post irradiation feeder capacity. *Blood* 83, 1799-1807.
- Thatava, T.; Nelson, T.J.; Edukulla, R.; Sakuma, T. et al. (2011). Indolactam V/GLP-1-mediated differentiation of human iPSCs into glucose-responsive insulin-secreting progeny. *Gene Ther.* 18, 283-293.
- Theodorakis, M.J.; Carlson, O.; Michopoulos, S.; Doyle, M.E. et al. (2006). Human duodenal enteroendocrine cells: source of both incretin peptides, GLP-1 and GIP. *Am. J. Physiol. Endocrinol. Metab* 290, E550-E559.
- Thompson, R.D.; Noble, K.E.; Larbi, K.Y.; Dewar, A. et al. (2001). Platelet-endothelial cell adhesion molecule-1 (PECAM-1)-deficient mice demonstrate a transient and cytokine-specific role for PECAM-1 in leukocyte migration through the perivascular basement membrane. *Blood* 97, 1854-1860.
- Thomson, J.A.; Itskovitz-Eldor, J.; Shapiro, S.S.; Waknrit, M.A. et al. (1998). Embryonic stem cell lines derived from human blastocysts. *Science* 282, 1145-1147.
- Thornton, J.E. and Gregory, R.I. (2012). How does Lin28 let-7 control development and disease? *Trends Cell Biol.* 22, 474-482.
- Tian, R.Q.; Wang, X.H.; Hou, L.J.; Jia, W.H. et al. (2011). MicroRNA-372 is down-regulated and targets cyclin-dependent kinase 2 (CDK2) and cyclin A1 in human cervical cancer, which may contribute to tumorigenesis. *J. Biol. Chem.* 286, 25556-25563.
- Tili, E.; Michaille, J.J.; Wemick, D.; Alder, H. et al. (2011). Mutator activity induced by microRNA-155 (miR-155) links inflammation and cancer. *Proc. Natl. Acad. Sci. U. S. A* 108, 4908-4913.
- Tomikawa, M.; Nishimoto, M.; Miyagi, S.; Katayanagi, T. et al. (2002). Identification of Sox-2 regulatory region which is under the control of Oct-3/4-Sox-2 complex. *Nucleic Acids Res.* 30, 3202-3213.
- Tommasi, S.; Zheng, A.; Weninger, A.; Bates, S.E. et al. (2012). Mammalian cells acquire epigenetic hallmarks of human cancer during immortalization. *Nucleic Acids Res.*
- Treiber, T.; Treiber, N.; Meister, G. (2012). Regulation of microRNA biogenesis and function. *Thromb. Haemost.* 107.
- Tripathi, B.K. and Srivastava, A.K. (2006). Diabetes mellitus: complications and therapeutics. *Med. Sci. Monit.* 12, RA130-RA147.
- Trokovic, R.; Weltner, J.; Manninen, T.; Mikkola, M. et al. (2012). Small Molecule Inhibitors Promote Efficient Generation of Induced Pluripotent Stem Cells From Human Skeletal Myoblasts. *Stem Cells Dev.*
- Tsai, C.C.; Chen, Y.J.; Yew, T.L.; Chen, L.L. et al. (2011). Hypoxia inhibits senescence and maintains mesenchymal stem cell properties through down-regulation of E2A-p21 by HIF-TWIST. *Blood* 117, 459-469.
- Tsai, Z.Y.; Singh, S.; Yu, S.L.; Kao, L.P. et al. (2010). Identification of microRNAs regulated by activin A in human embryonic stem cells. *J. Cell Biochem.* 109, 93-102.
- Tudor, D.; Chaudry, F.; Harper, L.; Mackenzie, I.C. (2007). The in vitro behaviour and patterns of colony formation of murine epithelial stem cells. *Cell Prolif.* 40, 706-720.
- Umeda, K.; Zhao, J.; Simmons, P.; Stanley, E. et al. (2012). Human chondrogenic paraxial mesoderm, directed specification and prospective isolation from pluripotent stem cells. *Sci. Rep.* 2, 455.
- Unwin, N.; Gan, D.; Whiting, D. (2010). The IDF Diabetes Atlas: providing evidence, raising awareness and promoting action. *Diabetes Res. Clin. Pract.* 87, 2-3.
- Utikal, J.; Polo, J.M.; Stadtfeld, M.; Maherali, N. et al. (2009). Immortalization eliminates a roadblock during cellular reprogramming into iPSCs. *Nature* 460, 1145-1148.

- Vaca, P.; Martin, F.; Vegara-Meseguer, J.M.; Rovira, J.M. et al. (2006). Induction of differentiation of embryonic stem cells into insulin-secreting cells by fetal soluble factors. *Stem Cells* 24, 258-265.
- Vacanti, V.; Kong, E.; Suzuki, G.; Sato, K. et al. (2005). Phenotypic changes of adult porcine mesenchymal stem cells induced by prolonged passaging in culture. *J. Cell Physiol* 205, 194-201.
- Vaithilingam, V.; Oberholzer, J.; Guillemin, G.J.; Tuch, B.E. (2010). The humanized NOD/SCID mouse as a preclinical model to study the fate of encapsulated human islets. *Rev. Diabet. Stud.* 7, 62-73.
- Valdes, A.M. and Spector, T.D. (2010). The clinical relevance of genetic susceptibility to osteoarthritis. *Best. Pract. Res. Clin. Rheumatol.* 24, 3-14.
- Vallier, L.; Mendjan, S.; Brown, S.; Chng, Z. et al. (2009a). Activin/Nodal signalling maintains pluripotency by controlling Nanog expression. *Development* 136, 1339-1349.
- Vallier, L.; Touboul, T.; Chng, Z.; Brimpari, M. et al. (2009b). Early cell fate decisions of human embryonic stem cells and mouse epiblast stem cells are controlled by the same signalling pathways. *PLoS. One.* 4, e6082.
- Van Assche, F.A.; Aerts, L.; De, P.F. (1978). A morphological study of the endocrine pancreas in human pregnancy. *Br. J. Obstet. Gynaecol.* 85, 818-820.
- Van der Jeught, M.; O'Leary, T.; Ghimire, S.; Lierman, S. et al. (2013). The combination of inhibitors of FGF/MEK/Erk and GSK3beta signaling increases the number of OCT3/4- and NANOG-positive cells in the human inner cell mass, but does not improve stem cell derivation. *Stem Cells Dev.* 22, 296-306.
- van, D.M.; Visser, A.; Posthuma, J.; Poutsma, A. et al. (2012). Naturally occurring variation in trophoblast invasion as a source of novel (epigenetic) biomarkers. *Front Genet.* 3, 22.
- Van, H.D.; D'Amour, K.A.; German, M.S. (2009). Derivation of insulin-producing cells from human embryonic stem cells. *Stem Cell Res.* 3, 73-87.
- Vera, A.; Stanic, K.; Montecinos, H.; Torrejon, M. et al. (2013). SCO-spondin from embryonic cerebrospinal fluid is required for neurogenesis during early brain development. *Front Cell Neurosci.* 7, 80.
- Verlinsky, Y.; Strelchenko, N.; Kukharensko, V.; Rechitsky, S. et al. (2005). Human embryonic stem cell lines with genetic disorders. *Reprod. Biomed. Online.* 10, 105-110.
- Virtanen, I.; Banerjee, M.; Palgi, J.; Korsgren, O. et al. (2008). Blood vessels of human islets of Langerhans are surrounded by a double basement membrane. *Diabetologia* 51, 1181-1191.
- Visvader, J.E. and Lindeman, G.J. (2008). Cancer stem cells in solid tumours: accumulating evidence and unresolved questions. *Nat. Rev. Cancer* 8, 755-768.
- Vollmers, A.; Wallace, L.; Fullard, N.; Hoher, T. et al. (2012). Two- and three-dimensional culture of keratinocyte stem and precursor cells derived from primary murine epidermal cultures. *Stem Cell Rev.* 8, 402-413.
- Wachs, F.P.; Couillard-Despres, S.; Engelhardt, M.; Wilhelm, D. et al. (2003). High efficacy of clonal growth and expansion of adult neural stem cells. *Lab Invest* 83, 949-962.
- Walia, B.; Satija, N.; Tripathi, R.P.; Gangenahalli, G.U. (2012). Induced pluripotent stem cells: fundamentals and applications of the reprogramming process and its ramifications on regenerative medicine. *Stem Cell Rev.* 8, 100-115.
- Wamhoff, B.R.; Bowles, D.K.; McDonald, O.G.; Sinha, S. et al. (2004). L-type voltage-gated Ca²⁺ channels modulate expression of smooth muscle differentiation marker genes via a rho kinase/myocardin/SRF-dependent mechanism. *Circ. Res.* 95, 406-414.
- Wang, J.; Rao, S.; Chu, J.; Shen, X. et al. (2006). A protein interaction network for pluripotency of embryonic stem cells. *Nature* 444, 364-368.
- Wang, N.; Li, Q.; Zhang, L.; Lin, H. et al. (2012a). Mesenchymal stem cells attenuate peritoneal injury through secretion of TSG-6. *PLoS. One.* 7, e43768.
- Wang, P.; McKnight, K.D.; Wong, D.J.; Rodriguez, R.T. et al. (2012b). A molecular signature for purified definitive endoderm guides differentiation and isolation of endoderm from mouse and human embryonic stem cells. *Stem Cells Dev.* 21, 2273-2287.
- Wang, P.; Rodriguez, R.T.; Wang, J.; Ghodasara, A. et al. (2011). Targeting SOX17 in human embryonic stem cells creates unique strategies for isolating and analyzing developing endoderm. *Cell Stem Cell* 8, 335-346.
- Wang, X. and Dai, J. (2010). Concise review: isoforms of OCT4 contribute to the confusing diversity in stem cell biology. *Stem Cells* 28, 885-893.
- Wang, X.; Misawa, R.; Zielinski, M.C.; Cowen, P. et al. (2013). Regional differences in islet distribution in the human pancreas—preferential beta-cell loss in the head region in patients with type 2 diabetes. *PLoS. One.* 8, e67454.
- Wang, Y.; Baskerville, S.; Shenoy, A.; Babiarz, J.E. et al. (2008). Embryonic stem cell-specific microRNAs regulate the G1-S transition and promote rapid proliferation. *Nat. Genet.* 40, 1478-1483.
- Wang, Y.; Liu, J.; Tan, X.; Li, G. et al. (2012c). Induced Pluripotent Stem Cells from Human Hair Follicle Mesenchymal Stem Cells. *Stem Cell Rev.*
- Wang, Y.; Medvid, R.; Melton, C.; Jaenisch, R. et al. (2007). DGCR8 is essential for microRNA biogenesis and silencing of embryonic stem cell self-renewal. *Nat. Genet.* 39, 380-385.
- Wang, Z. (2011). The guideline of the design and validation of MiRNA mimics. *Methods Mol. Biol.* 676, 211-223.
- Wang, Z.Z.; Au, P.; Chen, T.; Shao, Y. et al. (2007). Endothelial cells derived from human embryonic stem cells form durable blood vessels in vivo. *Nat Biotechnol.* 25, 317-318.
- Warren, L.; Manos, P.D.; Ahfeldt, T.; Loh, Y.H. et al. (2010). Highly efficient reprogramming to pluripotency and directed differentiation of human cells with synthetic modified mRNA. *Cell Stem Cell* 7, 618-630.
- Watabe, T. (2012). Roles of Dppa2 in the regulation of the present status and future of pluripotent stem cells. *J. Biochem.* 152, 1-3.
- Webster, J.D.; Yuzbasiyan-Gurkan, V.; Trosko, J.E.; Chang, C.C. et al. (2007). Expression of the embryonic transcription factor Oct4 in canine neoplasms: a potential marker for stem cell subpopulations in neoplasia. *Vet. Pathol.* 44, 893-900.
- Weedon, M.N.; McCarthy, M.I.; Hitman, G.; Walker, M. et al. (2006). Combining information from common type 2 diabetes risk polymorphisms improves disease prediction. *PLoS. Med.* 3, e374.
- Wei, D.; Wang, L.; Kanai, M.; Jia, Z. et al. (2010). KLF4alpha up-regulation promotes cell cycle progression and reduces survival time of patients with pancreatic cancer. *Gastroenterology* 139, 2135-2145.
- Wernig, M.; Meissner, A.; Foreman, R.; Brambrink, T. et al. (2007). In vitro reprogramming of fibroblasts into a pluripotent ES-cell-like state. *Nature* 448, 318-324.
- Wild, S.; Roglic, G.; Green, A.; Sicree, R. et al. (2004). Global prevalence of diabetes: estimates for the year 2000 and projections for 2030. *Diabetes Care* 27, 1047-1053.
- Willcox, A.; Richardson, S.J.; Bone, A.J.; Foulis, A.K. et al. (2010). Evidence of increased islet cell proliferation in patients with recent-onset type 1 diabetes. *Diabetologia* 53, 2020-2028.

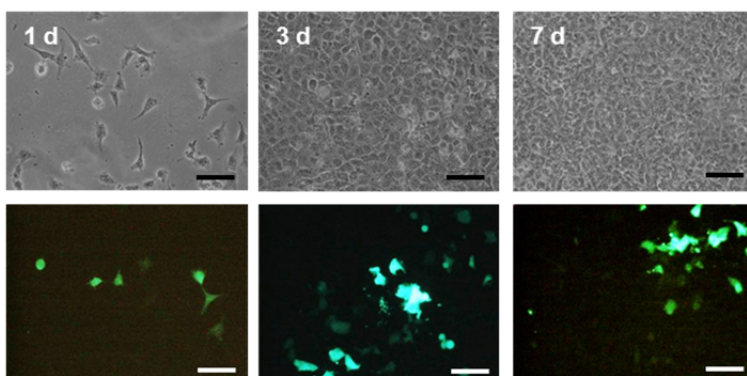
- Winbanks, C.E.; Beyer, C.; Hagg, A.; Qian, H. et al. (2013). miR-206 represses hypertrophy of myogenic cells but not muscle fibers via inhibition of HDAC4. *PLoS. One.* 8, e73589.
- Wobus, A.M. and Boheler, K.R. (2005). Embryonic stem cells: prospects for developmental biology and cell therapy. *Physiol Rev.* 85, 635-678.
- Wolgemuth, D.J. (2011). Function of the A-type cyclins during gametogenesis and early embryogenesis. *Results Probl. Cell Differ.* 53, 391-413.
- Wong, S.S.; Ritner, C.; Ramachandran, S.; Aurigui, J. et al. (2012). miR-125b promotes early germ layer specification through Lin28/let-7d and preferential differentiation of mesoderm in human embryonic stem cells. *PLoS. One.* 7, e36121.
- Woodford, C. and Zandstra, P.W. (2012). Tissue engineering 2.0: guiding self-organization during pluripotent stem cell differentiation. *Curr. Opin. Biotechnol.* 23, 810-819.
- Wu, X. and Brewer, G. (2012). The regulation of mRNA stability in mammalian cells: 2.0. *Gene* 500, 10-21.
- Xu, C.X.; Xu, M.; Tan, L.; Yang, H. et al. (2012a). MicroRNA miR-214 regulates ovarian cancer cell stemness by targeting p53/Nanog. *J. Biol. Chem.* 287, 34970-34978.
- Xu, R.H.; Chen, X.; Li, D.S.; Li, R. et al. (2002). BMP4 initiates human embryonic stem cell differentiation to trophoblast. *Nat. Biotechnol.* 20, 1261-1264.
- Xu, R.H.; Sampsel-Barron, T.L.; Gu, F.; Root, S. et al. (2008). NANOG is a direct target of TGFbeta/activin-mediated SMAD signaling in human ESCs. *Cell Stem Cell* 3, 196-206.
- Xu, X.; Browning, V.L.; Odorico, J.S. (2011). Activin, BMP and FGF pathways cooperate to promote endoderm and pancreatic lineage cell differentiation from human embryonic stem cells. *Mech. Dev.* 128, 412-427.
- Xu, X.; Gnatenko, D.V.; Ju, J.; Hitchcock, I.S. et al. (2012b). Systematic analysis of microRNA fingerprints in thrombocytic platelets using integrated platforms. *Blood* 120, 3575-3585.
- Xu, X.; Kahan, B.; Forgianni, A.; Jing, P. et al. (2006). Endoderm and pancreatic islet lineage differentiation from human embryonic stem cells. *Cloning Stem Cells* 8, 96-107.
- Xu, Y.; Wei, X.; Wang, M.; Zhang, R. et al. (2013). Proliferation rate of somatic cells affects reprogramming efficiency. *J. Biol. Chem.* 288, 9767-9778.
- Xu, Y.; Zhu, X.; Hahm, H.S.; Wei, W. et al. (2010). Revealing a core signaling regulatory mechanism for pluripotent stem cell survival and self-renewal by small molecules. *Proc. Natl. Acad. Sci. U. S. A* 107, 8129-8134.
- Yan, X.; Lv, A.; Xing, Y.; Liu, B. et al. (2011). Inhibition of p53-p21 pathway promotes the differentiation of rat bone marrow mesenchymal stem cells into cardiomyocytes. *Mol. Cell Biochem.* 354, 21-28.
- Yang, F.; Green, J.J.; Dinio, T.; Keung, L. et al. (2009). Gene delivery to human adult and embryonic cell-derived stem cells using biodegradable nanoparticulate polymeric vectors. *Gene Ther.* 16, 533-546.
- Yang, J.; Zhang, Z.; Chen, C.; Liu, Y. et al. (2013). MicroRNA-19a-3p inhibits breast cancer progression and metastasis by inducing macrophage polarization through downregulated expression of Fra-1 proto-oncogene. *Oncogene.*
- Yang, J.S. and Lai, E.C. (2011). Alternative miRNA biogenesis pathways and the interpretation of core miRNA pathway mutants. *Mol. Cell* 43, 892-903.
- Yang, Q.; Lu, Z.; Singh, D.; Raj, J.U. (2012). BIX-01294 treatment blocks cell proliferation, migration and contractility in ovine foetal pulmonary arterial smooth muscle cells. *Cell Prolif.* 45, 335-344.
- Yang, Y.P.; Thorel, F.; Boyer, D.F.; Herrera, P.L. et al. (2011). Context-specific alpha- to-beta-cell reprogramming by forced Pdx1 expression. *Genes Dev.* 25, 1680-1685.
- Yasunaga, M.; Tada, S.; Torikai-Nishikawa, S.; Nakano, Y. et al. (2005). Induction and monitoring of definitive and visceral endoderm differentiation of mouse ES cells. *Nat. Biotechnol.* 23, 1542-1550.
- Yates, F. and Daley, G.Q. (2006). Progress and prospects: gene transfer into embryonic stem cells. *Gene Ther.* 13, 1431-1439.
- Yi, F.; Pereira, L.; Hoffman, J.A.; Shy, B.R. et al. (2011). Opposing effects of Tcf3 and Tcf1 control Wnt stimulation of embryonic stem cell self-renewal. *Nat. Cell Biol.* 13, 762-770.
- Ying, Q.L.; Nichols, J.; Chambers, I.; Smith, A. (2003). BMP induction of Id proteins suppresses differentiation and sustains embryonic stem cell self-renewal in collaboration with STAT3. *Cell* 115, 281-292.
- Ying, Q.L.; Wray, J.; Nichols, J.; Battle-Morera, L. et al. (2008). The ground state of embryonic stem cell self-renewal. *Nature* 453, 519-523.
- Yochim, J.M. and Mitchell, J.A. (1968). Intrauterine oxygen tension in the rat during progestation: its possible relation to carbohydrate metabolism and the regulation of nidation. *Endocrinology* 83, 706-713.
- Yoo, J.K.; Kim, J.; Choi, S.J.; Noh, H.M. et al. (2012). Discovery and characterization of novel microRNAs during endothelial differentiation of human embryonic stem cells. *Stem Cells Dev.* 21, 2049-2057.
- Yoshida, Y.; Takahashi, K.; Okita, K.; Ichisaka, T. et al. (2009). Hypoxia enhances the generation of induced pluripotent stem cells. *Cell Stem Cell* 5, 237-241.
- Yoshitomi, H. and Zaret, K.S. (2004). Endothelial cell interactions initiate dorsal pancreas development by selectively inducing the transcription factor Ptf1a. *Development* 131, 807-817.
- Yu, J.; Hu, K.; Smuga-Otto, K.; Tian, S. et al. (2009). Human induced pluripotent stem cells free of vector and transgene sequences. *Science* 324, 797-801.
- Yu, J.; Vodyanik, M.A.; Smuga-Otto, K.; Antosiewicz-Bourget, J. et al. (2007). Induced pluripotent stem cell lines derived from human somatic cells. *Science* 318, 1917-1920.
- Yuan, H.; Corbi, N.; Basilico, C.; Dailey, L. (1995). Developmental-specific activity of the FGF-4 enhancer requires the synergistic action of Sox2 and Oct-3. *Genes Dev.* 9, 2635-2645.
- Yue, G.G.; Fan, J.T.; Lee, J.K.; Zeng, G.Z. et al. (2011). Cyclopeptide RA-V inhibits angiogenesis by down-regulating ERK1/2 phosphorylation in HUVEC and HMEC-1 endothelial cells. *Br. J. Pharmacol.* 164, 1883-1898.
- Zangrossi, S.; Marabese, M.; Brogini, M.; Giordano, R. et al. (2007). Oct-4 expression in adult human differentiated cells challenges its role as a pure stem cell marker. *Stem Cells* 25, 1675-1680.
- Zanone, M.M.; Favaro, E.; Camussi, G. (2008). From endothelial to beta cells: insights into pancreatic islet microendothelium. *Curr. Diabetes Rev.* 4, 1-9.
- Zeng, Y. and Cullen, B.R. (2003). Sequence requirements for micro RNA processing and function in human cells. *RNA.* 9, 112-123.
- Zhang, D.; Jiang, W.; Liu, M.; Sui, X. et al. (2009a). Highly efficient differentiation of human ES cells and iPS cells into mature pancreatic insulin-producing cells. *Cell Res.* 19, 429-438.
- Zhang, D.; Jiang, W.; Shi, Y.; Deng, H. (2009b). Generation of pancreatic islet cells from human embryonic stem cells. *Sci. China C. Life Sci.* 52, 615-621.

- Zhang, X.; Neganova, I.; Przyborski, S.; Yang, C. et al. (2009c). A role for NANOG in G1 to S transition in human embryonic stem cells through direct binding of CDK6 and CDC25A. *J. Cell Biol.* 184, 67-82.
- Zhang, Y.; Hu, H.; Song, L.; Cai, L. et al. (2013a). Epirubicin-mediated expression of miR-302b is involved in osteosarcoma apoptosis and cell cycle regulation. *Toxicol. Lett.* 222, 1-9.
- Zhang, Y.; Yang, P.; Sun, T.; Li, D. et al. (2013b). miR-126 and miR-126* repress recruitment of mesenchymal stem cells and inflammatory monocytes to inhibit breast cancer metastasis. *Nat. Cell Biol.* 15, 284-294.
- Zhang, Z.; Gao, Y.; Gordon, A.; Wang, Z.Z. et al. (2011). Efficient generation of fully reprogrammed human iPSC cells via polycistronic retroviral vector and a new cocktail of chemical compounds. *PLoS. One.* 6, e26592.
- Zhang, Z.; Xiang, D.; Heriyanto, F.; Gao, Y. et al. (2013c). Dissecting the Roles of miR-302/367 Cluster in Cellular Reprogramming Using TALE-based Repressor and TALEN. *Stem Cell Reports.* 1, 218-225.
- Zhao, Y.; Yin, X.; Qin, H.; Zhu, F. et al. (2008). Two supporting factors greatly improve the efficiency of human iPSC generation. *Cell Stem Cell* 3, 475-479.
- Zhao, Z.; Wu, Q.; Cheng, J.; Qiu, X. et al. Depletion of DNMT3A suppressed cell proliferation and restored PTEN in hepatocellular carcinoma cell. *J Biomed Biotechnol.*
- Zheng, J.; Benbrook, D.M.; Yu, H.; Ding, W.Q. (2011). Cloiquinol suppresses cyclin D1 gene expression through transcriptional and post-transcriptional mechanisms. *Anticancer Res.* 31, 2739-2747.
- Zhou, H.; Chang, S.; Rao, M. (2012). Human cord blood applications in cell therapy: looking back and look ahead. *Expert. Opin. Biol. Ther.* 12, 1059-1066.
- Zhou, J.; Su, P.; Li, D.; Tsang, S. et al. (2010). High-efficiency induction of neural conversion in human ESCs and human induced pluripotent stem cells with a single chemical inhibitor of transforming growth factor beta superfamily receptors. *Stem Cells* 28, 1741-1750.
- Zhou, Q.; Law, A.C.; Rajagopal, J.; Anderson, W.J. et al. (2007). A multipotent progenitor domain guides pancreatic organogenesis. *Dev. Cell* 13, 103-114.
- Zhou, W. and Freed, C.R. (2009). Adenoviral gene delivery can reprogram human fibroblasts to induced pluripotent stem cells. *Stem Cells* 27, 2667-2674.
- Zhu, B.; Mandal, S.S.; Pham, A.D.; Zheng, Y. et al. (2005). The human PAF complex coordinates transcription with events downstream of RNA synthesis. *Genes Dev.* 19, 1668-1673.
- Zhu, H.; Shah, S.; Shyh-Chang, N.; Shinoda, G. et al. (2010). Lin28a transgenic mice manifest size and puberty phenotypes identified in human genetic association studies. *Nat. Genet.* 42, 626-630.
- Zhu, T.S.; Costello, M.A.; Talsma, C.E.; Flack, C.G. et al. (2011). Endothelial cells create a stem cell niche in glioblastoma by providing NOTCH ligands that nurture self-renewal of cancer stem-like cells. *Cancer Res.* 71, 6061-6072.
- Zou, Q.; Yan, Q.; Zhong, J.; Wang, K. et al. (2014). Direct Conversion of Human Fibroblasts into Neuronal Restricted Progenitors. *J. Biol. Chem.*
- Zou, S.; Scarfo, K.; Nantz, M.H.; Hecker, J.G. (2010). Lipid-mediated delivery of RNA is more efficient than delivery of DNA in non-dividing cells. *Int. J. Pharm.* 389, 232-243.

8. APPENDICES

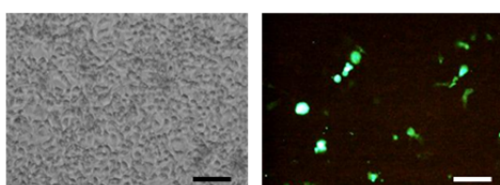
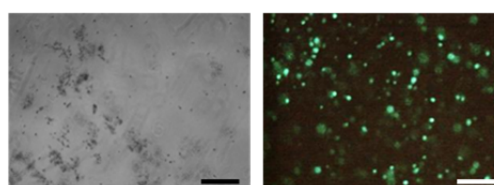
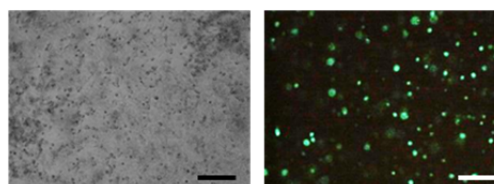
A

electroporation standard approach

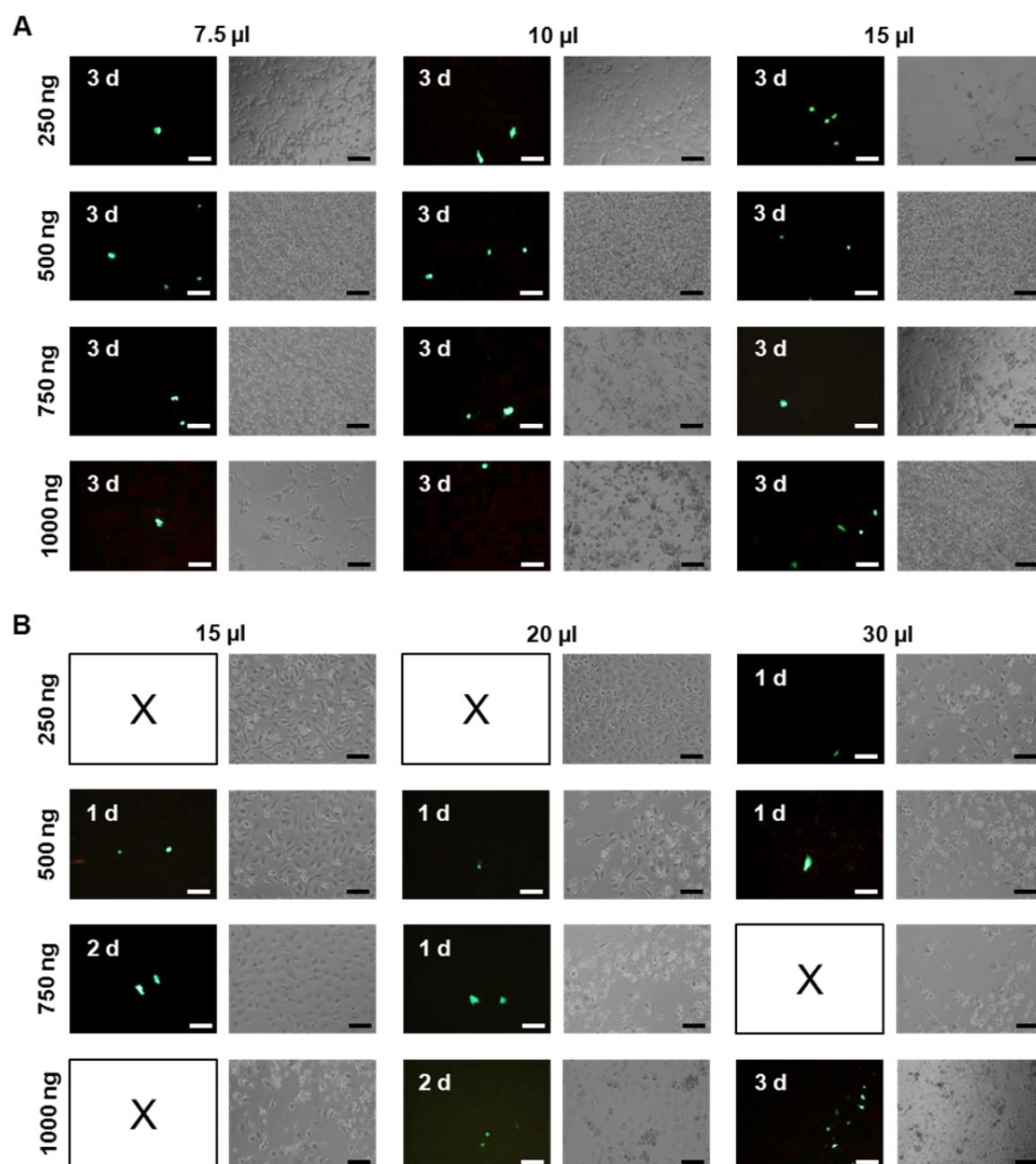


B

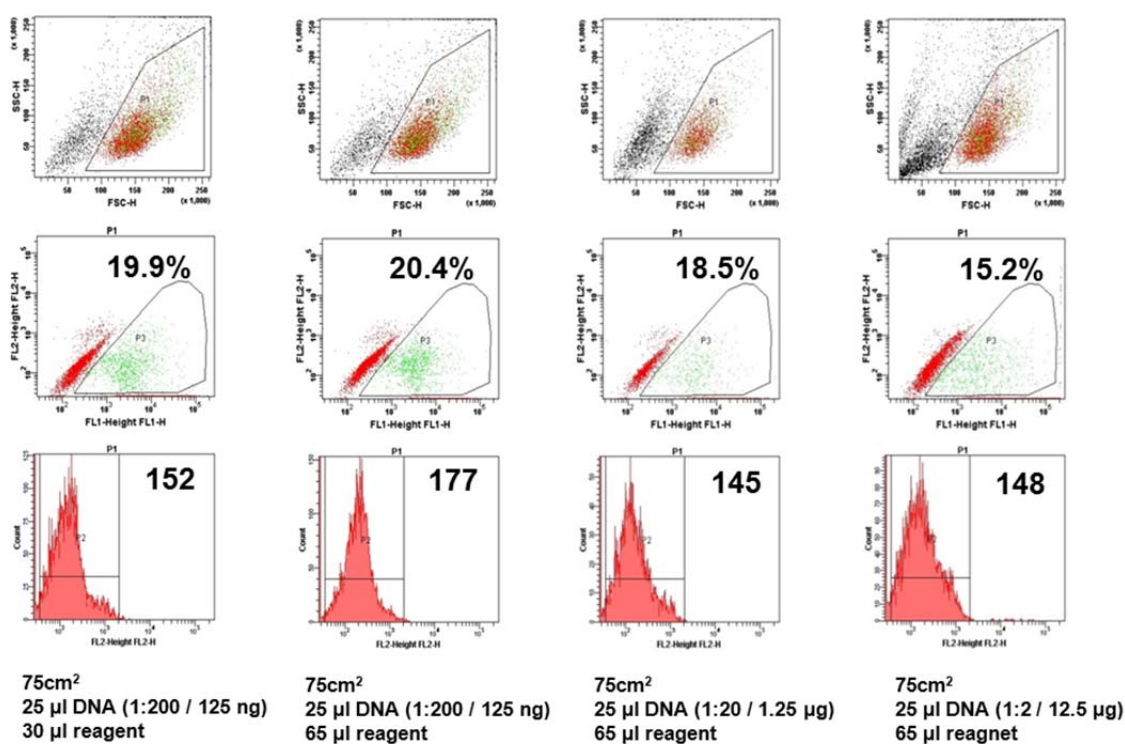
lipofection standard approach

more than 625 ng DNA/10⁵ cellsmore than 9.4 µl INTERFERin™/10⁵ cells

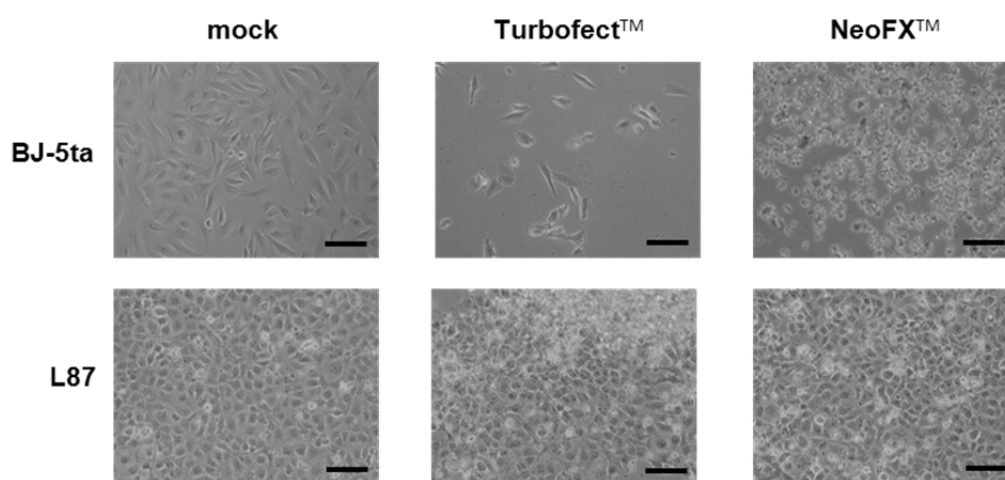
APPENDIX 1: Morphology and GFP expression after delivery of pEGFP-N1 by electroporation and lipofection. (A) Electroporation of pEGFP-N1 into L87 cells by application of different protocols. Morphology and GFP fluorescence are demonstrated from day 1 until day 7 for the standard approach. (B) Lipofection of pEGFP-N1 into L87 cells by application of different protocols at day 3. Morphology and GFP fluorescence of viable cells are demonstrated when 625 ng DNA and 9.4 µl INTERFERin™ were applied in 10⁵ cells (indicated as standard approach). Detachment indicating loss of viability is demonstrated by elevation of plasmid DNA and transfection reagent. Bars represent 100 µm.



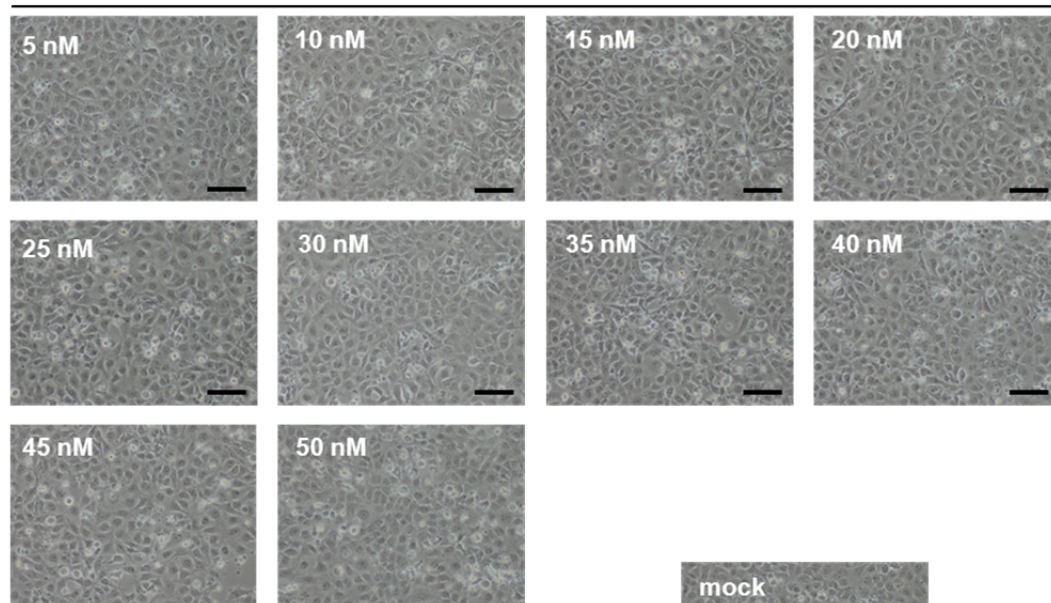
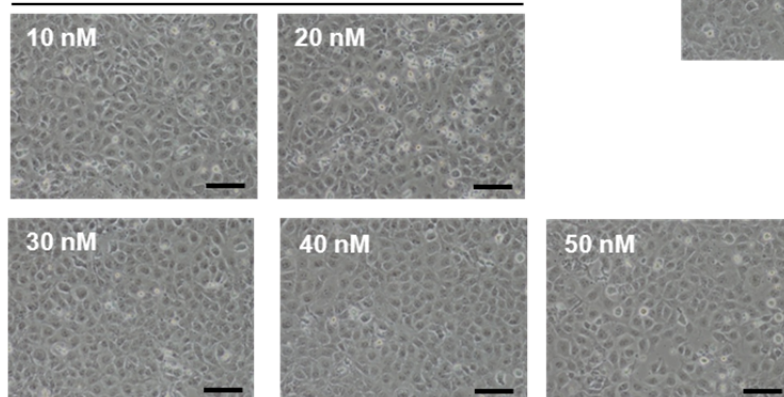
APPENDIX 2: Morphology and GFP expression after delivery of pEGFP-N1 using competitor reagents. (A) Optimization assay of Lipofectamine™ 2000. L87 cells were treated with 7.5-15.0 μ l Lipofectamine™ 2000 and 250-1000 ng DNA per 12-well containing 4×10^4 cells. Morphology and GFP expression is demonstrated at day 3. **(B)** Optimization assay of Lipofectamine™ LTX & Plus™ reagent. Cells were treated with 15.0-30.0 μ l diluted reagent and 250-1000 ng DNA per 12-well containing 4×10^4 cells. Morphology and GFP fluorescence is demonstrated at that when GFP expression occurred. [X] indicates that there was no GFP expression. Bars represent 100 μ m.



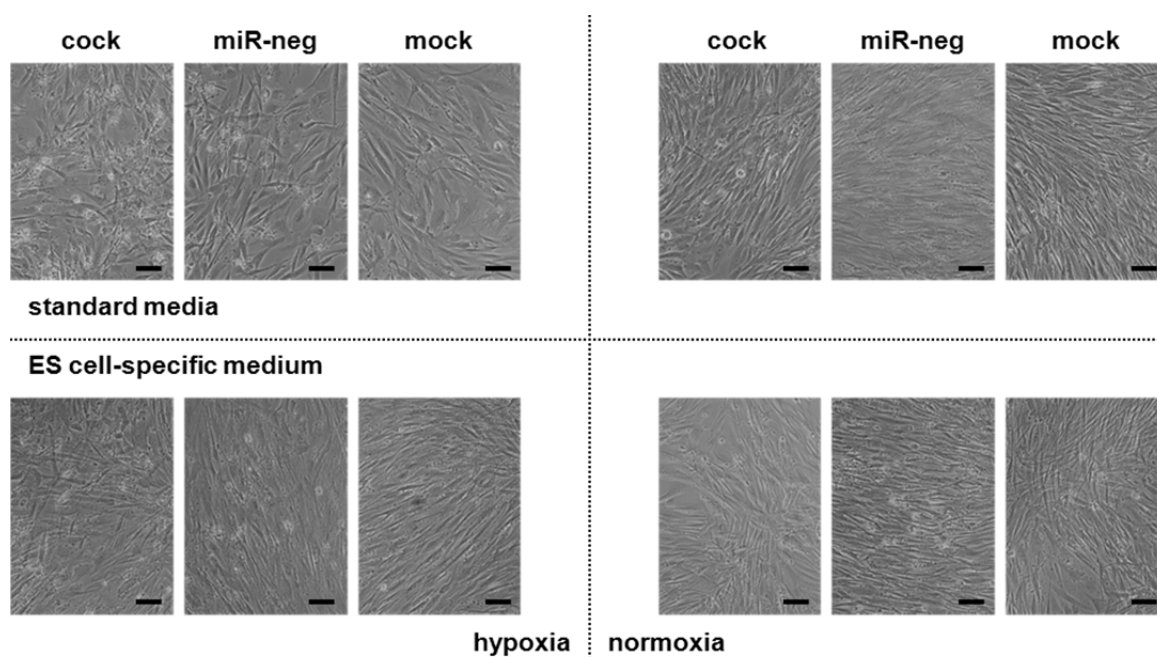
APPENDIX 3: Optimization of STEMcircles™ delivery. L87 cells ($1-1.5 \times 10^6$) were transfected with different amounts of INTERFERin™ transfection reagent (indicated as reagent) and episomal vector DNA (indicated as DNA). The presence of the GFP fluorescence was analyzed by flow cytometry at day 3. Representative data (n=2).



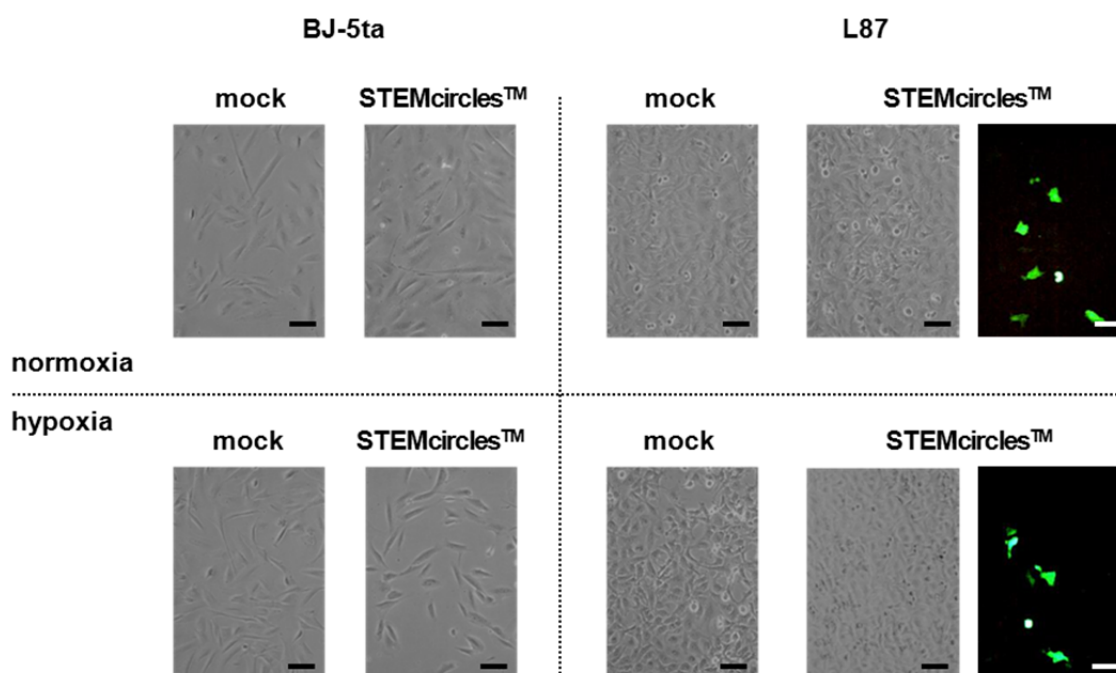
APPENDIX 4: Morphology after delivery of miRs using competitor reagents. Turbofect™ and NeoFX™ transfection reagents were analyzed in BJ-5ta cells and L87 cells at day 3 according to manufacturer's instructions by transfection of 50 nM miR-1 and mock transfection. Bars represent 100 µm.

miR-1**nonsense miR**

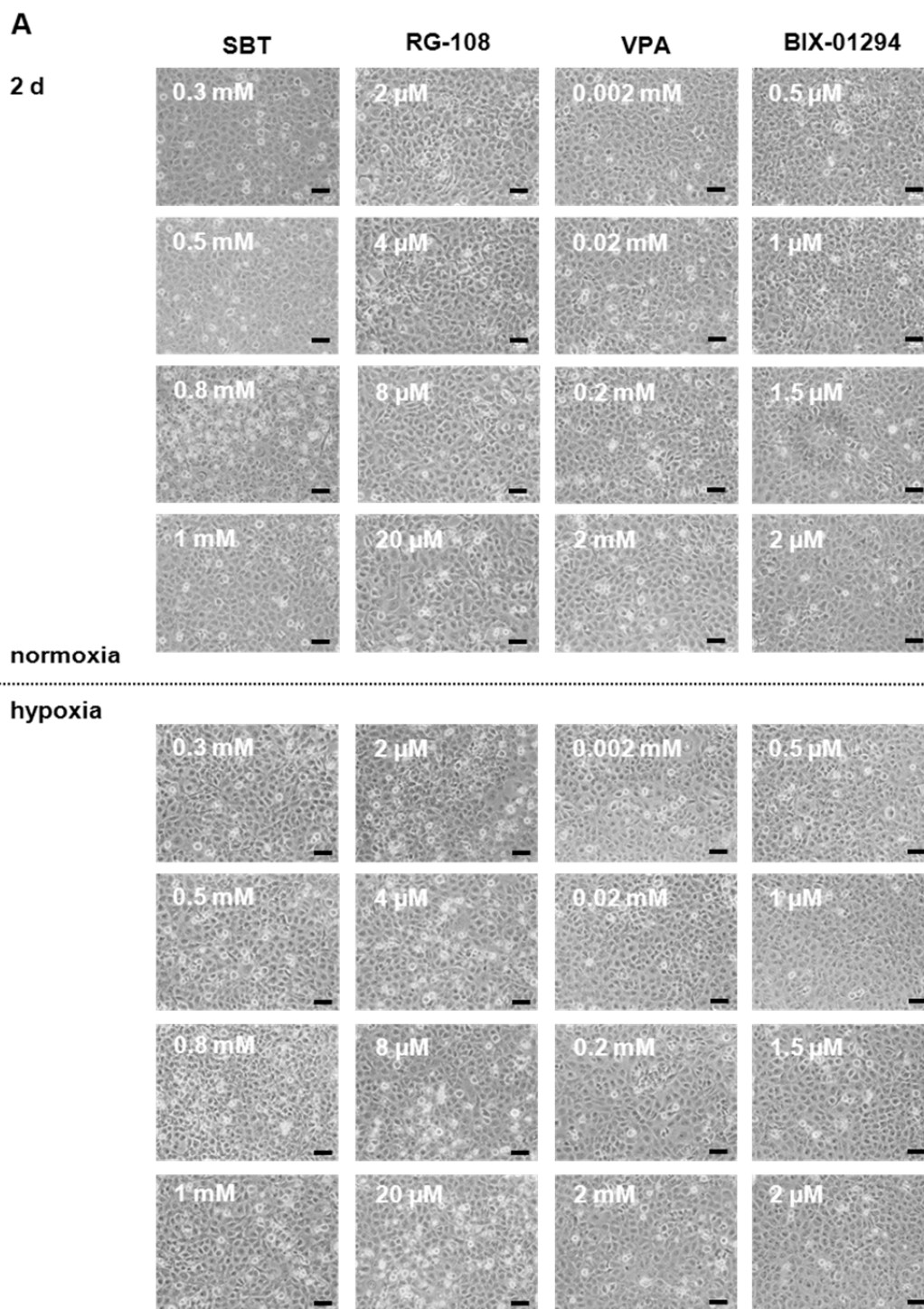
APPENDIX 5: Morphology after delivery of miRs using different concentrations. L87 cells were treated by INTERFERin™ according to manufacturer's instructions. Different amounts of miR-1, nonsense miR and mock transfection is demonstrated. Bars represent 100 μ m.

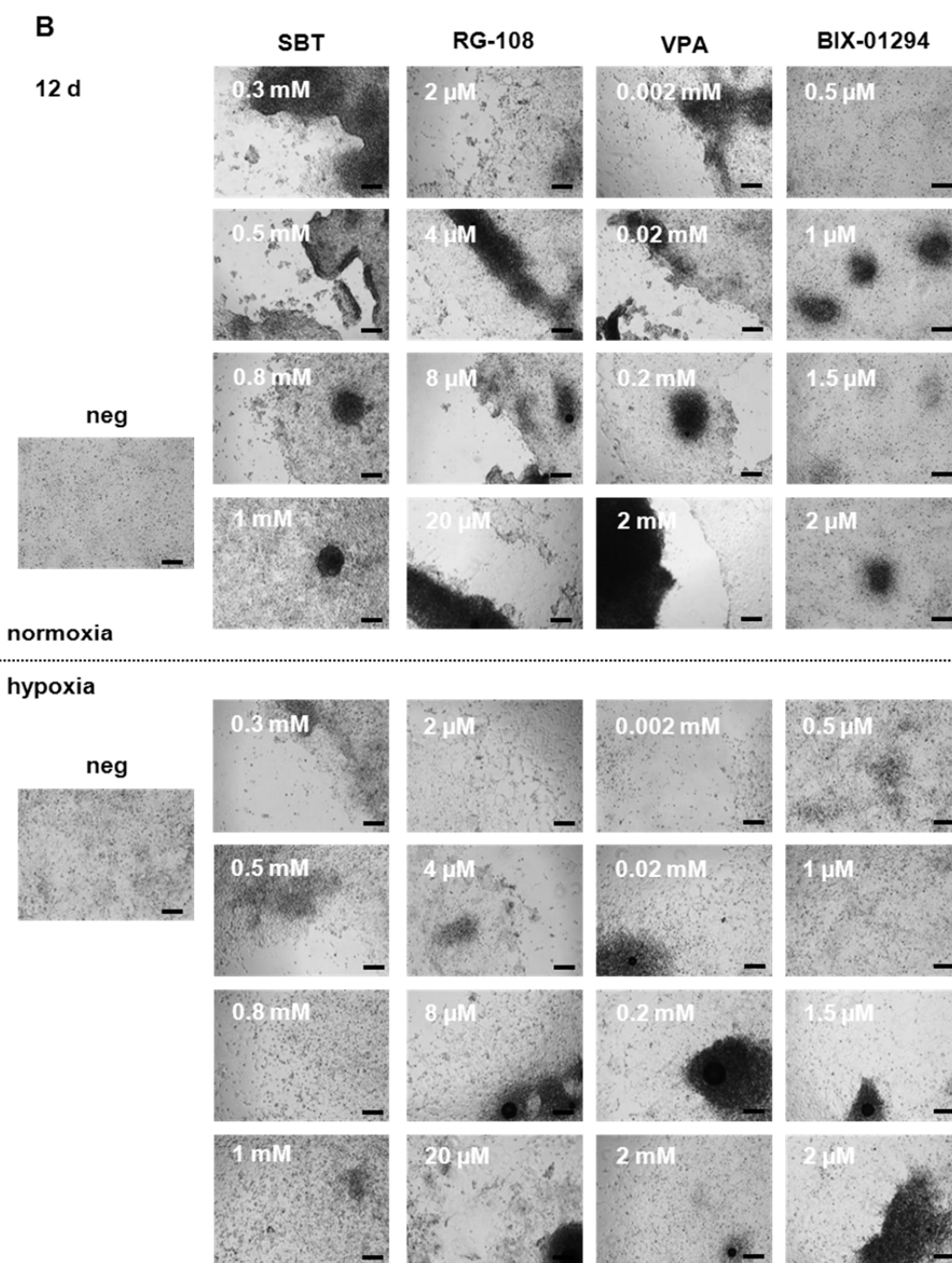


APPENDIX 6: Morphology and after delivery of miR-302a-d & 372 in the presence of hypoxia. BJ-5ta cells were transfected with 5×10 nM miR-302a-d & 372 (cock), 50 nM nonsense miRs (miR-neg), and mock-transfected (mock). Cells were seeded on MEFs and morphology is demonstrated using standard media and human ES cell-specific medium under normoxia and hypoxia. Representative data at day 5 (n=3).

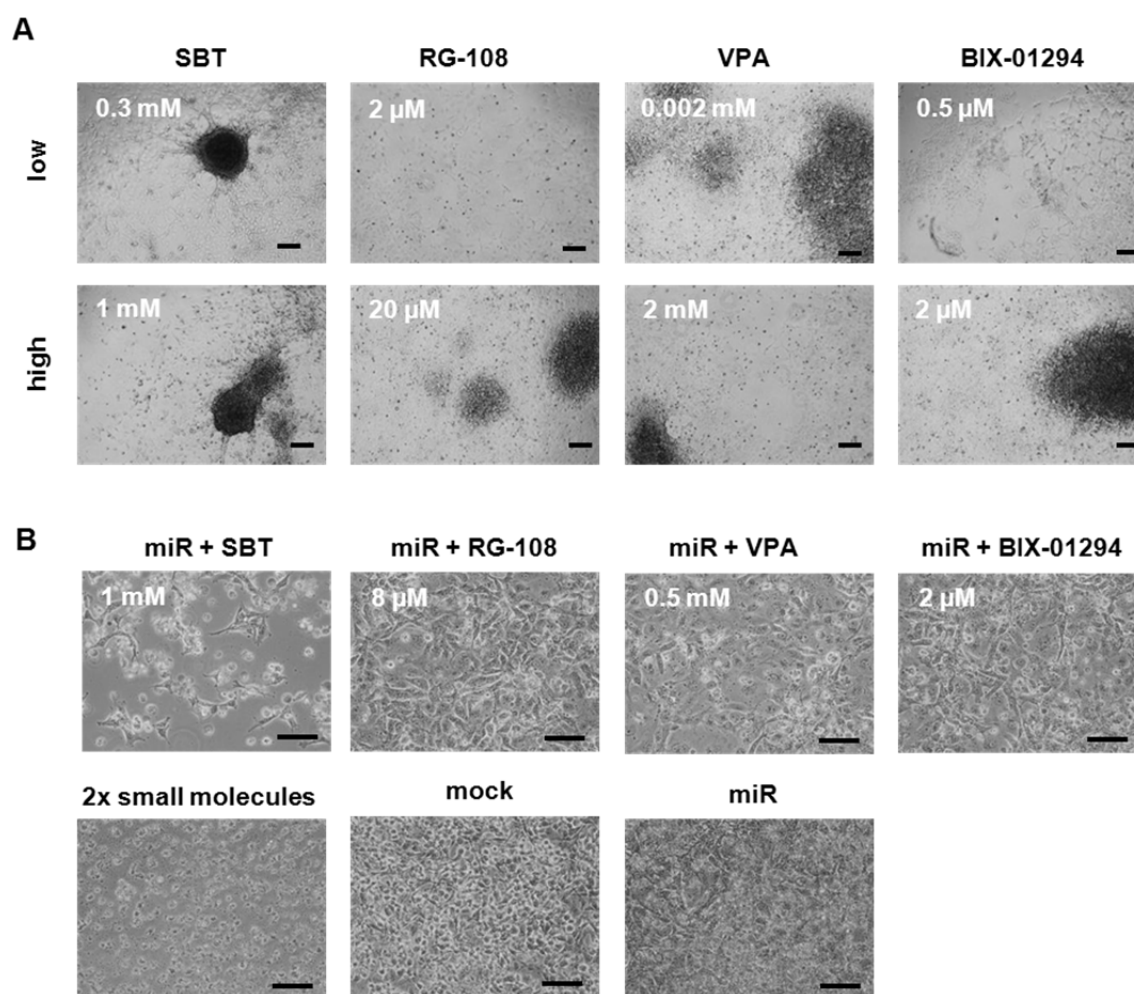


APPENDIX 7: Morphology and GFP expression after delivery of STEMcircles™ in the presence of normoxia and hypoxia. BJ-5ta cells and L87 cells were transfected with episomal vectors ($1-1.5 \mu\text{g} / 1 \times 10^6$ cells) or mock-transfected (mock). Morphology and GFP expression is demonstrated at day 2 under normoxia and hypoxia. Representative data (n=3).

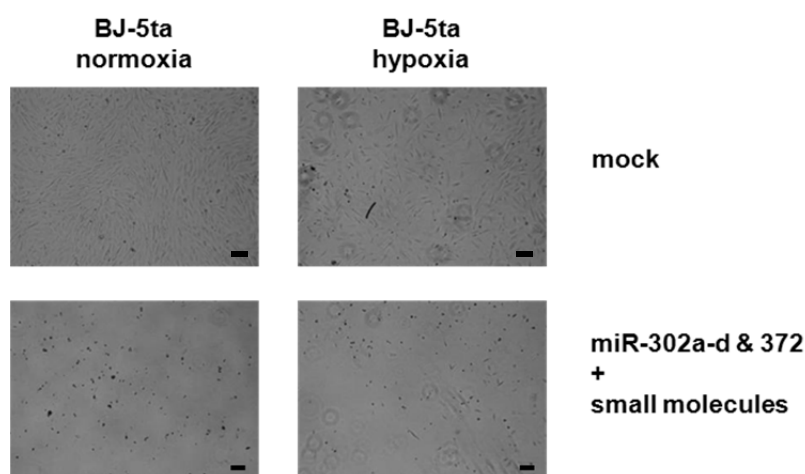




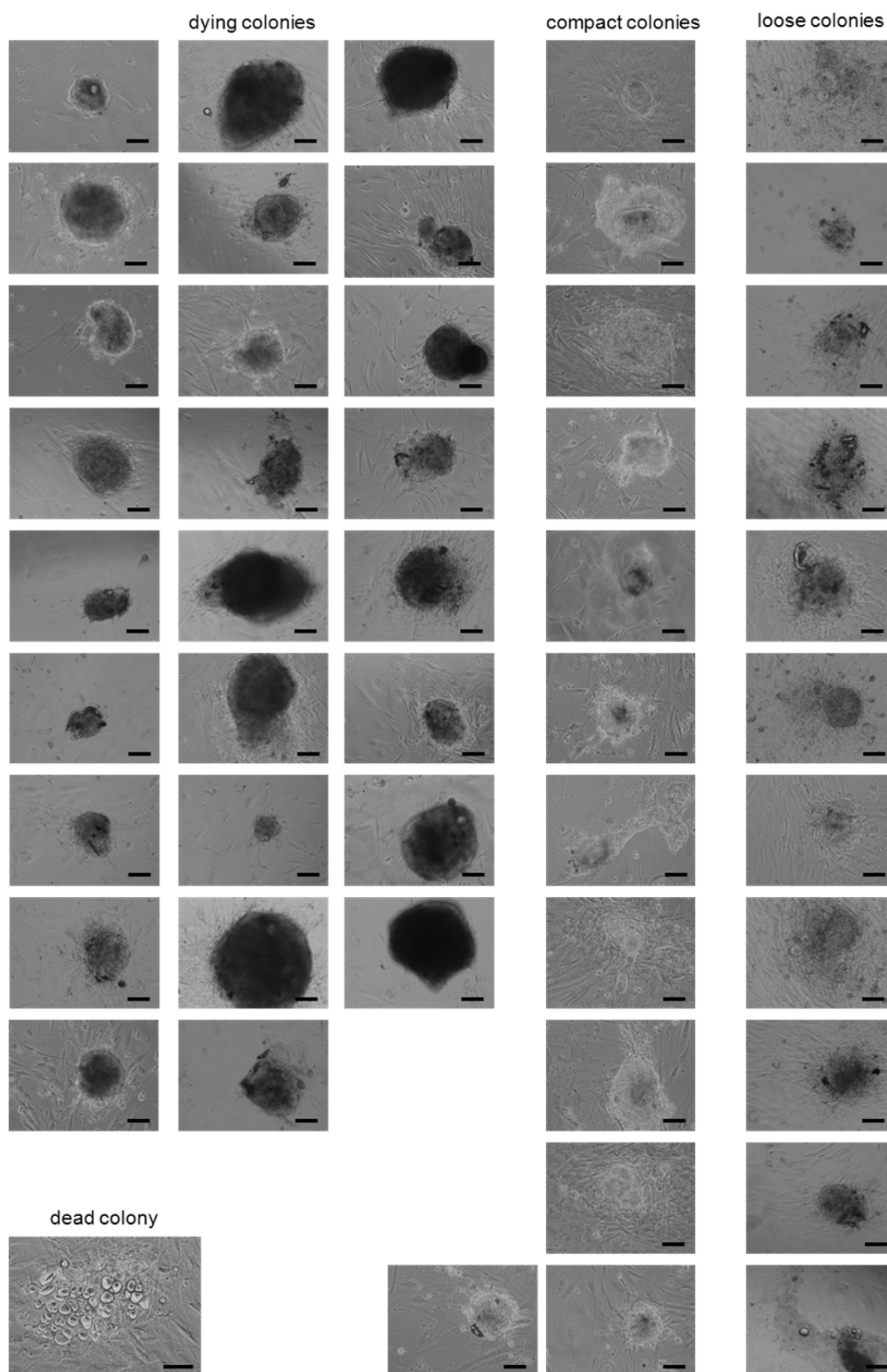
APPENDIX 8: Morphology after treatment with small molecule epigenetic modulators. (A) Optimization assay in L87 cells under normoxic and hypoxic conditions at day 2. Media supplements are indicated. Bars represent 100 μ m. **(B)** Optimization assay in L87 cells under normoxic and hypoxic conditions at day 12. Mock-treated cells (neg) are shown as a control. Bars represent 200 μ m.



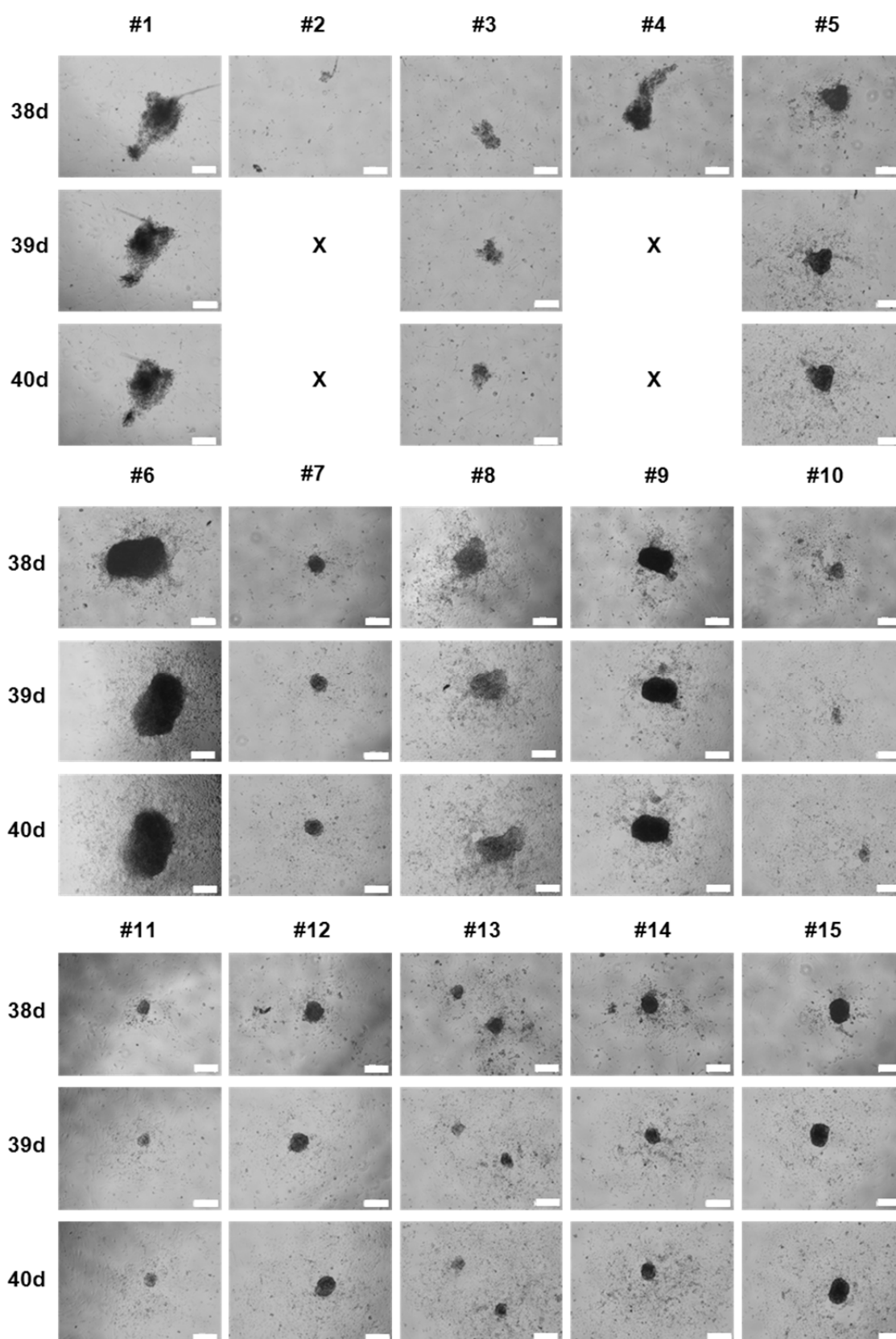
APPENDIX 9: Small molecule epigenetic modulators, miR-302a-d & 372, and hypoxia affect the morphology of L87 cells. L87 cells were cultured under hypoxia and treated with epigenetic modulators and miRs. **(A)** Morphological analysis at day 6 after treatment with RG-108, BIX-01294, VPA, and SBT using low and high concentrations. Bars represent 200 μ M. **(B)** Morphological analysis at day 6 after treatment with epigenetic modulators and miR-302a-d & 372. L87 cells were transfected with 5×10^6 nM miR-302a-d & 372. Further, another approach 2 epigenetic modulators using different combinations were applied in the presence of miRs. Morphology is shown for treatment with RG-108 and BIX-01294 (2x small molecules). Control cells were transfected with miRs or mock-transfected and cultured in presence of hypoxia without treatment. Bars represent 100 μ m.



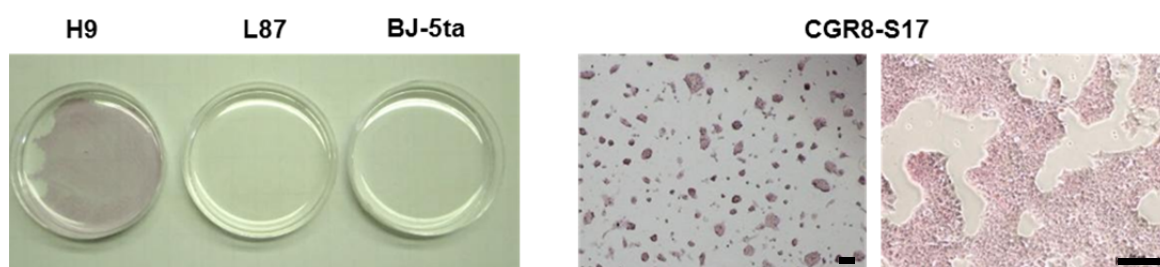
APPENDIX 10: Morphology after treatment with miR-302a-d & 372, small molecule epigenetic modulators, and ES cell-specific culture conditions. BJ-5ta cells were transfected with 5×10^6 nM miR-302a-d & 372 or mock-transfected (mock) and seeded onto MEFs at day 3 under normoxia in human ES cell-specific medium supplemented with set#1 of small molecules. Morphology is demonstrated at day 6. Bars represent 100 μ m.



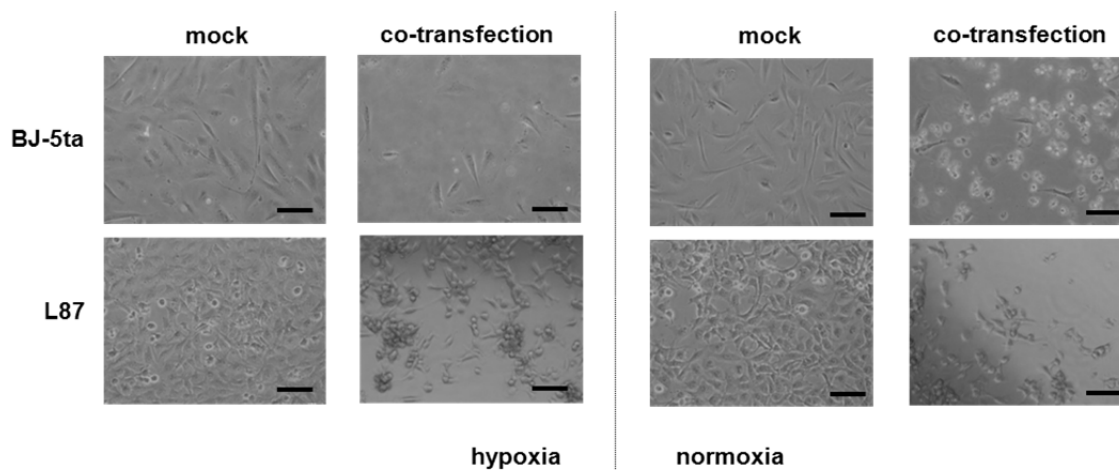
APPENDIX 11: Small molecule epigenetic modulators promote maintenance of colonies derived after transfection with miR-302a-d & 372. BJ-5ta cells were transfected with 5×10 nM miR-302a-d & 372 and seeded onto MEFs at day 3 under hypoxia in human ES cell-specific medium supplemented with set#6 and set#7 of small molecules. Clones were picked at day 27 and morphology is demonstrated one week later. Colonies were classified according to their morphology namely, dying colonies, compact colonies, and loose colonies. Bars represent 100 μ m.



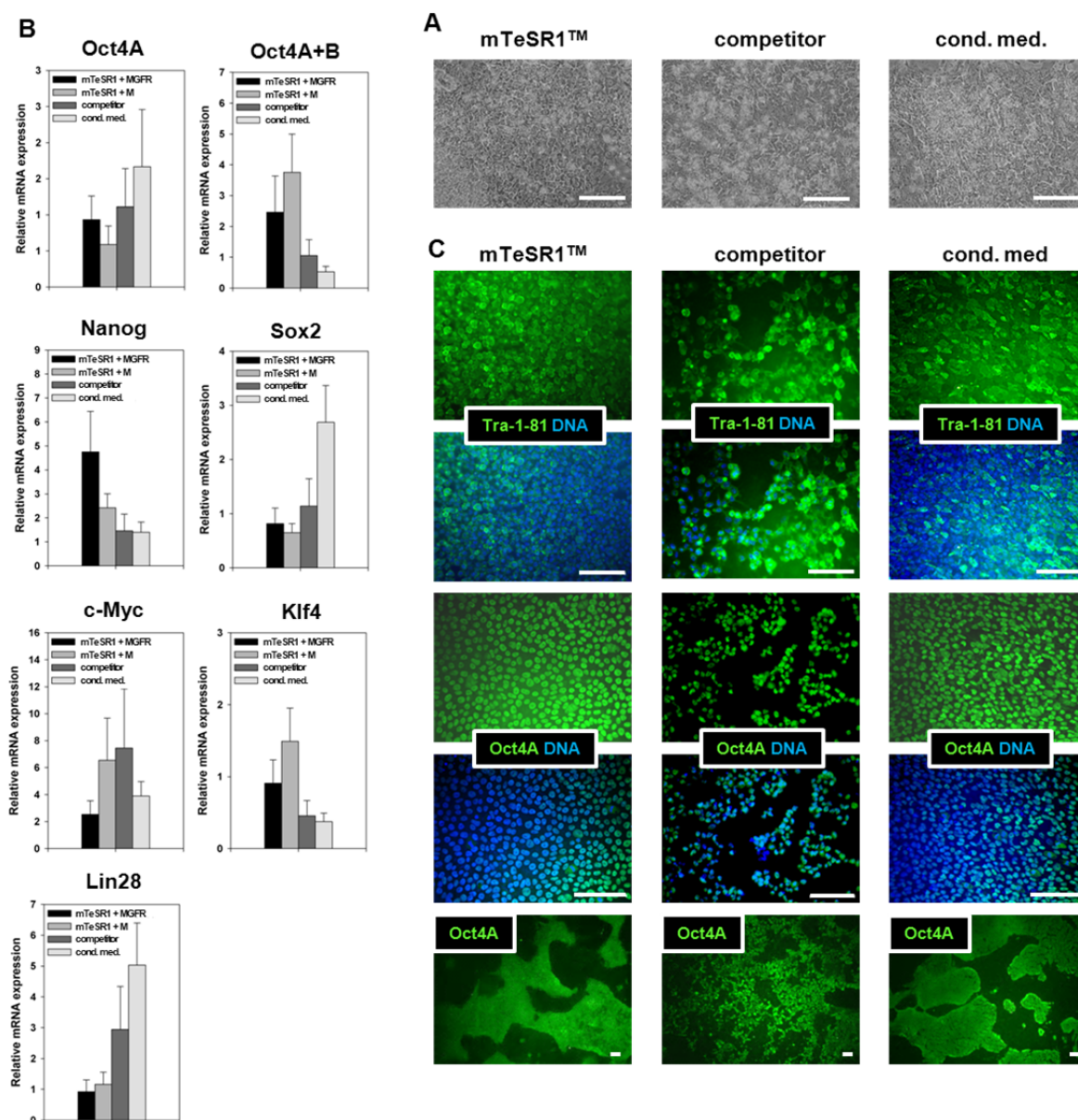
APPENDIX 12: Small molecule kinase inhibitors do not preserve proliferation of non-epithelial colonies established by STEMcircles™. L87-derived colonies obtained by transfection with 5×10 nM miR-302a-d & 372 and treatment with kinase inhibitors were cultured using hypoxic and human ES cell-specific conditions. The morphology of clones are shown after passage 2. Morphology of selected clones (indicated by #) is shown from day 1 to day 3 after passaging. Bars represent 200 μ m.



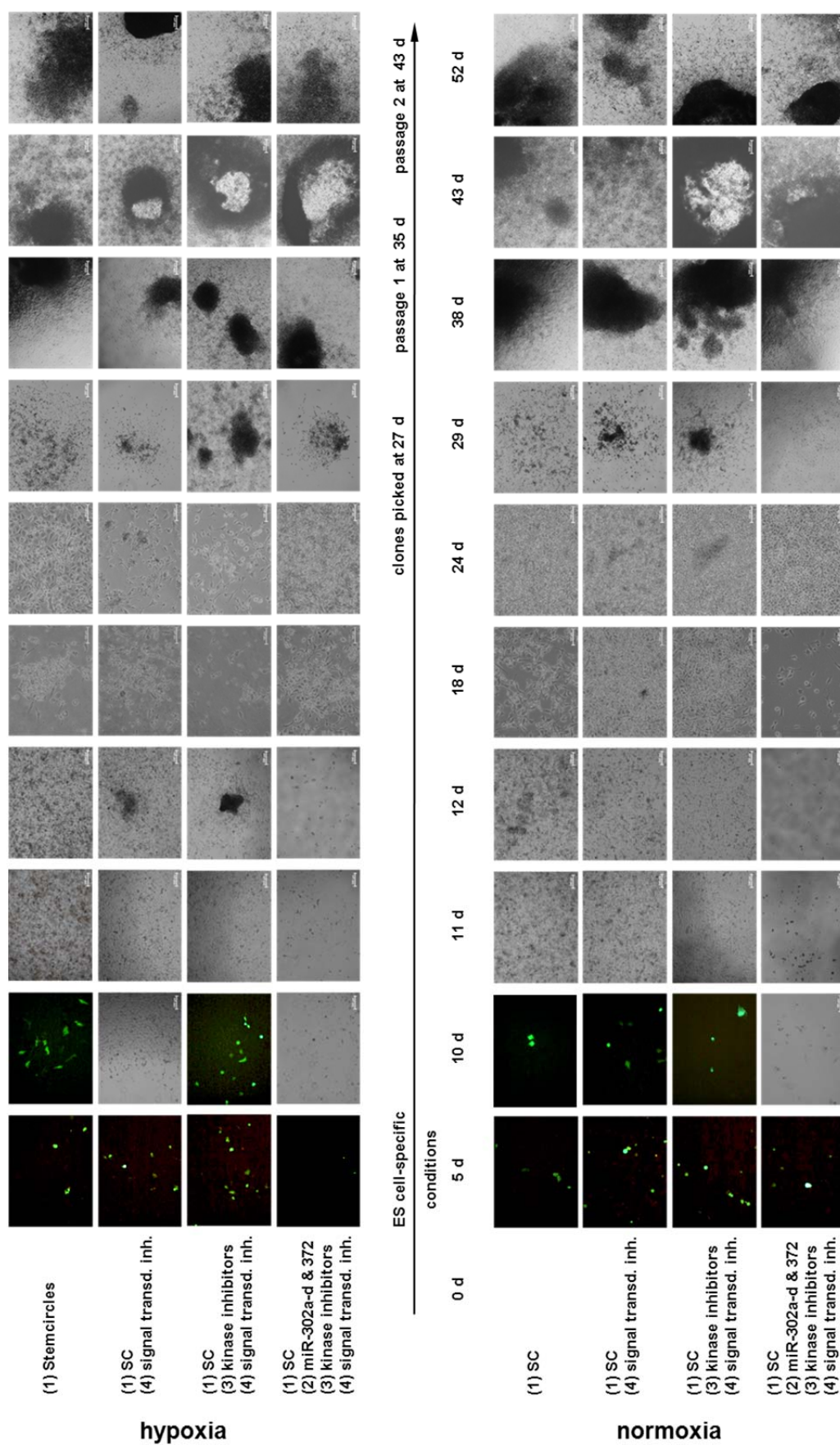
APPENDIX 13: Alkaline Phosphatase staining of pluripotent ES cells and somatic cells. Absence of alkaline phosphatase activity is demonstrated in human somatic L87 MSCs and BJ-5ta fibroblasts. Presence alkaline phosphatase activity is demonstrated in H9 human ES cells (H9) and CGR8-S17 murine ES cells (CGR8-S17). Bar represents 100 μ m.



APPENDIX 14: Morphology after co-transfection of STEMcircles™ and miR-302a-d & 372. BJ-5ta cells and L87 cells were transfected with episomal vectors and 5x 10 nM miR-302a-d & 372 and control cells were mock-transfected (mock). Morphology is shown at day 2. Bars represent 100 μ m.



APPENDIX 15: Characteristics of human ES cells are preserved in iPS cells by MEF-conditioned medium. IMR90 iPS cells were seeded onto GFR Matrigel™ (MGFR) and standard Matrigel™ (M) using mTeSR1™ medium. Further, cells were cultured in MEF-conditioned medium (cond. med.) and Nutristem™ culture medium (competitor) using GFR Matrigel™-coated dishes. After one passage, cells were analyzed at day 3. **(A)** Analysis of colony morphology. **(B)** qRT PCR analysis of pluripotency marker Oct4, Nanog, Sox2, c-Myc, Klf4 and Lin28 mRNA levels. Error bars represent SD of representative data. **(C)** IF analysis of Tra-1-81 and Oct4A. Bars represent 100 μ m.



APPENDIX 16: Morphology and GFP expression after subsequent treatment with STEMcircles™, miR-302a-d & 372, and small molecules. Morphology during reprogramming of L87 cells is demonstrated. The use of kinase inhibitors, signal-transduction inhibitors (indicated as signal transd. inh.), human ES cell-specific conditions and hypoxia is indicated. Bars represent 200 µm.

APPENDIX 17: List of human semi-quantitative PCR primers.

GENE	SEQUENCES	SIZE [bp]	TRANSCRIPTS / DNA SEQUENCES	DESCRIPTION
18SrRNA	(S) ACTCAACACGGGAAACCTCACC (AS) CGCTCCACCACTAAGAACGG	111	NR_046235.1 NR_003286.2	control
Poli	(S) TGAACCTTCTGCGGTGACTG (AS) TTGGATACGCTGAGCAACTG	409	NM_007195.2	proliferation
Mcm5	(S) CCCAGACACATGCAGCTCTA (AS) TGCTCCTCGGCGAGTAAGT	400	NM_006739.3	proliferation
miR302 cluster ¹	(S) GGGCTCCCTTCAACTTTAAC (AS) ATTCTGTGATTGGCTTAACAATCCATCACC	707	NR_029857.1 NC_018915.2	pri-miR-302
Nanog noCDS	(S) GACTGAGCTGGTTGCCTCAT (AS) ATGCTTCAAAGCAAGGCAAG	225	NM_024865.2	endogenous ONSL expression
Oct4 noCDS ²	(S) GCGATCAAGCAGCGACTA (AS) TTCACCTTCCCTCCAACC	400	NM_001285987.1 NM_203289.5 NM_001285986.1 NM_001173531.2 NM_002701.5	endogenous ONSL expression
Sox2 noCDS ²	(S) CCCTGTGGTTACCTCTTCC (AS) CTCCACCTTCCCTCGTTT	259	NM_003106.3	endogenous ONSL expression
Lin28 noCDS ²	(S) AGCCAAGCCACTACATTC (AS) AGATACGTCATTGCGACA	300	NM_024674.4	endogenous ONSL expression
Oct4A	(S) CAAGCCCTCATTTCAACCAG (AS) TTGATGTCCTGGGACTCCTC	467	NM_002701.5	pluripotency
Oct4A+B	(S) AGTGAGAGGCAACCTGGAGA (AS) CAAAACCTTGGCACAAAAC	447	NM_001285987.1 NM_203289.5 NM_001285986.1 NM_001173531.2 NM_002701.5	pluripotency
Sox2	(S) AGTCTCCAAGCGACGAAAAA (AS) GGAAAGTTGGGATCGAACAA	410	NM_003106.3	pluripotency
Nanog	(S) TTCCTTCCCTCATGGATCTG (AS) ACTGGATGTTCTGGGTCTGG	483	NM_024865.2	pluripotency
c-Myc	(S) TTCGGGTAGTGGAAAACCAG (AS) TAGGAGGCCAGCTTCTCTGA	490	NM_002467.4	pluripotency
Lin28	(S) GGTTCCGGTCTCTGTCCATGA (AS) GGTGGCAGCTTGCATTCCTTG	313	NM_024674.4	pluripotency
Klf4 ³	(S) TGATTGTAGTGCTTTCTGGCTGGGCTCC (AS) ACGATCGTGGCCCGGAAAAGGACC	387	NM_004235.4	pluripotency
Dnmt3b	(S) CCAGGACTCGTTCAGAAAGC (AS) CAAACTCCTTCCCATCCTGA	390	NM_001207055.1 NM_175850.2 NM_175849.1 NM_175848.1 NM_006892.3 NM_001207056.1	pluripotency
Chd1l	(S) GACATGCCACGAAAGGTTTT (AS) CTAGCAAGCTGGGGTCAAAG	388	NM_004284.4 NM_001256336.1 NM_024568.2 NM_001256337.1 NM_001256338.1	pluripotency
Myst3	(S) CCCATGTGTGGTGTATTGA (AS) TATAAAGCGGGTTTGCAGAT	279	NM_001099412.1 NM_006766.3 NM_001099413.1	pluripotency
Rest	(S) CCAGCACCCAACCTTACCAC (AS) ACCGACCAGGTAATCACAGC	333	NM_001193508.1 NM_005612.4	pluripotency
Tert	(S) AGGAGCTGACGTGGAAGATG (AS) GCACCTCTTCAAGTGTGT	273	NM_198253.2 NM_001193376.1	pluripotency
Terc	(S) CCCTAACTGAGAAGGGCGTA (AS) GCTGACAGAGCCCAACTCTT	271	NR_001566.1	pluripotency
Gdf3 ³	(S) CTTATGCTACGTAAGGAGCTGGG (AS) GTGCCAACCCAGGTCCCGGAAGTT	631	NM_020634.1	pluripotency
Esg1 ³	(S) ATATCCCGCGTGGGTGAAAGTTC (AS) ACTCAGCATGGACTGGAGCATCC	243	NM_001025290.2	pluripotency
Dppa4 ³	(S) GGAGCCCGCTGCCCTGGAAAATTC (AS) TTTTCTGATATTCTATTCCCAT	408	NM_018189.3	pluripotency

Dppa2 ³	(S) CCGTCCCGCAATCTCCTCCATC (AS) ATGATGCCAACATGGCTCCCGGTG	608	NM_138815.3	pluripotency
Gabrb3 ³	(S) CCTTGGCCAAAATCCCCTATGTCAAAGC (AS) GTATCGCCAATGCCGCTGAGACCTC	277	NM_000814.5 NM_021912.4 NM_001191320.1 NM_001278631.1 NM_001191321.2	pluripotency
TdGF1 ³	(S) CTGCTGCCTGAATGGGGGAACCTGC (AS) GCCACGAGGTGCTCATCCATCACAAGG	237	NM_003212.2	pluripotency
Gal ³	(S) TCGGGCCCGAAGATGACATGAAACC (AS) CCCAGGAGCTCTCAGGACCCTC	188	NM_015973.3	pluripotency
Lefty1 ³	(S) CTTGGGACTATGGAGCTCAGGGCGAC (AS) CATGGGACGAGTCACTCCGAGG	255	NM_020997.2	pluripotency
Lefty2 ³	(S) GCTGGAGCTGCACACCCTGGACCTCAG (AS) GGGCAGCGAGGCTCTCCGAGGC	274	NM_003240.3 NM_001172425.1	pluripotency
Fitm1 ³	(S) CCCCAAAGCCAGAAGATGCACAAGGAG (AS) CGTCGCCAACCATCTTCTGTCCTAG	229	NM_003641.2	pluripotency
Nodal ³	(S) GGGCAAGAGGCACCGTCGACATCA (AS) GGGACTCGGTGGGGCTGGTAACGTTTC	234	NM_018055.4	pluripotency
Utf1 ³	(S) CCGTCGCTGAACACCGCCTGCTG (AS) CGCGCTGCCAGAATGAAGCCAC	171	NM_003577.2	pluripotency
Grb7 ³	(S) CGCCTCTTCAAGTACGGGTGCAGCTGT (AS) TGGGACAGGTGAGGCGGTGTTTG	241	NM_001242443.1 NM_001242442.1 NM_001030002.2 NM_005310.3	pluripotency
Podxl1 ³	(S) TCCAGCCCCACAGCAGCATCACTACC (AS) CCGGGTTGAAGGTGGCTTTGACTGCTC	226	NM_005397.3 NM_001018111.2	pluripotency
CD9 ³	(S) GTGCATGCTGGGACTGTTCTTCGGCTTC (AS) CACGCCCCAGCCAAACCACAGCAG	220	NM_001769.3	pluripotency
Fgf4 ³	(S) CTACAACGCCTAGGAGTCTACA (AS) GTTGACACAGAAAAGTCAGAGTTG	371	NM_002007.2	pluripotency
Rex1 ³	(S) CAGATCTAAACAGCTCGCAGAAT (AS) CGGTACGCAAATTAAGTCCAGA	306	NM_174900.3	pluripotency
Tie2 ⁴	(S) CCAAACGTGATTGACACTGG (AS) TGTGAAGCGTCTCACAGGTC	261	NM_000459.3	characterization ECs
vWF ⁴	(S) TCGGGCTTCACTTACGTTCT (AS) CCTTCACTCGGACACTCA	180	NM_000552.3	characterization ECs
Ephb2 ⁴	(S) TGAGTGGGTGCGTGGTAT5 (AS) GGAGAGGTTGGGGTGATG	150	NM_004093.3	characterization ECs
Ephb4 ⁴	(S) GCCATCATCATGTCTGTTTCCA (AS) CACCAACTACCGCCCTTTTAC	129	NM_004444.4	characterization ECs
Eng ⁴	(S) GCCAGCATTGTCTCACTTCA (AS) GGCACACTTTGTCTGGATCA	135	NM_001278138.1 NM_000118.3 NM_001114753.2	characterization ECs
Pecam1 ⁴	(S) ACCGCAGGATCATTGAGTT (AS) CCCAGCCCAGGATTTCTTAT	165	NM_000442.4	characterization ECs
VEcad ⁴	(S) CAGCCCCAAAGTGTGAGAA (AS) TGTGATGTTGGCCGTGTTAT	162	NM_001795.3	characterization ECs
Vegfr2	(S) CCCACGTTTTTCAGAGTTGGT (AS) CTACCGGTTTGCACCTCAAT	563	NM_002253.2	characterization ECs
Bra	(S) AATTGGTCCAGCCTTGAAT (AS) TACTGGCTGTCCACGATGTC	290	NM_003181.3 NM_001270484.1	differentiation
Ngn3	(S) CGGACCCATTCTCTCTTCT (AS) GGGCAGGTCACTTCGTCTT	250	NM_020999.3	differentiation
Foxa2 ³	(S) TGGGAGCGGTGAAGATGGAAGGGCAC (AS) TCATGCCAGCGCCACGTACGACGAC	216	NM_021784.3 NM_153675.1	differentiation
Afp ³	(S) GAATGCTGCAAACTGACCAGCTGGAAC (AS) TGGCATTCAAGAGGGTTTTCACTCTGGA	281	NM_001134.2	differentiation
Sox17	(S) TAGTTGGGGTGGTCTGCAT (AS) CGCTTTCATGGTGTGGGCTA	166	NM_022454.3	differentiation

Pax6 ³	(S) ACCCATTATCCAGATGTGTTTGCCCGAG (AS) ATGGTGAAGCTGGGCATAGGCGGCAG	317	NM_001127612.1 NM_000280.4 NM_001604.5 NM_001258462.1	differentiation
Sdf1	(S) GCACTTTCACCTCTCCGTCAG (AS) CCACTTTAGCTTCGGGTCAA	323	NM_001033886.2 NM_199168.3 NM_001178134.1 NM_000609.6	differentiation
Pdx1	(S) ACCTTAGACCGAAGGGGAAA (AS) GCATCAATTCACGGGATCT	400	NM_000209	differentiation
Nkx2.2	(S) TGGCCATGTAAAGTTCTGA (AS) CCGAATAGCTGAGCTCCAAG	311	NM_002509	differentiation
Nkx6.1	(S) ATTCGTTGGGGATGACAGAG (AS) TCAACAGCTGCGTGATTTTC	219	NM_006168	differentiation
Gcg	(S) CATTACAGGGCACATTCAC (AS) GCGCGCAAGATTATCAAGAA	336	NM_002054	differentiation
Ins	(S) AGAAGAGGCCATCAAGCAGA (AS) GCTGGTAGAGGGAGCAGATG	245	NM_000207	differentiation
Mist1	(S) ACGCTGGCCAAGAACTACAT (AS) CTGTGGATCTGCGTGGAGTA	200	NM_177455.3	differentiation
Meox1	(S) GCAGCGTACCCTGACTTCTC (AS) CGGTTCTGGAACCACACTTT	497	NM_013999.3 NM_004527.3 NM_001040002.1	differentiation
Gfap ³	(S) GGCCCGCCACTTGCCAGGAGTACCAGG (AS) CTTCTGCTCGGGCCCTCATGAGACG	328	NM_002055.4	differentiation
Map2 ³	(S) CAGGTGGCGGACGTGTGAAAATTGAGAGTG (AS) CACGCTGGATCTGCCTGGGACTGTG	212	NM_002374.3 NM_001039538.1 NM_031845.2 NM_031847.2	differentiation

¹Suh et al., 2004; ²Jia et al., 2010; ³Takahashi et al., 2007; ⁴Wang et al., 2007

APPENDIX 18: List of mouse semi-quantitative PCR primers.

GENE	SEQUENCES	SIZE [bp]	TRANSCRIPTS	DESCRIPTION
TubV	(S) GGGAGGTGATAAGCGATGAA (AS) GGGCACACACTGAAGGTAT	452	NM_011655.5	control
Oct4	(S) GCGTTCCTCTTTGGAAAGGTGTTT (AS) CTCGAACCACATCCTTCTCT	313	NM_013633.3 NM_001252452.1	differentiation
Bra	(S) CTCTAAGGAACCACCGTCA (AS) AACCGAAGACGAGGACGTG	357	NM_009309.2	differentiation
Foxa2	(S) CCCGGGACTTAAGTGAACG (AS) CTAGCGACGGGCTCATT	290	NM_010446.2	differentiation
Sox17	(S) GGAGGGTACCACCTGCTTTA (AS) TGCTCATGGCTCTCCAGAC	358	NM_011441.4	differentiation
Cxcr4	(S) CATGGAACCGATCAGTGTGA (AS) TTTACGCCAGCAGTTTCCTT	467	NM_009911.3	differentiation
Shh	(S) TATCCCAACGTAGCCGAGA (AS) CAGTGGATGTGAGCTTTGGA	409	NM_009170.3	differentiation
FoxF1	(S) GAGTACCCGCACCACGAC (AS) GTAAGATCCTCCGCCTGTTG	390	NM_010426.2	differentiation
Sox7	(S) GACCGAGGGACTGGAGTGT (AS) GTTGGGTAATCCTGCATGT	304	NM_011446.1	differentiation
Pdx1	(S) ACAGCAGTCTGAGGGTGAGC (AS) TCCGTATTGGAACGCTCAAG	317	NM_008814.3	differentiation
Ngn3	(S) GAGGCTCAGCTATCCACTGC (AS) TCTTCGCTGTTTGCTGAGTG	347	NM_009719.6	differentiation
Amy2	(S) GGGTTGATATTGCCAAGGAA (AS) GGCCAGTCAGACACAATTT	423	NM_001160152.1 NM_001160151.1 NM_001160150.1 NM_001042711.2	differentiation
Pax6	(S) TCTAATCGAAGGGCCAAATG (AS) ATGCACGAGTACGAGGAGGT	296	NM_001244198.1 NM_001244200.1 NM_013627.5 NM_001244201.1 NM_001244202.1	differentiation
Sdf1	(S) TCTGTCTTCCCCACTTTTG (AS) CTTCCTGCAATCCATTTA	396	NM_001012477.2	differentiation

APPENDIX 19: List of human qRT-PCR primers.

GENE	SEQUENCES	SIZE [bp]	TRANSCRIPTS / DNA SEQUENCES	DESCRIPTION
18SrRNA	(S) ACTCAACACGGGAAACCTCACC (AS) CGCTCCACCACTAAGAACGG	111	NR_046235.1 NR_003286.2	control
Oct4 Qmethyl	(S) GACTCTCTGGACTGGCTTGG (AS) AATACCTGCCACAGGTCTGC	350	NC_018917.2	Oct4 promoter analysis
Nanog	(S) AAATCTAAGAGGTGGCAGAAAAACA (AS) CTTCTGCGTCACACCATTGC	60	NM_024865.2	pluripotency
Sox2	(S) CACTGCCCTCTCACACATG (AS) CCCATTTCCCTCGTTTTTCTT	81	NM_003106.3	pluripotency
c-Myc	(S) GACGATGCCCTCAACGT (AS) ACCGAGTCGTAGTCGAGGTCAT	60	NM_002467.4	pluripotency
Lin28	(S) CCCCCAGTGGATGTCTTT (AS) CCGGAACCTTCCATGTG	55	NM_024674.4	pluripotency
Klf4	(S) TCTGGGCCCCACATTAAT (AS) CGTCGCTGACAGCCATGTC	60	NM_004235.4	pluripotency
Oct4A	(S) CAAGCCCTCATTTCAACAG (AS) ATCACCTCCACCACCTGGA	108	NM_002701.5	pluripotency
Oct4A+B	(S) AGTTTGTGCCAGGGTTTTTG (AS) TTGTGTTCCCAATTCCTTCC	63	NM_001285987.1 NM_203289.5 NM_001285986.1 NM_001173531.2 NM_002701.5	pluripotency
Dnmt1	(S) ACGGCATCCTGTACCGAGTT (AS) CTTCCGTGGCGTTTCAC	83	NM_001379.2 NM_001130823.1	miR target analysis
Dnmt3a ¹	(S) TATTGATGAGCGCACAAAGAGAGC (AS) GGGTGTCCAGGTAACATTGAG	111	NM_175629.2 NM_022552.4 NM_153759.3	miR target analysis
Dnmt3b ²	(S) CCATTCGAGTCCTGTCAATG (AS) GCAATGGACTCCTCACACAC	176	NM_001207055.1 NM_175850.2 NM_175849.1 NM_175848.1 NM_006892.3 NM_001207056.1	miR target analysis
Wdr61	(S) CCAACCAGTACGGTATTCTCTTCA (AS) CGTCCCCAAGCAACTGA	74	NM_025234.1	miR target analysis
Ccna1	(S) TGGCATTGAGGATGTGTATGAA (AS) TGTGTTGAAATCCAGCAGGAAGT	77	NM_003914.3 NM_001111045.1 NM_001111046.1 NM_001111047.1	miR target analysis
Klf13	(S) TGCAGGACCCTGTCACTACTATACC (AS) TGCCCACTGTTTCCAACAAA	135	NM_015995.2	miR target analysis
Thy1	(S) CCTGACCCGTGAGACAAAGAAG (AS) GCTAGTGAAGCGGATAAGTAGAG	130	NM_006288.3	miR target analysis

¹Zhao et al., 2010; ²Rajendran et al., 2011

APPENDIX 20: List of mouse qRT-PCR primers.

GENE	SEQUENCES	SIZE [bp]	TRANSCRIPTS	DESCRIPTION
Gapdh	(S) CCTGCACCACCAACGCTA (AS) TCATGAGCCCTTCCACCATG	75	NM_008084.2	control
Sox17	(S) AGAAACTGCAGACCAGAAGCTATCA (AS) GCTCATTGTATCCATGAGGTGACA	122	NM_011441.4	differentiation

APPENDIX 21: Oligonucleotides for the generation of pmiRGLO-Dnmt1, pmiRGLO-nonsense, and pmiRGLO-302a.

VECTOR	SEQUENCES	SIZE [bp]	DESIGN
pmiRGLO-Dnmt1	(S) AAAC TAGCGGCCGCTTTAGTGATCAAATTGTGCAGTACTTTGTGCAT (AS) CTAGATGCACAAAGTACTGCACAATTTGATCACTAAAGCGGCCGCTAGTTT	47/51	Ensemble IDs: ENST00000340748 ENST00000359526
pmiRGLO-nonsense	(S) AAAC TAGCGGCCGCTTTAGTGATCAAATTGTGCTCGTGAATGTGCAT (AS) CTAGATGCACATTCACGAGCACAATTTGATCACTAAAGCGGCCGCTAGTTT	47/51	not complementary to miR-302a
pmiRGLO-302a	(S) AAAC TAGCGGCCGCTTGTCAACAAAACATGGAAGCACTTAATTTAT (AS) CTAGAAAAATTAAGTGCTTCCATGTTTTGGTGACAACGCGGCCGCTAGTTT	47/51	complementary to miR-302a

APPENDIX 22: Composition of media applied for pancreatic differentiation.

Spontaneous differentiation medium for the generation of EBs during spontaneous pancreatic differentiation of mouse CGR8-S17 cells.

spontaneous differentiation medium	
component	final concentration
IMDM	50%
F12	50%
L-glutamine	2.5 mM
NEAA	1%
monothioglycerol	450 μ M
FCS	20%

CDM for the generation of EBs during directed pancreatic differentiation of mouse CGR8-S17 cells.

CDM	
component	final concentration
IMDM	50%
F12	50%
L-glutamine	2.5 mM
LIF	2 U/ml
chemically defined lipid concentrate	1%
monothioglycerol	450 μ M
BSA	5.0 mg/ml
transferrin	150.0 μ g/ml
insulin	7.0 μ g
activin A	50 ng/ml

PDM for the differentiation of DE progenitors during pancreatic differentiation of mouse CGR8-S17 cells.

PDM1	
component	final concentration
IMDM	50%
F12	50%
L-glutamine	2.5 mM
monothioglycerol	450 μ M
NEAA	1%
FCS	2%
KAAD-cyclopamine	0.75 mM
indolactam V	300 nM

PDM2	
component	final concentration
IMDM	50%
F12	50%
L-glutamine	2.5 mM
monothioglycerol	450 μ M
NEAA	1%
FCS	2%
KAAD-cyclopamine	0.75 mM
RA	1 μ M

PDM3	
component	final concentration
IMDM	50%
F12	50%
L-glutamine	2.5 mM
monothioglycerol	450 µM
NEAA	1%
FCS	2%
progesterone	20 nM
putrescine	100 µM
laminin	1.0 µg/ml
insulin	25.0 µg/ml
sodium selenite	30 nM
nicotinamide	10 mM
transferrin	50.0 µg/ml
B27® supplement	1:50

HPDM for the differentiation of DE progenitors during directed pancreatic differentiation of human IMR90 iPS and H9 ES cells.

HPDM1	
component	final concentration
RPMI-1640	100%
KAAD-cyclopamine	0.25 µM
FGF10	50.0 ng/ml
Human VEGFa	50.0 ng/ml
FCS	2%

HPDM2	
component	final concentration
DMEM	100%
KAAD-cyclopamine	0.25 µM
FGF10	50.0 ng/ml
Human VEGFa	50.0 ng/ml
B27® supplement	1:50
RA	2 µM
10 µM	Dorsomorphin

HPDM3	
component	final concentration
DMEM	100%
Human VEGFa	50.0 ng/ml
B27® supplement	1:50

CURRICULUM VITAE**Personal Details**

Name	Matthias Jung
Sex	male
Nationality	German
Date and place of birth	13 th of January, 1984 in Jena

Education

since 08/2012	Research staff of the research group of Molecular and Stem Cell Biology of Psychiatric Disorders headed by Prof. Dr. med. Dan Rujescu
03/2009 – 07/2012	PhD student at the Martin Luther University (MLU) Halle-Wittenberg, Medical Faculty, Department Anatomy and Cell Biology headed by Prof. Dr. med. Dr. agr. Bernd Fischer, Junior Research Group Stem Cell Biology headed by Dr. Insa S. Schroeder Title: <i>The establishment of non-viral reprogramming methods and pancreatic differentiation in organotypic models for the production of patient-specific pancreatic cells.</i>
11/2011 – 02/2012	Teaching assistant at the MLU Halle-Wittenberg, Faculty of Natural Science, Department of Agricultural and Nutritional Science
03/2009 – 01/2012	Research assistant at the Translational Centre for Regenerative Medicine (TRM) Leipzig, Junior Research Group Stem Cell Biology headed by Dr. Insa S. Schroeder
05/2008 – 02/2009	Diploma thesis at the Leibniz Institute of Plant Genetics and Crop Plant Research (IPK) in Gatersleben in the research group <i>In Vitro</i> -Differentiation headed by Prof. Dr. Anna M. Wobus Title: <i>Pankreatische Differenzierung von ICA-CCF-GFP-exprimierenden embryonalen Stammzellen.</i>
10/2003 – 02/2009	Degree in Biology at Kassel University: Diplom Biologe
12/2007 – 02/2008	Student assistant at the University of Kassel, Department Biology, group animal physiology headed by Prof. Dr. M. Stengel
08/2007 – 11/2007	Research assistant at the Leibniz Institute of Plant Genetics and Crop Plant Research (IPK) in Gatersleben in the research group <i>In Vitro</i> Differentiation headed by Prof. Dr. Anna M. Wobus
06/2003	Secondary school in Gera: Allgemeine Hochschulreife

Awards

11/2011	1st Place for the Best Abstract World Conference on Regenerative Medicine in Leipzig, Germany
05/2011	Seige-Hasik-Preis Bilateral Symposium of Molecular Medicine in Halle/Saale, Germany
10/2010	Delegate/Representative TRM Leipzig/University of Leipzig World Stem Cell Summit in Detroit, United States of America

List of Publications

- Jung, M.** Uding, J. Trillhaase, A. Rujescu, D. (2014) Neural derivatives from patient-specific B cells for the analysis of psychiatric diseases. 27th European College of Neuropsychopharmacology Congress: 18.-21.10.2014 (Berlin); Eur Neuropsychopharmacol. in press
- Foja, S.* **Jung, M.*** Harwardt, B. Pelz-Ackermann, O. Schroeder, I.S. (2013) Hypoxia supports reprogramming of mesenchymal stroma cells via induction of embryonic stem cell specific miRNA-302 cluster and pluripotency-associated genes. Cell. Reprogram. 15(1): 68-79
- Jung, M.** Schroeder, I.S. (2013) Pluripotency and Early Cell Fate Decisions are Orchestrated by microRNAs. Sahu, S.C. (editor): microRNAs in Toxicology and Medicine. West Sussex, United Kingdom: John Wiley & Sons Ltd.
- Jung, M.** Trillhaase, A. Friedl, M. Hartmann, A.M. Giegling, I. Rujescu, D. (2013) Herstellung und Analyse von Patienten- und Krankheitsspezifischen Neuronen. 9. Mitteldeutsche Psychiatertage: 13-14.09.2013 (Jena); ISBN-Nr. 978-3-9816002-6-1
- Jung, M.** Schroeder, I.S. Rujescu, D. (2013) ES cell-associated microRNAs and hypoxia guide reprogramming of somatic cells. 4rd World Conference on Regenerative Medicine: 23.-25.10.2013 (Leipzig); Regen Med. 8(6s)
- Schroeder, I.S. Oelschlaegel, D. **Jung, M.** (2013) Stem Cell Applications for Pancreas Function. Calegari, F. Waskow, C. (editor): Stem Cells: From Basic Research to Therapy, Volume 2: Tissue Homeostasis and Regeneration During Adulthood, Applications, Legislation and Ethics. Woodland Hills, United States of America: Productivity PR Inc.
- Jung, M.** Kuhn, S. Foja, S. Schroeder I.S. (2011) Micro RNAs influence the generation of induced pluripotent stem cells and subsequent differentiation into the pancreatic lineage. 3rd World Conference on Regenerative Medicine: 02.-04.11.2011 (Leipzig); Regen Med. 6(6s)

List of Oral Presentations

- Jung, M.** Trillhaase, A. Uding, J. Friedl, M. Giegling, I. Rujescu, D. (23.06.2014) Title: *Herstellung von iPS-Zellen aus B-Lymphozyten schizophrener Patienten und deren Differenzierung in Neurone*. Course unit of the MLU Halle-Wittenberg, Faculty of Natural Science, Department Zoology in Halle/Saale, Germany
- Jung, M.** Trillhaase, A. Friedl, M. Giegling, I. Rujescu, D. (16.10.2013) Title: *Herstellung von iPS-Zellen aus B-Lymphozyten schizophrener Patienten und deren Differenzierung in Neurone*. Educational event of the University Hospital Halle/Saale, Department Psychiatry, Psychotherapy, and Psychosomatic Medicine in Halle/Saale, Germany
- Jung, M.** Foja, S. Sulzbacher, S. Harwardt, B. Schweyen, S.M. Oelschlägel, D. Kuhn, S. Schroeder, I.S. (21.05.2012) Title: *Herstellung von iPS-Zellen und deren pankreatische Differenzierung zur Analyse des Diabetes mellitus*. Course unit of the MLU Halle-Wittenberg, Faculty of Natural Science, Department Zoology in Halle/Saale, Germany
- Jung, M.** Kuhn, S. Foja, S. Schroeder I.S. (02.11.2011) Title: *MicroRNAs influence the generation of induced pluripotent stem cells and subsequent differentiation into the pancreatic lineage*. World Conference on Regenerative Medicine (WRM) in Leipzig, Germany
- Jung, M.** Foja, S. Schroeder I.S. (21.05.2011) Title: *Generation of disease/patient specific induced pluripotent stem (iPS) cells for the analysis of diabetes mellitus*. Bilateral Symposium of Molecular Medicine in Halle/Saale, Germany
- Jung, M.** Sulzbacher, S. Schroeder, I.S. Wobus, A.M. (27.05.2009) Title: *Pancreatic Differentiation of ICA-CCF-GFP-expressing ES cells*. University of Kassel in Kassel, Germany

List of Poster Presentations

- Jung, M.** Trillhaase, A. Rujescu, D. (11.-13.11.2013) Title: *Reprogramming of patient-specific B cells for the generation of disease-specific neural cells*. Annual Conference of the German Stem Cell Network (GSCN) in Berlin, Germany

- Jung, M.** Schroeder, I.S. Rujescu, D. (21.-23.10.2013) Title: *ES cell-associated microRNAs and hypoxia guide reprogramming of somatic cells*. World Conference on Regenerative Medicine (WRM) in Leipzig, Germany
- Jung, M.** Trillhaase, A. Friedl, M. Hartmann A.M. Giegling, I. Rujescu, D. *Herstellung und Analyse von Patienten- und Krankheits-spezifischen Neuronen*. (13.-14.09.2013) Mitteldeutsche Psychiatrietage (MDP) in Jena, Germany
- Jung, M.** Schroeder, I.S. Rujescu, D. (23.-27.04.2013) Title: *ES cell-associated microRNAs and hypoxia guide reprogramming of somatic cells*. International Meeting Stem Cell Network NRW in Cologne, Germany
- Jung, M.** Harwardt, B. Rujescu, D. Schroeder, I.S. (29.-30.11.2013) Title: *Induction of pluripotency by episomal vectors or miR-302 cluster*. Fraunhofer Life Science Symposium in Leipzig, Germany
- Jung, M.** Oelschlägel, D. Harwardt, B. Schroeder, I.S. (20.06.2012) Title: *Cells for the analysis diabetes: The understanding of disease development and progression*. Saxon Biotechnology Symposium in Leipzig, Germany
- Jung, M.** Kuhn, S. Foja, S. Schroeder, I.S. (11.-14.09.2011) Title: *Induced pluripotency in somatic cells and subsequent pancreatic differentiation of pluripotent stem cells is regulated by microRNAs*. Stem Cells in Development and Disease in Berlin, Germany
- Foja, S. **Jung, M.** Schroeder I.S. (11.-14.09.2011) Title: *Induction of embryonic microRNA (miR) cluster 302 and pluripotency genes in humane mesenchymal stroma cells under hypoxic culture conditions*. Stem Cells in Development and Disease in Berlin, Germany
- Jung, M.** Kuhn, S. Foja, S. Schroeder, I.S. (08.-09.09.2011) Title: *MicroRNAs (miRs) guide pluripotency on somatic cells and subsequent pancreatic differentiation*. RNAi Europe in München, Germany
- Jung, M.** Foja, S. Schroeder, I.S. (21.05.2011) Title: *Generation of disease/patient specific induced pluripotent stem (iPS) cells for the analysis of diabetes mellitus*. Bilateral Symposium Molecular Medicine in Halle/Saale, Germany
- Schweyen, S.M. Sulzbacher, S. **Jung, M.** Schroeder, I.S. (21.05.2011) Title: *Improvement of pancreatic differentiation through nutritional factors and small molecules*. Bilateral Symposium Molecular Medicine in Halle/Saale, Germany
- Jung, M.** Foja, S. Schroeder, I.S. (05.-06.04.2011) Title: *Non-viral reprogramming strategies in somatic cells: Approach for the study of diseases*. International Meeting Stem Cell Network NRW in Essen, Germany
- Schweyen, S.M. Sulzbacher, S. **Jung, M.** Schroeder, I.S. (05.-06.04.2011) Title: *Influence of glucose on definitive endoderm and early pancreatic progenitor formation*. International Meeting Stem Cell Network NRW in Essen, Germany
- Schroeder, I.S. Sulzbacher, S. Fuchs, J. Nolden, T. Himmelbauer, H. Czarnotha, J. **Jung, M.** Wobus, A.M. (29.-30.10.2010) Title: *Potential of SOX17-expressing mouse embryonic stem cells induced to differentiate into endoderm and early pancreatic lineages by Activin A*. Fraunhofer Life Science Symposium in Leipzig, Germany
- Jung, M.** Foja, S. Schweyen, S.M. Czarnota, J. Harwardt, B. Schroeder, I.S. (12.10.2009) Title: *In vitro differentiation of embryonic stem cells into the pancreatic lineage*. TRM Retreat in Wittenberg, Germany

Halle an der Saale, 26.06.2014

Ort, Datum

Matthias Jung

EIDESSTATTLICHE ERKLÄRUNG

Hiermit erkläre ich, Matthias Jung, dass diese Arbeit von mir bisher weder der Naturwissenschaftlichen Fakultät I – Biowissenschaften – der Martin-Luther-Universität Halle-Wittenberg, noch einer anderen wissenschaftlichen Einrichtung zum Zweck der Promotion eingereicht wurde und ich noch keine vergeblichen Promotionsversuche unternommen habe.

Ich erkläre ferner, dass ich diese Arbeit selbstständig, ohne Fremde Hilfe und nur unter zur Zuhilfenahme der angegebenen Hilfsmittel und Literatur angefertigt habe und weiterhin keine anderen als die von mir angegebenen Quellen und Hilfsmittel benutzt habe, sowie die den benutzten Werken wörtlich oder inhaltlich entnommenen Stellen als solche kenntlich gemacht habe.

Halle an der Saale, 26.06.2014

Ort, Datum

Matthias Jung